Uncovering neural patterns of cognition by aligning oscillatory dynamics

Sander van Bree

Submitted in fulfilment of the requirements for the
Degree of Doctor of Philosophy (PhD)

School of Psychology and Neuroscience
College of Medical, Veterinary & Life Sciences
University of Glasgow

November 2023

Abstract

A primary aim of cognitive neuroscience is to explain how cognition is physically realized by the brain. Toward this end, neuroscientists study consistent activity patterns produced across ensembles of neurons. Importantly, such ensembles are subject to excitability fluctuations imposed by neural oscillations, which are used in a self-organized way to realize windows of effective communication, coding schemes, a switch between memory processes, interareal information exchange, and other functions. Given the intimate link between oscillations and neural processing, this thesis explores the power of studying activity patterns of cognition with reference to brain dynamics. Specifically, I submit that spectral information like phase and oscillatory cycles offer a brain-intrinsic coordinate system by which the readout of neurocognitive patterns can be assisted. From this vantage point, I explore two methodological advances: (1) *brain time warping*, which incorporates oscillatory dynamics post-hoc after brain data has been acquired, and (2) *visual perturbation* or "*pings*", which artificially regularize oscillations as memory retrieval is ongoing. We demonstrate that brain time warping can reveal activity patterns otherwise left undetected, and we introduce a comprehensive toolbox to apply the algorithm and test its effects. On the other hand, we found no evidence that pings enhance the readout of memory representations from electroencephalography data. Together, these empirical and theoretical points underscore the need for a neurally inspired methodology in which scientists are cast as spectators with privileged access to external world variables.

Contents

List of tables

List of figures

Figures Main text

Figures Supplementary material Chapter 3

Figures Supplementary material Chapter 4

Publications

The following proceedings contain work presented in this thesis:

Journal articles

Chapter 3 contains material from:

van Bree, S., Melcón, M., Kolibius, L. D., Kerrén, C., Wimber, M., & Hanslmayr, S. (2022). The brain time toolbox, a software library to retune electrophysiology data to brain dynamics. *Nature Human Behaviour*, *6*(10), 1430–1439. https://doi.org/10.1038/s41562-022-01386-8

Conference presentations

van Bree, S., Mackenzie, A., Wimber, M. (2023). Evaluating visual pings as a method to enhance the readout of long-term memory contents. *Generative Episodic Memory (GEM)*

van Bree, S., Melcón, M., Kolibius, L. D., Kerrén, C., Wimber, M., & Hanslmayr, S. (2023). Clock time: a foreign measure to brain dynamics – introducing the brain time toolbox. *Learning & Memory (LEARNMEM)*

van Bree, S., Melcón, M., Kolibius, L. D., Kerrén, C., Wimber, M., & Hanslmayr, S. (2022). Clock time: a foreign measure to brain dynamics – introducing the brain time toolbox. *Organization for Human Brain Mapping (OHBM)*

van Bree, S., Melcón, M., Kolibius, L. D., Kerrén, C., Wimber, M., & Hanslmayr, S. (2022). Clock time: a foreign measure to brain dynamics – introducing the brain time toolbox. *International Conference of Cognitive Neuroscience (ICON)*

van Bree, S., Melcón, M., Kolibius, L. D., Kerrén, C., Wimber, M., & Hanslmayr, S. (2021). Clock time: a foreign measure to brain dynamics. *Society for Neuroscience (SfN)*

van Bree, S., Melcón, M., Wimber, M., & Hanslmayr, S. (2020). Brain Time Toolbox: Warping electrophysiological data to detect recurrence of active cognitive processes. S*fN: Global Connectome*

Acknowledgements

Thank you to my supervisors, colleagues, family, and friends for your pillaring support.

Maria Wimber, I appreciate your vigorous approach to science and supervision. Thank you for your trusting attitude and your continuous sharpness. Start to finish, it felt like we were at the ship's wheel together. You strike a balance between direction and freedom that allows students to flourish with their own identity—it has been an empowering journey.

Simon Hanslmayr, I appreciate your steadfastness and visionary approach, your forward thinking and scientific creativity, and frankly your sheer analytical prowess.

Abbie, Jacqueline, David, and Janvi, thank you for your helping hand and the companionship.

I am grateful for the background support from people working at the University of Glasgow and the University of Birmingham, including IT, psychology admins, lab organizers, cleaners, and other staff.

Mircea, Luca, Christopher, María, Christoph, Seán, Ralitsa, Katarina, Casper, Jonas, Pablo, Jelena, Eleonora, Bianca, Danying, Jack, Laura, Robin, and many others, thank you for your warmth and inspiration. I reserve a special thank you to those who prepared good food for us to eat together, and for me to take home.

Guido, Helmie, and Julian—thank you for a safe haven.

Declaration

I declare that all work contained in this thesis was carried out by the author unless it is stated otherwise. No large language model was used in writing this thesis.

Abbreviations

AUC	Area Under Curve
BOSS	Bank of Standardized Stimuli
DTW	Dynamic Time Warping
EEG	Electroencephalography
EPSP	Excitatory Post-Synaptic Potential
ERP	Event-Related Potential
E-I	Excitation-Inhibition
FDR	False Discovery Rate
FFT	Fast Fourier Transform
FOOOF	Fitting Oscillations and One Over F
GED	Generalized Eigendecomposition
GIMP	GNU Image Manipulation Program
ICA	Independent Component Analysis
IRASA	Irregular-Resampling Auto-Spectral Analysis
ITC	Intertrial Coherence
ITPC	Intertrial Phase Coherence
LDA	Linear Discriminant Analysis
LFP	Local Field Potential
LTM	Long-term Memory
M	Mean
MEG	Magnetoencephalography
ms	Milliseconds
MVPA	Multivariate Pattern Analysis
POD	Peak Order Distance
RGB	Red Green Blue colour values
RT	Reaction Time
s	Seconds
SD	Standard Deviation
SEM	Standard Error of the Mean
SOA	Stimulus Onset Asynchrony
STDP	Spike-Timing Dependent Plasticity
TGM	Temporal Generalization Matrix
WM	Working Memory

Chapter 1: General introduction

1.1 Scope

The motivating assumption of this thesis is that the brain works in ways that do not reveal themselves to naïve experimental observation. As neuroscientists, we study an information processing system that works via enshrouded internal processes, and our task is to work through this shroud and lay bare how the brain produces behaviour and cognition. The body of research presented in this manuscript suggests this project is more fruitful if we explicitly consider the relationship between scientists and their system of study in our approaches. By casting scientists as *spectators*, we confer a kind of primacy to the brain that has implications for how to analyse, experiment, and theorize.

What is this thesis *not* about? Some thinkers have argued that due to our position as outside observers, we have consolidated over time a cognitive ontology that is misaligned with reality. The proposal to match is that instead of inheriting terms like perception, attention, memory, emotion, language, and action, we should revise our vocabulary by leveraging neural data (Buzsáki, 2019), or phylogenetic evidence (Cisek, 2019). Now, although the research presented in this thesis is inspired by inside-out approaches, this work remains agnostic to cognitive ontology—that is to say, it neither endorses nor rejects a brain-driven revision of psychology. My key claim is critically different: Regardless of what cognition is like, inquiry into its neural underpinnings should start from the notion that the brain lacks direct access to information in the external world (Scharnowski et al., 2013).

To be sure, the brain encodes distances and durations, manipulating representations of space and time in the service of adaptive behaviour (Gallistel, 2011). But this is orthogonal to the question of how the brain endemically structures its activity. As I will review, neuronal processing is organized by non-linear fluctuations in neuronal excitability. Given that these dynamics govern how information processing unfolds, they offer a system-centric base unit for scientific analysis, experimentation, and description. Put differently, while the brain infers and reconstruct variables of the external world to support complex cognition, units of spacetime are by no means the brain's home court (Buzsáki & Llinás, 2017; Buzsáki & Vöröslakos, 2023).

Thus, this work is about *Methods*, not *Metaphysics*: How do we effectively study an opaque information processing system? How do neural dimensions relate to worldly dimensions? What units of measurement can we validly project onto the brain, and when should we?

1.2 The curious case of unit *t*

If there is one central message of this thesis, it would be that methodological trouble arrives when we collapse neural variables in favour of worldly variables. To introduce the issue, take the emblematic case of $t = 0$ in experiments of mind and brain. This represents a slice of time that marks the start of our recordings, the onset of an experimental intervention or stimulus, or some other striking event in the world. With our anchor firmly in place, we next track what happens within our system of study as a function of *t*. How do patterns of activity unfold? What consistent temporal structure do they display? When do participants press a button? What variability do we see in cognition and behaviour, within and across participants?

From the vantage point of the neural mechanisms we are studying, there is something peculiar about this way of doing neuroscience. Certainly, Newtonian time is indispensable to scientific investigation and conceptualization because it grounds measurements in the physical world. But this dimension of time is not all there is to it—and from the brain's perspective, it is not even most central.

The nuts and bolts of the brain process information on their own terms, using intrinsic dynamics which rarely comport to variables in the external world (Buzsáki & Llinás, 2017). In this sense, the brain is nothing much like a radio, with its perpetually receptive antenna and with its internal wirings that yield continuous processing. Instead, the brain fluctuates in excitability levels in ways that vary markedly across regions in the brain (Capilla et al., 2022). Even within the same region, individual ensembles display activity patterns that change nonlinearly with respect to Newtonian time from one moment to the next (Cole & Voytek, 2019). As a result of such spatiotemporal variability, neural computation becomes idiosyncratic from the vantage point of external observers. The normative claim of this thesis is that accounting for such eccentricities makes for a neuroscience that is more fruit-bearing, and the descriptive contributions underpin this aim. To this end, I present an empirical overview that explores how brain dynamics relate to cognition (Chapter 2), and I evaluate methodological approaches that have the potential to support a brain-centric neuroscience (Chapter 3 and 4). Before relaying these points, I first spell out this work's theoretical assumptions, and the basic principles of brain dynamics.

1.3 Assumptions

What are some assumptions that run through this thesis? First, neuronal activity is taken to *represent* and *compute*. That is to say, the brain is assumed to encode and transform

information in the service of cognition (Gallistel & King, 2009). While representationalism is taken on board axiomatically, it is not universally accepted (van Gelder, 1995).

Second, concerning time, it is often said that the brain is a dynamical system, but this does little to no conceptual work because any physical system that evolves over time is a dynamical system (Kelso, 2001), and it is hard to conceive of a system that does not. The more instructive lens is given by the distinction between analog and digital information processing. Unlike digital architectures in which a series of static state transitions discretely impinge on each other, the brain is an analog computational system which evolves continuously in a self-organized manner (Lashley, 1958, p. 539; but see Piccinini & Bahar, 2013). This contrast is important, as the core functional properties of a system influence what scientific path most effectively enables our understanding of it, and more fundamentally, how the system actualizes its capacities. In short, the second assumption is that the brain's processing regime is continuous and that these dynamics constrain brain function and guide methodology.

Now, a striking observation is that much of the brain's activity displays stereotypic rhythmic fluctuations, or *neural oscillations* (Berger, 1929), a finding which is perhaps unsurprising considering that networks of neurons are systems of coupled relaxation oscillators. And just as physicists leverage different vocabularies and observe distinct physical laws under oscillatory and non-oscillatory regimes of its systems of study (Hartman & Wintner, 1949), so too do neuroscientists observe changes in information processing during oscillatory and non-oscillatory states, each inviting a separate body of terms and analytical techniques. In this work, a third assumption is that oscillations are a genuine class of brain activity that is to be separated from activity that unfolds by other temporal structure. For instance, in Chapter 2, the functional role of oscillations is explicitly analysed in the context of memory processing. In Chapter 3, electrophysiology data is transformed based on user-selected frequency bands of oscillations. In Chapter 4, the phase reset of oscillations is taken as a plausible mechanism of action for why visual perturbations could refocus brain activity. With that said, a good deal of the observations and inferences across these chapters hold even when collapsing all forms of brain dynamics into a single unitary dimension. Or, in philosophical terms, much but not everything turns on oscillations being a *natural kind* of brain activity. As an illustrative example, in bats, neuronal ensembles discharge at specific phases of non-oscillatory fluctuations in the local field potential (Eliav et al., 2018), suggesting that the basic idea of excitability changes as a valid reference scheme persists across dynamical regimes.

A fourth question is whether oscillations are causal players in the brain or merely passive byproducts of neuronal activity. In other words, does the fluctuating brain activity, and specifically the electric field associated with it, feed back into neuronal populations to influence cortical and subcortical computation? This question will not be given extensive treatment. Rather, I consider what turns on its answer. Even if oscillations are nothing but a passive reflection of neuronal population states, then neuroscientific inquiry should factor in oscillatory dynamics all the same. Summary statistic alone, or top-down causal player over and above that, in either case oscillations offer information about how neural patterns of cognition unfold. Ergo, techniques that regularize or factor in oscillatory brain dynamics are important regardless—it is just that the reason for their importance varies. Even so, individual claims across these chapters depend in varying degrees on the hypothesis that oscillations causally influence neural computation and cognition at large, and I have attempted to support assertions that use causal terms with empirical and theoretical justification.

Finally, I have decided to tolerate vagueness and ambiguity toward the term neural oscillations, opting for the encompassing definition of fluctuating brain activity. There is currently no consensus on the necessary properties of neural oscillations. Some invoke the term when there is a rhythmic brain response of any kind, others require a (damping) rhythmic response after driving input has ceased (van Bree et al., 2021; van Bree, Alamia, et al., 2022; Zoefel et al., 2018), and further formulations still require active self-generative dynamics (Doelling & Assaneo, 2021). The reason to adopt a broad lens is that ultimately my claims concern temporally structured variance in brain activity, a point which transcends weak and strong oscillation accounts. By extension, I do not believe anything central turns on which formulation of neural oscillations is right.

In summary, ranging from most to least pivotal, the research in this thesis assumes representationalism, constraint of brain function by dynamics, the view that oscillations are real, that they are informative, and that they are causally relevant for cognition. Next, I introduce the scientific study of brain dynamics.

1.4 Brain dynamics

1.4.1 Characterizing temporal structure

How do neuroscientists get a handle on the orchestra of neural activity? A primary method to characterize brain dynamics is Fourier analysis, whereby signals recorded using neuroimaging techniques—such as electroencephalography (EEG),

magnetoencephalography (MEG), intracranial local field potential recordings (LFP), and functional MRI (fMRI)—are decomposed into a set of sinusoidal functions which faithfully recapitulate the original signal when summed. Such decomposition into underlying functions has at least three uses. First, it helps us uncover the distribution of fast- and slow-changing signal components, which have distinct neural origins (Capilla et al., 2022; Womelsdorf et al., 2014). Second, through signal decomposition we can modify the data systematically, removing frequency bands or coloured noise we assume to be unrelated to our phenomena of interest, increasing our effective signal-to-noise ratio (Widmann et al., 2015). Third and relatedly, frequency decomposition can help us separate oscillatory and non-oscillatory dimensions of brain activity, which as outlined in Section 1.2 call for separate methodologies and arise from distinct brain mechanisms (Gerster et al., 2022). For a mathematical exposition of Fourier analysis, see Körner, 1988.

In addition to Fourier analysis, there are a host of related techniques—such as Welch's method (Welch, 1967) and wavelet transform—which also achieve the goal of representing neuroimaging data in time and frequency space, each with its own upshots and limitations (Akin, 2002; Rahi & Mehra, 2014).

1.4.2 Non-oscillatory dynamics

Whereas oscillatory brain activity confines itself to band-limited segments in frequency space, non-oscillatory activity spreads out disparately across the spectrum with varying intensities. White noise refers to activity with equal intensities across the board, pink noise has a negative slope with intensity ramping down with increasing frequencies (in keeping with a $1/\text{frequency}$ law), and Brown noise drops off even more rapidly (with a $1/\text{frequency}^2$ law; Figure 1.1A). Pink noise—henceforth referred to as 1/f noise—shows up robustly across natural physical systems, and the brain is no exception (Fig. 1.1B). It is not understood why 1/f noise is so ubiquitous throughout the universe; though some accounts suggest it is a necessary byproduct of stationary random stochastic processes that arises regardless of the kind and number of system variables at play (Szendro et al., 2001).

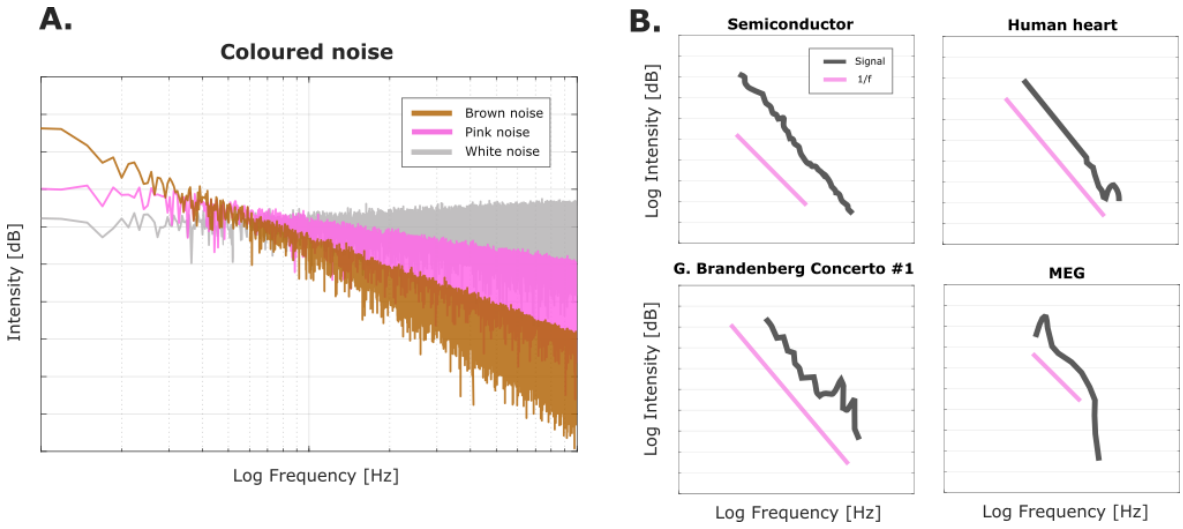

Figure 1.1. Non-oscillatory activity in natural systems. (A) White noise, pink noise (1/frequency), and Brown noise (1/frequency^2). (B) Examples of pink noise in nature. Figure 1B was adapted from Ward & Greenwood, 2007; see reference for original data sources.

Out of the different forms of noise, 1/f noise has been of most interest to neuroscientists because it shows up robustly across power spectra of brain activity (Donoghue et al., 2020). 1/f noise profiles are correlated with network spiking (Manning et al., 2009), blood-oxygen levels (Winawer et al., 2013), the relative distribution of excitatory and inhibitory synaptic activity (E-I balance; Gao et al., 2017), task-relevant changes in behaviour (Ouyang et al., 2020) and cognition (Herweg et al., 2020), disease (Molina et al., 2020), and cortical depth (Halgren et al., 2021).

Given such relations, and the distinct brain mechanisms believed to be at play for oscillatory activity, a longstanding analytical project has been to develop ways of teasing apart 1/f and oscillatory components—which as mentioned before blend in frequency space. This problem spawned a host of modelling tools, including but not limited to *Fitting Oscillations and One Over F* (*FOOOF*; Donoghue et al., 2020) and *Irregular-Resampling Auto-Spectral Analysis* (*IRASA*; Wen & Liu, 2016), each with its own applications (Gerster et al., 2022). The Brain Time Toolbox introduced in Chapter 3 depends on the extraction of oscillatory components of brain activity, and as such leverages these and other techniques for its reliable application.

This thesis places its focus on oscillatory dynamics. One reason for this is that oscillations come packaged with a relatively well-defined brain-inspired unit of time—excitability cycles—allowing us to strike at the heart of the problem identified in the opening paragraphs. Since my focus is on this class of brain dynamics, forms of non-oscillatory dynamics—1/f or other forms of coloured noise—are often discussed as something to be

filtered out. Crucially, this should not be taken to suggest that such brain activity is uninformative, as the previous empirical relations attest. Rather, this thesis centrally explores how brain oscillations coordinate (or, alternatively, offer a summary statistic of) masses of neuronal activity in the service of cognition—and under that goal, its distinct mechanisms should be targeted, and its relevant methodologies should be used.

1.4.3 Oscillatory dynamics

Spectral properties

Borrowing from physics, neuroscience has benefited from nomenclature used to denote different aspects of an oscillation. The first spectral property of interest is *frequency*, which refers to the number of cycles per second (Hz). Relatedly we can refer to the duration of a cycle, or its *period*, which is inversely proportional to frequency. Third, oscillations vary in amplitude, which indexes the maximum magnitude deflection of an oscillation. A fourth concept central to these Chapters is *phase*, which refers to instantaneous moments of a cycle, or more formally, the fraction of a cycle traversed after *t*. The phases across a cycle are usually quantified from 0 to 2π, or sometimes $-\pi \; and \; +\pi$. Each of these spectral properties offer ways to refer to aspects of the same phenomenon with potential empirical relations to molecular processes, neuronal information processing, cognition, and behaviour.

Oscillatory frequencies

In neuroscience, oscillations are categorized based on their membership to frequency bands. These bands are denoted by Greek letters, with delta (2-4 Hz), theta (4-7 Hz), alpha (7-13 Hz), beta (13-30 Hz), and gamma (over 40 Hz) as the most prominent examples. These categories are human-constructed—at minimum, the borders are fuzzy—but they do find grounding in nature (Cohen, 2021). For one, regions of the human brain settle into specific frequency bands during resting periods, consistently so across participants (Fig. 1.2; Capilla et al., 2022). Second, at least for alpha and beta, we observe a normal distribution of frequencies spanning aforementioned ranges, with the mode in the centre of these bands. This pattern holds between participants, and between cognitive tasks within participants (Haegens et al., 2014). Third, frequency bands go together with stereotypic underpinnings. For example, gamma oscillations are produced by fast-spiking interneurons and basket cells (Kopell et al., 2000; Whittington et al., 2000; Buzsáki & Wang, 2012), and modelling work suggests that alpha and beta oscillations emerge from separable generators (Jones et al., 2009; Kramer et al., 2008). Furthermore, on a functional level, activity at theta and gamma

frequencies carries feedforward signals, complemented by feedback-sending beta oscillations (Bastos et al., 2015). Thus, oscillatory frequency bands offer a useful and empirically justified vocabulary to study how cognition is realized by the brain.

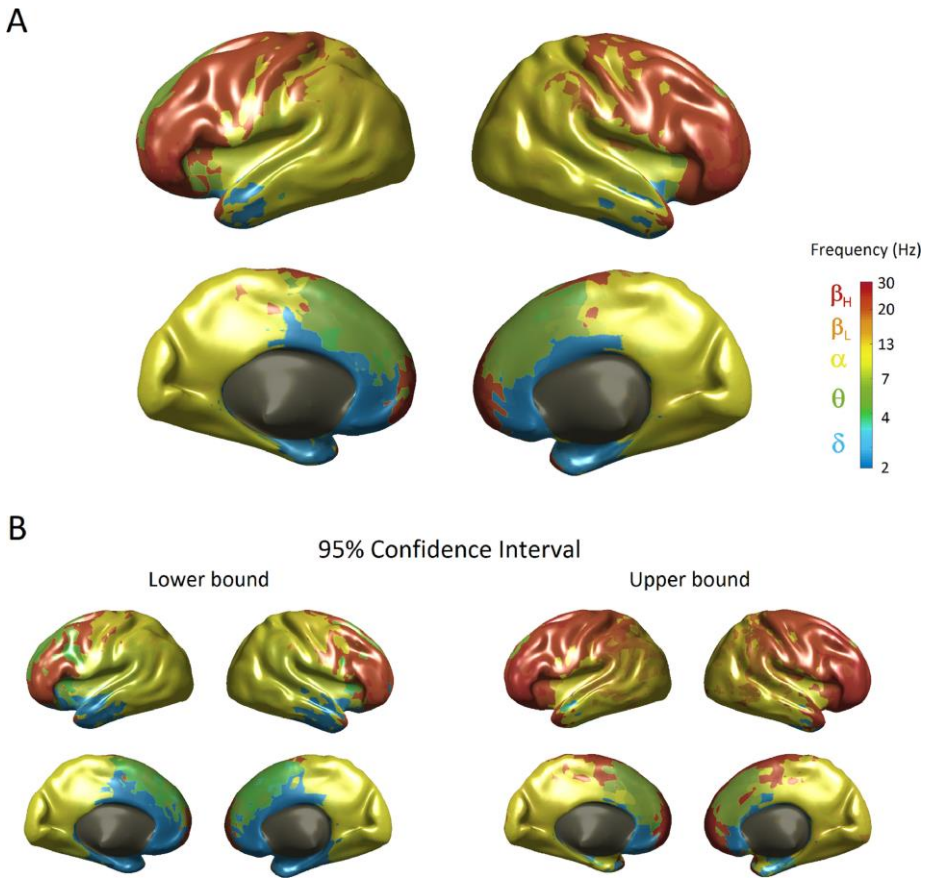

Figure 1.2. Natural frequencies of the human brain. (A) Spatial distribution of oscillations at the single-voxel level during rest. Typical frequency bands are colour coded and denoted by Greek letters on the colour bar. (B) A 95% confidence interval with lower and upper bounds derived using a bootstrapping technique. Figure 1.2 was borrowed from Capilla et al., 2022 (licensed under CC BY-NC-ND 4.0).

Spectral variation

The second point is that brain oscillations are themselves subject to dynamical fluctuations. Put differently, oscillations are not perfectly regular but instead vary along key spectral dimensions from one instance to the next. Such variation includes phase jumps and spontaneous resets, time-varying frequency modulations, dynamical shifts in amplitude, and interruption by sharp transients (Cole & Voytek, 2018; Rabinovich et al., 2008). As will be discussed, this picture of brain oscillations as containing a layer of non-linearity (with respect to Newtonian time) has consequences for neuroscientific practice and cognition itself. Specifically, if brain oscillations orchestrate information processing across neurons, then

their variability will cause changes to neural or behavioural patterns of interest. Or under the non-causal view that oscillations passively reflect information processing across neurons, tracking how oscillations unfold informs us about dynamical changes to the lower-level realizers of cognition and behaviour.

1.4.4 Determinants of temporal structure in brain activity

What physical factors underlie and shape brain dynamics? Neurobiological research suggests that factors at different levels of scale each leave their mark.

At the neuronal level, the distribution of ion types across segments of the neuron influences action potential patterning (Hutcheon & Yarom, 2000). Under certain ionic configurations, pristinely regular firing emerges at baseline, such as in the seminal case of neurons in the inferior olive of the medulla oblongata (Llinás & Yarom, 1981). In addition, the spatial distribution of ions across neuronal segments influences not only the baseline firing of neurons, but also their resonance—i.e., their rhythmic response profile to external stimulation (Llinás, 1988).

Furthermore, the activity of single neurons is dependent on how they are embedded in their local circuitry as well as the synaptic properties of cells in the circuit. Seminally, modelling work demonstrated that small circuits of mutually inhibiting neurons will, upon receiving an excitatory external drive, organically settle into a collective oscillatory regime (Matsuoka, 1985). This simplified example raised the possibility that recurrent inhibition in general produces oscillatory firing patterns. In line with this, subsequent empirical efforts have shown that reciprocally connected excitatory and inhibitory neurons instantiate a push-pull dynamic that naturally gives rise to rhythmic firing patterns on the neuronal level, and oscillations on the network level (Kopell et al., 2000; Börgers & Kopell, 2008; Buzsáki & Wang, 2012). Much of this work covers the emergence of gamma oscillations, but different frequencies emerge depending on the time constants of synaptic potentials and dendritic integration, as well as the conductance properties of feedback loops (Hutcheon & Yarom, 2000; Singer, 2018). Aside from these factors, there are increasingly complex arrangements of cell types and synaptic connections that produce distinct macroscopic network oscillations across the frequency spectrum (Womelsdorf et al., 2014).

Finally, properties described at the network level itself—i.e., macroscopic details above the circuit level—have their own relation to global activity patterns. Most characteristically, the size of a network influences the temporal structure of population activity over and beyond underlying motif (Lea-Carnall et al., 2016). For example, slow

oscillations in the delta and frequency range inhabit the largest networks of the brain, with small circuits and local ensembles recruiting fast frequencies in the gamma range (Buzsáki & Draguhn, 2004; Csicsvari et al., 2003; Steriade, 2001).

Taken together, fundamental neuroscience has found that factors at the level of neurons, circuits, and networks have interlocking effects that together determine the cacophony of neural activity. Importantly, insofar this neural symphony displays oscillatory structure, specific opportunities for information processing emerge.

1.4.5 Oscillatory dynamics and information processing

A fundamental property of neural oscillations is that they impose time windows for neuronal firing. Specifically, as oscillations fluctuate, they move between phases of low and high neuronal excitability, and this influences how cell ensembles in information-carrying circuits discharge over time. During low excitability phases, the membrane potential of neurons is reduced, requiring comparatively stronger excitatory post-synaptic potentials (EPSPs) from upstream ensembles to induce local action potentials (Singer, 2018). During such phases of functional inhibition, the combined input received from neuronal ensembles must produce relatively high levels of temporal and spatial summation for local firing thresholds to be reached. Conversely, at high excitability phases, the voltage difference between resting and threshold potentials is reduced, meaning less aggregate input is required for the induction of action potentials (Lakatos et al., 2007). In effect then, oscillations introduce temporal structure to an otherwise discordant brain.

From an information processing standpoint, the waxing and waning of neuronal excitability means that the exchange of impulses between up- and downstream ensembles becomes segmented into meaningful chunks (Buzsáki, 2010; Buzsáki & Draguhn, 2004). Indeed, the relative moments of silence and activity afforded by brain oscillations are reminiscent of Morse code and other communication systems that critically depend on boundaries to demarcate the start and end of encoded sequences.

On the network level, oscillations also establish functional communication channels between distant regions of the brain. When the neurons in two anatomically isolated regions fire synchronously at the same oscillatory phase, upstream action potentials during the excitable phase are more likely to elicit action potentials in downstream receiving areas because excitability levels will be high there also (Fries, 2005, 2015; Lisman & Jensen, 2013; Singer, 1999). The notion that phase coherence enhances the effective exchange of information across regions of the brain has given rise to fruitful theoretical pursuits. For

example, computational frameworks have been developed that posit the brain leverages oscillations through self-organizing principles to restrict communication to task-relevant brain regions, functionally inhibiting irrelevant and potentially interfering areas (Jahnke et al., 2014; Jensen & Mazaheri, 2010; Salinas & Sejnowski, 2001). In support of this, the allocation of covert attention to one hemifield increases alpha power in ipsilateral regions where task-irrelevant information is processed, inhibiting their activity levels (Thut et al., 2006; Worden et al., 2000; Händel et al., 2011; but see Jensen, 2023). With that said, an alternative explanation is that interregional synchronization, regardless of whether it is taken to reduce task-irrelevant computation or to send information onward, is merely the product of a region sending oscillatory patterns downstream through anatomical projections (Schneider et al., 2021). Nevertheless, with this critical note in mind, a picture emerges in which brain oscillations orchestrate information processing across the brain in the service of cognition at large, and as we will see, memory is a richly supported case in point.

1.5 Summary & looking ahead

To summarize the points made thus far, a preliminary intuition for the relevance of brain dynamics in cognitive neuroscience is that it offers a brain-centric coordinate system by which to understand how the brain implements cognition. Brain dynamics reflect continuously evolving excitability fluctuations which, in contrast to Newtonian time, are the brain's home court. Researchers characterize such dynamics by harnessing time-sensitive neuroimaging methods and a suite of mathematical approaches. What we learned as a result of these efforts is that brain activity displays stereotypic rhythms which unfold in natural frequency bands as dictated by factors at the neuronal, circuit, and network scale.

This raises the question of what all of this has to do with cognition. After all, this thesis submits that a science interested in the neural basis of cognition should incorporate internal dynamics of the brain into its inquiry, and so it must be established that these dynamics pertain to cognition in the first place. In the proceeding chapter, rather than shallowly touching on all cognitive functions and frequency bands, I will focus on the relation between the phase of theta oscillations and memory processes, which have a particularly well-established link (Chapter 2). This overview will serve as an illustrative starting point, with the remainder of this thesis intermittently branching out to other frequency bands and cognitive functions, mostly by referencing key studies and comprehensive overviews by others.

After a representative case has been made that oscillatory dynamics are relevant for studying the neural basis of cognition, I will then introduce the Brain Time Toolbox (Chapter 3). This part of the thesis fleshes out the importance of brain-intrinsic analysis, and spells out concretely how we might achieve this through algorithmic advances. In the penultimate chapter, I evaluate an alternative approach to accounting for brain dynamics (Chapter 4). Specifically, I outline an experiment that evaluates whether perturbing brain dynamics using visual stimulation regularizes relevant activity to enhance our study of memory representations. In this sense, while Chapter 3 covers the merit of weighing dynamics at the analysis end *after* the experiment is completed, Chapter 4 explores the possibility of factoring in brain dynamics as the experiment is ongoing. Finally, in Chapter 5 I collect and integrate insights across this body of work, discussing its implications and sketching a route forward.

Chapter 2: Theta phase and human memory

2.1 Introduction

2.1.1 Aims

The goal of this Chapter is to offer a comprehensive overview of the computational relevance of theta oscillations for memory processes in the human brain. My focus is on theta phase, and how its instantaneous excitability is leveraged by memory areas to enable information processing (for older reviews on theta phase, see Fell & Axmacher, 2011; Klimesch et al., 2008; Nyhus & Curran, 2010; for a recent review on theta power, see Herweg et al., 2020). Throughout the following paragraphs, I begin by tracing the origin of influential hypotheses to modelling research and empirical studies on the rodent brain. Then, once a scientific context has been established, I turn to the central aim and ask to what extent the ideas generalize to the human brain.

The structure of this Chapter unfolds as follow. First, I make a case for the existence and importance of theta oscillations in rodent and human memory areas. I briefly consider whether theta is homologous between the species to see if it is warranted to leverage rodent evidence to inspire human research. Then, I outline basic evidence for the notion that theta oscillations realize a phase-based coding scheme, which dynamically updates with goal-directed behaviour. After that, I discuss two ways in which a theta phase code empowers memory processing: (1) it compresses event sequences to assist synaptic plasticity, and (2) it provides a neurally accessible scheme of the relative order of events and our position within it. Moving on from the phase code, I argue theta phase also implements a switch between encoding and retrieval processes. This efficiently makes available circuitry multipurpose, and it paves the way for learning algorithms that dynamically update memory representations. Finally, I argue that theta-based phase synchronization across distant regions makes it possible for memories to become integrated locally, and for neocortical patterns to become reinstated globally.

2.1.2 The hippocampal theta rhythm in rodents and humans

Theta oscillations in rodents

In the rodent brain, theta oscillations between ~6 and 10 Hz dominate the frequency spectrum (Vanderwolf, 1969) of hippocampal activity—a brain region deeply implicated in memory processing (Bird & Burgess, 2008; Broadbent et al., 2004). Theta oscillations show up robustly when rodents explore a new environment, and display frequency and power-

specific changes with running speed (Kennedy et al., 2022; McFarland et al., 1975). Beyond a movement signal, hippocampal theta has proven critical for the integrity of memory processes. Indeed, disrupting theta oscillations in rodents pharmacologically or using lesions has detrimental effects on memory performance (Buzsáki, 2005; Givens & Olton, 1994; McNaughton et al., 2006; Petersen & Buzsáki, 2020; Winson, 1978).

How are theta oscillations produced in the rodent brain? It is helpful to distinguish the mechanisms that orchestrate rhythmic structure from those that produce the electric fields picked up by electrodes (Buzsáki, 2002). On the former, theta's patterning results in part from circuit architectures (Cutsuridis & Hasselmo, 2012) and inputs from the medial septum (Petersen & Buzsáki, 2020; Petsche et al., 1962; Vertes & Kocsis, 1997). The electric fields on the other hand are mostly a product of synaptic currents and to a lesser extent action potentials (Einevoll et al., 2013; Kamondi et al., 1998; Mazzoni et al., 2015; Reimann et al., 2013), with the exact proportions for future work to uncover (Buzsáki et al., 2012).

Theta oscillations in humans

In humans, theta oscillations have been widely implicated in the encoding (Joensen et al., 2023), consolidation (Marshall et al., 2011), and retrieval (Herweg et al., 2020) of information. In general support of this, successfully remembered memory items show differences in theta power from forgotten items (Backus et al., 2016; Kota et al., 2020; Ter Wal et al., 2021; Hanslmayr & Staudigl, 2014), and causal enhancements of theta synchronization improve performance on memory tasks (see Hanslmayr et al., 2019 for an overview).

There are three ways in which theta in the human hippocampus differs from its rodent counterpart (for overviews, see Foo & Bohbot, 2020; Jacobs, 2014). First, the rhythm is overall less prominent in humans, showing up less reliably across measurements, and lasting fewer cycles when it does (Watrous, Lee, et al., 2013). Second, theta emerges at slower frequencies—around 1 to 4 Hz (Kahana et al., 2001; Lega et al., 2012; Mormann et al., 2005; Watrous et al., 2011)—compared to the 6 to 10 Hz fluctuations in rodents (Vanderwolf, 1969). Third, rather than displaying a uniform frequency distribution, the human hippocampus seems to carry two functionally distinct rhythms (Lega et al., 2012); a slow signal dominating anterior regions, and a faster rhythm clustering in posterior regions (Goyal et al., 2020; Kota et al., 2020). Thus, in human hippocampal areas there seems to be a band residing at lower frequencies, though with a higher frequency component in addition to that.

Due to the lack of opportunities for invasive measurements and interventions, substantially less is known about the generating mechanisms of human theta oscillations. Indeed, given the lack of delicate causal control it is hard to establish whether theta is generated by mechanisms within the hippocampus and septum as with rodents, and an alternative hypothesis remains that the patterns are induced by neocortical inputs (Herweg et al., 2020; Box 3).

What explains interspecies discrepancies?

At first glance, these rodent-to-human discrepancies in hippocampal theta suggest that we are dealing with non-homologous neural phenomena instantiated by distinct mechanisms. However, a number of factors could explain away putative differences between the species.

First, electrode implantation in rodents is carried out for scientific reasons alone, whereas electrode implantation in humans is performed for medical reasons—such as to identify the source of epileptic seizures. This confers more degrees of freedom in rodent electrophysiology, making it is possible to record from loci where theta is most striking. This could partially or fully explain interspecies differences in the prominence and reliability of theta.

Second, whereas rodents typically move freely during recordings, human patients are for the most part recorded at the bedside. Given that locomotion modulates theta power (Terrazas et al., 2005) and frequency (Kennedy et al., 2022; McFarland et al., 1975), differences in mobility could account for interspecies variation. Indeed, in exceptional circumstances where human LFP is recorded during movement—such as during a virtual reality task (Bush et al., 2017; Ekstrom et al., 2005; Goyal et al., 2020) or when a mobile intracranial setup is employed (M. Aghajan et al., 2017; Stangl et al., 2021, 2023)—theta oscillations show increases in power. This suggests that discrepancies in theta robustness may be explained by a mobility confound. With that said, concerning other differences, the separation of high and low theta peaks in the human hippocampus seems to persist during virtual locomotion (Bush et al., 2017; Vivekananda et al., 2021), possibly highlighting one true difference.

Third, variation in brain size rather than distinct mechanisms could explain inter-species discrepancies in the dominant theta frequency. In support of this, theta oscillations are slower as a function of brain size across the animal kingdom (Buzsáki et al., 2013). And within the same species, dominant frequencies slow down with network size (Chapter 1; Section 1.4.4). To speculate, perhaps the larger human hippocampus means longer axons are

in place to connect information across the module, thus increasing conduction delays and slowing down the dominant frequency as a result.

Together, while more research is needed, it is highly plausible that theta oscillations are evolutionarily conserved across mammals, with interspecies variation in scientific methodology and brain size explaining away differences in theta frequency and power. One exception seems to be the existence of slow and fast theta components, which appear in humans from distinct hippocampal regions. Based on this, I will assume in the remainder of this chapter that findings on theta phase in rodents offer at minimum a jumping off point for the investigation of human memory processing. With that assumption in mind, I next turn to theta phase, the codes it embeds, and the computational benefits it affords.

2.2 Theta phase

2.2.1 Phase code

Rodent phase code

When theta oscillations—which are inhibitory in nature (Vertes & Kocsis, 1997)—are at their maximally inhibitory phase, only neuronal ensembles that have high pre-existing levels of excitation will be able to withstand global inhibition and trigger action potentials. Then, as inhibition ramps down, ensembles less strongly activated by the task will be able to withstand global inhibition, activating sequentially as a function of their relative input levels (Jensen & Lisman, 1996; Mehta et al., 2002; see Burgess et al., 2007 for a related mechanistic account). This instantiates a *phase code*, comprising a systematic activation of memory representations across the theta cycle through self-organizational principles.

Research on rodents has amassed evidence for the existence of a theta phase code (Dragoi & Buzsáki, 2006; Foster & Wilson, 2007; Wikenheiser & Redish, 2015; Zheng et al., 2021). Seminally, place cells which encode spatial locations fire at distinct theta phases as an animal moves across a previously experienced track, with these cells activating in a relative order matching the order of represented locations across the path (O'Keefe & Recce, 1993; Skaggs et al., 1996). To enable the phase code, theta oscillations synergize with gamma oscillations, which recruit specific information-coding ensembles (including place cells). Through such *theta-gamma coupling*, a striking nested structure emerges in which the overarching theta cycle becomes parcelled up by a concatenation of gamma subcycles (Bragin et al., 1995). In philosophical terms, we might say that theta introduces a vehicle that bears the representational content, with such content inserted through gamma's activation of ensembles (see Martínez & Artiga, 2023; Murphy, 2024 for relevant accounts).

Human phase code

While the most compelling evidence for theta phase codes stems from rodent work, a growing body of studies strongly suggests humans carry a similar code to support the brain's ability to encode, maintain, and retrieve information. Here, I cover each function in turn.

First, as participants encode sequences of images, brain regions that represent each image display gamma peaks at distinct theta phases in the MEG signal, with a relative order that recapitulates the ground truth positional sequence (Heusser et al., 2016). These findings generalize to the spiking behaviour of information-coding ensembles. In Reddy et al., 2021, neurons in the human temporal lobe were recorded as participants encoded sequences of images. They found that during learning, neurons part of image-representing ensembles fired in a sequence-preserving fashion across the theta cycle.

Similar findings were found in a study where participants carried out the Sternberg task, which requires the active maintenance of information in working memory. Analyses of simultaneously acquired intracranial recordings showed that letter-specific sites in the hippocampus displayed gamma power increases at distinct phases of high theta (or low alpha) frequencies (Bahramisharif et al., 2018) with dynamics that retained the original stimulus order. In another experiment, stimulus-selective neurons in medio-temporal regions fired at specific theta phases during sequence maintenance—although in this case, the reactivation patterns did not follow stimulus presentation order (Liebe et al., 2022).

Finally, the theta phase code has been linked to human memory retrieval. In a recent study, participants learned associations between visual cues and locations in a virtual environment (Kunz et al., 2019). The authors found that each of eight cue representations were reactivated at distinct phases of the hippocampal theta cycle (but not in keeping with the original order). In further support, similar experiments revealed that spatial locations themselves—not just memory cues—were coded across separate phases of the theta cycle in the human hippocampus (Qasim et al., 2021; Watrous et al., 2018).

Together, these studies support the notion that memory representations activate at distinct theta phases to instantiate a coding scheme. Interestingly, the fact that multiple kinds of representations (retrieval cues, spatial locations, letters, and images) and memory functions (encoding, maintenance, and retrieval) are involved in the theta phase code suggests we may be tapping into a general mechanism of the memorizing brain (for further discussions, see Griffiths & Jensen, 2023; Lisman, 2005; Lisman & Buzsáki, 2008; Lisman & Jensen, 2013; Yamaguchi et al., 2007).

Phase precession

Research has shown that the theta phase code, at least in rodents, is anything but stationary over time. Rather, during a phenomenon called *phase precession*, information-coding cells fire at progressively earlier phases as a function of the organism's position in the overall sequence (Dragoi & Buzsáki, 2006; Mehta et al., 2002; O'Keefe & Recce, 1993; Skaggs et al., 1996; Terada et al., 2017). This finding has been mostly demonstrated in the context of the navigating animal, during which place cells fire progressively earlier as a function of how much headway the animal makes across the track (Jensen & Lisman, 1996).

Interestingly, this finding has recently been extended to humans. First, in the previously mentioned study by Qasim et al., 2021, neurons part of the ensemble representing spatial locations fired during progressively earlier phases as participants virtually moved through that location. Similarly, neurons tuned to behaviourally relevant goal states showed phase precession during virtual movement toward the relevant goal. And second, in the study by Reddy et al., 2021, neurons part of image-coding ensembles shifted their firing to earlier phases as a function of their serial distance to currently presented images. To our knowledge, these are the only two demonstrations of human phase precession, and further work is needed to see if these results replicate and generalize. For further reading on computational and rodent evidence for phase precession, see Jaramillo & Kempter, 2017; Lisman, 2005; Malhotra et al., 2012; Maurer & McNaughton, 2007. Next, I will take this evidence for the existence of phase codes and phase precession in humans and explore their benefits to information processing.

2.2.2 How theta phase codes support memory

Neural compression and synaptic plasticity

As rodents, humans, and other animals move through the world, they experience connected events that must be remembered to generate adaptive behaviour. Such event sequences typically unfold on the order of seconds, minutes, and longer still. Yet the synaptic plasticity mechanisms that strengthen and weaken the connection between groups of neurons that encode such events depend on Hebbian firing rules at play on the order of milliseconds (Bi & Poo, 1998, 2001). This introduces a conceptual tension that has been used to criticize Hebbian learning and the idea of synaptic memory storage in general (Gallistel & Matzel, 2013).

Theta phase codes could partially resolve this temporal paradox by collapsing behavioural timescales into neural timescales (Jaramillo & Kempter, 2017; Reifenstein et al., 2021; Skaggs et al., 1996; Wang et al., 2023). Specifically, as memory networks recruit theta-gamma coupled oscillations, the activation of represented sequences of events becomes compressed to the period of a theta cycle, which lasts roughly 125 to 250 milliseconds. These ranges are compatible with spike-timing dependent plasticity (STDP) rules established in rodents (Bi & Poo, 1998; Markram et al., 1997) and humans (Mansvelder et al., 2019), which dictate the order and timing with which ensembles need to fire to induce a strengthening or weakening of synaptic connections (Abbott & Nelson, 2000).

Importantly, beyond the theta phase code, sharp-wave ripples could offer an alternative or additional way for the brain to warp external event sequences to endemic timescales. Indeed, in rodents these brief bursts of activity also recapitulate events in compressed formats (Buzsáki, 2015; Nádasdy et al., 1999), and they figure prominently during memory consolidation and retrieval (Fernández-Ruiz et al., 2019; Jadhav et al., 2012; Ólafsdóttir et al., 2018)—especially during sleep (Girardeau et al., 2009; Ji & Wilson, 2007). In humans, sharp-wave ripples (or at least replay bursts) have also been observed across contexts, including restful periods (Higgins et al., 2021), transfer learning (Y. Liu et al., 2019), and memory recollection (Michelmann et al., 2019; Y. Norman et al., 2019).

To summarize this section then, it appears theta phase codes compress the neural activation of event sequences, making it possible for STDP-based plasticity mechanisms to flexibly modify associations between neural representations. With that said, sharp-wave ripples make it possible in their own right to compress sequences into neural timescales, introducing an additional or alternative resolution to the problem of mismatching timescales.

Sequence and positional information

To achieve goal-directed behaviour, animals must learn states of the world and construct internal models of how these states relate to each other (Pezzulo et al., 2014). The functional dissociation between these processes is supported by work in rodents, with optogenetic interference of place cell sequencing disrupting the neural prediction of state transitions without affecting event-specific information such as the spatial tuning of place cells (C. Liu et al., 2023). Theta phase codes are well-geared to assist in the build-up of event sequence representations. For one, since theta oscillations ride on top of many clusters of neurons at once, its cycles offer a neurally accessible reference point by which sequence representations become widely interpretable. Specifically, some event representations activate late and

others early within the overarching theta clock, and this relays details about the relative distance between serially connected events to downstream readers. Theta phase precession adds to the scheme by introducing another degree of freedom that can be used to dynamically encode the animal's position within the sequence. Specifically, as the relation between the overarching theta cycle and spiking behaviour of information-coding ensembles steadily shifts as a function of task progression, a compact code manifests that can be accessed by connected areas.

These ideas are based on an array of modelling and empirical work in rodents (Burgess et al., 2007; Canavier, 2015; Dragoi & Buzsáki, 2006; Hasselmo, 2012; Jensen, 2001; Lisman & Buzsáki, 2008; Lisman & Jensen, 2013). One way to test these hypotheses is by exploring the relative contribution of theta phase-locked firing versus other neural variables toward predictions of an animal's current location in a memorized sequence (Jensen & Lisman, 1996; Lisman & Buzsáki, 2008). The reasoning here is that if it is correct that theta phase sets a grounding template for neural ensembles to parse event and position information by, then a decoder fed the same information should be able to infer event and position information.

Promisingly, when including theta phase beyond phase-agnostic spike rates to decoders, position readouts are improved by more than 43% (Jensen & Lisman, 2000) or even 80%, reaching centimetre-level precision (Reifenstein et al., 2012). While such improvements may indicate that phase coupling between spikes and the overarching theta cycle confers positional information, a caveat remains. Namely, a longstanding question is whether our ability to use neural variables as information justifies the inference that such variables are legible and informative for the human brain itself (for discussions on the scope and limits of decoding, see de-Wit et al., 2016; Ritchie et al., 2019; van Bree, 2023). In light of this debate, I invite the reader to decide for themselves how much evidential weight they wish to grant to these results.

In terms of causal work, the discussed findings that theta disruptions worsen memory performance further suggests computational relevance of the dynamically updating theta phase (Buzsáki, 2005; Givens & Olton, 1994; McNaughton et al., 2006; Petersen & Buzsáki, 2020; Winson, 1978)—though it needs to establish whether such impairments are due to a disruption of theta phase codes or due to other neural processes promoted by theta oscillations. Ambitious research could try to disentangle theta oscillations from spike-field coupling, for example through pharmacological intervention (Douchamps et al., 2013) or optogenetic manipulation (Strüber et al., 2022).

Finally, to establish whether the theta phase code confers computational utility to the human brain, it could similarly be explored what the relative contribution is between spike-field coupling and other neural variables in predicting sequence position across memory tasks (subject to the previous considerations). This question is actively being pursued (e.g., Watrous et al., 2018), with advancements in intracranial tools inviting a more holistic mapping (Ye et al., 2023). More basically, some of the human research in Section 2.2.1 could be taken as preliminary evidence for not only the existence of a human theta phase code itself, but also its computation-enhancing role. Finally, one way to evaluate the computational role of the theta phase code is to test whether momentary aberrations to the theta phase code—for example, specific goal locations incorrectly activating too late or too early in the scheme—produce expected behavioural errors.

2.2.3 Mode switching

We have established that rodent and human brains represent information across the theta cycle through ensemble-recruiting gamma waves. We have also seen that the sweep of event representations that results from this moves progressively earlier during goal-directed behaviour. It appears the purpose of this scheme is to make information about event sequences and an animal's current position accessible to other areas for subsequent processing. As I will discuss next, separate from this, the phase of theta oscillations may introduce a circuit processing switch that makes it possible for the brain to flexibly alternate between encoding and retrieval.

Rodent evidence

The hypothesis for a theta phase-based switch goes back to the seminal discovery that stimulation to hippocampal region CA1 results in long-term potentiation (LTP) when it is applied during one phase, and in long-term depression (LTD) when it is applied during the opposite phase (Hölscher et al., 1997; Huerta & Lisman, 1995; Hyman et al., 2003; Pavlides et al., 1988). These findings inspired a model which proposed that during the LTD-conducive phase, hippocampal dynamics show weak synaptic transmission from the entorhinal cortex such as to gear neural systems toward the retrieval of old information. Conversely, during the LTP-conducive phase, the model takes entorhinal input to be strong in order to promote the encoding of new information (Hasselmo et al., 2002). Subsequent research confirmed the notion that the phase of hippocampal theta oscillations initiates a

switch in network processing (Colgin et al., 2009; Colgin & Moser, 2010; Cutsuridis & Hasselmo, 2012; Hasselmo & Stern, 2014; Kunec et al., 2005; Manns et al., 2007).

Crucially, it has been found that the theta phase switch exerts effects on the cognitive-behavioural level. In environments where encoding predominates, such as in novel locations, spikes organically cluster to theta peaks in CA1. Conversely, in familiar environments, where retrieval predominates, spikes tend to coincide with theta troughs (Douchamps et al., 2013). Furthermore, optogenetic inhibition of CA1 during theta peaks produced deficits selectively during encoding stages of a memory task, with stimulation at theta troughs conversely impairing performance during retrieval stages, demonstrating a double dissociation (with compelling effect sizes; Siegle & Wilson, 2014). Together, these studies strongly suggest that the phase of theta oscillations in the rodent hippocampus initiates a switch between encoding and retrieval by cyclically biassing the routing of information towards pathways that subserve one or the other function.

Human evidence

Subsequent research suggests that these findings carry over to the human brain. First, theta oscillations in medial temporal regions showed significant phase differences between the encoding and retrieval of letters in a working memory task (Rizzuto et al., 2006). These findings generalize to long-term memory contexts, where the encoding and reinstatement of specific items trends to opposite hippocampal theta phases (Pacheco Estefan et al., 2021). Similarly, ERPs arising from memory cues that prompted the encoding and retrieval of information displayed opposing phase relations (Ter Wal et al., 2021). Moreover, in this last study, a marked theta rhythm emerged in the cross-trial distribution of reaction times following retrieval cue onset. This is consistent with the phase switch hypothesis, which predicts that retrieval processes wax and wane at theta frequencies.

On the level of neural representations, it has been found that the EEG-based decodability of memory items fluctuates at theta rates, importantly at opposite phases during encoding and retrieval (Kerrén et al., 2018). Finally, high-resolution fMRI suggests that encoding and retrieval initiate distinct functional connectivity patterns across hippocampal and midbrain areas (K. Duncan et al., 2014), though temporally sensitive techniques are required to test if this is theta-locked. Together, these results strongly indicate that a theta switch mechanism exists in humans. However, further inquiry is needed to establish whether the observed phase-to-cognition relations are causal, as they are in the rodent brain.

Computational utility

How might a theta phase switch support memory? One promising answer is that it prevents neural circuits from conflating internally generated and externally received information. For context, while encoding and retrieval in humans are partially subserved by different regions of the hippocampus (Eldridge et al., 2005; Small et al., 2001; Zeineh et al., 2003), they also recruit overlapping circuitry (Greicius et al., 2003). By delegating encoding and retrieval to distinct theta phases, a functional separation emerges in time that makes it possible for networks generally equipped to process information to operate over both encoded and retrieved events without cross-interference. Moreover, a phasic separation of processing regimes is likely energetically cheap, considering that theta oscillations are self-sustaining processes (Giovannini et al., 2017), meaning they require little drive to continue once they are active. In short, a theta switch offers a metabolically inexpensive way to make available brain circuitry multipurpose.

More broadly, dynamic mode-switching between processing states could facilitate learning in the brain (Honey et al., 2018). As the brain cyclically processes perceptual inputs (during encoding) and internally generated predictions (during retrieval), such representations can be contrasted against each other. Then, prediction errors can be used to update memory representations (see Sauseng et al., 2015 for a related idea). In a similar vein, a theta switch might offer the backbone for learning algorithms where target memory representations are strengthened during one oscillatory phase, followed by a weakening of competitor memories during the opposing phase (K. Norman et al., 2006). In direct support of this idea, a recent MEG study found that target and competing memories become processed at distinct theta phases following repeated recall (Kerrén et al., 2022).

2.2.4 Interareal synchronization

Most of the ideas explicated up until this point suggest that the phase of theta oscillations empowers local information processing within the hippocampus and regions in its vicinity. However, for this to happen, such memory modules need to have access to information housed across the brain. During learning for example, multimodal perceptual inputs, error signals, goal states, and other elements need to be integrated before a holistic memory can be formed (see also Singer, 2007). And as widely maintained across theories, retrieval involves the (re-)activation of relevant neural patterns distributed across neocortical networks (Battaglia et al., 2011; Buzsáki, 1996; Eichenbaum, 2000; McClelland et al., 1995;

Preston & Eichenbaum, 2013; Rolls, 2013; Sekeres et al., 2018; Squire et al., 2015; Teyler & DiScenna, 1985).

The phase synchronization of theta oscillations between distant regions likely plays an important role in realizing these ends (Fell & Axmacher, 2011; Klimesch et al., 2008; Nyhus & Curran, 2010). Specifically, by aligning excitable phases of distant areas, theta oscillations initiate functional communication routes that support the readout and reinstatement of relevant representations (see also Chapter 1, Section 1.4.5). Interestingly, compared with the previous relevancies of theta phase, most evidence for the importance of phase synchronization comes from research in humans—and so I turn to this question directly.

A primary line of work supporting the notion that theta phase synchronization benefits binding and reinstatement is the highly replicable finding that memory processes coincide with phase connectivity changes at theta frequencies. Namely, during encoding, hippocampal theta waves synchronize with neocortical regions, and their consistent phase relation predicts memory performance across tasks, such as during the integration of new and old memories (Backus et al., 2016), the encoding of unexpected items (Gruber et al., 2018), and during word list learning (Solomon et al., 2019). Similar results have been obtained for retrieval, with cues that prompt the recollection of spatial information resulting in increases in theta phase coupling between medial temporal regions and prefrontal areas (Kaplan et al., 2014), as well as across large networks of the neocortex generally (Watrous, Tandon, et al., 2013). Indeed, I emphasize that the communication-enhancing function of theta phase is not specific to the hippocampus, with the observed effects generalizing across the human brain (Weiss et al., 2000; Weiss & Rappelsberger, 2000).

This raises the question of whether correlations between theta phase synchronization and memory reflect a causally relevant mechanism. Recent evidence that leverages oscillatory entrainment paradigms suggests that the answer may be yes. In one study, participants learned associations between rhythmically fluctuating audio and visual clips, which is a manipulation that can synchronize brain oscillations (Clouter et al., 2017). Interestingly, the synchronous presentation of the stimuli resulted in better memory performance than asynchronous presentation, but only when the stimuli had luminance fluctuations at theta frequencies (the effects did not manifest at delta and alpha rates). Subsequent research confirmed these findings, with phase differences between visual and auditory regions reliably predicting memory performance (Wang et al., 2018). Furthermore, non-invasive brain stimulation can be used to address this question (Hanslmayr et al., 2019).

Importantly, in brain stimulation work it is important to target regions simultaneously to attain full control over their phase relation.

2.3 Summary & looking ahead

Let us take a step back and evaluate how the findings covered in this Chapter contribute to the overall claims of this manuscript. As a start, these are the five most important assertions of this Thesis:

1) Scientists study evolving neural patterns to investigate how cognition is implemented by the brain.

2) Oscillatory dynamics strongly influence or covary with the evolution of neural patterns of cognition.

3) As such, oscillatory dynamics offer a reference point or anchor by which the study of neural patterns can be improved.

4) We can adopt this reference point algorithmically by transforming recorded brain data in concordance with coordinating oscillations of interest.

5) Alternatively, we can adopt it by experimentally regularizing oscillatory dynamics during data acquisition.

The purpose of this Chapter has been to justify claim (2). In support of this, theta oscillations are deeply connected with memory processing. As we have seen, theta waves instantiate an evolving phase code, a phasic processing switch, and functional communication channels. Together, these confer computational benefits: they promote neural access to event order and position information, they achieve sequence compression for synaptic learning, they support multiplexed computations within neural circuits, and they promote the integration and reinstatement of memory patterns. As a result, systematic changes emerge in the neurocognitive patterns that scientists seek to capture to construct scientific explanations. I maintain that the symbiosis between brain oscillations and computational processes naturally invites an integration of spectral information into our investigations, and the remainder of this thesis is about exploring specific solutions toward this end. In the next Chapter, I will evaluate an algorithmic technique that can be used to bring electrophysiology data toward key dynamics (Chapter 3). Its contents establish points (3) and (4) in the inference train outlined above, and—to a lesser extent—points (1) and (2).

Chapter 3: Aligning brain dynamics with the Brain Time Toolbox

This chapter contains material from van Bree et al., 2022:

van Bree, S., Melcón, M., Kolibius, L. D., Kerrén, C., Wimber, M., & Hanslmayr, S. (2022). The brain time toolbox, a software library to retune electrophysiology data to brain dynamics. *Nature Human Behaviour*, *6*(10), 1430–1439. https://doi.org/10.1038/s41562-022-01386-8

3.1 Aims

This Chapter opens by concretizing the abstract problem identified in Chapter 1—namely that researchers risk missing informative neural patterns by projecting external worldly variables onto a brain that has no direct access to them. To make this problem more tangible, I elaborate on the notion of time in neuroscientific methodology, outlining why it is a thorny concept. Specifically, I highlight the problems that come with adopting *clock time* as a reference point in neural analysis rather than brain-centric measures such as oscillatory dynamics, the latter of which I shorthand with the term *brain time*. Importantly, clock time is similar to the concept of Newtonian time introduced in Chapter 1, but with the added connotation of timekeeping and measurement. Clock time refers to milliseconds, seconds, minutes, or any other unit that quantifies a magnitude order of Newtonian time.

After expanding the intuition, I claim that brain time is more appropriate because, as we have seen in Chapter 2, it relates intrinsically to the unfolding of neural patterns of cognition. I specify how clock and brain time are in tension with each other, and what we might expect to happen if we do not internalize their differences in our research practices. Then, I introduce the Brain Time Toolbox, a software library that retunes electrophysiology data in line with oscillations that orchestrate such neurocognitive patterns. The toolbox overcomes mismatches between clock time and brain dynamics by warping the data based on the temporal structure of coordinating oscillations. This enforces oscillatory cycles as the data's new time axis, which I demonstrate can be used to detect activity patterns.

3.2 Introduction

Everyday tasks involve a plethora of cognitive functions that operate dynamically in tandem. Something as mundane as taking notes during a meeting or battling your friend in a video game requires attention, motor activity, perception, memory and decision-making, each evolving over time. How does the brain achieve dynamic cognition? To answer this question, neuroscientists closely study how brain activity unfolds from one moment to the next using temporally precise neuroimaging methods. These include electroencephalography (EEG), magnetoencephalography (MEG) and single and multi-unit recordings—grouped together under the term electrophysiology.

3.2.1 Seconds are foreign to the brain

In a typical electrophysiology study, neuroscientists first probe cognition by introducing an experimental manipulation. For example, an attention researcher might introduce a set of moving dots. Then, to understand cognition in the brain, they perform a series of analyses on the recorded data. They might study changes in scalp topography over a second of data, apply machine learning to characterize how the representation of the dots evolves or perform any other time-dependent analysis.

Critically, from the raw output of neuroimaging devices to the analysis of recorded brain signals, time is operationalized as clock time—sequences of milliseconds. We claim that clock time, with all its benefits for human affairs, is generally inappropriate for neuroscience. This is because clock time is defined by us and for us, on the basis of how long it takes for Earth to rotate its axis. The brain itself, however, uses its own regime of time, dictated by its own dynamics.

As such, the brain is indifferent to how many milliseconds, seconds, minutes or hours have passed unless it is expressly relevant for specific behaviour, such as maintaining circadian rhythms (Antle & Silver, 2005) tracking a time-dependent reward (MacDonald et al., 2011), . Instead, the brain is concerned with coordinating communication between cells in a delicate time-sensitive manner, such as sending information at one moment and receiving feedback signals at the next. Hence, the brain's intrinsic time format—brain time—is dictated by the internal processes that clock brain activity (for an explanation of key terms, see Table 3.1).

Term	Description
Antiphase	Two oscillations are in antiphase when they stand in opposite phase relation to each other—for example, when the peak of one oscillation co-occurs with the other's trough.
Brain oscillations	Rhythmic fluctuations of brain activity generated by populations of cells.
Brain time	Time as sequences of cycles of a coordinating brain oscillation.
Brain time warping	Algorithm that uses dynamic time warping to transform electrophysiology data in accordance with brain time dynamics.
Brain time toolbox	Software library that implements brain time warping and tests its effects.
Clock time	Time as sequences of seconds.
Dynamic time warping (DTW)	Algorithm that can measure the similarity between signals and minimize their difference.
Frequency	Number of cycles per time window (typically a second).
Linear discriminant analysis (LDA)	Machine learning method that maximizes the separability between two classes of data by applying linear transformations to it.
Local field potential (LFP)	The electric potential recorded from extracellular space around cells.
Neural signature	Brain activity that systematically correlates with, in the present context, a cognitive process.
Periodicity	Fluctuating patterns of a neural signature.
Phase	Metric to indicate the specific point in the cycle of an oscillation. Two oscillations are in phase when (for example) their peaks align.
Phase precession	Phenomenon where place cells fire at progressively earlier phases of theta oscillations as an animal moves across a trajectory.
Temporal generalization matrix (TGM)	Representation of how a classifier trained to separate classes of data on one timepoint performs on other timepoints. When a classifier generalizes, it indicates that the neural signature remains stable.
Warping path	Representation obtained from DTW that shows how two signals need to be resampled to minimize their difference.
Warping source	Data structure containing potential coordinating brain oscillations used for brain time warping.

Table 3.1. Glossary of key terms used in this Chapter.

3.2.2 Cycles as the brain's native unit

How is brain activity organized? A defining feature of the brain is that its activity waxes and wanes (Llinás, 1988), pointing to a central role of brain oscillations. Brain oscillations are well-geared to structure brain activity. For one, each cycle of an oscillation contains a

window of excitability where cells are more likely to fire (Buzsáki & Draguhn, 2004; Engel et al., 2001). Moreover, oscillations vary in their frequency, meaning that the excitability windows vary in duration. The functional role of oscillations has been shown across a wide array of cognitive functions, including attention (Capotosto et al., 2009; Jensen & Mazaheri, 2010; Klimesch, 2012), perception (auditory; Lakatos et al., 2005; Luo & Poeppel, 201, visual; Busch et al., 2009; Romei et al., 2010 and tactile; Ai & Ro, 2013; Ruzzoli & Soto-Faraco, 2014), action (Joundi et al., 2012; Nowak et al., 2018), memory (Hanslmayr et al., 2019; Hasselmo et al., 2002; Kerrén et al., 2018) and decision-making (Jacobs et al., 2006; Polanía et al., 2015). Together, this situates brain oscillations as the brain's clocking mechanism, clustering brain activity in flexible ways to organize dynamic cognition. The brain's base units of time then, are the cycles of oscillations that coordinate neural firing, not the milliseconds with which we format our data.

3.2.3 Clock and brain time are usually out of tune

Why does it matter that we use a foreign time format? When neuroscientists study dynamic cognition, they repeat measurements across trials, resetting their stopwatch at the start of each. However, some oscillations do not reset (Jansen et al., 2003; Mazaheri & Jensen, 2006). Even when most do, oscillations evolve continuously in frequency and show jumps in phase (Fig. 3.1). Thus, besides a potential mismatch between clock and brain time from the get-go caused by variable starting phases, the disharmony between the dimensions accumulates due to frequency drift and phase jumps. These are prime examples of eccentricities in brain dynamics (and there are more; Cole & Voytek, 2017). Their presence makes clock time an ill-suited format to study temporal patterns of dynamic cognitive function—it distorts how the brain itself carries information forward in time.

To demonstrate this point, take again the case of spatial attention. Studies show that alpha oscillations (8–12 Hz) in parietal regions orchestrate the dynamics of spatial attention (Capotosto et al., 2009; Sauseng et al., 2005). If these oscillations vary in their starting phase across trials, then the neural patterns of spatial attention will vary along with it. Likewise, if the oscillations slow down in frequency, the patterns slow down too. If a researcher is interested in, say, decoding the locus of covert attention in the visual field over time, it would muddy the waters to do so in clock time, ticking away with its equal periods. The slowing down of alpha oscillations means brain time falls behind relative to clock time, so analysing the data in its default format yields a sped-up readout of attention's true pattern. Instead, we argue that the dynamics of clocking oscillations should heavily inform data analysis. As a

general mantra, the optimal approach to analyse the brain, like any other system, is with recourse to its own dynamics—from inside out (Buzsáki, 2019; Scharnowski et al., 2013; Fig. 3.2).

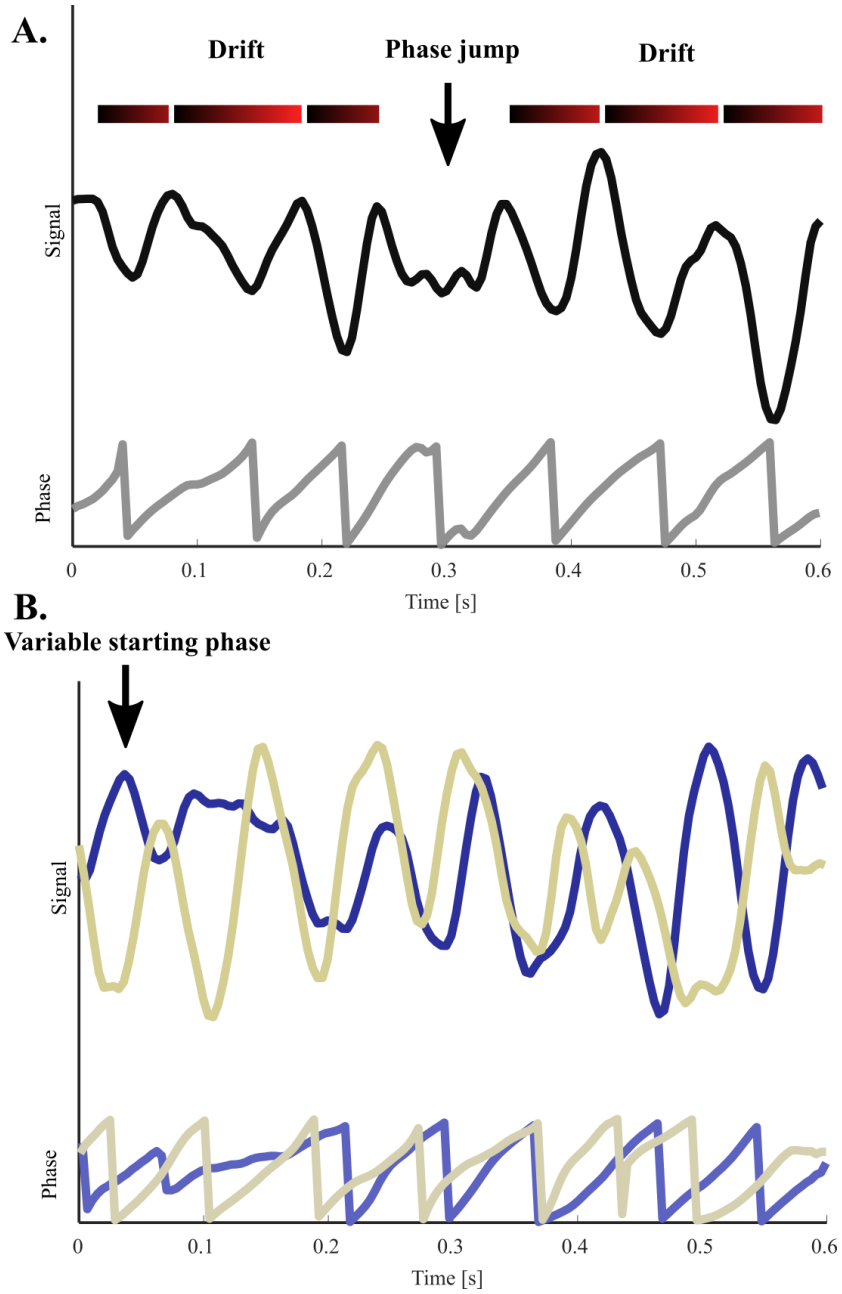

Figure 3.1. Sources of disharmony between clock and brain time. (A) Brain oscillations display spectral variation, which causes a non-correspondence or 'disharmony' between the brain's internal dynamics and clock time. An oscillation shows frequency drift and a spontaneous jump in phase, resetting itself. **(B)** Two oscillations with different starting phases. The blue oscillation starts with a rising phase, while the sand-coloured oscillation starts with a falling phase. The top rows of each panel show the amplitude fluctuations of oscillations, while the bottom rows show the phase.

The problem of disharmony does not end here. Neuroscientists repeat measurements across participants to establish whether effects found in the data are representative and statistically robust. But different brains have different dynamics, resulting in disharmony across brains too. In the attention experiment, it is highly relevant that the clocking alpha oscillations differ in frequency from person to person (Klimesch, 1999) as it means the patterns differ too. Looking for evolving patterns of spatial attention by averaging across participants is like asking when spring turns to summer in a solar system that contains diverse planets—it only makes sense after correcting for individual dynamics (Fig. 3.2).

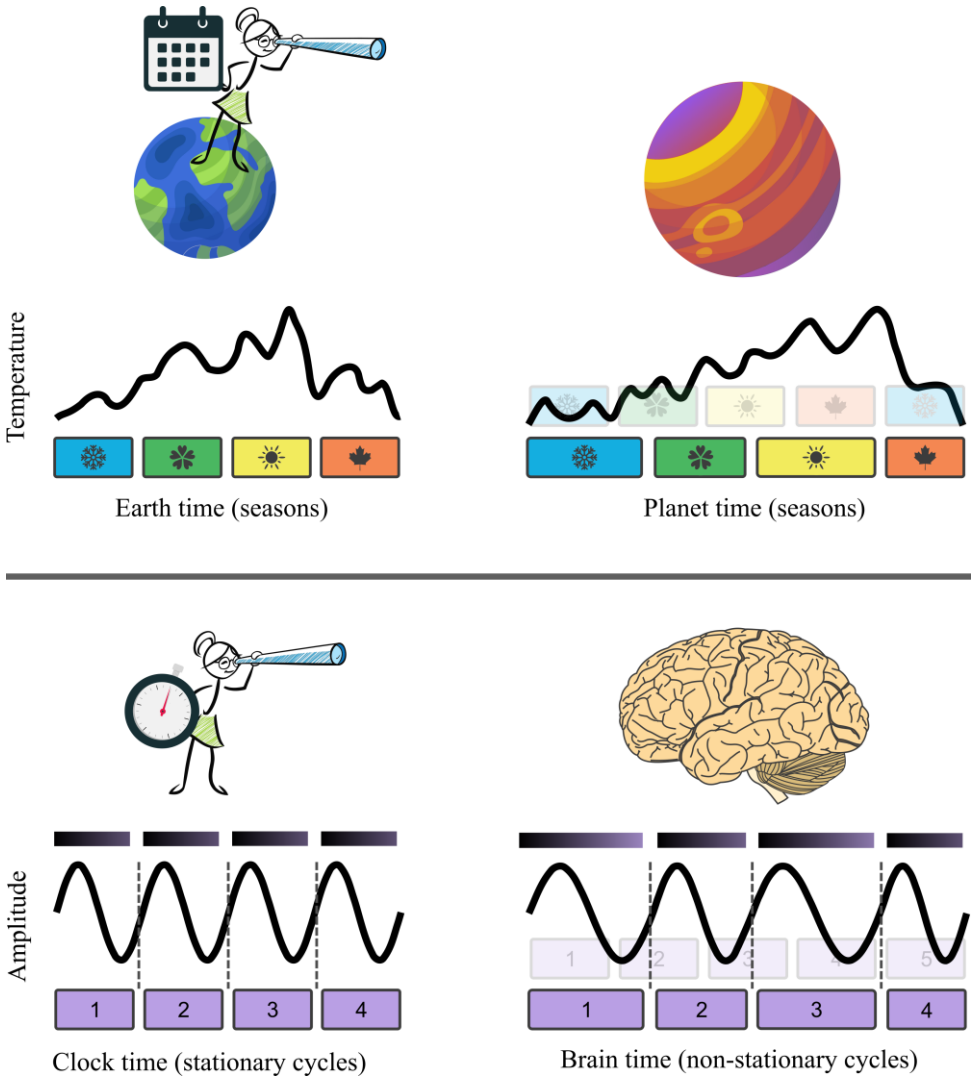

Figure 3.2. What is the best way to study a foreign system? (Top) Imagine a planet with seasonal dynamics radically different from Earth's, where the duration of each season differs substantially (as a real-world example, planet Kepler-413b has erratic seasons due to its eccentric orbit; Kostov et al., 2014). To understand the system, we measure a variable of interest across time, such as surface temperature. Critically, how do we define time here? If we plot temperature as a function of Earth's seasons (Earth time), the data will be heavily

distorted, hampering interpretation. Instead, if we were to study the system with recourse to its own dynamics (system time), the same temporal patterns in the data become interpretable. **(Bottom)** As neuroscientists, we are in an analogous position—we are studying a foreign system with its own dynamics. So, in the same vein, we should interpret data patterns with reference to the brain's dynamics, enabling an accurate readout of evolving patterns of information.

3.2.4 Approaches to factor in brain time

Disharmony between clock and brain time impedes scientific analysis within and across brains. To overcome this problem, approaches have been developed that factor in brain dynamics (Panzeri et al., 2014). At minimum, the phase of oscillations can be tracked to explain some of the variance in brain data (Kerrén et al., 2018) or behaviour (Kösem et al., 2014; Ter Wal et al., 2021) and analyses can be locked selectively to oscillatory peaks or troughs (Bonnefond & Jensen, 2015) or, more expansively, to a range of oscillatory phase bins (C. Kayser et al., 2012). Then there are more techniques where the electrophysiological data are restructured before any analysis is carried out. These include organizing the data with phase as the time axis (Eliav et al., 2018; Qasim et al., 2021), as well as linear time warping approaches that transform a template signal on the basis of trial-by-trial variations in brain dynamics (Williams, 2020).

Such approaches can reveal brain patterns of interest that are otherwise obstructed by clock time's distorting effects. For example, the phenomenon of phase precession has been extended from rodents to humans when using phase as the time axis, with no such effect visible in clock time (Qasim et al., 2021). As another example, linear time warping uncovers oscillatory brain patterns on the trial average by correcting for differences in brain time across trials (Williams et al., 2020). Over and beyond oscillatory reference frames, relative spike timings offer a brain-centric coordinate system that is agnostic to clock time as well (Chase & Young, 2007; Panzeri et al., 2014; Sotomayor-Gómez et al., 2023).

While these approaches come a long way in factoring in brain dynamics, each is limited in their scope. Using phase to explain variance in the data or locking analyses to peaks or troughs provides insights about selective data samples but does little to enable the readout of dynamic patterns. Setting the time axis to phase may not always be possible and departs significantly from the original data structure—such that unique phase-based analyses are needed. Linear time warping can equalize brain time across trials but is less equipped to deal with spectral variation throughout the trial due to its linear nature.

In this Chapter, we introduce brain time warping as a non-linear method to account for the disharmony between clock and brain time. This algorithm tracks disharmony between

clock and brain time in electrophysiology data and it transforms the data to mitigate such mismatches. We offer a software library for MATLAB (The MathWorks), the Brain Time Toolbox, which implements brain time warping and evaluates its effects. This toolbox was built for electrophysiology data analysis, including EEG, MEG and single and multi-unit recordings. It allows users to select a brain time signal from one or more warping sources (for example, channels or independent components extracted from a data structure). This signal then serves as the basis for brain time warping as laid out in Fig. 3.3.

In the remainder of this Chapter, we first introduce the methodological details of brain time warping. Then, we briefly introduce three datasets which we used to evaluate whether brain time warping can uncover effects absent in clock time. We discuss the details of several basic and advanced analyses that were used to this end. Then, we offer a more detailed exposition of each dataset's methodology. In the Results section, we describe the outcome of each dataset's basic and advanced analyses. Finally, the Discussion covers possible circularity concerns, criteria which determine whether brain time warping is appropriate, and various other considerations. The full methodological details of the toolbox itself are provided in the supplementary material of Chapter 3, as are additional analyses mentioned throughout these paragraphs.

3.3 Methods

3.3.1 Brain time warping

Here, we introduce brain time warping as a method to account for the disharmony between clock and brain time. This approach overcomes previous limitations in the following way. First, it identifies segments throughout each trial where clock and brain time fall out of tune. Then, it adapts the data to reduce their difference—winding back clock to brain time sample by sample (Fig. 3.3). Brain time warping incorporates an algorithm called dynamic time warping (DTW), which characterizes the similarity of two signals (Berndt & Clifford, 1994; Sakoe & Chiba, 1978). DTW computes a warping path, which shows how the samples of each signal need to be transformed to optimize their alignment. For brain time warping, those signals are clock and brain time (Fig. 3.3a). How are clock and brain time operationalized? Brain time can be characterized as the phase of the oscillations hypothesized to orchestrate the dynamics of a process, with its variable starts, drift and phase jumps. Clock time can be characterized as the phase of a stationary sine wave, fluctuating away faithfully to seconds. Such a signal is what brain time would look like without the three sources of disharmony;

here milliseconds and cycles map directly onto each other. (For example, in Fig. 3.3a, multiples of 100 ms correspond to each zero-crossing of the clock time signal.)

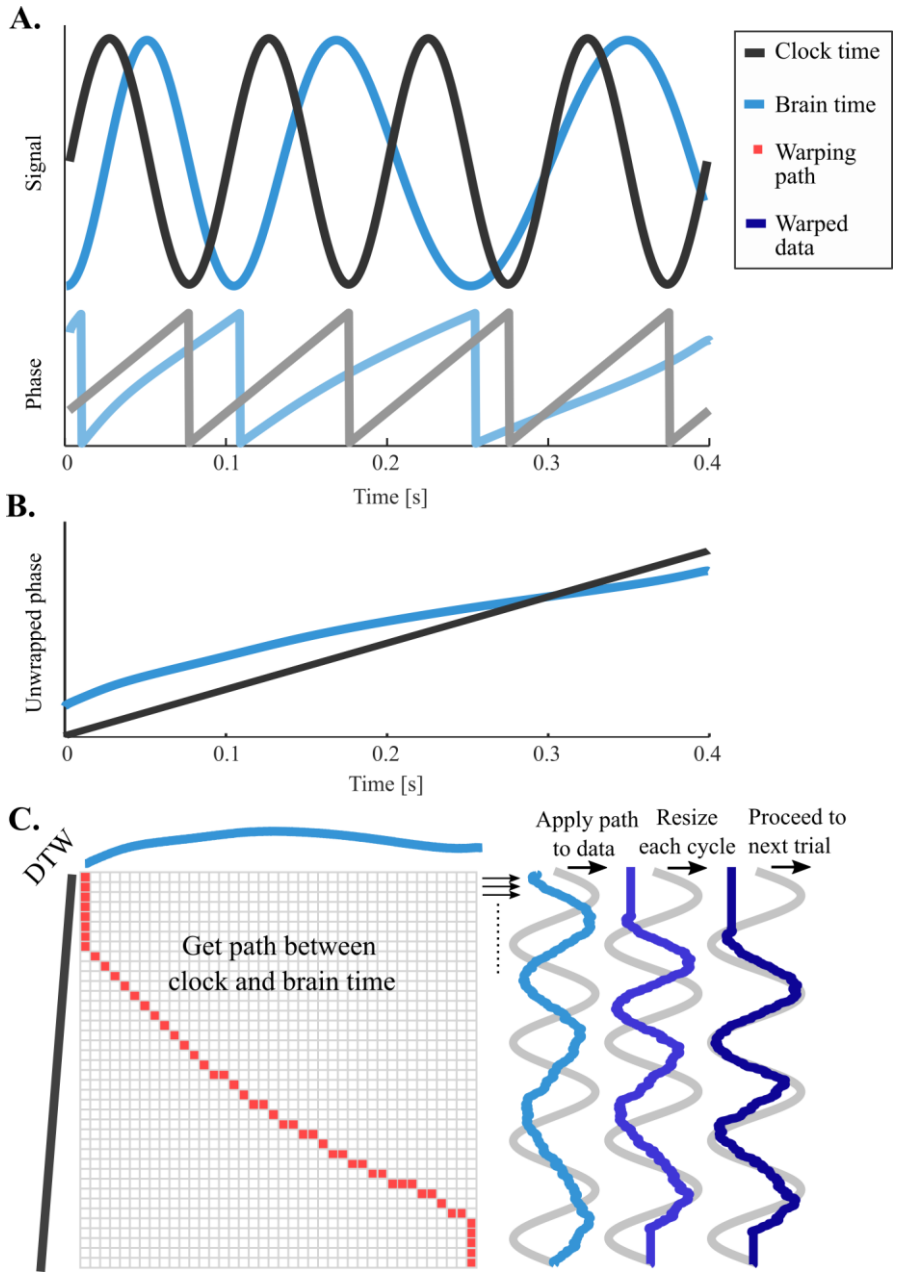

Figure 3.3. Brain time warping between clock and brain time. (A) Brain time starts in its rising phase and slows down its frequency over the course of the trial, both causing a mismatch to clock time (defined as a sinusoidal signal fluctuating in synchrony with a researcher's stopwatch). **(B)** To facilitate warping, the phase of clock and brain time is unwrapped, meaning phase is computed without cycle resets. **(C)** On the left-hand side, the unwrapped clock time (left; black line) and brain time phase vectors (top; blue line) are displayed, with a matrix between their individual samples representing possible mappings between the dimensions. DTW calculates a warping path (red squares) which amounts to a resampling procedure that efficiently minimizes the distance between the two signals—in this context, clock and brain time phase dynamics. Cycle by cycle, this warping path is applied to the input electrophysiology data, transforming its dynamics in accordance with

the brain's dynamics. To enable alignment of brain time across trials, the data of each cycle are resized to a constant number of samples. The previous steps are repeated for all remaining trials. Upon completion, the data's time axis is changed from seconds to cycles of brain time. The data are no longer in clock time but in brain time.

DTW highlights during which samples clock and brain time fall into disharmony and offers a warping path to mitigate such disharmony. Concretely, at samples where the warping path suggests that brain time needs to repeat itself before ramping back up to clock time, brain time warping repeats samples in the original data (Fig. 3.3c). Looping back to our attention example, at segments where DTW indicates that alpha oscillations slow down, brain time warping stretches the data by repeating samples in an attempt to bring its structure closer to the true dynamics of spatial attention.

The toolbox extracts the warping path between clock time (`ct_phs`) and brain time (`bt_phs`) using the following MATLAB code:

```
[~,ix,iy] = dtw(bt_phs,ct_phs)
```

`ix` is the warping path which, when applied to `bt_phs`, will minimize its distance to `ct_phs`, and vice versa for `iy`. Since `ct_phs` is a sinusoidal signal without frequency drift or phase jumps, `ix` indicates (1) segments with spectral eccentricities in `bt_phs` and (2) how `bt_phs` needs to be resampled to overcome these. Crucially, rather than applying `ix` to `bt_phs` to get it closer to `ct_phs`, brain time warping instead applies `ix` to the clock time data structure, transforming all of its dynamics based on the dynamics of the warping signal.

Whilst applying each trial's `ix` to transform clock time data in a trial-by-trial fashion, the toolbox implements a cycle-by-cycle resizing. This ensures that the data of each cycle per trial has a constant number of samples. Without this step, if the warping path contains an extended segment of data repetitions for some trials, which would stretch out the data extensively, introducing a misalignment of brain time across trials. In other words, cycle-by-cycle resizing ensures brain time unfolds with a similar time course across trials by aligning its cycles. To resize data, the toolbox uses MATLAB's `imresize` (which uses nearest-neighbour interpolation). *Braintime* determines the start and end of cycles using the warping path `iy` (the warping path from `ct_phs` to `bt_phs`), which has an equal length to `ix` but more closely reflects the dynamics of clock time. An additional side-effect of

cycle-by-cycle resizing is that the number of samples of the original data remains unchanged after brain time warping.

As brain time warping loops over trials, it continuously corrects disharmony by applying the warping path cycle-by-cycle. The result is a dataset in brain time rather than clock time and, as such, the time axis has changed from seconds to cycles. As the data are referenced to individual dynamics, it also becomes easier to look for temporal patterns across brains.

3.3.2 Dataset introduction

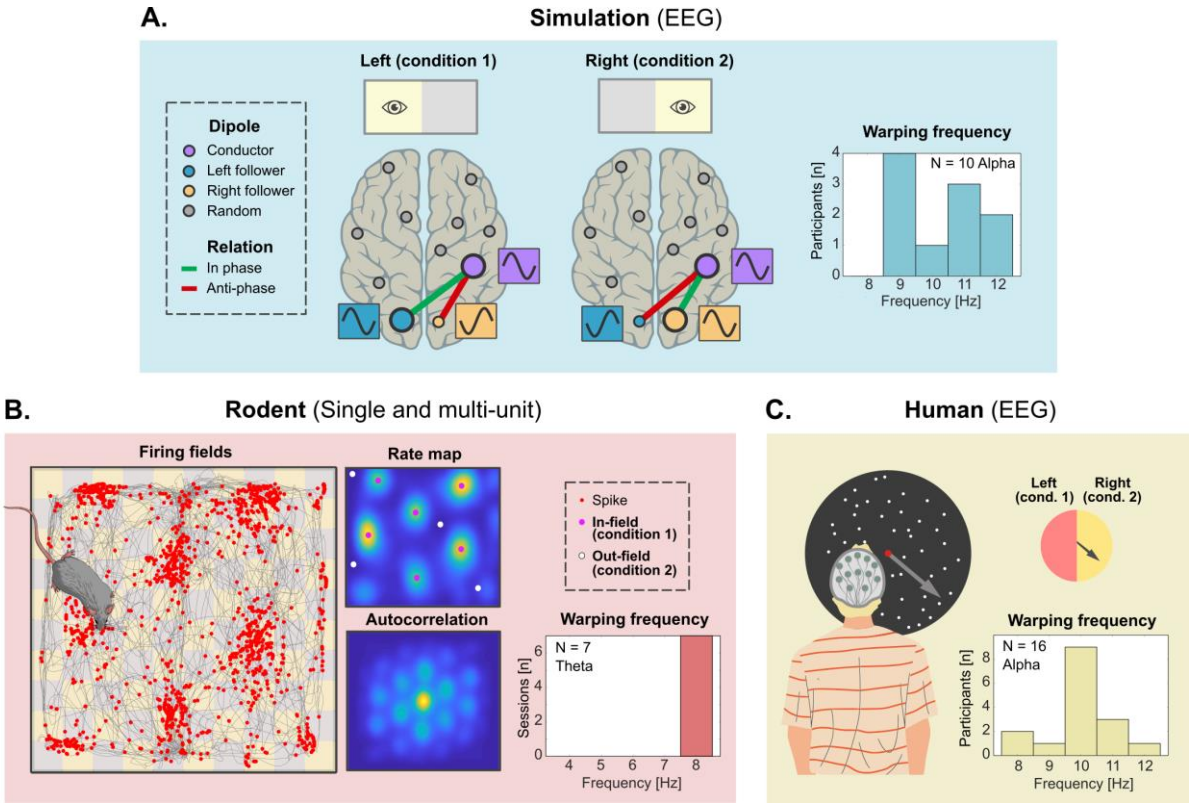

Figure 3.4. Electrophysiology datasets used to validate brain time warping. (A) Simulated EEG data (n = 10 virtual participants). We developed a basic attentional spotlight model with dipoles oscillating at alpha frequencies (8–12 Hz). One parietal conductor dipole controlled two follower dipoles, one in each visual cortex. Two conditions differed in brain activity due to the phase relation across dipoles and the suppressed amplitude of the contralateral follower dipole, together yielding attention's neural signature. To introduce disharmony between clock and brain time, we added frequency drift and variable starting phases to the data. We brain time warped to alpha oscillations in visual regions (right). **(B)** Rodent single and multi-unit data (n = 7 sessions). Long-Evans rats navigated through a square environment while single units and LFP were recorded from the entorhinal cortex. We identified grid cells and cut the data depending on whether the animal was travelling through a location coded by a grid cell (condition 1) or not (condition 2). We display cell spike locations in the field, its smoothed representation (rate map) and this representation's

autocorrelation. We then brain time warped grid cell firing patterns to theta oscillations (4–8 Hz) measured in LFP recordings (bottom right). **(C)** Human EEG data (n = 16 participants). Participants viewed random dot kinematograms, with dots moving at one of two levels of coherence (25.6% or 51.2%) in a direction ranging from 1° to 360°. We pooled the levels of coherence and binarized direction toward leftward (condition 1) or rightward (condition 2) motion. We then brain time warped the EEG data to parietal alpha oscillations (bottom right).

We tested the algorithm's effects across three electrophysiology datasets. In the first dataset (n = 10 participants), we simulated a basic attentional spotlight model, giving us full control over the ground truth brain patterns (Fig. 3.4a). Briefly, we placed one conducting dipole in the right parietal cortex, which exerted top-down control over the phase of two follower dipoles, one located in each visual cortex. We generated two conditions, one where attention was oriented to the left hemifield and one to the right. These conditions systematically differed in their underlying brain activity. Specifically, the conducting dipole always forced its contralateral follower to the same phase while setting an antiphase relation with its ipsilateral follower (drawing upon experimental findings Sauseng et al., 2005; Thut et al., 2006; Worden et al., 2000). In addition, the conducting dipole inhibited the contralateral follower dipole, reducing its amplitude (Jensen & Mazaheri, 2010). We then injected the data with variable starting phases and frequency drift to mimic natural brain activity.

In a second dataset (n = 7 sessions), we warped intracranial data from rodents navigating through a square environment (Fig. 3.4b; data obtained from Newman & Hasselmo, 2014). Here, we were interested in characterizing the dynamics of the local field potential (LFP) and grid cell firing patterns in the entorhinal cortex. Just like in the simulation, we again formatted the data into two conditions. Specifically, the data were split on the basis of whether the animal was travelling through a firing field of the grid cell or through another location not in the firing field of the grid cell.

In a third dataset (n = 16 participants), we warped EEG data recorded while human participants observed moving dots (Fig. 3.4c; data obtained from Bae & Luck, 2019). The two conditions were set around the motion direction of dots—with one condition comprising trials with leftward motion and the other comprising rightward motion. We report additional details on each dataset after describing methodological details of the analyses applied to each.

3.3.3 Analysis

Basic analyses

In basic analyses, we asked whether warping recovers oscillatory neural activity for each dataset by comparing clock and brain time on a number of measures. For these analyses, we

pooled across conditions—focusing on general effects of brain time warping on electrophysiology data and ignoring cognition for the moment.

Event-related potentials

Brain time warping is expected to overcome frequency drift, variable starting phases, and phase jumps, which in conjunction should result in a strong oscillatory structure in the event-related average, where trials are collapsed. We tested this hypothesis by applying a timelocked analysis in *FieldTrip* (Oostenveld et al., 2011) to each of the three datasets, separately for both conditions. We then selected a channel near the location of the warping signal to obtain a qualitative indication that brain time warping increases the simulated or predicted oscillatory structure (with similar results for neighbouring channels). In short, we tested whether warping increases the oscillatory structure of event-related potentials of channels near the predicted location of coordinating brain oscillations. This analysis provides a qualitative indication on the question of whether brain time warping overcomes mismatches between clock and brain time.

Power spectrum

Second, we performed a time frequency analysis across all channels and tested whether warped data reveal a higher peak at the predicted frequency of interest in the power spectrum. This quantifies the degree to which brain time warping is able to overcome frequency drift and phase jumps in the data.

We obtained Welch's power spectral density estimates for each trial and channel per participant. We used the *fitting oscillations & one over f* (FOOOF) toolbox (the MATLAB implementation; Donoghue et al., 2020) to remove the aperiodic 1/f component, after which we averaged across trials and channels per participant. As such, each power spectrum we display shows the average model fit with the aperiodic component removed. For each dataset, we analysed the clock time data from 2 to 30 Hz. For brain time spectra, we re-referenced the frequency space to each participant's individual warping frequency – which we then aligned in terms of spectral resolution and frequency space via the method explained in Supplementary material section 2.3.4 (*Filtering to common frequencies*). We equalized the y-axis (power) between clock and brain time according to the minimum and maximum values between them to enable a direct visual comparison.

Intertrial coherence

Third, we compared the intertrial coherence (ITC) across all channels between clock and brain time. This measure tests for the consistency of oscillatory phase across trials and thereby additionally taps into the degree to which the algorithm overcomes variable starting phases (which ordinarily reduce ITC by jittering the phase relation across trials). We predicted that brain time warping increases ITC at the predicted frequency of interest by equalizing brain time across trials. In the next paragraphs, we offer additional detail on each basic analysis.

For each dataset, we used *FieldTrip*'s `ft_freqanalysis` to obtain the Fourier spectrum of each channel and trial, using a wavelet analysis that fits 5 cycles. We calculated the intertrial phase coherence (ITPC) across time and frequency for each participant in the following way. We divided the Fourier spectrum by its amplitude, summed the resulting angles, took the absolute value and normalized based on the number of trials (adapting the scripts provided by https://www.fieldtriptoolbox.org/faq/itc/). We averaged ITPC across all channels within participants, and then averaged across participants – separately for clock and brain time. We used the same brain time frequency re-referencing, spectral alignment approach, and axis equalization step as described in the previous paragraph.

Advanced analysis

In advanced analyses, we tested whether brain time warping unveils dynamic patterns of cognition. For each dataset, the conditions were set up such that their contrast was expected to yield a difference in brain activity that makes for a neural signature of cognition. For example, in the human dataset, the difference in neural activity between leftward and rightward motion trials estimates the neural signature of spatial attention because activity unrelated to attending to one or other spatial direction is factored out. If oscillations of interest dynamically clock the neural processes underlying cognition, this should cause the neural signature to vary along with the oscillations.

Pattern classifiers capitalize on neural signatures to make predictions about condition (that is, class) membership of untrained data. As such, classifier performance makes for a useful index of the fidelity of neural signatures of cognition—with fluctuations of classifier performance indicating fluctuations in the neural signature (periodicity; Bouwer et al., 2020). Building off these assumptions, we predicted that brain time warping enhances periodicity of these neural signatures by adapting for spectral variation in the data.

To test this, we used a linear discriminant analysis (LDA) to classify condition in each dataset. We trained the LDA on each timepoint and tested how well it generalized to all other timepoints (King & Dehaene, 2014). This resulted in a two-dimensional temporal generalization matrix (TGM) that provides a robust map of classification performance over time (and so too of the fidelity of the neural signature). In summary, we assumed that periodicity in TGMs is a high-level measure to detect periodic brain patterns of cognition and we predicted that brain time warping would increase such patterns by factoring in the dynamics of clocking oscillations.

Classification

We trained an LDA with 5 folds and 10 repetitions on the data and obtained 50 empirical TGMs and a null distribution of 50 permuted TGMs (obtained by class label shuffling). Classifier performance was defined in terms of accuracy (i.e., the proportion of correctly classified trials).

Quantifying periodicity

For the advanced analyses, we quantified TGM periodicity by applying a Fast Fourier Transform (FFT) over each row and column of TGMs. Then, we averaged the resulting spectra into a single spectrum—the periodicity spectrum. This spectrum quantifies how much the neural signature fluctuates at different frequencies. To test our hypothesis that brain time warping increases the oscillatory structure of neural signatures, we contrasted the spectra obtained from clock and brain time data against each other—comparing the periodicity at predicted frequencies of interest.

Moreover, to aid visual inspection of periodicity, we also report autocorrelation maps of TGMs for each dataset. These maps are generated by correlating TGMs with iteratively shifted versions of itself, resulting in a representation of its self-similarity that brings out latent periodic structure (Hafting et al., 2005).

Henceforth, the term “periodicity spectrum” refers to this analysis outcome of the decoding data. The more commonplace term “frequency spectrum” refers to the spectrum derived by applying FFT to the electrophysiology directly, not to classifier output. This distinction will be maintained throughout this thesis.

Statistically testing periodicity

To evaluate which frequencies in the periodicity spectrum are statistically reliable, we compared the empirically derived spectrum with the periodicity spectra obtained under the null hypothesis that there is no fluctuating neural signature of cognition. To do so, we used the pool of 50 TGMs trained using randomly permuted classification labels. This procedure destroys the true class structure inherent to the data (Grootswagers et al., 2017), leaving the classifier with pseudo neural signatures that do not contain generalizable information about the cognitive process under investigation. To obtain second-level results, we set the toolbox settings such as to obtain 10^6 permuted power values for each periodicity frequency by randomly grabbing (with replacement) from the total pool of 50 permuted TGMs, from which p-values are calculated. This was done for both the clock and brain time data.

Cluster correction

We established whether the classifier was able to differentiate both classes of data above chance using cluster correction in *MVPA Light*. We use 10^4 permutations to test for significant clusters.

Warping source extraction

For the simulation and human analyses, we use independent component analysis (ICA) to decompose the input clock time data into additive subcomponents with statistically independent characteristics. Each component served as a warping source, meaning each contained a potential warping signal that could be designated as brain time. After brain time warping, we removed the warping source (ICA component) that was used for warping from the data before continuing to periodicity analyses. This removes the warping signal from the output data, introducing data independence (see Supplementary Material section 2.4.1).

For the rodent analysis, we warp using local field potential channels, and introduce independence by removing the selected channel from the data, leaving only the warped single-unit data.

Brain Time Toolbox settings

We used *braintime*'s default *consistenttime* method to ensure the brain time warped data restricts itself to the specified time window for each analysis (for details, see Supplementary Material section 2.4.2). To obtain time frequency information of each warping source, we

applied a wavelet analysis (fitting 5 cycles to the data). To correct for multiple comparisons across the tested frequencies in the periodicity spectra, we adjusted p-values for the false discovery rate (FDR). We implemented the FDR correction as described in (Benjamini & Yekutieli, 2001), which is optimized for analyses with statistical dependencies between tests – as is the case with frequencies across the periodicity spectra.

Classifier reliability

The previous analyses evaluate whether brain time warping can uncover periodic patterns of the neural signature—either in basic analyses of electrophysiology (ERP, ITC, power spectrum), or on a higher-level in time-generalized decoding results. A further question is whether brain time warping can increase classifier performance or, relatedly, its statistical reliability, in and of itself regardless of periodic fluctuations. The logic is that since brain time warping artificially regularizes brain dynamics, neural signatures coupled to such oscillations might artificially align across trials. This is expected to increase the performance of MVPA methods such as LDA because these techniques capitalize on neural patterns of cognition that unfold in a consistent manner across trials to generate predictions. In short, brain time warping serves to align neural codes, and since LDA relies on the cross-trial alignment of neural codes, brain time warping is expected to increase the performance and statistical reliability of LDA if variably unfolding neural codes are present in the data.

We tested this prediction using the attentional simulated dataset by systematically comparing the difference in the proportion of significantly classified timepoints between clock and brain time data as a function of the number of simulated trials. We predicted that brain time warping would introduce a higher proportion of significantly classified timepoints compared to what is present in the clock time data, with this difference between the dimensions increasing as more trials are tested. Furthermore, we use this analysis to offer a secondary evaluation of whether brain time warping can uncover periodic patterns in the neural signature. For this additional analysis, we predict that brain time warping introduces more evidence for periodicity than clock time, with the difference between these dimensions also scaling as a function of the number of simulated trials.

Throughout these analyses, we focused on classifier output that was not cross-time generalized—which is equivalent of testing only the diagonal of a TGM. The reason for this is twofold. First, most applications of LDA in the neuroscience literature are not time-generalized, so demonstrating its applicability in this more basic context means researchers

can use brain time warping without making further assumptions. Second and relatedly, it could be that brain time warping detectably increases classifier performance and reliability only on data trained and tested on the same timepoints (on diagonal in the TGM), but not on cross-time generalized timepoints (off-diagonal in the TGM). Since the absence of off-diagonal reliability increases could drown out on-diagonal reliability increases across these analyses, we limit tests to the diagonal only.

Comparing classifier reliability

We generated a version of the simulated attentional dataset with 600 left (class 1) and right (class 2) trials, resulting in 1200 trials in total (for details on the simulation, see the next section; 3.3.4). We brain time warped these data and compared the statistical reliability of accuracy values between the clock time and brain time data structure.

For both data structures, we iteratively subsampled from the full distribution of class-specific trials with increments of 40 trials. For example, in the first iteration, we randomly grabbed 40 left trials, and 40 right trials. Then, during the next iteration, we increased the number of randomly grabbed class-specific trials by 40. This resulted in 17 total iterations ranging from 40 subsampled trials to a sampling of all 600 trials. Furthermore, we repeated each iteration 20 times to avoid a subsampling of trials which are not representative of the ground truth pattern (for example, a set of trials where frequency drift is minimal, or where the starting phase of each trial coincidentally aligns). We averaged the analysis outcomes across all 20 repetitions of each iteration to get a robust estimate.

For each iteration, we calculated the proportion of significantly classified timepoints in the clock time and brain time classifier outcome. Specifically, for both data dimensions, we computed how many of the individual timepoints of the classifier performance time series contained accuracy values that exceeded 95% of the accuracy values for that timepoint derived across 60 permuted results (derived by shuffling class labels). In other words, for each iteration, we counted the proportion of samples where the p-value was lower than 0.05, where the p-value is defined in terms of the percentile of the empirical value among a null distribution of shuffled values (e.g., if the empirical accuracy is larger than 98.3% of shuffled values, a p-value of 0.017 obtains for that sample).

Comparing periodicity reliability

We performed a similar analysis to evaluate whether the difference in evidence for classifier *periodicity* between clock and brain time data scales parametrically with simulated trial number. All of the procedures were identical to the previous analysis, except for the statistical outcome computed per iteration. Namely, instead of calculating the proportion of significantly classified timepoints between classifiers trained on clock and brain time data structures, we computed the average p-value for periodicity at the warping frequency across repetitions of the same iteration (Supplementary Material, section 2.3.4). The reason for evaluating the reliability of periodicity in this way is that periodicity is definitionally calculated across timepoints, resulting in one p-value per frequency across all timepoints rather than one p-value per timepoint. We predicted that the average p-value for brain time data at the warping frequency would be lower than in clock time, and that this difference between the dimensions scales across iterations.

Warping source extraction

We extracted warping sources in the same way as described in the advanced analysis.

Classification

As with the advanced periodicity analyses, we trained an LDA with 5 folds and 10 repetitions and used accuracy as classifier performance.

Quantifying periodicity

We quantified periodicity using FFT as in the advanced analysis, but this time over only a single vector (the one-dimensional classifier results across time; TGM diagonal). For more details on quantifying periodicity in this way, see Supplementary Material section 2.3.1.

Brain Time Toolbox settings

The toolbox parameters were the same as they were for the advanced periodicity analyses.

3.3.4 Dataset methods

Simulated dataset

We simulated a basic attentional spotlight model (Figure 3.4) with dipoles oscillating at an alpha frequency (8 to 12 Hz). To introduce disharmony between clock and brain time, we introduced variable starting phases and frequency drift in the primary dipoles. We predicted that brain time warping would selectively increase periodicity at the ground truth frequency by adjusting for spectral eccentricities in the warping signal. The Brain Time Toolbox contains the MATLAB (The MathWorks, Natick, Massachusetts, USA) code used to generate the simulated dataset, which includes options to change simulation parameters (such as the degree of frequency drift, pink noise amplitude, the number and duration of trials, and so forth).

We used *FieldTrip*'s (Oostenveld et al., 2011) `ft_dipolesimulation` function to generate an electrophysiology dataset where the ground truth consists in a periodic fluctuation of covert attention at alpha frequencies. For the basic and advanced analyses, we simulated $n = 10$ datasets with 120 trials and two conditions (covert attention to the left and right hemifield; LHF and RHF). For the parametric analyses, we simulated $n = 1$ dataset with 1200 trials and two conditions. Each trial lasted one second and had a sampling rate of 200 Hertz (Hz). Across both conditions and all participants, we held constant the orientation and location of the primary dipoles that instantiated the neural signature of attention. The remaining parameters were randomized, such as the frequency, location, and orientation of non-primary dipoles ("random" dipoles), as well as each dipole's starting phase. We modelled 3 primary dipoles, and 8 random dipoles. The primary dipoles contained different parameters across the two classes of data. In contrast, the random dipoles contained parameters that were uncorrelated to each class, yielding no meaningful average difference in neural activity between conditions. In this simulation, our primary focus was to create a dataset suitable to test brain time warping (with a neural signature and spectral phenomena like drift and phase jumps) rather than to accurately model attention in close accordance with theoretical models.

Primary dipole configuration

We placed the conductor dipole in the right parietal cortex with an amplitude of 1 (in arbitrary units), oscillating at a random alpha frequency. This conductor dipole "conducted" the phase of two follower dipoles, one located in each visual cortex, oscillating at the same frequency and oriented with the same x, y, and z coordinates. We generated two classes: trials of LHF and RHF data. The two conditions contained a difference in parameters – and

thereby brain activity – that the classifier could exploit to differentiate the data and obtain the ground truth signature of attention. Specifically, for both conditions, we changed two parameters:

- The relative amplitude between follower dipoles. The follower dipole contralateral to the hemifield condition oscillated at half the amplitude (0.5) compared to the ipsilateral dipole (1) – mimicking contralateral inhibition of alpha.
- Phase relation between primary dipoles. The conductor dipole oscillated in antiphase with the follower dipole contralateral to the hemifield. In contrast, it oscillated in phase with the follower dipole ipsilateral to the hemifield (barring a $\frac{\pi}{6}$ phase delay to mimic signal conductance delay).

In addition to these condition-specific differences, each primary dipole contained 1/F noise, variable starting phase, and frequency drift. We implemented frequency drift through a random walk approach, where the frequency of all three primary dipoles decreased or increased by 0.05 Hz per sample.

Random dipole configuration

To decrease the signal to noise ratio of the neural signature exerted by primary dipoles, we introduced 8 random dipoles that oscillated at random frequencies, limited to 2 Hz above and below the primary dipole's frequency to avoid interference with the neural signature. These dipoles oscillated at an amplitude of 1, contained 1/F noise, and were placed randomly across the brain with a random orientation.

Brain time warping

For the main and advanced analysis with multiple simulated datasets, we considered each as separate participants with their own alpha frequency. Across all analyses, we used ICA to obtain warping sources and warped each participant to a source with (1) a topographical activity profile around occipital and parietal regions, (2) and a high amplitude alpha peak.

Rodent dataset

We brain time warped a rodent dataset obtained from (Newman & Hasselmo, 2014). In this study, local field potentials (LFP) and single units were measured from the entorhinal cortex

of Long-Evans rats as they navigated through a rectangular open field. In the following section, we describe how we reformatted and analysed the data to test the effects of brain time warping. For methodological details on the recordings such as data acquisition, surgical procedures, and behavioural protocols, we refer to (Newman & Hasselmo, 2014). We hypothesized that brain time warping would increase the periodicity with which a classifier is able to differentiate when an animal is inside or outside the firing field of a grid cell. To this end, we brain time warped grid cell activity to theta oscillations in the LFP. The logic is that if theta clocks grid cell activity, then periodic patterns in their spiking activity should be enhanced after brain time warping (through its correcting of spectral eccentricities in brain time).

Primary grid cells

We inspected single cell recordings from 7 recording sessions (N = 2 rodents) and extracted one primary grid cell for each recording, which we used to define the in- and outfield condition. We selected a primary grid cell by comparing each cell's firing rate map for triangular structure and the periodicity of these maps using a 2D autocorrelation analysis (Hafting et al., 2005). In Supplementary Material section 3.2.2, we display the smoothed firing rate maps of each session's primary grid cell and how we devised classes based on their firing fields.

Spike-field coupling

Brain time warping is only expected to enhance periodicity if grid cells phase lock to theta. Thus, we verified spike-field coupling for selected grid cells. In Supplementary Material section 3.2.3, we show the spike-field coupling of one example grid cell.

Data preparation

For each session, we created a separate structure for the spike activity of grid cells (between 2 and 4 channels; convolved with a Gaussian) and LFP recordings (2 channels). We split each structure into two classes of data based on when rodents were inside a firing field of the primary grid cell's firing field (defined by local maxima in the smoothed firing rate map) or outside of it (defined by local minima). As a consequence of this split, the data at t = 0 reflected the animal's presence in a firing field (class 1), or not (class 2). This trivially

introduces high classifier performance around these timepoints. However, we were not interested in the classifier's performance to differentiate in- and out-field conditions. Rather, we tested whether brain time warped data increased periodicity in classifier performance at the warping frequency. We brain time warped 2.5 seconds of data (from 1.25 seconds before to after t = 0). The number of trials per session ranged from 60 to 168 (mean: 104.8 trials, standard deviation: 39).

Brain time warping

The average waveshape of LFP theta was asymmetric, so we generated the clock time template signal (used to detect segments of frequency drift and phase jumps in LFP theta) based on a smoothed version of the average waveshape rather than a symmetric sine wave (which is the default method). This optimizes brain time warping by reducing differences between the clock and brain time signal, improving the accuracy of the warping path (see Toolbox methods). In Supplementary Material Section 3.2, we show TGMs and their autocorrelation map for each session. The prepared data and scripts used for analysis are included in the Brain Time Toolbox. For our warping signal, we selected the highest power theta frequency from the component that displayed the overall highest power across theta frequencies (always resulting in an 8 Hz signal).

Human dataset

We brain time warped a human dataset obtained from Bae & Luck (2019), which is available for download at https://osf.io/bpexa/. In this study, electroencephalography (EEG) was recorded while participants viewed random dot kinematograms, where a proportion of dots moved coherently toward a direction in 360° space. Each trial contained, in order, a fixation period of 1.5s, a motion period of 1.5s, and a direction report of variable duration. Again, we restrict our description to how we reformatted and analysed the data. For the full methodological details, see Bae & Luck (2019). We hypothesized that brain time warping to occipital-parietal alpha oscillations would increase the periodicity with which a classifier is able to differentiate whether motion is leftward or rightward, resting on evidence for alpha's role in controlling spatial attention (Capotosto et al., 2009).

Data preparation

First, we pooled both recording sessions and coherence levels (with 25.6% and 51.2% of dots moving coherently in one direction). We used only the 1.5s motion period for decoding, as we predicted the neural signature of spatial attention is most detectable during motion. We filtered each participant's data (N = 16) to the 80% most accurate trials (defined based on the error between reported and presented motion angle), reducing the number of trials from 1280 to 1024. This removes the subset of trials where a rare reversal effect occurred in which participants report motion in roughly the opposite direction to the presented motion. Next, we defined two classes of data based on whether motion was leftward (class 1; angles between 90° and 270°), or rightward (class 2; the remaining angles).

Brain time warping

We extracted warping sources by applying ICA to the data. For each participant, we chose a component with sustained alpha power and a topographical profile that suggested an occipital-parietal origin in line with previous research (Capotosto et al., 2009; Sauseng et al., 2005). Out of components that met these criteria, we chose the component with the largest amplitude at alpha. In Supplementary Material section 3.3, we show TGMs and autocorrelation maps for each participant.

3.4 Results

3.4.1 Brain time warping recovers oscillatory activity

In the simulated dataset, the event-related average of clock time data shows no robust oscillatory shape. After warping, the oscillatory structure hidden in the data becomes qualitatively uncovered (Fig. 3.5a). Moreover, we found that the algorithm sharpens the power spectrum selectively around the warping frequency (Fig. 3.5b) and, in line with our hypothesis, increases the peak's magnitude. Third, the ITC in clock time shows comparatively low values around simulated alpha rates—with only weak clustering at low alpha (Fig. 3.5c). ITC is enhanced by brain time warping, revealing a strong cluster at participants' warping frequency. We find similar results for the rodent dataset (Supplementary Material section 3.2.1). For the human data, we found a prominent increase in ITC at the warping frequency but not in the peaks of the power spectrum (Supplementary Material section 3.3.1). Together, these results demonstrate that warping can reveal oscillatory activity that is lost due to clock time's distorting effects on the data. As mentioned in Figure 3.5, brain time spectra are normalized with respect to individual participants' brain

time warping frequency ($\frac{clock\ time\ frequency}{brain\ time\ frequency}$). While we denote these ratios in terms of Hz throughout this Thesis, we recognize that Hz is a unit that refers to cycles per clock time second, making it a technically inadequate brain time-based frequency unit.

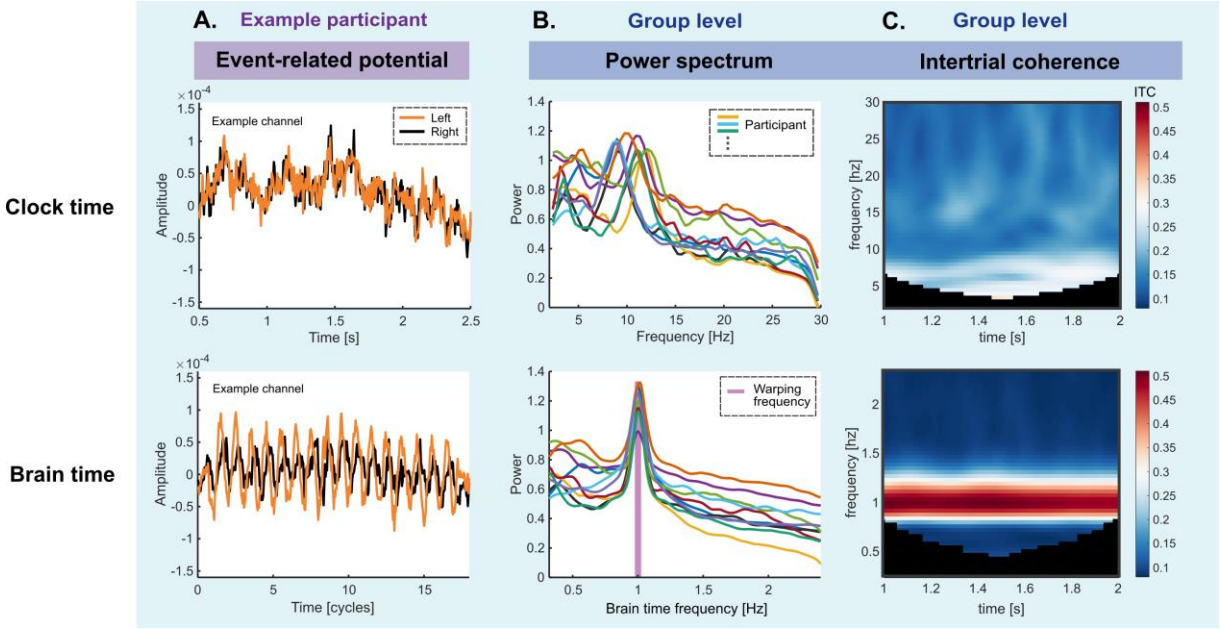

Figure 3.5. Results of basic analyses in the simulated dataset. (A) ERPs in the left visual cortex of one example virtual participant. In clock time, averaging across trials destroys the simulated oscillatory structure. By repairing disharmony, brain time warping recovers this structure. **(B)** Power spectra averaged across all channels and participants. Brain time warping increases the power of alpha oscillations at the simulated rate for each participant. Brain time results are always rereferenced to individual participants' brain time rate ($\frac{clock\ time\ frequency}{brain\ time\ frequency}$). This sets 1 Hz as each participant's warping frequency (and, for example, 0.5 Hz as half the warping frequency). We removed the aperiodic (1/*f*) component of the power spectrum using the FOOOF toolbox (Donoghue et al., 2020). **(C)** ITC averaged across all channels and participants. Brain time warping increases ITC at the (ground truth) alpha frequency. The analysis window was restricted to 1–2 s to reduce artefacts. We equalized the *y* axis in (B) and the colour axis in (C) between clock and brain time based on maximum values to enable a visual comparison between dimensions (this step is performed in all figures).

3.4.2 Brain time warping recovers neural patterns of cognition

In the simulation, the neural signature provided by the classes reflected attention. The simulated patterns of this signature were not detectable in a default clock time format but did emerge after brain time warping (Fig. 3.6).

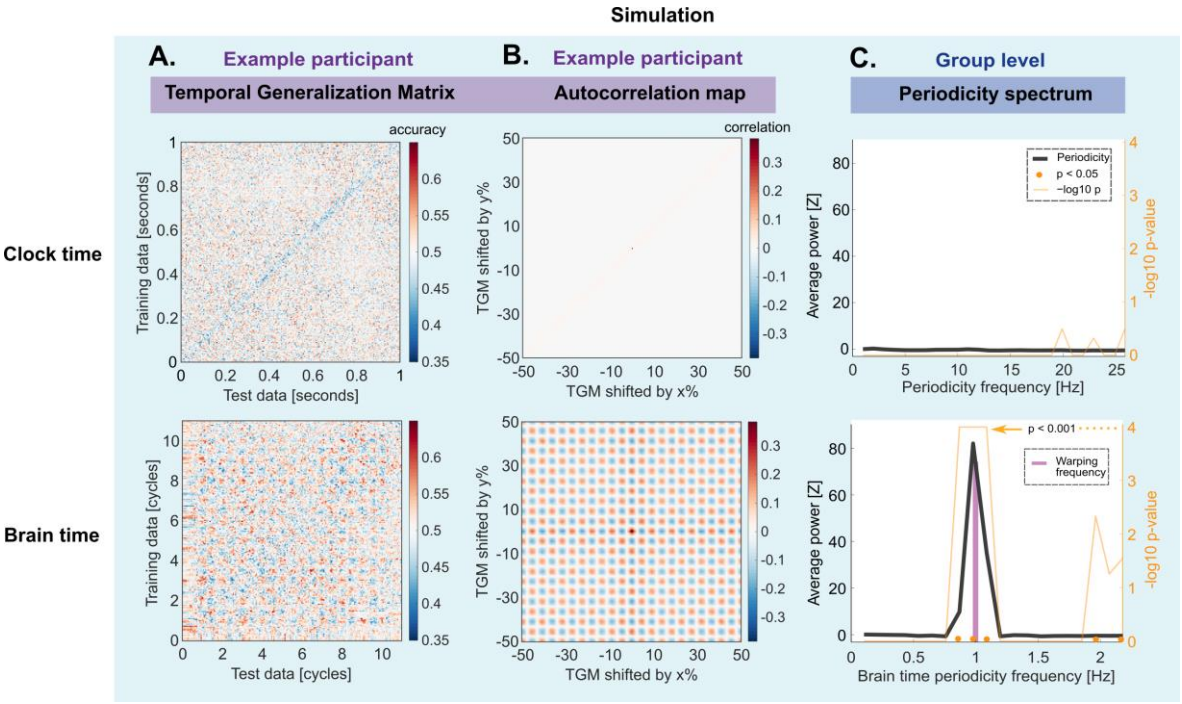

Figure 3.6. Results of advanced analyses in the simulated dataset. We tested for periodic patterns in the classifier's TGM, which provides an index of neural signatures of cognition by demonstrating how the classifier's performance generalizes across time. **(A)** An example participant's TGM shows no periodic structure in clock time (top). After brain time warping, the simulated periodic structure in the neural signature is recovered—as evidenced by the chequerboard pattern (bottom). **(B)** The difference between clock and brain time becomes qualitatively striking in the TGM's autocorrelation maps. **(C)** We quantified periodicity by applying an FFT over all rows and columns of TGMs. Then, we perform second-level statistics by comparing empirical periodicity with permuted periodicity (obtained by shuffling class labels). Only brain time spectra show significant periodicity at the warping frequency ($P < 0.001$) and its first harmonic ($P < 0.05$), demonstrating that brain time warping corrects for disharmony and unveils ground truth neural signature dynamics (bottom and top). Each participant showed periodicity peaks selectively at their warping frequency. We corrected for multiple comparisons (using false discovery rate (FDR); Benjamini & Yekutieli, 2001), except at specific frequencies in the brain time spectra at which we hypothesized classifier periodicity (0.5, 1 and 2 Hz; 1 Hz remains significant when applying FDR. We provide additional plots, including all TGMs, autocorrelation maps and periodicity spectra in Supplementary Material section 3.1.2).

In the rodent data, the difference in activity between classes reflected whether the animal was in a firing field of the grid cells, yielding a signature of the neural basis for spatial navigation (Jacobs et al., 2013). In clock time, no periodicity is evident over time (Fig. 3.7a; top) despite grid cells strongly phase locking to theta oscillations (Burgess & O'Keefe, 2011; Supplementary Material section 3.2.3). Importantly, brain time warping the firing rates of grid cells to theta oscillations obtained from the LFP does result in periodicity (Fig. 3.7a; bottom).

In the human data, the neural signature reflected spatial attention, provided by the difference in brain activity during leftward and rightward motion. While the clock time data qualitatively show some periodicity at alpha, the peaks do not stand out reliably from the peaks in periodicity spectra obtained with permuted labels (Fig. 3.7b; top). In contrast, brain time warping reveals prominent and reliable periodicity at participants' individual alpha frequency (Fig. 3.7b; bottom). Together, the basic and advanced results indicate that brain time warping is a promising tool to repair disharmony between clock and brain time, facilitating the study of the dynamic cognitive brain.

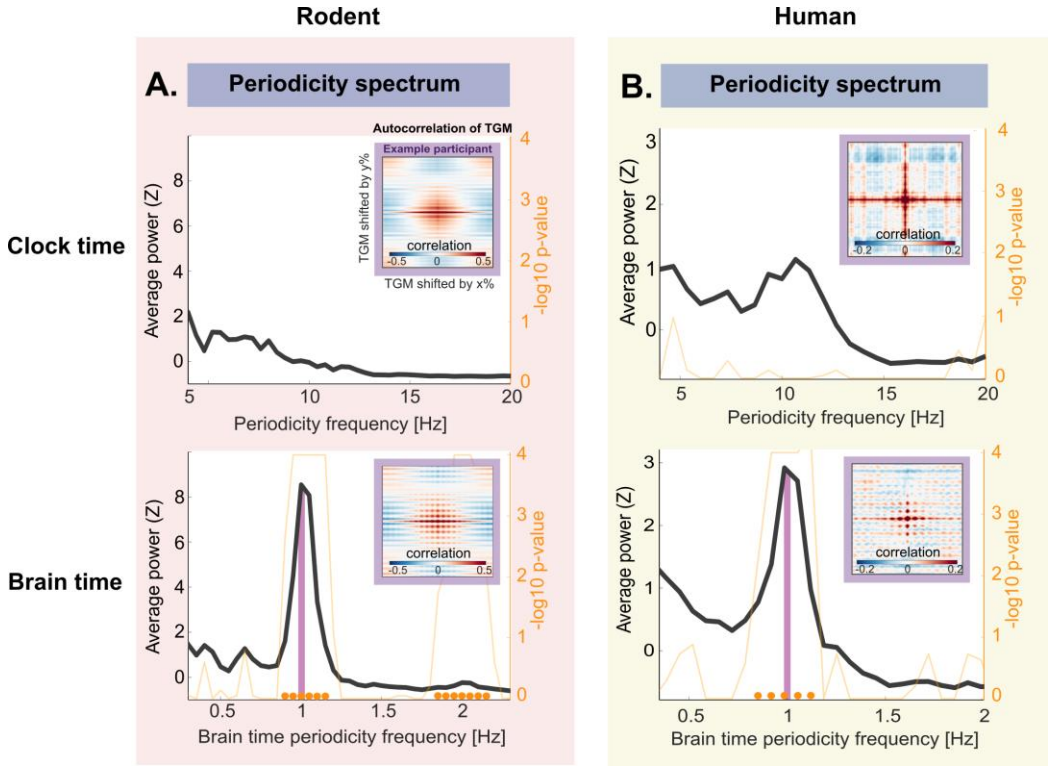

Figure 3.7. Results of advanced analyses in the rodent and human dataset. (A) Warping the rodent data to LFP theta unveils statistically robust periodicity around the warping frequency and its first harmonic ($P < 0.001$), while the clock time spectrum shows no significant peaks. **(B)** In the human dataset, brain time warping reveals periodic patterns around the warping frequency ($P < 0.001$), indicating that the neural signature of attention fluctuates during motion perception. For the rodent data, each session showed periodicity peaks selectively at their warping frequency. For the human data, not all participants showed periodicity peaks and there was some variance in the brain time frequency of peaks. The insets display autocorrelation maps of TGMs from example sessions (for the rodent dataset) or example participants (for the human dataset). We provide additional plots in Supplementary Material section 3.2 and 3.3. These plots include TGMs, autocorrelation maps, periodicity spectra, grid cell maps and spike-field coupling between theta and single unit spikes.

3.4.3 Brain time warping parametric classifier reliability

As mentioned in the Methods section, a further question is whether brain time warping can be used to increase the readout of neural signatures regardless of whether the algorithm can increase the readout of their periodicity. In the simulated data, we found evidence for a parametric increase in the proportion of significantly classified timepoints for brain time warping, with the difference in this proportion to clock time scaling with the number of considered trials (Figure 3.8). This situates brain time warping as a promising approach to uncover cognition-specific brain activity.

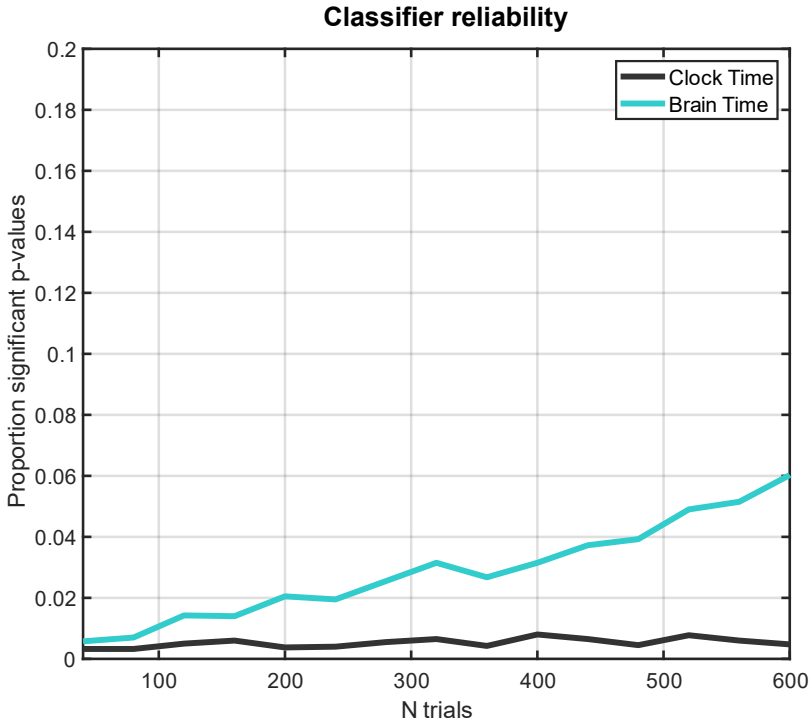

Figure 3.8. Results of parametric analysis classifier reliability. The proportion of classifier timepoints with accuracy values that exceed the top 5 percent of null distribution accuracy values (i.e., $p < 0.05$) as a function of the number of subsampled simulation trials per class. While a classifier trained and tested on clock time data contains approximately the same proportion of significantly classified timepoints with increasing trial numbers, brain time results show a gradual increase in this proportion. With increasing trial numbers, the difference between clock and brain time classifier reliability increases.

3.4.4 Brain time warping parametric classifier periodicity

We used the same analytical setup to offer a secondary way to address the question of whether brain time warping can uncover periodicity in the neural signature (Figure 3.9).

While the evidence for periodicity in a classifier carried out on clock time data retains approximately the same average p-value regardless of how many trials are used for classification, a classifier performed on brain time data shows decreasing average p-values for periodicity at the warping frequency. This corroborates the idea that brain time warping can be used to uncover periodicity in neural signatures of cognition.

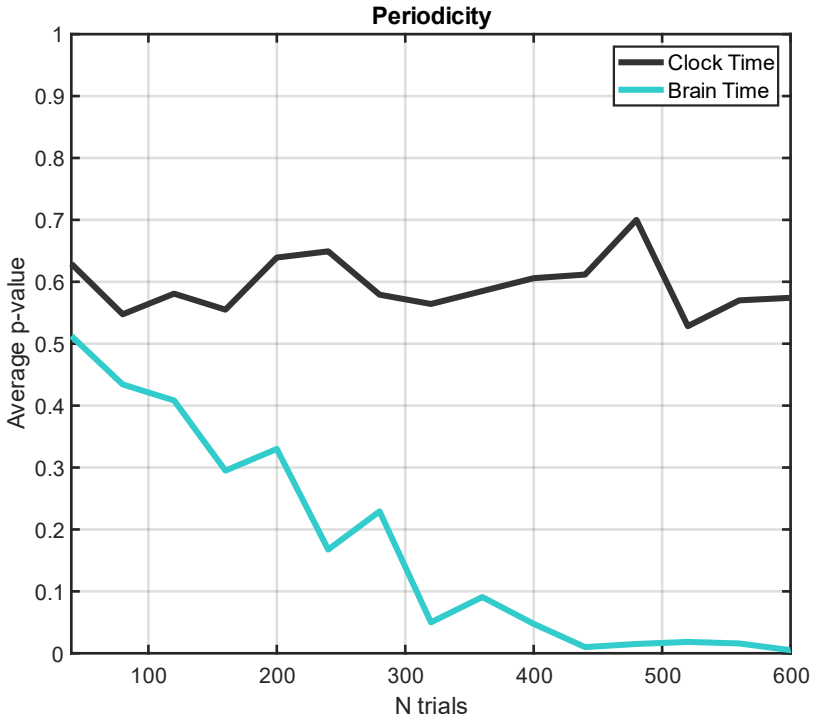

Figure 3.9. Results of parametric analysis classifier periodicity. The average p-value at the warping frequency as a function of the number of subsampled simulation trials per class. While a classifier trained and tested on clock time data does not show systematic changes in the average p-value at the warping frequency across simulated trial numbers, brain time results show a decrease in average p-value as the number of trials increases.

3.5 Discussion

3.5.1 Is retuning using brain time warping circular?

A potential concern with brain time warping could be that it trivially imposes oscillatory structure onto the data. The worry here is that the algorithm makes data patterns fluctuate at the warped frequency no matter which frequency is selected. In this section, we examine when the algorithm is on safe grounds and when vigilance is needed.

First, as a note of clarification, the path used for brain time warping does not contain oscillatory structure. That is to say, if the path were applied to a random time series, it would

not mould it to increase its oscillatory shape. This is because the path is instead designed to show when the oscillation used for warping undergoes spectrally variable behaviour. Nevertheless, an important concern remains. Brain time warping applies the path to the data to align it with brain dynamics, so if the warping signal is within the data, its stationarity will increase—introducing some oscillatory structure after all. Whether circularity is a problem depends on two factors: the type of analysis carried out and the dependence between warping signal and warped data. We discuss these points in turn, first covering each type of analysis.

Basic analyses

Brain time warping is expected to enhance oscillatory structure in the event-related potential (ERP), power spectrum and ITC at least somewhat because there are usually at least some oscillations at any frequency to begin with. So, warping to a random frequency will cause those oscillations to have their frequency drift, variable starting phase, and phase jumps reduced, affecting subsequent results. Hence, any increase around warping frequencies in basic analyses should not be taken as evidence that those frequencies are critical for cognition—there needs to be a further relation to independent measures (such as cognitive or orthogonal neural variables). In this sense, brain time warping can be used as a preprocessing step to aid subsequent high-level approaches that are sufficiently independent (to avoid circular inference; Kriegeskorte et al., 2009).

With that said, we find that warping to weak simulated oscillations results in only weak frequency-specific enhancements compared to warping to strong oscillations—speaking to the specificity of brain time warping even before cognition enters the scene (Supplementary Material section 1.1).

Advanced analyses

We have presented the advanced classification analysis as a circularity-free high-level approach and it is the central analysis implemented in the Brain Time Toolbox. By tapping into neural signatures of cognition rather than oscillations themselves, warping-induced changes are non-trivial. Specifically, only warping to those oscillations that coordinate the underlying activity relevant for cognition is expected to yield fluctuations in cognition's neural signature. In support of this, we performed a control analysis where we warp to control frequencies (Pletzer et al., 2010), resulting in no evidence of periodicity (Supplementary Material section 1.1). A further safeguard of the advanced analysis is that

the obtained null distributions benefit equally from any trivially imposed oscillatory structure as the empirical distribution.

Data dependence

Beyond the type of analysis that is used, the dependence between warping source and transformed data is another factor to consider. After all, if the cause for circularity lies chiefly in changes to the warping signal, then removing it from the warped data reduces circularity concerns. We report suggestions on how to achieve data independence for each electrophysiology method, describing how they can be implemented before or after warping (Supplementary Material section 2.4.1). We also report cases in which independence between warping source and data is impossible. Here, it is important to determine on a case-by-case basis whether circularity is a concern on the basis of the previous points (that is, are subsequent analyses orthogonal or not?). To aid this process, the toolbox tracks dependence between warping source and warped data and raises a warning when circularity could become an issue.

Statistical false positives

With these reflections in mind, we finally emphasize that brain time warping is a hypothesis-driven method that capitalizes on the temporally coordinating nature of oscillations. Hence, we recommend warping only using oscillations predicted to fit that bill to avoid false positive results by chance or to apply multiple testing correction when rewarping to a different signal in the data. To enable hypothesis-driven warping, the Brain Time Toolbox computes a variety of information about warping signals—including their time frequency characteristics, waveshape and topographical profile—allowing users to make informed decisions about which signal they wish to designate as brain time.

3.5.2 When is retuning clock and brain time necessary?

The need to use brain time warping or other methods to retune depends on (1) the degree to which clock and brain time are in disharmony and (2) the degree to which such disharmony interferes with analyses. Below, we elaborate on both criteria.

The degree to which disharmony is present depends on the levels of processing involved in the experimental paradigm used. Take once again the spatial attention study. Between the moving dots' light hitting the participant's retina and their pressing of the button to indicate motion direction, a vast amount of subcortical and cortical processing transpires.

While internal dynamics start to coordinate stimulus processing as early as the thalamus (Hughes, 2004; Vijayan & Kopell, 2012), or even earlier (Koepsell et al., 2009), disharmony is most prevalent in higher level regions—where processes such as attention and decision-making operate in full swing. This is because, at this late stage, information has passed through many cell ensembles where different oscillations have each exerted a temporal footprint. As these footprints add up, clock time falls increasingly out of tune with brain time. As a result, we lose track of brain dynamics and the information they provide about cognition, such as whether dots make it to awareness (VanRullen, 2016) or whether features of the dots (such as their colour) are available to working memory (ten Oever et al., 2020). Thus, there is a gradation in clock time's distorting effect which depends on the extent of cortical processing. Research that restricts analyses to low-level subcortical processing or very early evoked potentials benefits comparatively little from retuning, while retuning may be a vital step to understand brain patterns in late stages—with at least one exception: retuning is unnecessary for analyses that do not rely on temporal variations of the neural signature. For example, a researcher may want to study the trial-average activity in parietal regions as a function of the proportion of dots that moved or map aggregate differences in network connectivity between participants. Here, it is true as ever that brain dynamics play their part in the subprocesses involved but the analyses are insensitive to time variations, leaving them unafflicted by the footprints of oscillations.

Finally, in some experimental contexts, the evolution of brain activity with reference to clock time is informative in its own right, with brain time warping potentially distorting such insights. For example, theta frequencies in the rodent hippocampus covary with running speed (Kennedy et al., 2022; McFarland et al., 1975), individual alpha frequencies are higher in human participants who display high memory performance (Klimesch et al., 1993), and prefrontal oscillatory activity has lower frequencies in schizophrenia patients (Uhlhaas & Singer, 2013).

In short, retuning clock and brain time is necessary depending on the degree to which both the mechanisms of study and the analyses used depend on the brain's internal dynamics. On the whole, few electrophysiology studies are exempt from the distorting effects of clock time.

3.5.3 Brain time is not unitary

The phrase "brain time" is used to emphasize the conceptual departure from a format extrinsic to the brain. We do not mean to suggest that there is a single brain time. Rather,

different cognitive processes are clocked by different groups of oscillations, each with their own frequency and source. In this sense, brain time is analogous to a concept like “Earth time”, which contrasts itself with time on other planets whilst further decomposing into different time zones. Finally, brain time in the present context does not refer to timekeeping in the brain. Instead, it refers to the oscillatory dynamics by which the brain coordinates cognition generally, of which temporal cognition is a specific instance (Wassenhove, 2016).

3.6 Summary & looking ahead

In this Chapter, I have argued that rather than imposing a foreign unit of time onto the brain while studying its function, the brain is best understood as a system with its own dynamics and temporal organization. Upon inspection, the brain operates rhythmically, with brain oscillations as a key player. This has important consequences for scientific analysis. If it is true that oscillations clock brain activity to coordinate cognition, then their dynamics should heavily inform how we study evolving data patterns. In contrast, analysing such patterns in the default clock time format is likely to yield a distorted readout as the brain’s internal dynamics do not scale linearly to sequences of (milli)seconds. We introduce brain time warping as a method to account for disharmony in brain data, dynamically transforming electrophysiology data structures in a way that brings them in line with brain dynamics. The Brain Time Toolbox implements brain time warping, facilitating analysis on the oscillatory dynamics of the cognitive brain.

In the next Chapter, I will explore a different method to tackle the same problem. Specifically, returning to the context of memory encoding and retrieval, I evaluate whether the presentation of striking visual stimuli can reset brain dynamics to regularize neural patterns of memory representations across measurements. This method constitutes a methodologically more invasive approach to factor in brain dynamics into neuroscientific inquiry because it involves the direct interference with oscillatory dynamics rather than post-hoc algorithmic transformations.

Chapter 4: Evaluating visual perturbation as a method to refocus brain dynamics

4.1 Introduction

A central question in memory research is how the brain retrieves information stored in long-term memory (LTM) in the service of adaptive behaviour. This research topic has inspired work from a variety of angles, involving different experimental protocols and methods—including neuroimaging modalities. Electroencephalography (EEG) and magnetoencephalography (MEG) have proven an important part of this project because they capture brain dynamics on a sub-second resolution. Such granularity is crucial, given that memory retrieval typically unfolds on the order of seconds, with the neural cascades underpinning memory retrieval evolving even faster (Staresina & Wimber, 2019).

To study the evolution of retrieved contents in the brain, one widely pursued family of techniques is multivariate pattern analysis (MVPA)—more broadly known as classification or decoding (Haxby et al., 2014; Grootswagers et al., 2017). These tools extract and upweight signal dimensions that robustly covary with retrieved memory contents, effectively boosting the signal-to-noise ratio of associated neural activity. MVPA has been successfully used to enrich our understanding of memory, including how information is encoded (Fritch et al., 2020; Kragel et al., 2017; Kuhl et al., 2012), consolidated (Deuker et al., 2013; Maguire, 2014; Schreiner et al., 2021), and reinstated during memory recall (i.e., pattern completion; Danker & Anderson, 2010; Favila et al., 2020; Rissman & Wagner, 2012; Xue, 2018).

Despite such advancements, the decoding of long-term memory contents in electrophysiology data typically remains only slightly above chance, impairing our ability to study the evolution of neural patterns of interest. One reason for this limitation is that memory processes and their associated brain activity are highly dynamic, which results in variable patterns across trials and participants (ter Wal et al., 2021; Madore & Wagner, 2022). Indeed, MVPA and most other EEG-based analyses rely for their robust predictions on the existence of a detectably constant cascade of neural patterns across measurements (van Bree, Melcón, et al., 2022). This clash between variability in neural processes on the one hand and the constancy assumption of our analyses on the other may cause us to miss representations of interest, or to obtain different results depending on what experimental event we timelock EEG data to (e.g., retrieval cues vs button presses; Linde-Domingo et al., 2019). A factor that further hampers our ability to robustly decode representations is that retrieval comes with fainter neural patterns to begin with compared to perception (Favila et al., 2020; Pearson et al., 2015). Together, these points invite creative techniques that improve our ability to infer long-term memory representations from dynamic brain activity.

In this study, we explore a perturbational method that has the potential to mitigate two issues at the same time: low signal fidelity at the level of measurement, and variability in neural processing dynamics. Specifically, in this EEG study we evaluated whether the presentation of a high contrast visual stimulus—henceforth referred to as a "ping"—during LTM retrieval enhances the readout of signatures of retrieved content. In motivating the hypothesis that *pings* boost the decodability of LTM representations, we built directly onto recent successful efforts in the domain of working memory (WM). In that context, pings have been used to enhance the decodability of the orientation (Wolff et al., 2015, 2017, 2020; ten Oever et al., 2020; Yang et al., 2023) and colour (Kandemir et al., 2023) of objects actively maintained in WM, as well as anticipated target locations (D. H. Duncan et al., 2023). An explanation for these findings is that pings produce a robust sweep of activity that interacts with WM representations to enhance their SNR, either by cascading through networks of activity-silent synaptic traces that encode WM contents (Stokes, 2015; Mongillo et al., 2008), or by interacting with generators responsible for memory-specific functional activity that persists during the delay period (Barbosa et al., 2021).

More broadly, pings may regularize neural dynamics across trials and participants by producing a phase reset of brain oscillations that coordinate information processing across neuronal populations. In support of this, visual stimuli presented during memory tasks have been shown to reset the phase of low-frequency brain oscillations that are implicated in encoding and retrieval (Rizzuto et al., 2003; Haque et al., 2015; audiovisual stimuli in Cruzat et al., 2021). Thus, by inducing pings at experimentally controlled moments, researchers may gain a level of control over variability in synchronized activity across information-coding neurons, making their dynamics more similar across measurements to improve the predictive power of MVPA.

Importantly however, while ping-based methods have been shown to work in WM contexts, to our knowledge it has not been explored whether they generalize to LTM research in which information is retrieved from stored representations. The purpose of this study then, is to systematically explore the possibility that pings can enhance the readout of reactivated long-term memory contents. To this end, we presented participants with pings as memory processes were actively engaged during cued recall, evaluating whether retrieved representations are more robustly discernible after ping onset.

4.2 Methods

4.2.1 Participants

We recruited thirty-three volunteers (22 women, M_{age} = 23.8 years, SD_{age} = 2.6 years, range = 18 to 31) with normal or corrected-to-normal vision, and with no history of epileptic attacks or neuropsychological conditions that could interfere with the examined study effects. The sample size required to derive a reliable effect was estimated based on Wolff et al., 2017, though our estimation was limited by the fact all previous work was in a WM context. One participant did not finish the experiment because they were unwell, and following data inspection, two participants were removed because of poor data quality due to a large number of high impedance channels, and one because of stimulus trigger issues. Thus, EEG-based analyses were conducted based on 29 participants. For behavioural analyses, the first four participants were excluded because of missing button press triggers, which, with the further exclusion of the participant who did not complete the experiment, resulted in an analysis of 28 participants (participants with noisy EEG data were included in the behavioural analysis).

Participants were informed about the details of the experiment in advance—including its duration, protocol, and methods—but were left naïve with respect to the purpose and hypotheses associated with the presentation of visual pings. Participants provided their written consent, and after the experiment, they were debriefed and given information about the central manipulation and hypothesis upon request, and they were compensated for their time with £9 per volunteered hour. The study was approved by the Ethical committee of the College of Science and Engineering of the University of Glasgow (Application number: 300210113).

4.2.2 Stimulus and apparatus

The presentation of stimuli was controlled using PsychoPy (version 2021.2.3; Peirce et al., 2019) running on Windows 10. Stimuli were presented on a CRT monitor (53.3 cm; 1024 by 768 pixels) operating at a refresh rate of 60 Hz. Participants were seated in a magnetically shielded room in a chinrest 65 cm from the screen, or at an approximately similar distance from the screen outside the chinrest if they experienced discomfort. Throughout the experiment, a fixation cross (with a visual angle of 0.44°) was presented in the centre of a constantly presented grey background (RGB = 128 128 128; PsychoPy default). All centrally presented stimuli overrode the fixation dot. The visual impulse (i.e., ping) was a single full-contrast bullseye stimulus presented at the centre of the screen for 200 milliseconds (ms;

with a diameter of 13° and 0.31° cycles per degree). The ping was generated using MATLAB and edited using GIMP (GNU Image Manipulation Program version 2.10.32).

In the main memory task, participants learned associations between action verbs and images, and were later prompted with the action verb to retrieve the associated image. The action verbs were selected based on usage frequency (largely based on Linde-Domingo et al., 2019) and the image stimulus set was a combination of 192 colour images collated across various royalty free databases, including the Bank of Standardized Stimuli (BOSS, Brodeur et al., 2010), and the SUN database (Xiao et al., 2010). The selected 192 images were constructed to follow a nested category structure of three embedded hierarchical levels. At the top level, the set consisted of 96 objects and 96 scenes, which were in turn composed at the middle level of 48 animate and 48 inanimate objects and 48 indoor and 48 outdoor scenes. Moving down to the bottom level, each of the middle level categories branched out into 4 categories (e.g., for animate objects: birds, insects, mammals, and marine animals), each of which contained 12 specific instances (e.g., twelve specific birds). We chose this nested hierarchy of stimulus categories because we did not know a priori what dimension of retrieved memories would be effectively decodable, so we included multiple levels of abstraction and chose one level based on pre-defined criteria (See *Level Selection*). The objects were presented on a white square matching in size to scene images (i.e., the visual degrees of all stimulus categories were 13°). Key presses were registered using a standard QWERTY keyboard.

4.2.3 Procedure

The main experiment consisted of 8 blocks, each with an encoding, distractor, recall, and recognition phase (Fig. 4.1A). In total, the main experiment lasted between approximately 45 and 65 minutes depending on the duration of self-paced breaks and electrode impedance maintenance. Before the main experiment, participants were provided with a practice run that covered each phase using example verbs and images that were not used in the main experiment. A standardized set of verbal instructions were provided to guide participants through the practice run. If the participant reported not understanding the task or if they did not give accurate responses, the practice run and instructions were repeated. Then, the main experiment commenced, throughout which EEG was acquired. At the start of each experimental phase, a screen was presented with a reminder of the task instructions and required response keys.

In the encoding phase, participants learned to build a mental association between action verbs and paired images. First, a verb was presented for 1500 ms (white, *OpenSans* font). Then, after 1000 ms, the associated image was presented until the spacebar was pressed to indicate the association was encoded (with a 6000 ms limit). Then, after a 1000 ms delay, the next verb was presented. During each block's encoding phase, 10 unique verb-image pairs were learned in one shot. This resulted in 80 encoded pairs across the full experiment, with the images pseudo-randomly selected from the full stimulus set such as to maintain an equal distribution of top-level stimulus categories (40 objects and 40 scenes) and fully random selection over nested middle and bottom levels.

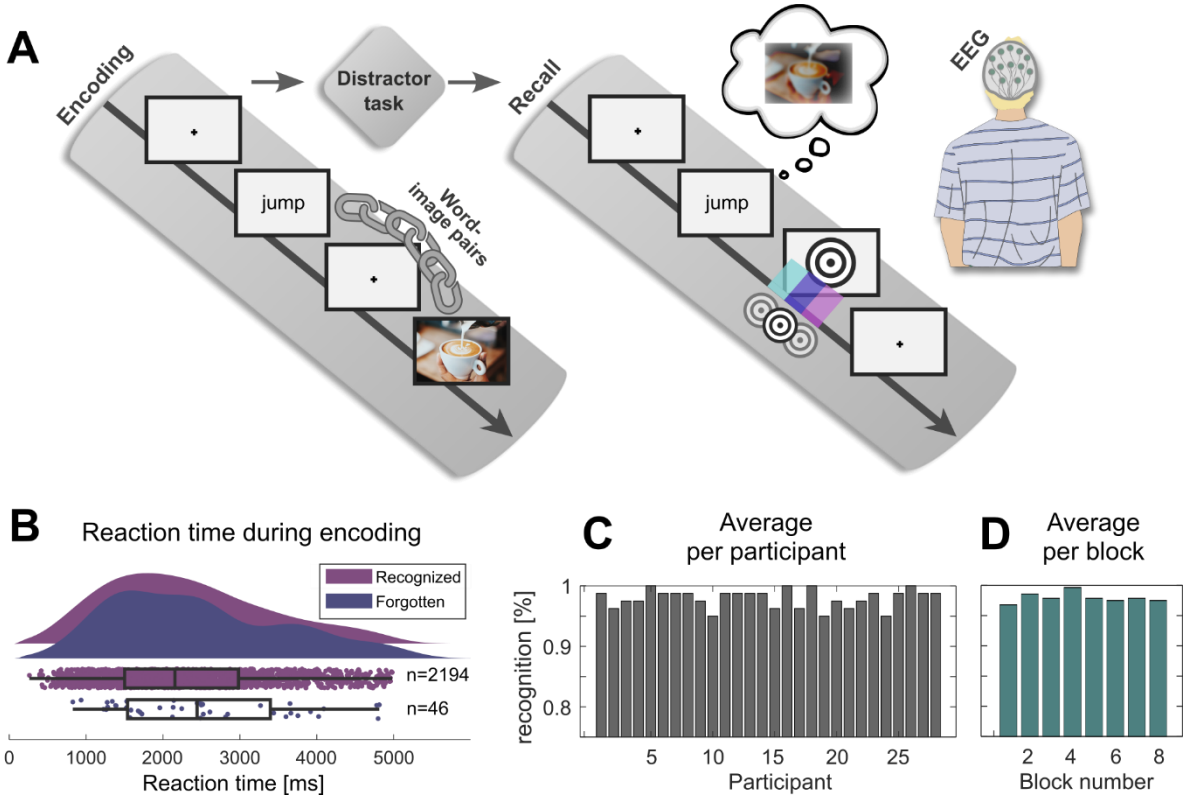

Figure 4.1. Paradigm and behavioural results. **(A)** Experimental paradigm. The encoding phase consisted of a word-image pair learning task. This was followed by a distractor task intended to wash out working memory effects. Then, during the recall phase, individual word-image pairs were retrieved while visual perturbations (pings) were presented in 75% of trials. In a fourth phase, recognition performance was tested (not displayed). **(B)** Reaction time during encoding for subsequently recognized and forgotten trials (collapsed across participants and blocks). **(C)** Average recognition performance per participant. **(D)** Average recognition performance per block.

The distractor phase that followed was included to flush out WM effects. Here, participants performed an odd-even task lasting 20 seconds. A number between 1 and 99

was presented in the centre of the screen (white, *OpenSans* font), and participants were instructed to press left key for odd numbers, and right key for even numbers. Following a left or right key press, the next number was presented immediately. Participants' average performance was displayed at the end of the distractor phase, marked as the proportion of correct responses. This data was not further analysed.

Next in each block, the recall phase tested our central manipulation of a ping-based visual perturbation. In this phase, participants recalled the learned verb-image associations of the encoding phase. First, one of the ten encoded verbs was presented for 2000 ms, serving as the retrieval cue that prompted recall of the associated image. In 75% of trials, a visual impulse was presented in either of three time bins: between 500 to 833.33 ms ("early ping"), 833.34 to 1116.67 ms ("middle ping"), or 1116.68 to 1500 ms ("late ping") after the onset of the retrieval cue, with a uniform distribution of possible ping times within each bin. This window was chosen on the basis that previous research on cued recall paradigms suggests this is the moment of maximum memory reinstatement (Staresina & Wimber, 2019). In 25% of trials, no visual impulse was presented in order to derive a baseline for statistical hypothesis testing. Participants pressed the left key to indicate that they had forgotten the image associated with the verb cue, or right key to indicate they remembered it. Key presses only resulted in a new trial after 1700 ms following retrieval cue onset (i.e., 200 ms after the latest possible ping). With presses earlier than that, nothing happened. Participants were given a visual indication that key presses were available via disappearance of the retrieval cue (at its offset; 2000 ms). During the recall phase, each of the 10 encoded verb-image pairs were tested four times, resulting in 40 recall trials per block, and 320 trials in total, comprising 160 objects and 160 scenes. Within participants, each of the four conditions—early, middle, late, and no ping—were configured to present object and scene images equally often (i.e., the top-level stimulus category), with the nested mid and bottom-level categories randomized. The sequence of presented stimulus level categories, pinging conditions, and verb-image pairs was fully randomized within and across blocks to mitigate order effects.

Finally, since the cued recall phase only included subjective memory judgments, a recognition phase was included to obtain an objective measure of memory performance for the verb-image pairs. During this two-alternative forced choice task, one of the 10 encoded verbs was presented in the centre of the screen, with two images (visual angle of 7.8°) presented underneath, one on the left-hand, and one on the right-hand side of the screen. Participants chose which of the two images was paired with the central action verb using a left or right key press (with a 5000 ms time limit). The location of the correctly paired image

was randomized between the left and right location. The lure image was always another old image from the immediately preceding encoding phase. Each of the 10 encoded verb-image pairs was tested once in a random sequence. Note that we designed this study to expend most of the available study time on the recall phase to maximize the statistical power of our main analysis, with the recognition phase serving chiefly as a basic check to ensure participants were not skipping through the experiment without memorizing verb-image pairs.

4.2.4 EEG acquisition and preprocessing

The data was recorded using a 64-channel passive EEG BrainVision system (BrainAmp MR; Brain Products) with a sampling rate of 1000 Hz. For our recording software we used BrainVision Recorder (Brain Products). The 64 Ag/AgCl electrodes were positioned in accordance with the extended international 10-20 system. Due to a necessary change in the recording system, a different EEG cap type (EasyCap) was used for participants 1 to 14 (subset 1) and 15 to 33 (subset 2). In the first subset, the ground electrode was located on the back of the head, below occipital electrode Oz, and two EOG channels were used to monitor eye movements (placed below and next to the eye; VEOG and HEOG). In the second subset, the ground electrode was on the midline frontal location AFz, and one EOG channel was used to measure eye movements (placed below the eye; VEOG). Furthermore, the cap used in the second subset included channels FT9 and FT10. For event related potential analyses, we included only electrodes common to both caps to enable a universal visualization of brain activity. Most electrode impedances were kept below 25 kiloΩ, and electrodes with outlier impedances were removed during preprocessing, with their associated data interpolated (see below).

Preprocessing was performed using FieldTrip (Oostenveld et al., 2011) in MATLAB (the MathWorks). First, the continuous EEG data was split up into two datasets: one with all trials epoched relative to retrieval cues, and one with trials epoched relative to pings and no-ping (defined by randomly sampling ping times of the pinged trials, yielding so-called "pseudo-pings"). Put differently, the data was locked once to $t = 0$ defined as the retrieval cue, and once to $t = 0$ defined as the manipulation of interest or a baseline alternative. In both cases, the epoched trials were 4 seconds in duration (-1 to 3 seconds relative to the event of interest).

Each dataset was filtered between 0.05 and 80 Hz and downsampled to 250 Hz. Next, bad trials and channels with outlier impedance levels were manually removed via visual inspection. Subsequently, eye movement and muscle artefacts were identified and removed

using ICA decomposition, and removed channels were interpolated using spline interpolation (with the FieldTrip function *ft_scalpcurrentdensity*). Finally, the data was re-referenced using a common average and a Laplacian method (current source density), deriving separate data structures for cue-locked and ping-locked analyses.

4.2.5 Behavioural analysis

The experiment was designed to result in high or even ceiling memory performance in order to obtain a maximal number of successfully remembered trials, and to optimally evaluate the central hypothesis of a ping-induced decodability enhancement. We report objective performance for the memory test conducted in the recognition phase, both across participants (Fig. 4.1C) and across blocks (Fig. 4.1D). We also report subjective judgments during the recall phase, quantifying how often participants report remembering versus forgetting the word-image pair. Reaction time (RT) during the recall phase is uninformative, because as described in the Procedure section, the response key was locked until 1700 ms after cue onset, at which point participants likely had already retrieved the associated image (Staresina & Wimber, 2019). Indeed, participants reported actively waiting for response buttons to become available. Thus, we instead analysed RT during the encoding phase as a function of whether the word-image pair was subsequently recognized or not. These RT data were collapsed across participants and blocks (Fig. 4.1B). For the proceeding analyses, both recognized and forgotten trials were included.

4.2.6 ERP analysis

For the ERP analyses, only channels common to both electrode cap subsets were used. We applied two types of ERP analyses, one locked to (pseudo-)pings and one to retrieval cues. FieldTrip was used to downsample the data to 250 Hz and a band-pass filter between 0.2 and 40 Hz was used. The data was baseline-corrected from -200 ms to 0 ms from events of interest. For ERP traces, we calculated the average activity across posterior channels (C3, C4, P3, P4, O1, O2, Cz, Pz, Oz, CP1, CP2, C1, C2, P1, P2, CP3, CP4, PO3, PO4, PO7, PO8, CPz, POz). For ERP topographies, we used the 61 channels common to both ERP cap types. We statistically evaluated whether pings resulted in higher amplitude ERPs compared to no-ping trials using non-parametric Monte Carlo permutation tests applied to each channel, correcting for multiple comparisons using Bonferroni correction as implemented in FieldTrip, averaging activity from 200 to 400 ms after pseudo-pings (alpha = 0.05; 10^5 randomizations).

4.2.7 MVPA analysis

For MVPA, all available EEG channels available per electrode cap type were used except EOG channels. Depending on the analysis, we trained and tested either a multi-class LDA using FieldTrip (*ft_timelockstatistics*), or a binary-class LDA using the MVPA Light toolbox (Treder, 2020). We classified EEG data re-referenced using a Laplacian transform on the basis that it accentuates local patterns (J. Kayser & Tenke, 2015). All classifier analyses were performed on the recall phase, where our main hypothesis could be evaluated. Unless specified otherwise, analyses were carried out on the retrieval cue-locked dataset. We downsampled the data from 250 Hz to 50 Hz by applying a moving average with a window length of 140 ms in length, moving in steps of 20 ms. During each step, a Gaussian-weighted mean was applied in which the centre data sample of the window was multiplied by 1, and the tail samples by 0.15 (FWHM = ~81 ms). In a subsequent step, sample by sample, the data was z-scored across channels (i.e., setting every channel to mean = 0 and standard deviation = 1), followed by training and testing using LDA. To evaluate decoder performance, we applied k-fold cross validation (5 folds, with 25 repetitions). For binary class decoding, we used area under the receiver operating characteristics curve (AUC) as a performance metric because it adjusts for class imbalances (Grootswagers et al., 2017; Xie & Qiu, 2007). For multi-class decoding, where standard AUC is unavailable, we used accuracy and factored in level-specific differences in chance levels. To infer decoding performance values under the null hypothesis, depending on the analysis, we either used no-ping trials or ping trials with shuffled class labels (100 1^{st}-level permutations, each with 3 repetitions). All analyses were restricted to the period before button presses were made (i.e., < 2000 ms).

4.2.8 Level selection

We used a multi-class LDA on no-ping trials to determine which retrieved stimulus category (top, middle, or bottom level) is most robustly detectable in the data when our main experimental manipulation was not applied. This level was then locked in for subsequent analyses that relate to our key hypothesis of ping-induced decoder enhancement. We selected the level with a high baseline performance to offer a conservative starting point from which we could establish whether pings are a powerful tool to further enhance decodability. However, as we will see in the results, stimulus selection rationales matter minimally because we found no reliable level differences in the no-ping decoder across levels to begin

with. For statistics, we performed a Wilcoxon rank sum test comparing the empirical and shuffled decoding performance for each level, in the way described in the next section.

4.2.9 Main analysis

For our statistical analysis of our main hypothesis, we used two-level permutation testing for the ping versus shuffle decodability comparison, and a Wilcoxon ranked sum test for the ping versus no-ping comparison. The former approach, which is based on van Bree et al., 2022, implemented the following algorithm in pseudo-code—applied window-by-window:

1) For each 2^{nd}-level permutation (10^5 times): Grab one random window-specific decodability value from the 1^{st}-level distribution of permutations of each participant and average the result. This yields 10^5 permuted averages.
2) Generate one p-value by calculating the percentile of the average empirical decoding value within the distribution of permuted averages.

The latter approach involved taking the Wilcoxon signed-rank test between the distribution of empirical decoder results and 1^{st}-level permutation results across participants. We opted for a Wilcoxon test over cluster-based methods because it makes minimal assumptions about the distribution of decoding results (Wilcoxon, 1945; Grootswagers et al., 2017). For both approaches, we adjusted the resulting p-values across windows for their false discovery rate (FDR). Since the p-values are not independent across time, we applied the approach by Benjamini & Yekutieli (2001).

Finally, for ping-locked analyses we restricted statistical analyses between 0 and 500 ms from ping onset. For analyses locked to retrieval cue, we analysed 500 to 2000 ms from cue, which is the approximate range where memory retrieval processes are active (Staresina & Wimber, 2019).

4.2.10 Condition-relative decoding peaks

In addition to our main analysis, we carried out a presumably more sensitive analysis to evaluate the possibility of ping-induced decoding enhancements. We reasoned that even if visual pings do not offer an enhancement of LTM decoding performance that is strong enough to emerge in a direct ping-to-no ping or ping-to-shuffle comparison, there could still be a weaker effect that is detectable by factoring in the relative order of pinging conditions. Specifically, we tested whether trials with an early, middle, and late ping tended to have, respectively, earlier, later, and even later decoding performance peaks. In other words, we

tested to what extent decoding peaks captured ping presentation orders (see Linde-Domingo et al., 2019; Mirjalili et al., 2021 for similar peak selection approaches).

First, we took every participant's SOA-specific decoding time series—early, middle, and late—and extracted one peak (specified below). Then, we calculated a *peak order distance* (POD) per participant, defined as the absolute serial distance between the order of extracted peaks and true ping presentation order, given by the formula:

$$POD_{non-normalized} = \sum abs(peak - \ true)$$

For example, if the decoder peak came first for early ping trials (1 − 1), third for middle pings (3 − 2), and second for late ping trials (2 − 3) this would amount to a POD of two. We divided PODs by the maximum distance (4), normalizing the score between zero and one:

$$POD = \frac{\sum abs(peak - \ true)}{maximum \ distance}$$

On this distance metric, lower values indicate a closer correspondence between ping-induced peaks and condition presentation order, which in turn confers stronger evidence for ping-based decoding enhancement. For our statistical evaluation, we used a two-level permutation approach (similar to van Bree et al., 2022). Specifically, we compared the distribution of empirical PODs with PODs calculated across 10^6 second-level permutations, randomly grabbing from the pool of first-level shuffled decoder time courses. The p-values were defined by the resulting percentile of the empirical POD within the distribution of second-level shuffled PODs (one-sided test, empirical < permuted).

For the detection of decoder peaks in this analysis, we detected the maximum peak in the derivative of the cumulative sum of decoding time series. We chose this peak detection method over more standard approaches—such as simply extracting the largest peak from raw decoding series—because independent simulations revealed that this algorithm is most powerful at detecting true POD effects, outperforming a range of competing approaches (Supplementary Material Chapter 4, section 2).

4.2.11 Brain time warping

As we will see, no compelling evidence was found for category decoding across conditions or category levels. Given that brain time warping appears suited to improve the statistical reliability of decoding (Chapter 3), we evaluated whether the algorithm increases the number of significantly classified timepoints in these data. Specifically, we used the cue-locked no ping trials at the top category level as a basis to apply the brain time algorithm. The reason to use trials without a ping is that striking ping-evoked activity could interfere with brain time warping, which requires a lack of contamination by extraneous signals that could impede the phase estimation of warping signals. We used cue-locked data because—as we will see—it has higher accuracy values compared to the ping-locked data. We brain time warped and classified the top category level (objects versus scenes) for the same reasons as with the main analysis (i.e., it affords binary classification).

Warping signal

We extracted ICA components from the no ping cue-locked trials and ranked them based on the average power at alpha frequencies (8 to 12 Hz). Then, we manually selected a warping signal based on which candidate warping signals optimally met two criteria: (1) the presence of an alpha peak, (2) a topographical profile that suggests media-temporal areas as a possible source. The reason for choosing alpha frequencies is that these rates are prominent and implicated in memory processing (Klimesch, 1997, 1999). Importantly, in spite of the important role of theta oscillations in memory (Chapter 2), we opted against theta-based warping signals because we did not observe theta peaks or high theta power in our data. After brain time warping, we removed the warping component before classification.

Brain Time Toolbox settings

The toolbox settings were set as in the analysis described in Chapter 3; Section 3.3.3.

Decoding parameters

For the decoding of brain time warped data, we used the same configuration as for the main analysis on clock time data (Section 4.2.7)—allowing for a direct comparison of the number of significantly decoded timepoints.

4.3 Results

4.3.1 Behavioural results

As expected in light of our experimental design, participants achieved high memory performance. This is evidenced by the high rate of remembered to forgotten judgments during the recall phase (M = 0.819; SD = 0.022) and the near-ceiling objective performance during the recognition phase across participants (M = 0.980, SD = 0.015; Fig. 4.1C) and blocks (M = 0.980, SD = 0.009; Fig. 4.1D). The average RT during encoding was 2313 ms for subsequently recognized trials (SD = 1041 ms; n = 2194 trials), and 2472 ms for subsequently forgotten trials (SD = 1105 ms; n = 46 trials; Fig. 4.1B).

4.3.2 Event-related potentials

We observed a robust evoked EEG response after pings (Fig. 4.2). Specifically, for each of the three stimulus onset asynchrony (SOA) conditions, we observed an extended peak of activity across occipitoparietal channels that followed the distribution of ping times for retrieval cue-locked data, peaking approximately 200 to 300 ms after pings. To further confirm that pings successfully evoked a visual response, we applied a ping-locked analysis across all channels and found significantly higher ERP amplitudes after pinged than no-pinged trials in posterior channels (Fig. 4.2, insets). Together, the ERP analysis suggests pings yielded a strong time-locked response that could putatively interact with ongoing LTM representations. For cue-locked and ping-locked ERPs for each participant, time-resolved topographical plots, and for p-values of each channel in Fig. 4.2 inset topographies, see the Supplementary Material Chapter 4; Section 1.

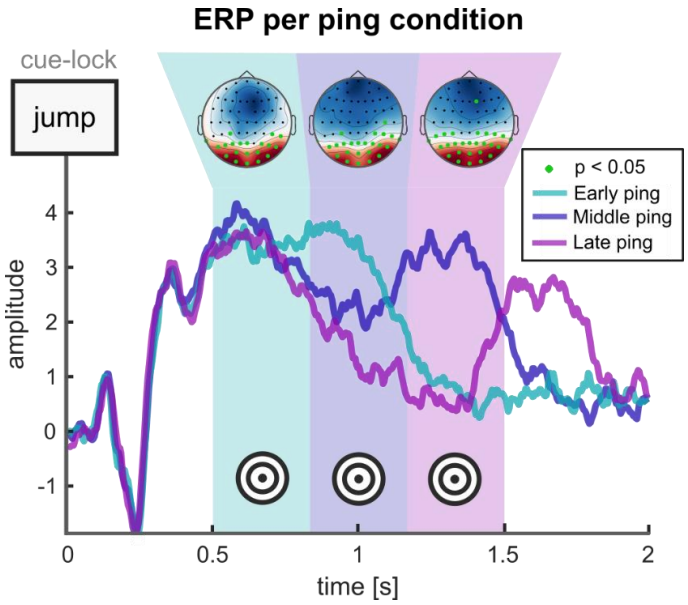

Figure 4.2. Ping-induced event-related potential. Average evoked response in posterior EEG channels across early (turquoise), middle (blue), and late ping (purple) trials during the recall phase. The inset topographies reveal higher posterior amplitudes following ping trials as contrasted with no-ping trials (Monte Carlo permutation test; Bonferroni-corrected).

4.3.3 Decoding results

Stimulus category selection

We used a multi-class LDA on no-ping trials (25% of the overall recall trials) to determine which retrieved stimulus category (top, middle, or bottom level) is most robustly decodable when our main experimental pinging manipulation was not present (Fig. 4.3). We found that none of the three levels displayed significant windows of decodability during our retrieval period of interest from 500 to 2000 ms after cue onset (Wilcoxon signed-rank test; $p > 0.11$ for top; $p > 0.25$ for middle; $p > 0.07$ for bot). We proceeded with the top-level, which with its two classes (objects and scenes) afforded simple binary classification with comparatively low variability in decoding performance. Next, during our main analysis, we investigated whether pings enhance the decodability of LTM contents.

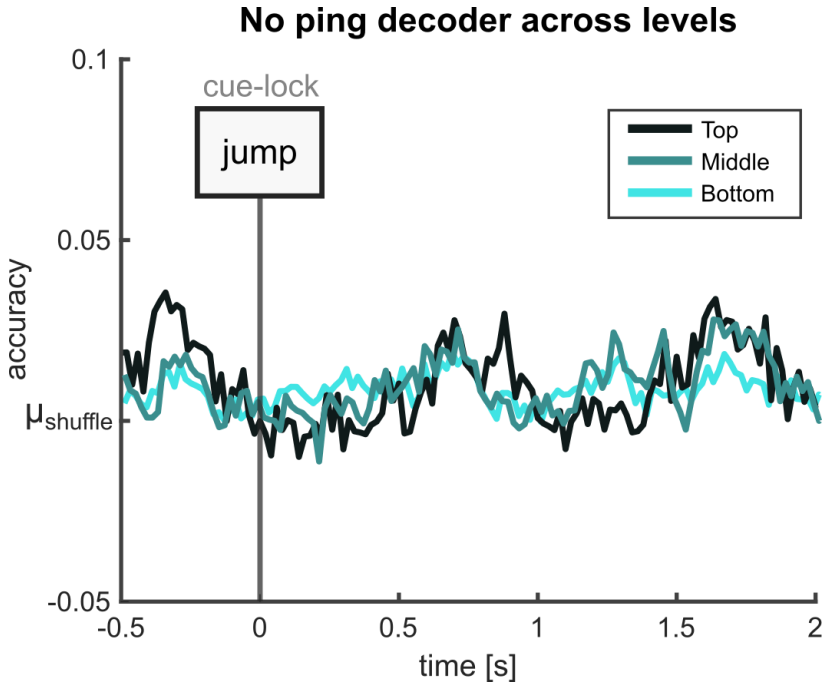

Figure 4.3. Stimulus category selection. Average decoding accuracy across stimulus category levels (top, middle, bottom). Decoding accuracy was quantified relative to the average performance across shuffled decoding results. No significant differences were observed for any level (Wilcoxon signed rank test, controlled for multiple comparisons using FDR).

Main analysis

For our central analysis, we compared decoder performance between ping and no-ping trials for top-level (objects vs scenes) classification, both with the data locked to retrieval cues, and to pings/pseudo-pings (i.e., artificial markers derived from the pool of ping timings; Fig. 4.4). For the cue-locked analysis, we found no windows where decoding was above chance for no-ping trials (two-level Monte Carlo permutation; $p > 0.49$; Fig. 4.4A), while the ping trials showed several significant windows of content decodability ($p < 0.05$; Fig. 4.4B). To validate our analysis we carried out a direct comparison between the ping and no-ping trial decoder, as opposed to contrasting each condition with a shuffled baseline. In this analysis, we found no evidence for a ping-induced decodability enhancement; neither in the cue-locked (Wilcoxon signed-rank test; $p > 0.99$; Fig. 4.4C) nor in the (pseudo-)ping-locked data ($p > 0.99$; Fig. 4.4D).

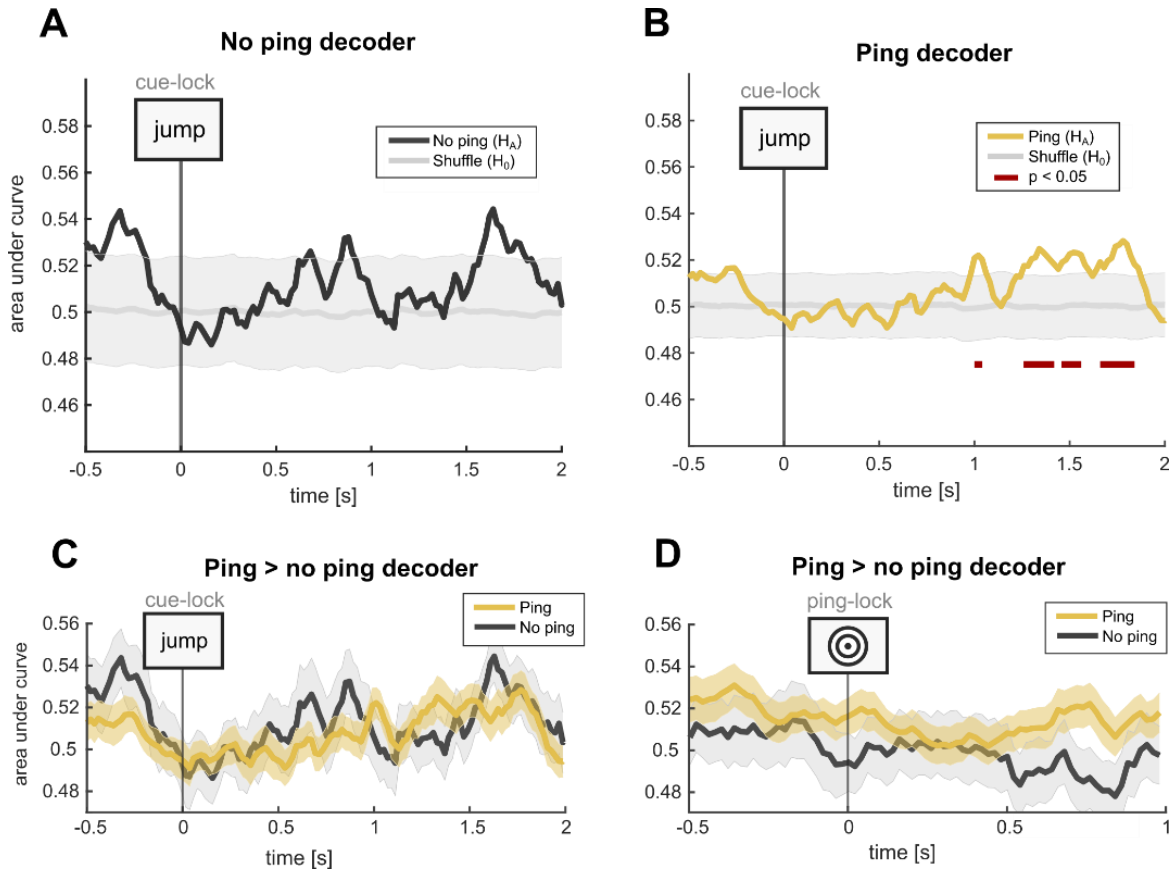

Figure 4.4. Main decoder analysis. **(A)** Cue-locked decoding across no-ping trials compared with a shuffled baseline. **(B)** Cue-locked decoding across ping trials compared with a shuffled baseline. **(C)** Direct comparison between on ping and no-ping trials. **(D)** Same as (C), but with the data time-locked to pings and (artificially marked) pseudo-pings. In (A) and (B) the shaded area represents the 5th and 95th percentile of the distribution of 2nd-level permutations of the shuffled decoder, and in (B) and (C) it represents the SEM of the empirical decoder. In (A) and (B), p-values were derived using two-level Monte Carlo

permutations, and in (C) and (D) using Wilcoxon signed-rank test (all p-values were corrected using FDR).

In light of an important methodological observation, we place more importance on the latter analysis, which directly compares the empirical decoding performance for ping and no-ping conditions without leveraging shuffled results. Specifically, we observed that the standard error of the mean (SEM) of the shuffled distributions varies substantially between ping (μ_{SEM} = 0.047) and no-ping (μ_{SEM} = 0.028), which we speculated could be explained by trial number differences alone. We inferred that since the ping trial decoder was trained and tested on three times more trials than the no-ping trial decoder, this might naturally shrink SEM values of the shuffled distribution and thereby modulate test statistics. In support of this interpretation, we build a simulation which confirms that an increase in the number of trials (and the number of decoding classes) reduces p-values, but only if there is an effect in the data (Supplementary Material Chapter 4; Section 3). Therefore, instead of relying on ping-to-shuffle and no-ping-to-shuffle comparisons where power differences might misleadingly lead us to infer a ping-related enhancement, we put most credence in the direct comparison between ping and no-ping trials in which shuffled results are sidestepped (Fig. 4.4C & Fig. 4.4D; see the Supplementary Material Chapter 4; Section 3.3 for an extended discussion).

Condition-relative decoding peaks

Next, we turn to the presumably more sensitive peak-order analyses. Qualitatively, we observed no ordered structure in decoder peaks when averaging across participants for each SOA pinging condition (Fig. 4.5A). For a quantitative analysis, we formally compared peak

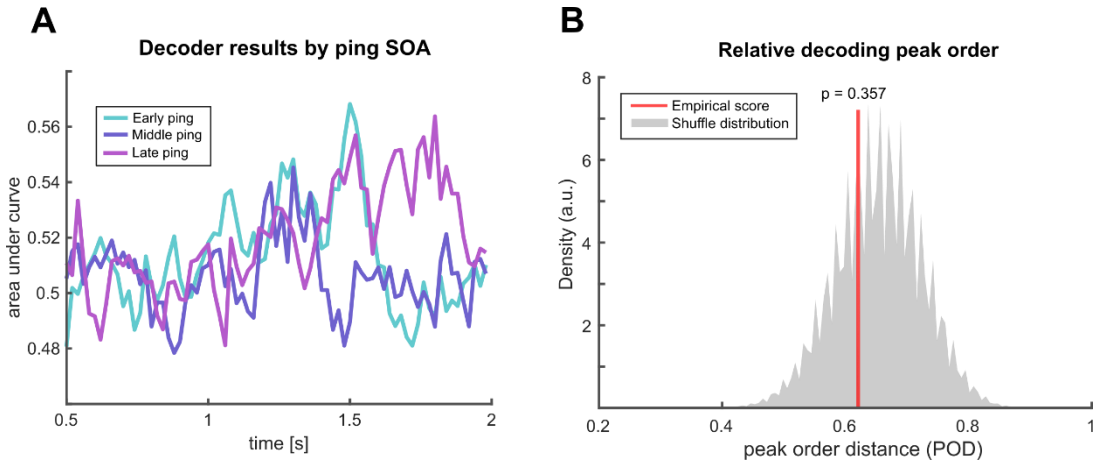

Figure 4.5. Condition-relative peak analysis. **(A)** Decoding results specific to for early (cyan), middle (blue), and late (purple) ping conditions, averaged across participants. **(B)**

Peak order distance scores for the empirical decoder (red line) among a pool of 2nd-level permutations derived from the shuffled decoder (grey distribution).

order structure by comparing POD scores for the empirical and shuffled decoder using two-level permutation tests. This analysis confirmed the previous result by revealing no significant evidence for the hypothesis that pings induce systematic differences in the order of decoding peaks ($p = 0.357$; Fig. 4.5B).

4.3.4 Brain time warping

Given the lack of compelling evidence for significant decoding across conditions, we applied brain time warping under the assumption that it could increase evidence for the read-out of neural activity underpinning cognition. We predicted that the cue-locked no ping decoder—which has no significant windows in clock time (Figure 4.4A)—would have significant windows after the application of warping. Contrary to our expectations however, the decoder trained and tested on the brain time warped data did not display any windows of significant classification either (Figure 4.6; two-level Monte Carlo permutation; $p > 0.99$). Qualitatively, the classifier time series trained and tested on brain time data looks similar to the classifier applied to the default clock time version of the no ping trials. Statistically, brain time warping does not increase the proportion of decoding windows with AUC values above chance levels following multiple testing correction (FDR). This suggests that brain time warping, in this experimental and analysis context, is not able to facilitate the readout of neural signatures that differentiate between the retrieval of object or scene images. If anything, the fact that classification looks qualitatively noisier over time, and the reduction in markedness of the late decoding peak (compare with figure 4.4A; circa 1700 ms) suggests that brain time warping could have deteriorated the consistency of the neural code in the data. One possible reason for this is that alpha oscillations do not coordinate the neural patterns associated with paired object and scene memory representations, with hard-to-detect theta oscillations or non-oscillatory dynamics orchestrating this neural code instead.

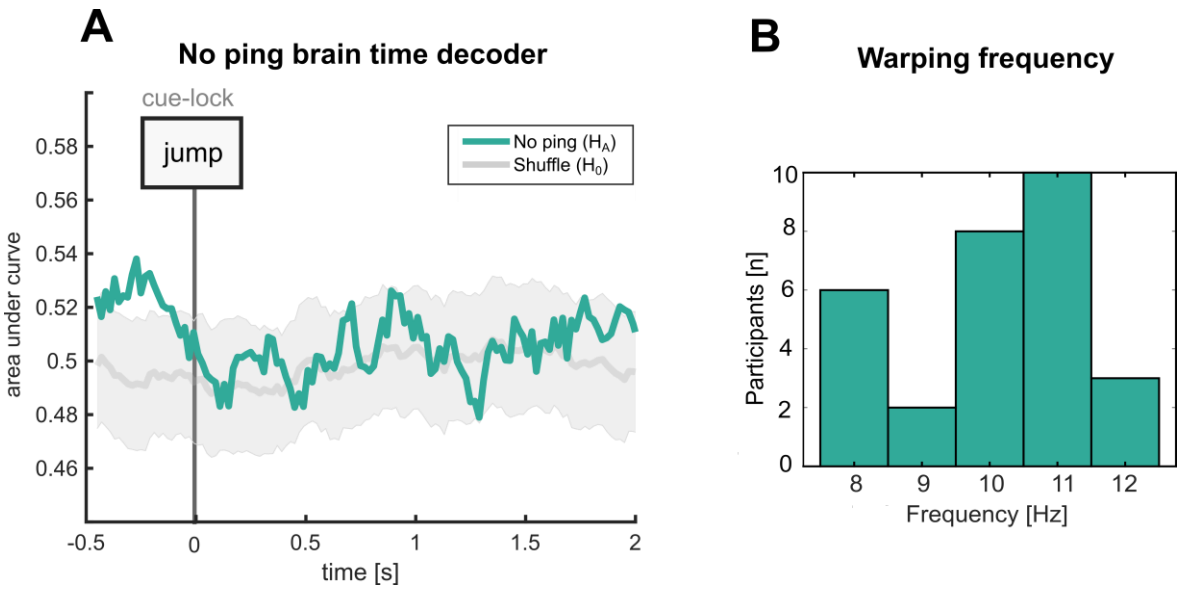

Figure 4.6. Brain time warping results. (A) Cue-locked decoding across brain time warped top category level no-ping trials compared with a shuffled baseline (i.e., a decoder applied to the same data with permuted class labels). As with the decoder trained and tested on clock time data, no significant classification windows obtain. **(B)** The distribution of alpha warping frequencies across participants.

4.4 Discussion

In this study, we set out to systematically evaluate visual perturbation, or ping-based stimulation, as a method to dynamically enhance the decodability of reactivated neural representations during memory recall. Such an approach could supplement offline analytical approaches by adding further read-out enhancements online at the experiment side. Despite promising results in the WM literature, in this LTM context we found no evidence for a ping-based enhancement across several time-resolved decoding analyses. While pings evoked a strong brain response, they did not detectably boost neural signatures of memory representations in EEG data. We draw this conclusion based on two key results. First, in the main comparison between pinged trials and non-pinged trials, we found no significant decoding difference regardless of whether the data was locked to (pseudo-)pings or retrieval cues. Second, in a more advanced analysis that leverages the constraining information of ping presentation timings during the experiment, we also found no evidence for ping-related decoding increases.

There are three overarching explanations for these null results. First, there could be an effect in the data that was left undetected analytically or statistically. Second, there could be an effect that manifests across other experimental contexts, but not with this study's

parameters. Third, there could be no effect in principle, with LTM-based retrieval eluding the enhancement of representational readouts using pings. We consider each option in turn.

First, the signal analysis parameter space is high, with variability in parameters across preprocessing and statistical analysis steps potentially altering the results. One important source of variability concerns the implementation of decoding techniques. Namely, we do not rule out that untested decoding methods such as linear approaches beyond LDA or non-linear classifiers would have resulted in performance enhancements induced by pings. More trivially, our analyses could have been optimal, with our key statistical results containing a type-II statistical error.

Second, the parameter space on the experimental side is also high. Here, we opted for a word-image association task, which has previously been shown to afford classification-based inferences about memory processing in the brain (Linde-Domingo et al., 2019; Martín-Buro et al., 2020; Mirjalili et al., 2021). However, other LTM tasks might be better situated to reveal ping-based enhancements. Besides the memory task itself, a key set of parameters concerns the presentation of pings. In this study, we chose a high-intensity, short-lasting ping presented with a uniform distribution between 500 and 1500 ms after retrieval cues. This time window was selected based on a review of the timeline of memory reactivation during cued recall, which suggested a maximal content reinstatement within this period (Staresina & Wimber, 2019). However, we observed that decoding was highest late within and even after this range, at approximately 1200 – 2000ms after cue (see Fig. 4.4D). Decoding plateaus that exceed 1500ms have also been observed in recent work that employed a similar task and analysis pipeline (Kerrén et al., 2022). This raises the possibility that the aforementioned 500 to 1500 ms window is biased to be too early—perhaps because it was estimated based on intracranial EEG research where recordings tend to focus on the hippocampus and other regions that activate early during retrieval (Merkow et al., 2015; Mormann et al., 2005). Put differently, it is possible that we did not find significant effects because the signatures of retrieved contents tended to arise robustly only after our ping presentation times. We recommend that future work considers later ping times, potentially informed by maximum decodability periods found in this and other work, or ideally in newly acquired pilot data. Moreover, additional research could explore parameters such as ping duration, intensity, and strength. Furthermore, besides visual pings, a plethora of other perturbational approaches are on stock that could realize the ping's proposed effects. Also inspired by WM research, stimulation using auditory impulses might offer a multimodal route to improving the readout of LTM contents (Kandemir & Akyürek, 2023). Furthermore,

brain stimulation methods like transcranial magnetic and ultrasound stimulation have the potential to regularize brain activity through the induction of a dynamics-altering magnetic or ultrasound pulse (Moliadze et al., 2003; Mueller et al., 2014).

A third possibility is that none of these factors explain our null results, with ping-based approaches restricting their utility to WM tasks. One specific possibility could be that WM and LTM differ in their mechanisms of action, with separate kinds of neural processes underpinning them. Indeed, classically WM is believed to involve the active maintenance of stimulus-induced information (Fuster & Alexander, 1971; Goldman-Rakic, 1995), whereas LTM is assumed to be based on a generative reconstruction of past experience based on the activation of silent information-storing engrams (Josselyn & Tonegawa, 2020). Perhaps the sweep of activity associated with the ping interacts more effectively with functional brain activity maintained continuously from stimulus onset, thus explaining WM-to-LTM differences. Speaking against this interpretation is work that suggests WM representations are encoded in activity-silent networks through short-lasting synaptic changes (Kamiński & Rutishauser, 2020; Masse et al., 2020; Stokes, 2015), which would not be fundamentally different from how LTM works. Contradicting this in turn is a critique which argues that evidence for activity-silent networks in WM tasks could alternatively be explained by LTM processes kicking in (Beukers et al., 2021). Thus, since it is both unclear to what extent the mechanisms of WM and LTM differ and to what extent WM and LTM intertwine in studies where ping-based effects have been demonstrated, we avoid firm interpretations in this part of the possibility space. In summary, although pings unambiguously elicited expected patterns of visual activity (Fig. 4.2), we failed to observe effects on memory decoding, either because they were left undetected in our analysis, because they do not show up in our experimental protocol, or because they do not exist.

This study builds on decoding research that investigates the physical basis of memory, leveraging its findings for a strictly instrumental purpose: the systematic enhancement of LTM readouts. This undertaking is key because the field presently lacks temporally sensitive neuroimaging methods that enable the consistent and clear readout of memory representations, which is needed to explain how the brain implements memory processes. Thus far, most efforts to improve memory-readouts from electrophysiology data have been restricted to the signal analysis end. Here, we advocate for research that explores online manipulations as memory tasks are unfolding, which has previously shown to complement or synergize with decoding techniques. For long-term memory decoding in particular however, such interventions are scarce, which limits research because memory involves low

decodability to begin with. Thus, even if a further carving out of the parameter space does not demonstrate a notable benefit of visual perturbations, future research should creatively explore alternative online methods such as multimodal stimulation and non-invasive brain stimulation.

Chapter 5: General discussion

5.1 Retrospective

Let us return to the five most central claims of this manuscript:

1) Scientists study evolving neural patterns to investigate how cognition is implemented by the brain.

2) Oscillatory dynamics strongly influence or covary with the evolution of neural patterns of cognition.

3) As such, oscillatory dynamics offer a reference point or anchor by which the study of neural patterns can be improved.

4) We can adopt this reference point algorithmically by transforming recorded brain data in concordance with coordinating oscillations of interest.

5) Alternatively, we can adopt it by experimentally regularizing oscillatory dynamics during data acquisition.

The first claim has been given comparatively little treatment because it is uncontroversial, and more akin to a starting point. With that said, we have seen that neuroscientists have developed methodologies to parse neural activity under oscillatory and non-oscillatory regimes, with elaborate quantification methods to specify how such activity evolves. Furthermore, the veracity of claim (1) is underscored by the large body of discussed neuroimaging research that utilizes pairwise correlations, multivariate techniques, and other linear approaches to detect neural activity which is consistently correlated with cognition.

The second claim (2) was principally covered in Chapter 1 and 2, and to some extent in Chapter 3. First, we saw that oscillations impose (or at minimum reflect) excitability fluctuations across populations of neurons. This induces alternating temporal windows during which message-passing becomes promoted or inhibited, and this contributes to the grammar of neuronal computation. Second, for cognitive functions such as memory, oscillations play a distinctive role. The phase of theta oscillations indexes excitability states, and using self-organizational principles these states are leveraged to generate coding schemes along which memory representations get slotted. These phase-based coding schemes dynamically update with goal-directed behaviour, and they appear to give ensembles access to sequence and positional information. Theta phase also allows neural circuits to compute over confoundable internal and external representations through a delegation of these processes to opposing phases. Beyond dynamic phase codes and a phase-based switch, theta oscillations also phase-synchronize across distributed networks to

promote functional communication. This makes it easier for memory integration to happen and for retrieval processes to successfully reinstate dispersed neural representations.

In support of claim (3), the aforementioned points sketch a picture where excitability fluctuations become a kind of coordinate system by which external observers can parse neural patterns of cognition. The logic is roughly this: if neural patterns of cognition are generated by neuronal ensembles, and if the timing and way in which such ensembles operate depends on oscillatory phase and other spectral measures, then such measures offer a system-centric way by which spectators can parse the emerging patterns. Bolstering this point, the clock time by which we currently analyse our data seems inadequate in most cases, firstly because the brain lacks direct access to clock time, and secondly because from the perspective of neural mechanisms, milliseconds are less consequential than oscillatory cycles.

Insofar one accepts these arguments, one might ask what solutions are on offer to facilitate the brain-centric analysis of neuroimaging data. Further than that, even if one does not fully accept these arguments, one might nevertheless wish to try out analyses based on internal brain metrics to see if additional insights can be gleaned. Toward this end, I have presented two techniques. First, brain time warping offers a way to analytically bring neural activity closer in line with oscillatory components hypothesized to be relevant or informative to cognitive phenomena of interest (claim 4). We found that the resampling of electrophysiology data based on the dynamics of these key oscillations produces evidence for neural patterns of cognition that are harder to pick up in clock time. Second, visual perturbational methods might be used to regularize oscillatory dynamics on the fly. However, we disappointingly did not find evidence that visual *pings* detectably improve the readout of neural patterns of interest under the attempted experimental, analytical, and stimulus parameters. Thus, while this thesis confirmed claim (4), our own research found no evidence to support claim (5). With that said, as evidenced by a review of the literature in Chapter 4, point (5) still stands in light of promising applications in working memory tasks shown by other research groups.

5.2 Intellectual roots and targets

In essence, this thesis suggests that a brain-centric methodology for cognitive neuroscience is both required and feasible. This idea builds onto a series of previous contributions. First, these writings have benefitted significantly from György Buzsáki's book *The Brain from Inside Out*, which sketches an ambitious agenda for a neurally inspired science (Buzsáki,

2019). Furthermore, contributions before mine have already introduced the issue of experimenters imposing their interpretation of space and time onto ensembles, arguing that for those ensembles, space and time are instead grounded in interneural communication dynamics (Scharnowski et al., 2013). Interestingly, this work introduces the term *Neurorelativity*, which intuitively captures the points of this thesis and the emerging perspective with a single word.

I would like to take this term and use it to reiterate a distinction between two kinds of views. First, *Methodological Neurorelativity* considers the merits of a brain-centric approach in scientific experimentation, analysis, and methodology in general. Second, *Ontological Neurorelativity* considers the merits of a data-driven revision of psychological terms, especially their potential replacement with neural concepts (Buzsáki, 2019). I will take a brief moment to sharpen this distinction further.

Methodological Neurorelativity takes a fixed explanandum, such as cognition or goal-directed behaviour, and asks a series of questions about scientific approach. What methodological tension exists between experimental and neural dimensions? How might this lead us to miss out on neural patterns in our analysis, and what ramifications does it have for our scientific interpretations? What experimental and analytical solutions are available that bring neuroscience methods toward the language of neural information processing? In which situations is it safe to parse brain activity with reference to external temporal or spatial measurement units, and when is this prohibitive towards our goals?

Ontological Neurorelativity on the other hand concentrates on explananda themselves, asking questions of the following kind. What evidence does neuroimaging data provide for the integrity of concepts like attention? What do cytoarchitectonic, connectomic, and functional data tell us about the makeup of the human mind (Poldrack, 2006; Poldrack & Yarkoni, 2016)? What does the evolution of neural structures suggest about the nature and parts list of mental function (Cisek, 2019)? Essentially, Ontological Neurorelativity places significant evidential weight to brain data. So for example, if the question is whether imagery and retrieval are identical or separate processes, possible overlap in neural correlates and circuitry matters more than psychological findings on the cognitive-behavioural level.

Importantly, one can coherently maintain both, one, or neither of these two views. In this thesis, I advocate for Methodological Neurorelativity, but I remain agnostic to Ontological Neurorelativity. That is to say, it does not matter for any of my writings here whether neuroscience's explanandum is cognition in psychological terms, cognition in

neural terms, or a less metatheoretically loaded explanandum like goal-directed behaviour. In each case, the conflation of internal and external variables is on the lure.

5.3 Future directions

In general, if the problem identified across these writings is the illicit collapse of neural and worldly dimensions, then the solution naturally consists in neuroscientific approaches that avoid that. This calls for brain-inspired methodologies where variables related to oscillatory and non-oscillatory forms of brain activity are placed in the foreground, and where clock time and metric space are moved backwards. Encouragingly, research across cognitive and systems neuroscience is already moving in this direction. For example, spectral units like phase, power, frequency, phase synchronization, and phase-amplitude coupling are increasingly seen as not only basic variables with which cognitive correlations can be established, but also as a reflection of deeper principles by which activity patterns are organized (Bressler & Kelso, 2001). Indeed, as we have seen in Chapter 2 and Chapter 3 (Section 3.2.4), phase is not only being used as a covariate or behavioural correlate, but also as a theoretically relevant index of excitability states which influence how information is neurally represented and manipulated. The same goes for non-oscillatory dynamics, where the 1/f trend in the frequency spectrum of neuroimaging data is seen as not merely a cognitive correlate, but also as a proxy of the contributions of excitatory and inhibitory synaptic currents—which unquestionably determine how neural patterns of cognition unfold (Gao et al., 2017; Lombardi et al., 2017). I expect that this shift will continue, especially with technological advances that make it easier to track brain dynamics with high temporal and spatial precision (Trautmann et al., 2023; Ye et al., 2023).

In this manuscript, I have explored brain-inspired techniques that can be leveraged during data analysis (Chapter 3) and acquisition (Chapter 4). In a nutshell, we found that an approach falling in the former category managed to align brain dynamics to support the extraction of neural codes. On the other hand, we found no readout enhancements for a perturbational method applied during data acquisition. In my estimation, this is poetically reflective of the broader methods literature, in which algorithmic innovation is running ahead of approaches implemented while the experiment is ongoing. To be clear, the field of brain stimulation is flourishing, but much of this work seeks to establish causal relations between parts of the brain and cognition. A fruitful future avenue is to systematically explore whether and how these interventionist techniques can control brain dynamics for the express reason of improving the readout of unfolding neural patterns of cognition. Ultimately, the most

effective course of action may be for the field of cognitive neuroscience to encourage and explore creative pursuits that have a potential to bridge variables inside and outside the brain.

Appendix

Note: Unless otherwise stated, sections in the Appendix denote sections within the Supplementary Material. For example, if section 2.1 is called, this refers to section 2.1 within the Supplementary Material of the associated Chapter, not the main body of text. References to the main body are explicitly phrased with the term "main".

Supplementary material Chapter 3

1. Additional analyses

1.1. Control analysis

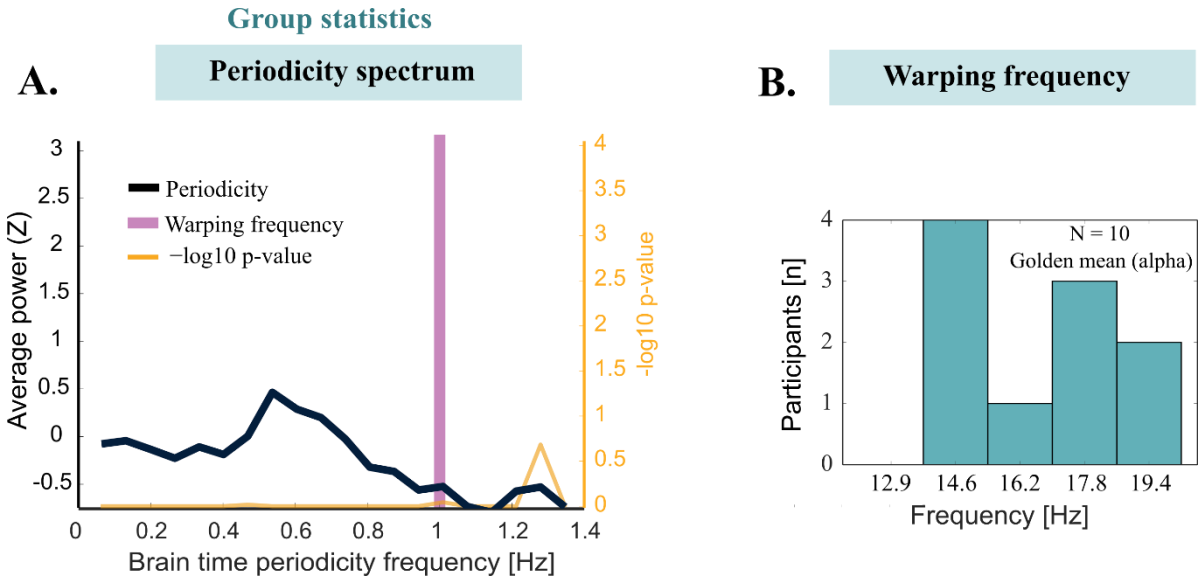

Supplementary Figure 1: Advanced control analysis of the simulation dataset. (A) We found no significant periodicity when warping to the golden mean of each participant's alpha oscillation. **(B)** Summary statistics of the warping frequency across participant.

Advanced analysis

To test for the specificity of brain time warping, we warped to the golden mean of each participant's warping frequency as obtained in the main analysis (Supplementary Figure 1). The logic is that if brain time warping is non-specific and prone to false positive results by trivially imposing oscillatory structure, then it should do so even for frequencies predicted to not have a clocking role in cognition. To test this possibility, we repeated the main analysis by warping to the golden mean of each participant's warping frequency (≈

$warping\ frequency \times 1.618$). We chose the golden mean as our control frequency because, at this frequency, the warping signal (which is predicted to be the clocking oscillation) is least expected to synchronize to different oscillations (Pletzer et al., 2010). The control analysis changed the warping frequencies from alpha (8 to 12 Hz) to approximately 12.9 Hz to 19.4 Hz. All other parameters were unchanged from the main analysis. The control analysis does not show significant periodicity at any frequency. We provide TGMs, autocorrelation maps and first-level periodicity spectra in 3.1.3.

These results demonstrate that brain time warping does not trivially impose oscillatory structure in high-level analyses by virtue of warping to a specific frequency if there are no such signatures hidden in the data. We next established whether the same conclusion extends to the family of basic analyses. Specifically, warping should not manifest in prominent peaks in the power spectrum, or high values in the ITC, at warping frequencies when those frequencies are only minimally present in the data.

Basic analysis

We repeated the control analysis to test for the effects of brain time warping on basic results like power spectra and ITC. As explained in the main text (*Is retuning using brain time warping circular?*), we expect brain time warping to at least show some increased power and ITC at any frequency because electrophysiology data is made up of different frequencies of oscillations which each have at least some non-stationarities that can be reduced. However, it should be the case that warping to oscillations not primarily simulated should result in lower power and ITC increases than warping to oscillations primarily simulated. To test this, we changed the main frequency of the random (1/f) dipoles to match the individual alpha frequency of the primary dipoles – strongly clustering the ground truth signals around alpha. We then again warped to the golden mean of alpha. We found that brain time warping to control frequencies only resulted in low spectral peaks and ITC at the control frequency (Supplementary Figure 2). In the power spectra, the primarily simulated frequency overshadows the brain time data even when warping to control frequencies.

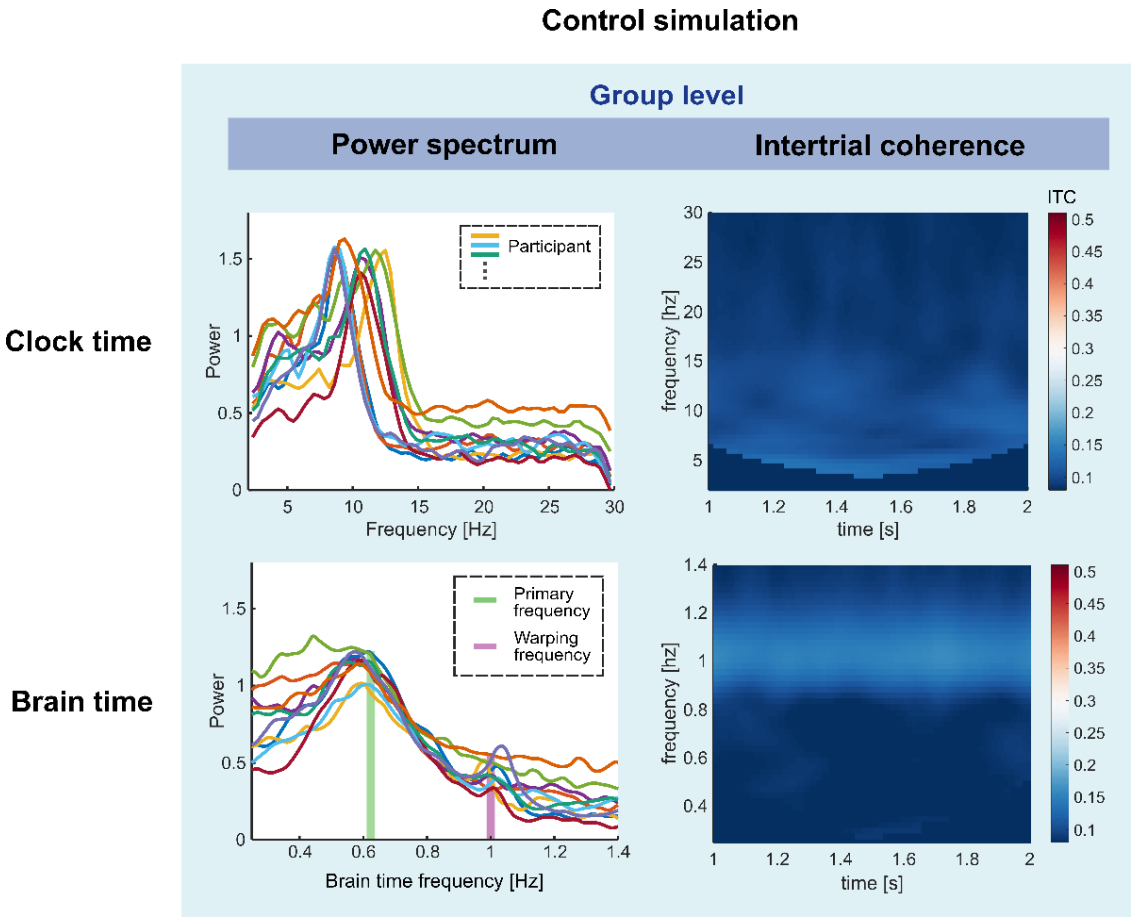

Supplementary Figure 2. Basic control analysis for the simulation dataset. Brain time warping to control frequencies (i.e., at the golden mean of the primarily simulated frequency) resulted in weak increases of power and ITC at control frequencies. The brain time data shows stronger peaks at the primarily simulated frequency. The color axis of ITC is held constant from the main analysis to enable visual inspection of the difference in magnitude between main and control analyses.

1.2 Nested oscillations

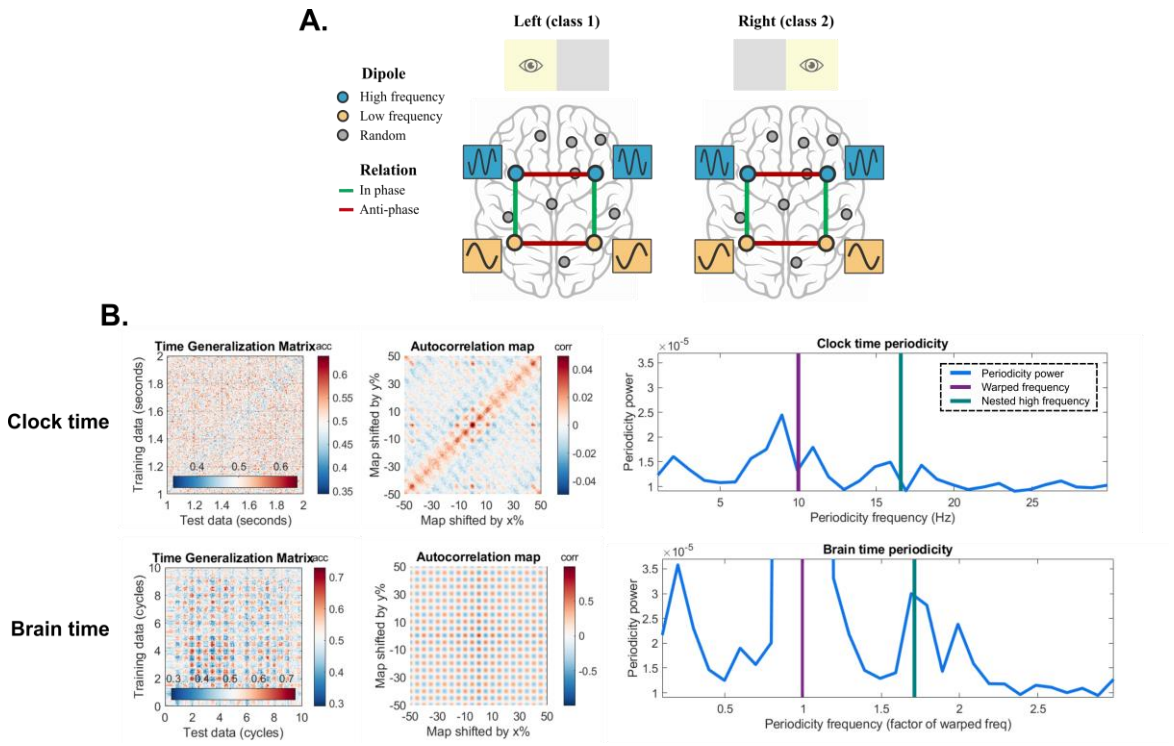

Supplementary Figure 3. Dipole configuration for the nested oscillation simulated dataset. (A) Dipole configuration for the nested oscillation simulation. A high and low frequency oscillator in each hemisphere were nested by means of phase-amplitude and phase-phase coupling. The two sets of nested oscillators had an anti-phase relationship with respect to each other, resulting in a classifiable neural signature that varies between left and right hemifield conditions. **(B)** Brain time warping shows a stronger peak at the frequency of the nested oscillator that was not apparent in clock time. These results are inconsistent across repetitions.

What is the effect of brain time warping if there are multiple nested oscillations that coordinate cognition? To address this question, we simulated a single dataset with two sets of nested oscillators that were cross-frequency coupled (Jensen & Colgin, 2007). Specifically, the nested oscillators were phase-amplitude coupled, and we added phase-phase coupling to further enhance the nested nature of the oscillators (Siebenhühner et al., 2016). One set of oscillators was in the left, and one set was in the right hemisphere (Supplementary Figure 3A). Within each set, one oscillator fluctuated at a high frequency and one at a lower frequency. As with the primary attentional dataset simulation, we generated a different phase relation between two hemifield conditions to create a classifiable neural signature. We tested whether warping to the lowest frequency oscillator reveals periodicity at the frequency of the nested high frequency oscillator. This simulation script is added in *braintime* under `bt_dipsim_cfc` and the relevant analyses are provided and documented in `tutorial8_crossfrequency`.

We found that brain time warping is able to reveal the high frequency oscillator when warping to the low frequency oscillation's frequency under some circumstances (Supplementary Figure 3B). However, the magnitude of the effect is small compared to standard analyses where we tested for periodicity at the warped frequency (i.e., in the simulation where no nested oscillations are present; main manuscript). Moreover, generating the same dataset several times – which introduces slight ground truth variability due to randomness in the simulation – showed that warping-induced periodicity increases around the coupled high frequency arose inconsistently across analyses. This suggests that while brain time warping can be used to study cross-frequency coupling, it is not optimally suited to do so and better methods are available (see Hülsemann et al., 2019 for an overview). From a different perspective, these results do demonstrate that if one is solely interested in the brain dynamics orchestrated by a single class of oscillators, brain time warped results are unlikely to be contaminated by extraneous brain dynamics – because even maximally coupled oscillators infrequently impinge on each other.

2. Toolbox

2.1 Introduction

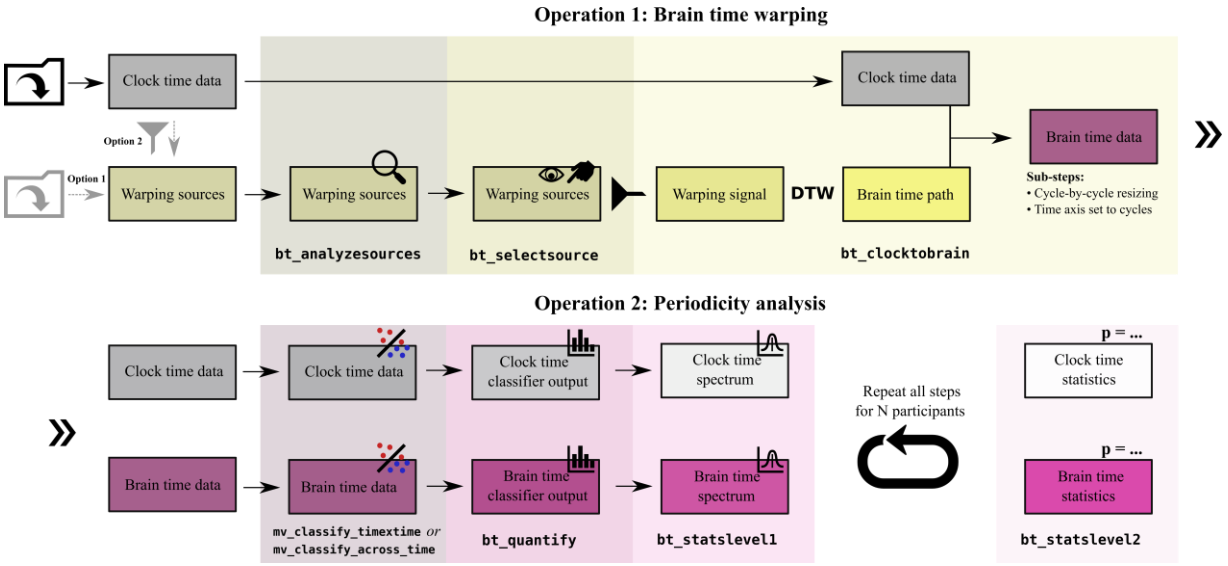

Supplementary Figure 4. the default Brain Time Toolbox pipeline. *Braintime* has two primary operations. **(Top row)** For brain time warping, the user first loads a FieldTrip formatted data structure that will be transformed (clock time data). Separately, a data structure with warping sources is required. This structure contains potential warping signals – the oscillation used to transform the data. The warping sources may be loaded separately (option 1) or extracted from the clock time data (option 2). `bt_analyzesources` analyzes each warping source for warping signals based on user parameters. Next, using `bt_selectsource`, the user can inspect each warping source's characteristics (such as

spectral information) and designate a warping signal as brain time. Finally, `bt_clocktobrain` dynamically time warps (DTW) the warping signal to either a stationary sine wave or the warping source's average waveshape. The resulting warping path is applied to the clock time data, cycle-by-cycle, and resized to the original length. The function also sets the time axis from seconds to cycles of brain time. **(Bottom row)** For the periodicity analysis, *braintime* first calls MVPA Light to test a classifier on two classes of data, prespecified by the user. The resulting output is one dimensional for `mv_classify_across_time`, or two dimensional, when testing for time generalization of the classifier using `mv_classify_timextime`. Then, across this output, `bt_quantify` tests for periodic patterns in classification performance, resulting in a periodicity spectrum. Next, `bt_statslevel1` performs first-level statistics by comparing the empirical spectrum with a user-specified number of permuted spectra (obtained by shuffling class labels). Finally, `bt_statslevel2` obtains group level results of the classifier's periodicity, and calls MVPA Light to perform cluster correction over the classifier's performance.

The Brain Time Toolbox, abbreviated *braintime*, is a MATLAB software library designed for use with electroencephalography (EEG), magnetoencephalography (MEG), and single and multiunit intracranial recordings (Supplementary Figure 4). The toolbox has two primary uses: brain time warping data structures (transforming them from clock to brain time; operation 1) and testing for periodic patterns in the data that reflect dynamic cognition (operation 2). The standard pipeline is to brain time warp data and test for a change in periodicity at frequencies of interest. However, each operation can be carried out without the other – brain time warped data may be analysed outside the toolbox and periodic patterns may be tested on data that has not undergone warping (clock time data).

In this manuscript, we describe *braintime* in extensive technical detail with limited emphasis on user flow. For a practical guide, we recommend the more concise and step-by-step documentation on *braintime*'s Github page (https://github.com/sandervanbree/braintime). For a quick start, we recommend *braintime*'s tutorials.

2.1.1 Requirements

Braintime interfaces with the following software packages, requiring each to be installed:

- MATLAB Signal Processing Toolbox (The MathWorks)
- FieldTrip (Oostenveld et al., 2011)
- MVPA Light (Treder, 2020)

Besides these software dependencies, *braintime* requires the electrophysiology data to be structured in a FieldTrip format. For data structures that are not in this format, FieldTrip has built-in tools to convert a wide array of common file types. See the FieldTrip documentation for information on how to convert data.

In case *braintime*'s second operation will be used (testing for periodicity), the input clock time data needs to consist of two classes of data hypothesized to yield the neural signature of the studied cognitive process. Moreover, trials in the data structure need to be labelled based on their class membership. For more details on how to do this, see section 2.3.

2.1.2 Download and installation

Before setting up *braintime*, ensure FieldTrip and MVPA Light are downloaded and fully initialized (download links above). *Braintime* can be downloaded on the toolbox Github page. First, download the ZIP folder and unzip it to a preferred path. Then, run the function `setup_braintime` (in the setup folder). To get started with the toolbox, see *braintime*'s tutorials.

2.2 Operation 1: Brain time warping

Brain time warping transforms data according to the phase dynamics of an oscillation hypothesized to clock the studied cognitive process. This changes the time axis of the data from seconds to cycles of the warping frequency.

2.2.1 Obtaining warping sources

Warping sources may either be ad hoc extracted from the clock time data or loaded from a separate data structure. The warping sources contain warping signals – potential oscillations used for brain time warping. There are only two restrictions to what constitutes warping sources: the data structure needs to be in a FieldTrip format, and the data needs to align in time with the to-be-warped clock time data. Users are encouraged to decide on a case-by-case basis what data serve as the best warping sources. Below, we describe two methods of obtaining warping sources, and provide several examples for each.

Ad hoc extraction

Warping sources may be extracted from clock time data on the fly, for example using independent component analysis (ICA). ICA is a popular method to decompose electrophysiology data into additive subcomponents (Makeig et al., 1995). The resulting components aggregate data with statistically uncorrelated spectral characteristics, making for suitable warping sources. Each component contains potential warping signals. The toolbox automatically detects when the warping sources are ICA components, and suggests removal of the selected component from the brain time warped data when continuing analyses outside the toolbox. For single- and multiunit recordings, an example of ad hoc extraction is to separate one (or more) local field potential channels into a warping source(s) structure.

Preloaded data structure

Warping sources may also be obtained from a separate preloaded data structure, in the form of previously extracted data. An example could be a study where magnetometer and gradiometer channels underwent separate preprocessing steps, with their data saved in separate files. Or perhaps a user has created a set of virtual channels using source localization, intending to warp sensor-level data using source-level phase estimation. Warping sources may also be obtained from a separate recording altogether. For example, a user may opt to warp EEG data using warping signal obtained from MEG data, or vice versa.

2.2.2 Analysing warping source

In `bt_analyzesources`, *braintime* uses FieldTrip to perform time frequency analyses on each warping source. Users may choose between a variety of time frequency analysis parameters based on FieldTrip's `ft_freqanalysis`, and may opt to include 1/F correction. In addition, users select a range of frequencies predicted to contain the coordinating oscillation. For example, a user interested in spatial attention may specify a range of 8 to 12 Hertz (Hz). The toolbox estimates the phase of high power oscillations in this range in anticipation of brain time warping. Upon completion of the time frequency analyses, the toolbox sorts the warping sources based on power in the range of interest. Optionally, for EEG and MEG, the sorting of warping sources may be weighted by the hypothesized topographical activity of warping sources. For example, a researcher may want to focus on warping sources with parietal activity, or a lateralized source. To enable topography weighting, users first call `bt_templatetopo` and draw a topographical

profile on a template layout. *Braintime* then loads the template topography and adapts the ranking of warping sources to their topography's correlation with the template topography, instead of the default setting which sorts solely by maximum power at frequencies of interest.

Asymmetry and waveshape

For each warping source, *braintime* detects the average waveshape and the asymmetry of each cycle in it. This allows users who have predictions about the symmetry of their coordinating oscillation to decide between warping sources. In addition, the amount of asymmetry may also inform parameter selection during subsequent steps in *braintime*.

The waveshape and asymmetry of data are obtained via the following steps. First, *braintime* applies a band-pass filter in a 2 Hertz (Hz) window around the warping frequency. Then, trial-by-trial, the toolbox finds local minima and maxima in the filtered data, reflecting troughs and peaks, respectively. Then, based on the location of these minima and maxima, *braintime* extracts associated data in the (non-filtered) warping sources, calculating a peak-triggered wave. Thus, the peaks are located in the filtered data, while the shape of waves themselves are obtained by extracting data samples in the raw data around the peak locations. This is repeated for all cycles. Then, the asymmetry is calculated for each cycle, while the average waveshape is obtained by averaging each cycles' data. We defined asymmetry as the difference in duration between the ascending and descending flank of a cycle, normalized by its duration (Belluscio et al., 2012):

$$asymmetry\ index = \frac{(t_{peak} - t_{trough_{left}}) - (t_{trough_{right}} - t_{peak})}{t_{cycle}}$$

The toolbox visually displays the average waveshape during warping signal selection (2.2.3). To aid the visual inspection of waveshape asymmetry, peak-triggered averages are rescaled to a fixed number of samples regardless of their frequency—i.e., the signal is displayed in phase instead of clock time.

2.2.3 Selecting a warping signal

In `bt_selectsource`, the user selects a warping source and its associated warping signal, designating brain time. In this step, *braintime* creates a graphical user interface that displays each warping source's information as calculated by `bt_analyzesources` (Supplementary Figure 5). This information comprises (1) a textbox with recommended

criteria for warping source selection and browsing instructions, (2) the topography of the warping source (if requested), (3) the asymmetry and shape of the average waveshape, (4) the time frequency representation of the warping source's data, and (5) its power spectrum. Users may visually inspect each warping source and combine all information to designate the warping signal predicted to clock the studied cognitive process of interest, in keeping with a hypothesis-driven approach.

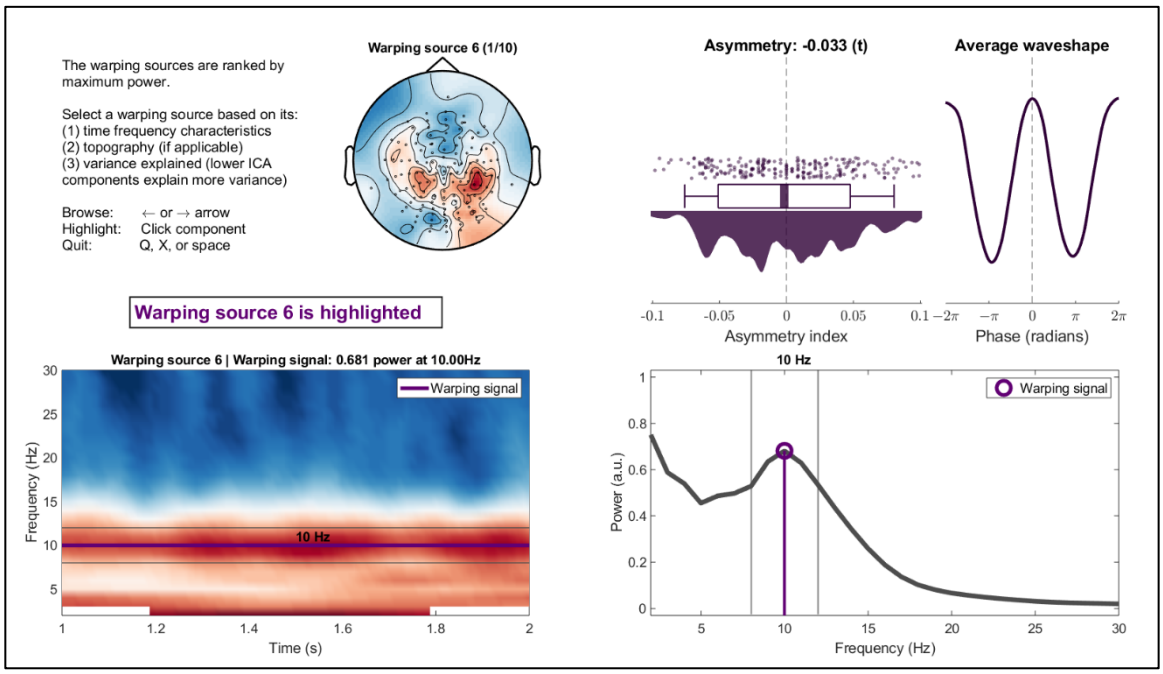

Supplementary Figure 5. Selecting a warping source. The graphical user interface generated by `bt_selectsource`. **(Top row)** A textbox is displayed with suggested criteria for warping source selection, as well as instructions for browsing. Next, optionally for EEG and MEG, the topography is displayed. On the right, the average asymmetry of cycles in each warping source is displayed (one dot represents one cycle in the warping source). This serves two purposes: users may want to discriminate between sources based on their asymmetry, or check levels of asymmetry to inform parameter selection during subsequent steps. **(Bottom row)** The warping source's time frequency representation is displayed, along with the power spectrum. For both plots, the borders of the frequency range of interest and the location of the warping signal are highlighted.

2.2.4 Warping clock to brain time

In `bt_clocktobrain`, the phase of the selected warping signal is used to warp the clock time data structure (Supplementary Figure 6). Here, we discuss two parameters that determine what DTW is applied to.

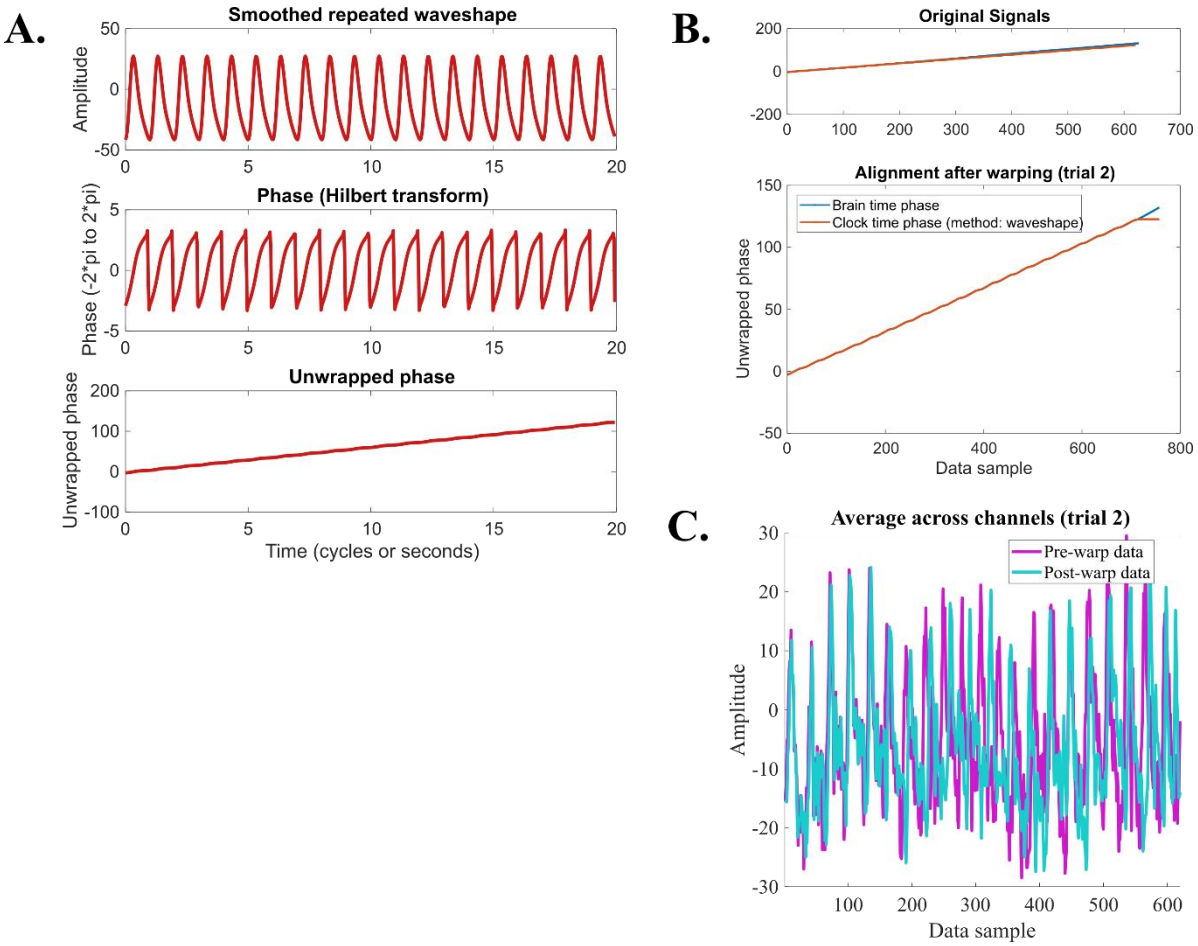

Supplementary Figure 6. Warping clock to brain time. *Braintime* prints a series of plots upon completion of bt_clocktobrain to show the application of brain time warping to the data at hand. **(A)** In this example, the user has set *braintime* to warp to the smoothed average waveshape of the selected warping source (top). The toolbox extracts the angle of its Hilbert transform (middle) and unwraps the phase in preparation for warping (bottom). **(B)** The unwrapped phase vector of the warping signal and the stationary sine wave (representing clock time) are displayed (top), and so is their alignment after applying dynamic time warping (bottom). **(C)** Here, the warping path has been applied to the original clock time data, yielding a dynamic resampled version of the original data based on the brain's dynamics.

Warp method

We define clock time as a stationary oscillation, oscillating away faithfully to seconds. This is what the warping signal will be dynamically time warped onto. We implement two ways of generating this stationary oscillation. First, users may choose the default method, where a stationary sine wave is generated with MATLAB. However, for data with asymmetric waveshapes, using a sine wave with perfect symmetry may impede DTW's attempt to minimize Euclidean distance between the phase of clock and brain time. Thus, we include

the option to warp using a concatenation of the smoothed average waveshape of the warping source, yielding a sinusoid with matching asymmetry (Supplementary Figure 6).

Phase method

Besides control over what constitutes clock time phase, users may opt to estimate brain time's phase in two ways. The standard way of estimating brain time's phase is by calculating the phase of the Hilbert transform of band-pass filtered data of the warping source, where the filter is centred on the warping frequency. However, the toolbox also offers Generalized Eigenvalue Decomposition (GED) as an alternative method to estimate the warping frequency's phase holistically across all warping sources. This method is appropriate when the warping sources are all considered to contain information about brain time. For example, the user's warping sources may be local field potential channels in the hippocampus. In this case, the user may not want to choose one local field potential channel given their interest in the phase of theta oscillations across the entire hippocampus. Similarly, a user may have source localized parietal cortex channels which each provide valuable phase information. In these cases, GED is the optimal choice. GED finds a spatiotemporal filter that differentiates all the warping source data into components with high and low power of the warping frequency (Cohen, 2017; Parra et al., 2005). When users specify this option, *braintime* extracts the component with the highest weight, yielding a time series of the GED component (after which the phase is again estimated via the Hilbert transform). To perform GED, the toolbox uses a modified version of the functions provided by Mike X Cohen (reported in Cohen, 2017). In short, FFT offers a classical and source-specific phase estimation of the warping frequency, while GED estimates the warping frequency's phase holistically across warping sources.

2.3 Operation 2: Periodicity analysis

Braintime allows users to test for dynamic patterns of information using machine learning techniques. This requires the data to contain two classes of conditions, which, when taking their difference in neural activity, reflects the studied cognitive process. We define this difference as the *neural signature*. The assumption of operation 2 is this: if the warping signal clocks the cognitive process, then the warped data should show an increase in the periodic dynamics of the neural signature. Thus, we compare the periodicity of a classifier's performance between clock and brain time data to test for a difference in such patterns. The

general pipeline is that each participant's clock and brain time data undergoes classification (2.3.1), quantification of classifier performance (2.3.2), and first-level statistics (2.3.3). Then, second-level statistics can be initiated on the first-level results (2.3.4).

Requirements

To get started with the second operation, both the clock time and brain time warped data need to have each trial's class membership labelled. This is necessary for *MVPA Light* and *braintime* to understand the class structure present in the data. *Braintime*'s tutorials describe how to do this using example code, but briefly, the user sets `bt_data.trialinfo` and `ct_data.trialinfo` to a vector of 1's and 2's in line with the trial structure (class labels). For example, for a dataset on motor processing, a triplet of trials that are in left, right, and left movement conditions would need to be labelled as `[1 2 1]` or `[2 1 2]`.

When using the second operation, it is important for users to establish the absence of high-pass filtering artefacts in the data. In a recent publication, it is reported that high-pass filtering may result in temporal displacement of information, causing leakage of classification performance (van Driel et al., 2021). These artefacts may influence the periodicity analysis. In light of this, we suggest using high-pass filtering with care, testing for a temporal leakage of classification performance (e.g., by testing whether filtering introduces classification peaks before stimulus presentation). Alternatively, trial-masked robust detrending may be applied as an artefact-free method of removing low frequencies (van Driel et al., 2021). Users are made aware of potential high-pass filtering artefacts in all sources of *braintime*'s documentation.

2.3.1 Classifying the data

To perform pattern classification, *braintime* calls *MVPA Light* (Treder, 2020). *MVPA Light* can be used to perform multivariate pattern analysis using different models (e.g., support vector machines, logistic regression, and linear discriminant analysis; LDA), classification metrics (e.g., accuracy, area under the curve, fidelity values), and cross-validation methods (e.g., k-fold, hold-out, leave one out). Classification may be performed in the standard way using `mv_classify_across_time` or with temporal generalization using `mv_classify_timextime` (Supplementary Figure 7). The former results in a one-dimensional (1D) time series that reflects how a classifier trained on each timepoint performs

when tested on that timepoint in held out data. The latter results in a two-dimensional (2D) temporal generalization matrix (TGM) that reflects how performance generalizes from each trained timepoint to all other timepoints in held out data (King & Dehaene, 2014). The diagonal of the TGM is identical to 1D classification, while the off-diagonal provides information about generalization of performance. This provides information about the degree of constancy of the neural code ("temporal generalization"). As such, `mv_classify_across_time` is appropriate when the neural signature is predicted to evolve beyond classifier recognition from one moment to the next, while `mv_classify_timextime` is appropriate when there is some constancy of the neural code across time. For analysis with *braintime*, if some constancy is expected, we strongly recommend `mv_classify_timextime` as it yields exponentially more data to perform periodicity analysis over – substantially increasing the power of the analysis.

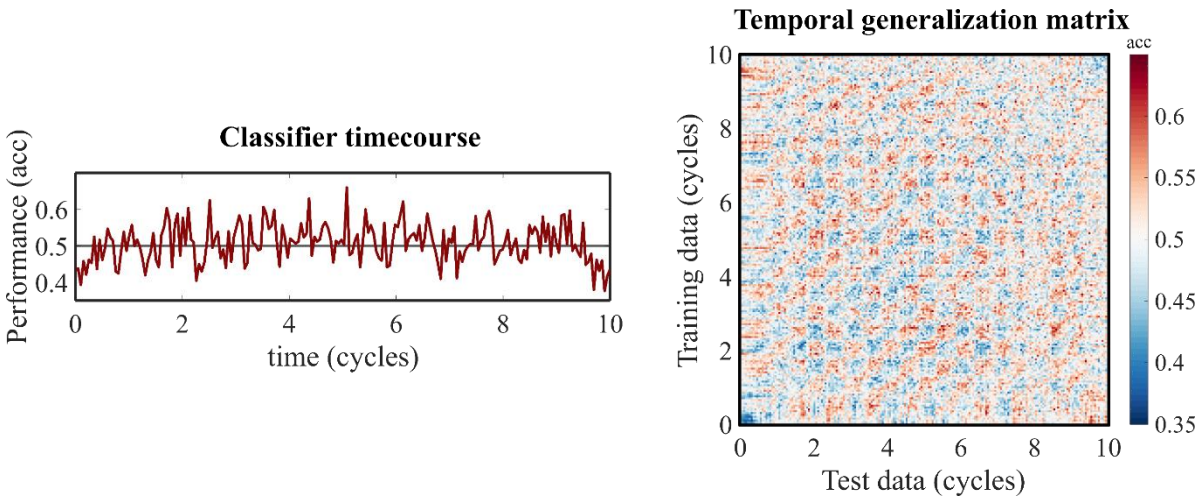

Supplementary Figure 7. Two types of classification
Braintime calls *MVPA Light* to perform standard classification across time (1D; left) or temporal generalization (2D; right). The classification timecourse on the left equals the diagonal of the TGM on the right. The off-diagonal represents how well classification generalizes when trained on one timepoint and generalized to each other timepoint in held-out data. *Braintime* can perform periodicity analyses over both types of classification. (*acc* = accuracy).

2.3.2 Quantifying classifier periodicity

In `bt_quantify`, classifier periodicity is quantified by an FFT over the classifier timecourse (1D results), or over each row and column of the time generalized classifier performance (TGM; 2D results). We use FieldTrip to apply the FFT using a multitaper

frequency transformation (using discrete prolate spheroidal sequences and Hanning window tapers). The FFT is performed across frequency ranges specified by the user.

For the time generalized classifier performance, users can specify whether the periodicity is done over the rows and columns of the TGM itself, or over its autocorrelation map (Supplementary Figure 8). The autocorrelation map correlates the TGM with all shifted versions of itself. That is, it iteratively shifts the TGM in each X and Y direction and plots the correlation of the shifted map with itself in coordinate space. The most powerful option depends on the uniformity of periodic patterns. Generally, the autocorrelation map is a more powerful approach, as it accentuates periodic patterns that are present in the TGM. However, when multiple periodicity rates are present in the TGM, the autocorrelation may drown out the weaker periodicity. Similarly, when periodicity is present in only a small part of the TGM, changing its rate or disappearing across time, the autocorrelation map may fail to detect it. In short, when uniform periodicity patterns in the data are expected, analysing the autocorrelation map of TGMs is a powerful approach. When the pattern is expected to only be present partially, or when multiple rates are predicted, it is more powerful to analyse the TGM itself.

Periodicity referenced to brain time

For brain time data, just as the time axis has been changed from seconds to cycles, periodicity is redefined from clock time to brain time. Specifically, each participant's periodicity is $(\frac{default\ frequency}{warping\ frequency})$. For example, if a user decides to quantify periodicity between 5 and 13 Hz for a participant with a 9 Hz warping frequency, the resulting periodicity will range from 0.56 Hz (= 5 / 9 Hz) and 1.44 Hz (= 13 / 9 Hz), see Supplementary Figure 8 (bottom). This referencing to brain time allows participants to be compared with reference to each brain's own dynamics. For example, if periodicity across participants were to cluster at 0.5 Hz, this would mean participants tend to show periodic patterns in their neural signature at half the rate of their clocking oscillations.

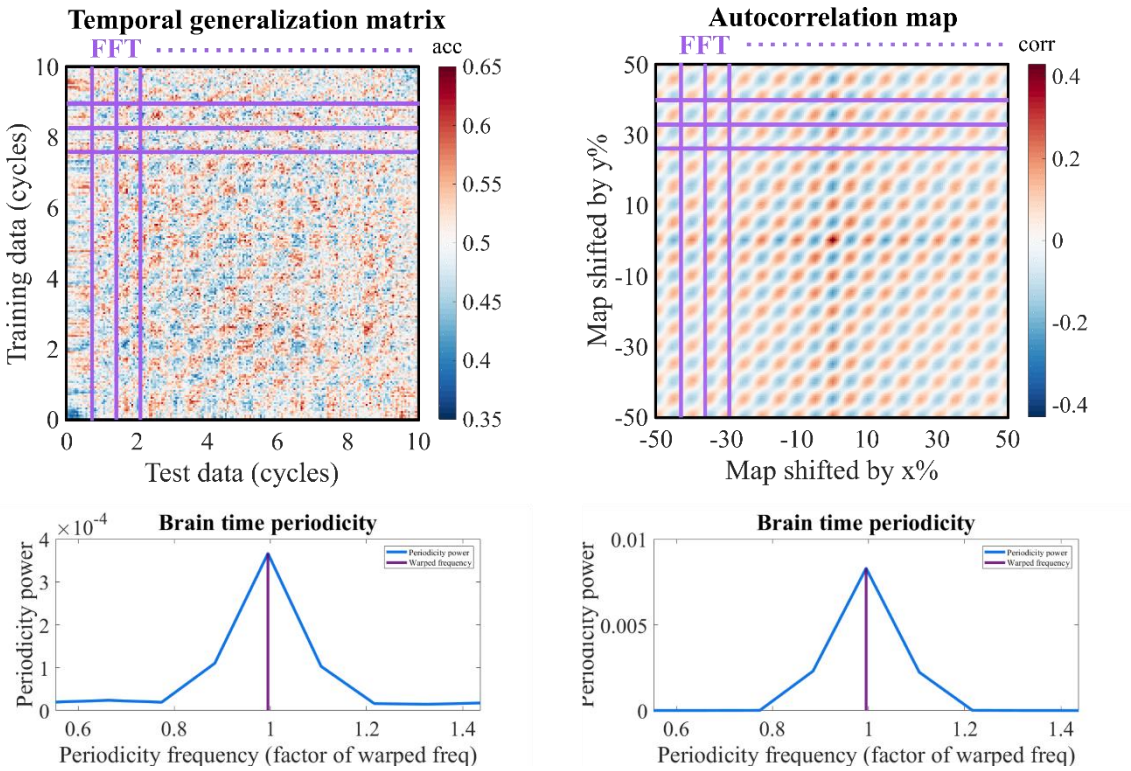

Supplementary Figure 8. Two ways of performing 2D periodicity analysis. (Top) Row-by-row and column-by-column, *braintime* performs an FFT over the TGM by itself, or its autocorrelation map. The former is more powerful when periodicity is present in small segments of the TGM, or if multiple periodicity frequencies are present. The latter is more powerful when the periodic pattern is present in most of the TGM (as is the case in this dataset). **(Bottom)** The resulting power spectra are averaged across all rows and columns, resulting in one participant's "periodicity spectrum". (*corr* = correlation)

2.3.3 First-level statistics of periodicity

In `bt_statslevel1`, quantified periodicity is subjected to first-level statistics to establish its statistical robustness. The user specifies a range of frequencies that will be tested, and the desired number of first-level permutations (`numperms1`). *Braintime* obtains a null distribution by repeating data classification (2.3.1) and quantification of its periodicity (2.3.2) `numperms1` times with the class labels shuffled randomly (destroying correspondence between trials and their associated condition). This yields a pool of *permuted periodicity spectra* that offers a confidence interval for each frequency. P-values are not provided until the second-level statistics are completed.

2.3.4 Second-level statistics of periodicity

Upon completion of the previous steps for all participants, users are requested to combine the first-level periodicity data structure of each participant into one superstructure. Next, in anticipation of `bt_statslevel2`, users specify the number of second-level permutations (`numperms2`) and the desired method of multiple testing correction across periodicity frequencies (false discovery rate; FDR, Bonferroni correction, or no correction). `bt_statslevel2` undertakes the following steps:

Z-scoring

Braintime performs z-scoring on each participant's periodicity spectra for two reasons. First, the output of FFT has amplitudes with arbitrary values, creating arbitrary differences in amplitude between participants. Second, we want to avoid participants with high periodicity (even after correcting for arbitrary differences) to drive a group effect. The toolbox implements z-scoring by normalizing both the permuted spectra and empirical spectra to the mean and standard deviation of the permuted spectra (i.e., by subtracting the mean and dividing by the standard deviation). With this method, the permuted spectra are considered a noise floor for which the empirical spectra are corrected.

Filtering to common frequencies

As discussed before (2.3.2), participants' range of tested periodicity frequencies are normalized to their warping frequency. This creates some variability in the range of tested frequencies across participants. For second-level statistics, *braintime* filters each participant's spectra to the frequencies that are common to all participants. For example, when quantifying periodicity between 5 and 13 Hz for a participant with a 9 Hz warping frequency in clock time, the evaluated frequencies for periodicity normalized to brain time will range from 0.56 Hz (= 5 / 9 Hz) and 1.44 Hz (= 13 / 9 Hz). If another participant has a different warping frequency (e.g., 8 Hz), the emerging frequency range in brain time will be slightly different (e.g., 0.62 Hz to 1.63 Hz). To enable cross-participant analyses, we bring periodicity spectra into the same range by cropping to brain time frequencies that are shared across all participants. Finally, to overcome potential variations in the frequency resolution between participants, *braintime* uses `imresize` to interpolate all participants' spectra according to the mode spectral resolution across participants. This establishes an equal number of samples for the application of multiple testing correction.

Obtaining p-values

On the second-level, each clock and brain time periodicity frequency is statistically tested across participants. This is done in the following way. For each participant, the toolbox grabs one random spectrum of each participant's `numperms1` permuted spectra. This is repeated `numperms2` times, yielding a pool of `numperms2` new spectra. For each frequency, *braintime* compares the average empirical periodicity power to the distribution of power in the `numperms2` pool spectra. The p-value of each frequency is defined as the proportion of `numperms2` power values that are equal or higher to the average empirical power value ($p = \frac{N}{numperms2}$, where N is the number of times the permuted pool equals or exceeds empirical power).

Multiple testing correction

Users may correct for multiple comparisons (where the comparisons are the tested frequencies) by using false discovery rate (FDR) or Bonferroni correction. For brain time spectra, three frequencies are exempted by default for multiple testing correction because, in line with the hypothesis-driven approach of *braintime*, periodicity is a priori expected at these rates. Specifically, these are at 0.5×, 1×, and 2× the warping frequency (i.e., 0.5 Hz, 1 Hz, and 2 Hz) in the brain time spectra. Depending on both the underlying dynamics and the classifier method used (`mv_classify_across_time` or `mv_classify_timextime`), periodicity is predicted at one or more of these rates (if the warping signal clocks the cognitive process of interest). In this sense, *braintime* performs two statistical tests: one primary test across the three hypothesized frequencies, and an additional one across the specified frequency range of interest. In the second-level periodicity spectra, the uncorrected p-values at the three frequencies of interest are combined with the corrected p-values of the remaining frequencies of interest.

Cluster statistics

Besides establishing the statistical robustness of periodicity in the classifier's performance, *braintime* also displays robustness of classifier performance per se. That is, it displays at which timepoints the classifier is able to differentiate the two classes of data above chance. The toolbox calls *MVPA Light* to perform cluster correction over the results obtained from `mv_classify_across_time` or `mv_classify_timextime`. Users may specify a

variety of parameters for cluster correction that are read and implemented by *MVPA Light*, including test methods (e.g., binomial or permutation based-cluster correction) as well as the number of permutations used to determine significant clusters. *MVPA Light* implements cluster correction as described by (Maris & Oostenveld, 2007). More information on cluster correction in *MVPA Light* can be found on its Github page.

2.4 Methodological considerations

Here, we describe several methodological concerns and considerations when using *braintime*.

2.4.1 Circularity concerns

As mentioned in the main text, a concern with brain time warping could be that it trivially imposes oscillatory structure at the warping frequency, causing either the activity or neural signature of a cognitive process to fluctuate even when warping to oscillations that do not clock it. A first point is that the warping path generated by DTW is not oscillatory, but instead represents how the warping signal needs to be transformed to reduce its non-stationarity. That is to say, application of the warping path to a random signal is not expected to alter its oscillatory structure in any way. Nevertheless, the concern persists. If the warping signal is present in the data, the oscillatory structure of the data is likely enhanced because the warping signal has its non-stationarities removed as a consequence of the path being applied to all the data. Below, we describe for which analyses circularity could be a concern, and how it can be avoided.

Analysis

Circularity is not a concern when testing for periodic patterns using the toolbox (operation 2). This is because of *braintime*'s method of obtaining a null distribution against which empirical periodicity is tested. Specifically, the only difference between this permuted pool and the empirical data is the shuffling of class labels. Besides this difference in data-to-condition allocation, the trials themselves remain unchanged. As a consequence, any trivially imposed oscillatory structure into the data is present equally between the permuted and empirical set. To the extent a classifier is able to exploit circular patterns (if they are present),

it will be able to do so for both dimensions. Thus, where circularity is present, it is expected to cancel out through *braintime*'s statistical method.

However, when using brain time warped data outside the toolbox, it may be that a researcher's analyses tap into the circular patterns (if they are present). Following the same logic, circularity is an issue to the extent it differentially affects the empirical and null distribution.

Dependence

Since circularity may arise from the warping signal, whether circularity is present at all critically depends on whether the warping signal is present in the transformed data. We call this concept data dependence. If the warping signal is present in the transformed data, the transformed data are said to be dependent. Below, we provide several examples with varying levels of dependence. Most caution and vigilance is needed for highly dependent data. To emphasize, the level of dependence is only relevant when analysing brain time warped data outside *braintime*, and only with analyses that can exploit circular patterns.

High dependence

H1) The warping signal was obtained from a channel in the clock time data, and it is still present in the brain time data.

H2) The warping signal was obtained from an ICA component in the clock time data, and it is still present in the brain time data.

Medium dependence

M1) The warping signal was obtained from source localized virtual channels obtained from within the clock time data, and these channels are still present in the brain time data.

M2) The warping signal comes from a set of anterior channels of an EEG or MEG dataset, which was used to warp posterior sensors.

M3) The warping signal is from low pass filtered MEG data, which is used to warp high pass filtered data.

Independence

These include all cases where the signal used for warping is absent from the brain time data. For example:

L1) The warping signal is obtained from local field potentials (LFP) in multi-unit recordings, which is used to warp single-cell recordings.

L2) The warping signal is from an ICA component that is absent in the brain time data.

L3) The warping signal is from a channel that is absent and spectrally orthogonal to channels in brain time data.

Solution

Circularity can be minimized by removing the warping source from the brain time warped data. An obvious example is the case where the warping source structure comprises ICA components (H2). *Braintime* automatically detects when warping sources are ICA components, and both recommends their removal and assists in this process (H2 → L2). Similarly, most of the aforementioned examples can be made independent. For example, in example M1, the spatial filters used for virtual channel generation could be used to filter those channels from brain time warped data. Or, if a brain time warped data structure comprises both LFP and single-unit channels, and the LFP channels were used to warp, then these channels can be removed from the brain time warped data.

2.4.2 Warping artefacts

Sometimes, brain time warping introduces a long series of sample repetitions at the start and/or end of the data that are too extended for the cycle-by-cycle resizing operation to compress them (Supplementary Figure 9). These extended data repetitions tend to occur at the start of brain time warped data, because this is where DTW attempts to repair initial differences in the phase between clock time and the warping signal. In other words, typically clock and brain time start out of tune, and so brain time warping repeats brain time data from the get-go until the two dimensions fall back in tune. These data repetitions are not intrinsically artefactual – they represent a true mismatch between the brain's dynamics and clock time that brain time warping accounts for. Nevertheless, they could in principle affect subsequent analyses, such as *braintime*'s periodicity analysis, causing them to exert an artefactual low-frequency footprint on it. For simplicity, we therefore refer to these data repetitions as warping artefacts.

Generally, warping artefacts are too small to exert an effect on *braintime*'s periodicity analysis. Their effects on analyses outside the toolbox depends on the degree to which the data repetitions affect it. The toolbox has built-in tools to avoid the artefact, if so desired. Specifically, the toolbox has a "cutartefact" parameter that brain time warps an additional 0.5 seconds before and after the specified window of interest, which is subsequently removed at the end of `bt_clocktobrain`. Here, the data repetitions at the start (end) of the brain time warped data (shown in Supplementary Figure 9) are shifted to the 0.5 seconds before (after) the window of interest. The advantage of this method is that the warping artefact is cut. The downside of this method is that because a longer time window of data is brain time warped (e.g., -0.5 to 1.5 seconds, instead of 0 to 1 seconds), more parts of the data are brought away from its default clock time format, making it increasingly difficult to consistently identify for example t = 0 seconds across trials. As such, there is also an increase in the amount of mismatch across trials in the true and specified clock time window of interest in the order of several milliseconds (for this reason, the default method that implements no artefact cutting is called "consistenttime"). Researchers may decide on a case-by-case basis which method is appropriate – cutartefact or consisttenttime – depending on the relative importance of the absence of warping artefacts and the constancy of the data's timing.

The two methods warp over different time periods and may therefore vary in their determination of which data belong to which cycle (the cycle-by-cycle resizing step, see 2.2.4). *Braintime* has a special function (`bt_checkallocation`) that visualizes how each of the two methods allocates data to cycles, allowing users to make informed decisions about which method to use and how much they diverge.

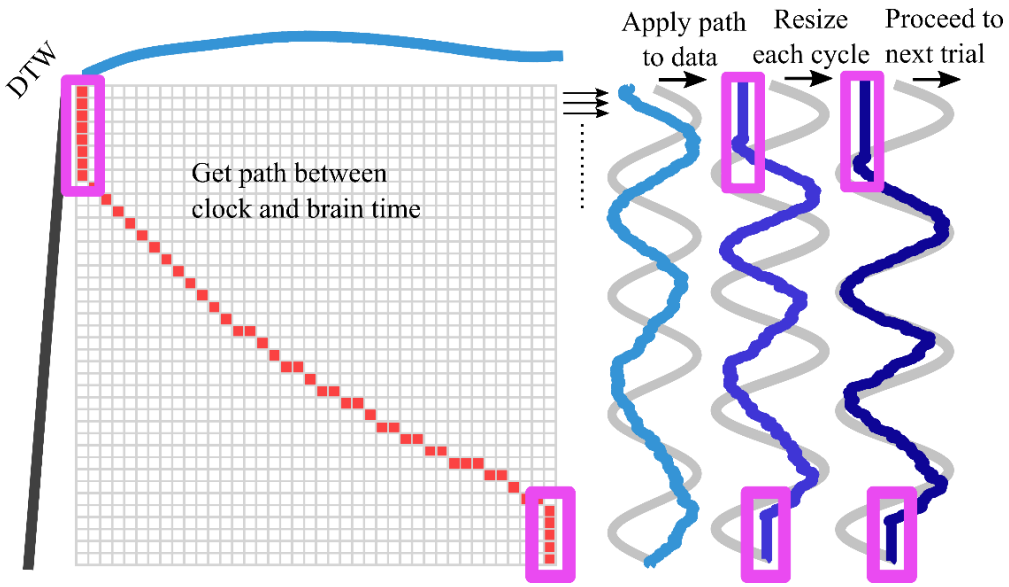

Supplementary Figure 9. Warping artefacts. Brain time warping may repeat samples for an extended period at the start and end of the data, depending on the disharmony between clock and brain time at the onset of trials (purple boxes). *Braintime* includes a method to remove the artefact, which warps additional data before and after the window of interest which is subsequently removed.

3. Supplementary results

For the plots of each dataset analysis, the y-axis of periodicity spectra and the colour scale of TGMs and autocorrelation maps are fixed to a constant range across (1) participants and (2) clock and brain time results to enable a visual comparison of magnitude. For a description of each type of classification plot, see section 2.3.

Note: Subsequent Supplementary figures are not numbered. Figure numbering returns in the Supplementary material for Chapter 4.

3.1 Simulation

3.1.1 ERP difference

To test whether the simulation yielded a fluctuating signature, we analysed the difference in average activity (event-related potentials; ERP) between left and right hemifield conditions. When using brain time warping to mitigate non-stationarities and other spectral eccentricities, the simulated periodic neural signature becomes unveiled.

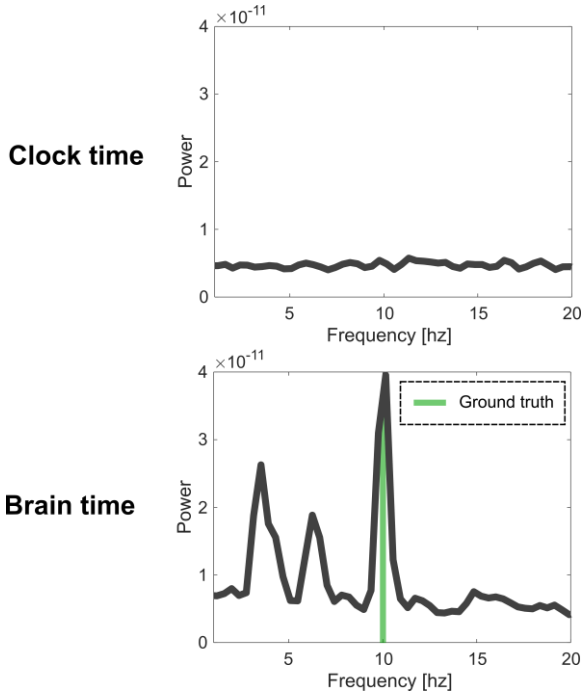

These frequency spectra concern the event-related potential.

3.1.2 Advanced (main analysis)

Brain time TGM

Brain time autocorrelation

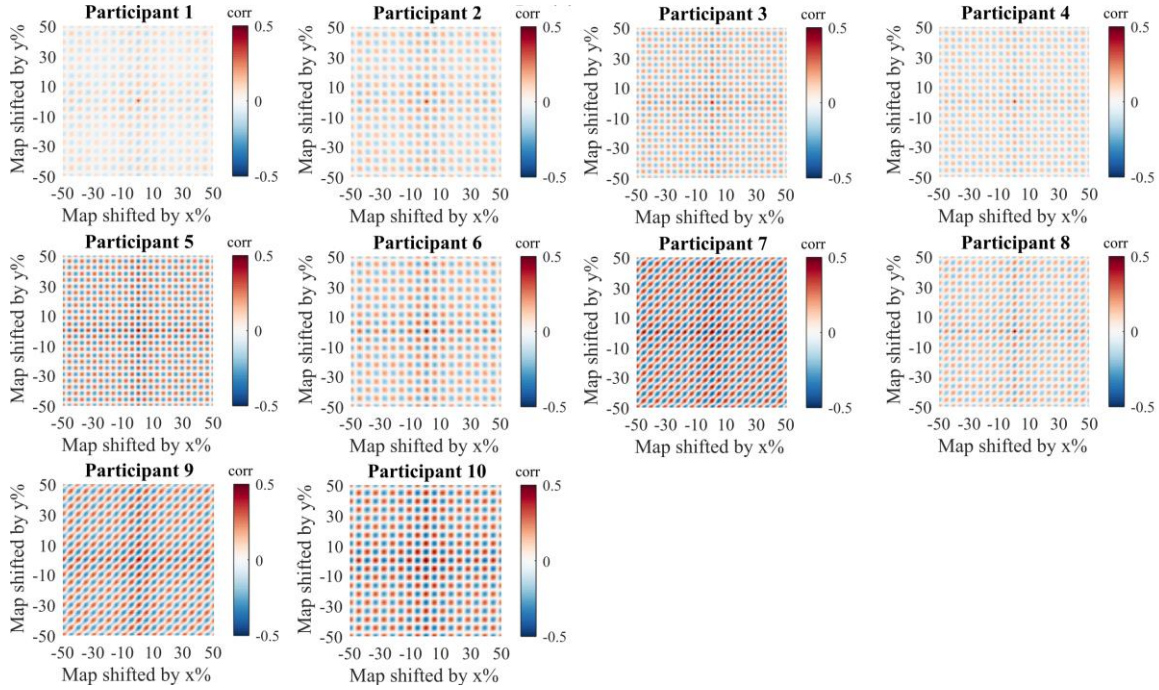

Brain time periodicity spectra (1st level)

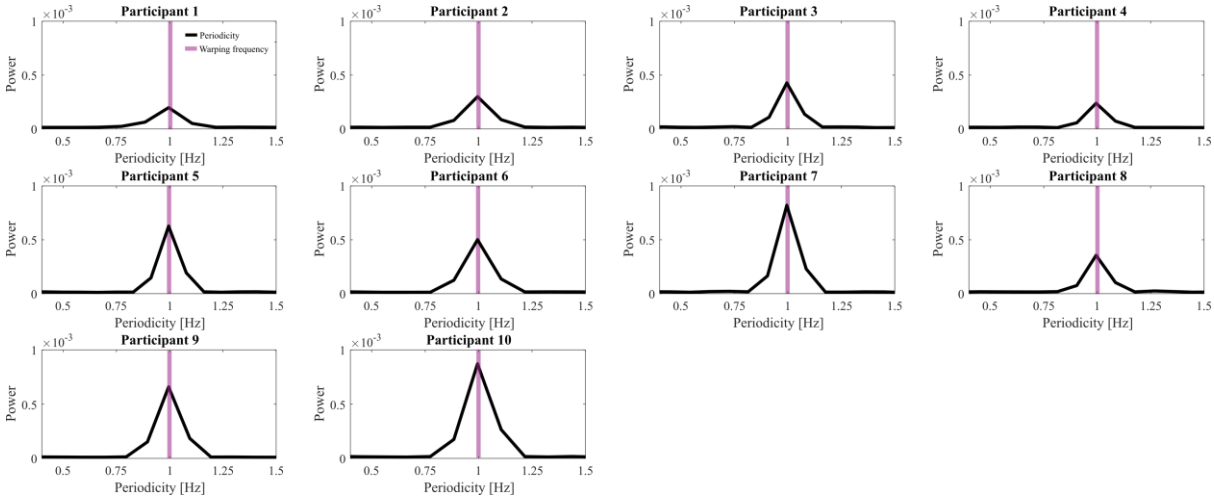

Periodicity spectra quantify rhythmic fluctuations in the temporal generalization matrix.

Brain time clusters

For the simulated dataset, we found few significant clusters with an alpha set at 0.05 and a critical t-value set at 1.96. We interpret these findings as indicating that the difference in simulated activity between left and right hemifield conditions is too small to be robustly detected by the classifier. However, since we know there is a difference in the ground truth between classes, we know this lack of significant results reflects a type II error. The fact that

the periodicity analysis does show significant results indicates that, between empirical and permuted data, differences in the fluctuations of the neural signature are easier to detect than a mean baseline shift in signature fidelity.

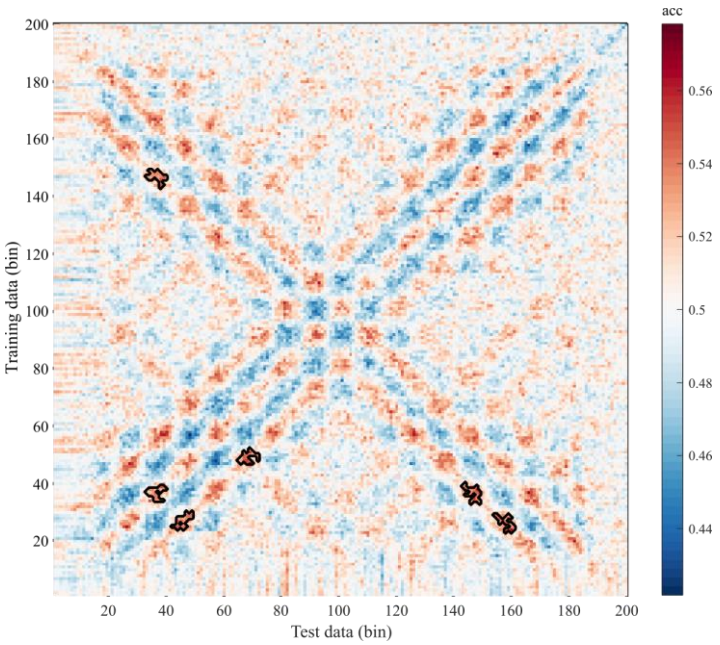

Clock time TGM

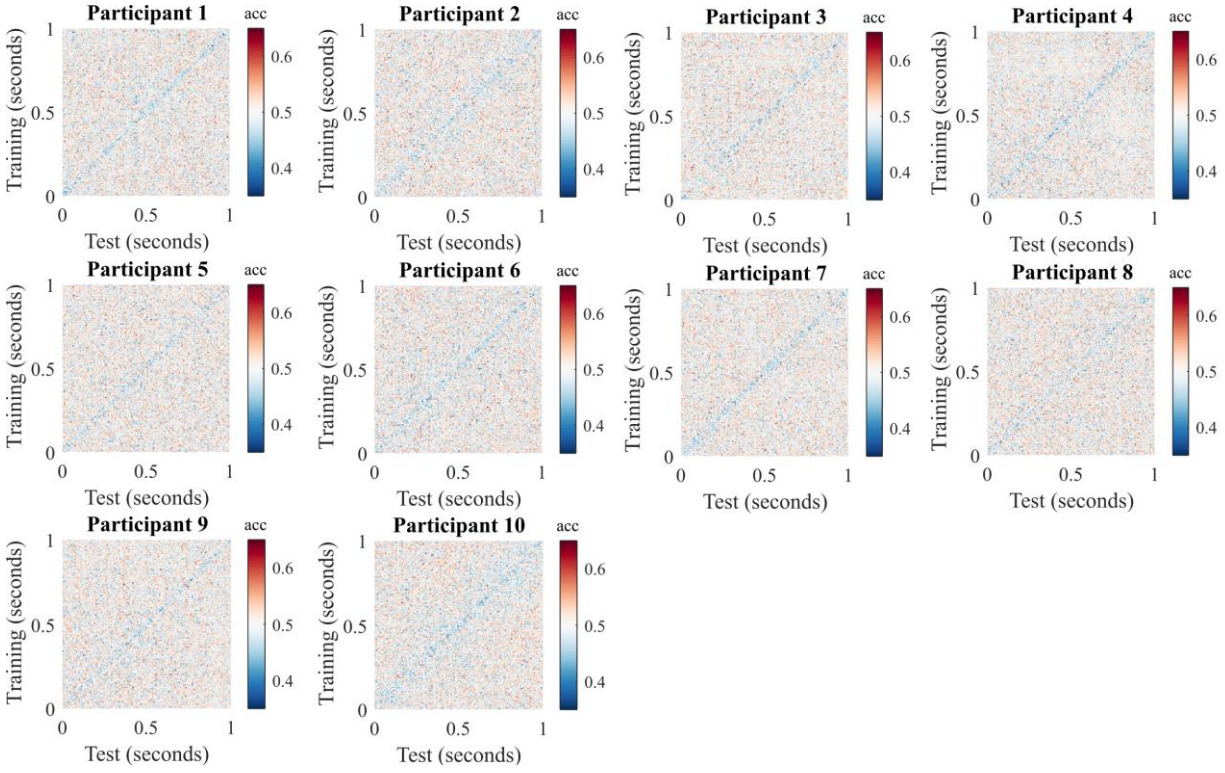

Clock time autocorrelation

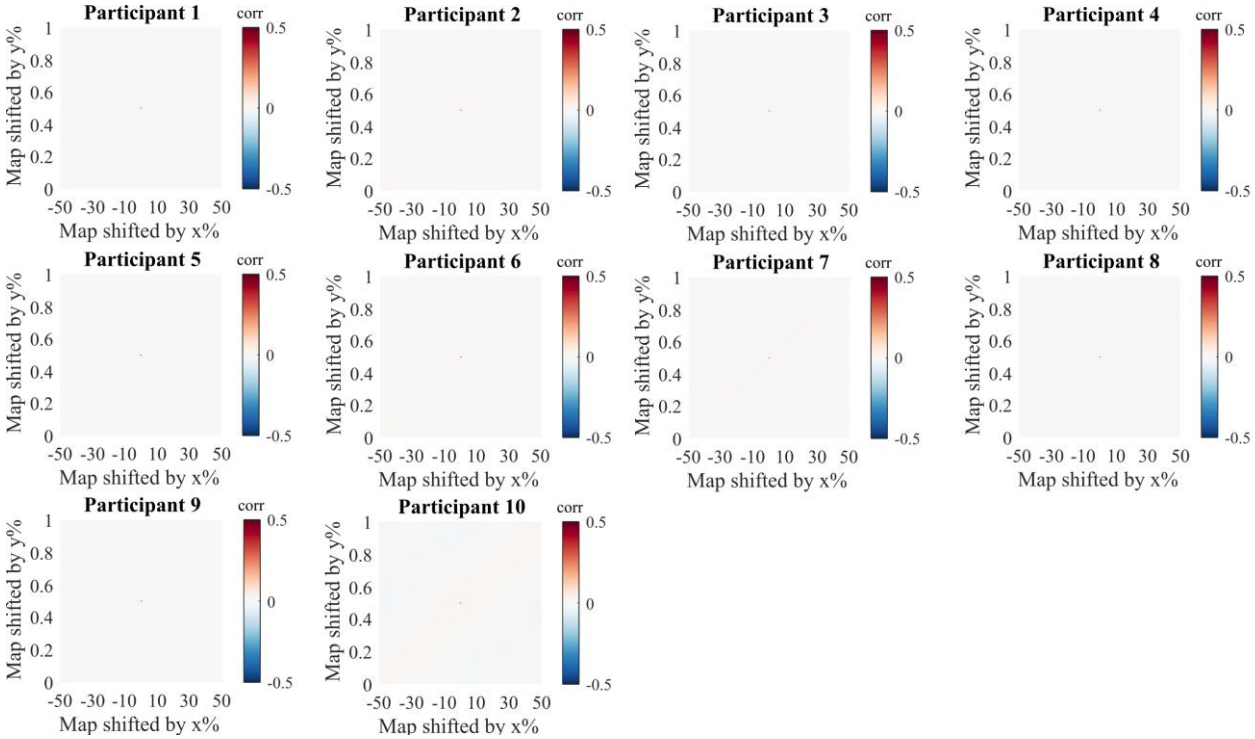

Clock time periodicity spectra (1st level)

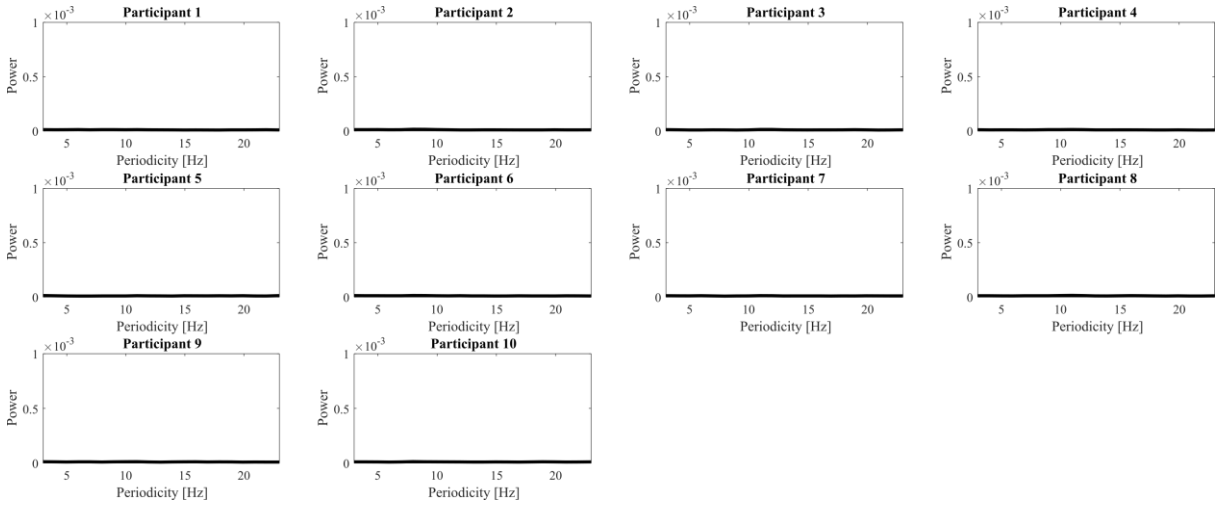

Clock time clusters

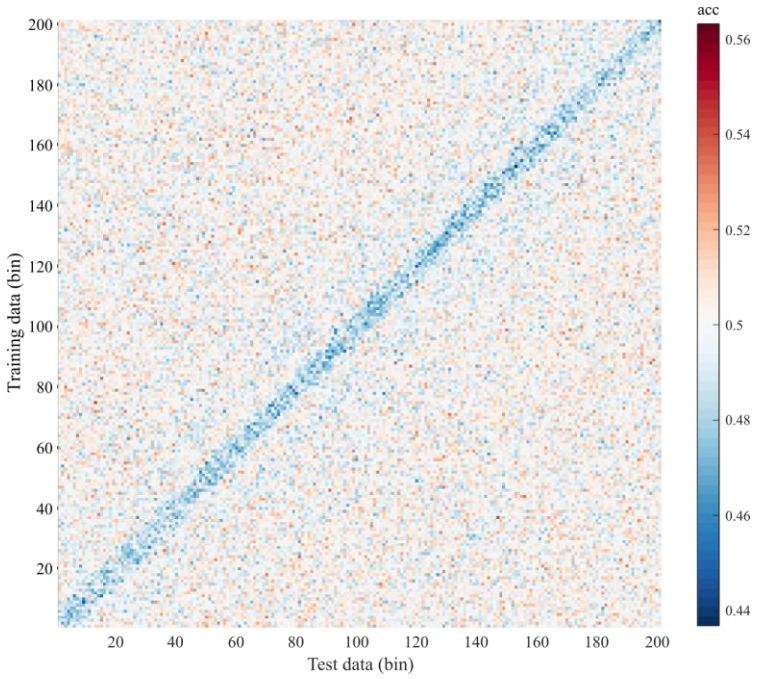

3.1.3 Advanced (control analysis)

In control analyses, we brain time warped to control frequencies. Specifically, we repeated the main analysis by warping to the golden mean of each participant's warping frequency (≈ warping frequency × 1.618), in which no harmonics are expected to be present. The purpose of this analysis was to test whether brain time warping artificially induces effects where no strong effects are present in the ground truth brain activity.

Control brain time TGM

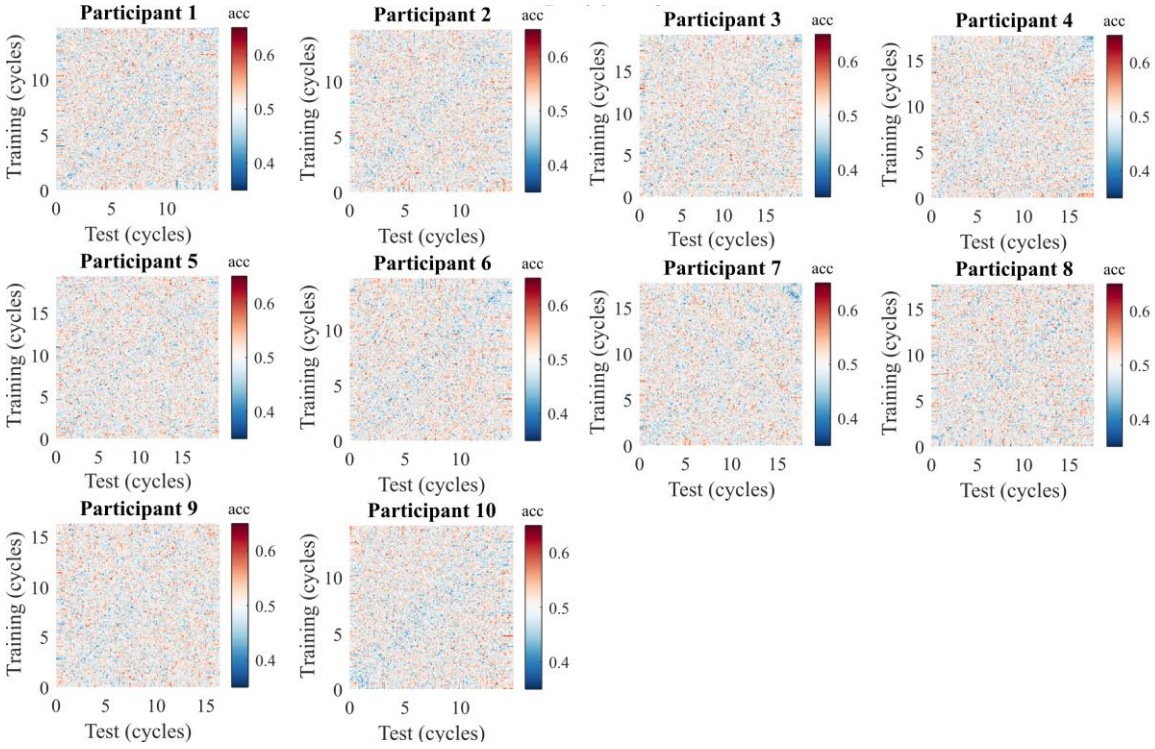

Control brain time autocorrelation

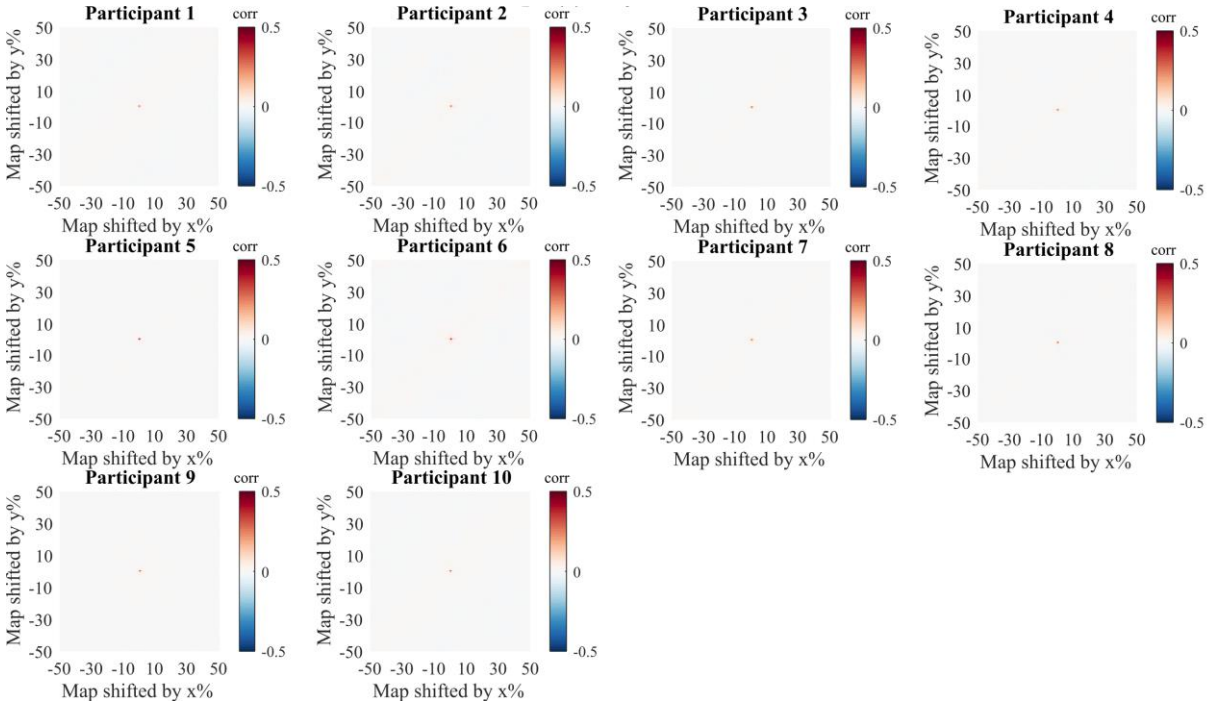

Control brain time periodicity spectra (1st level)

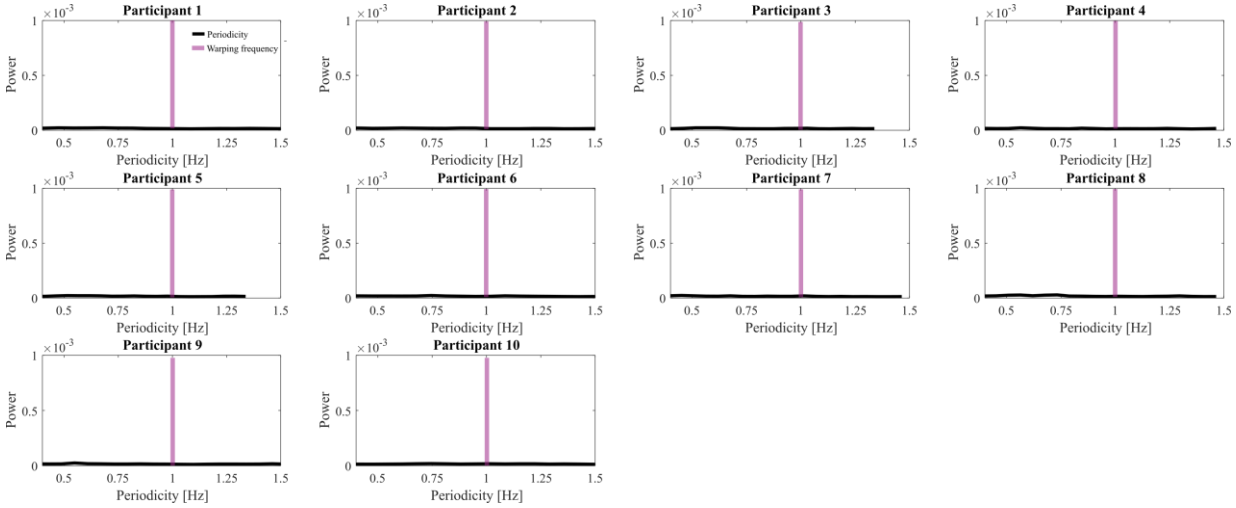

Control brain time clusters

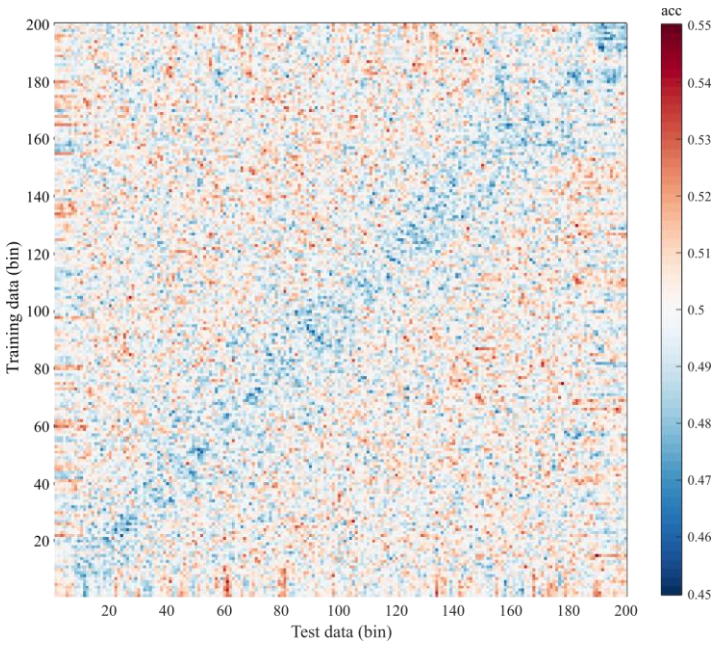

3.2 Rodent

3.2.1 Basic (main analysis)

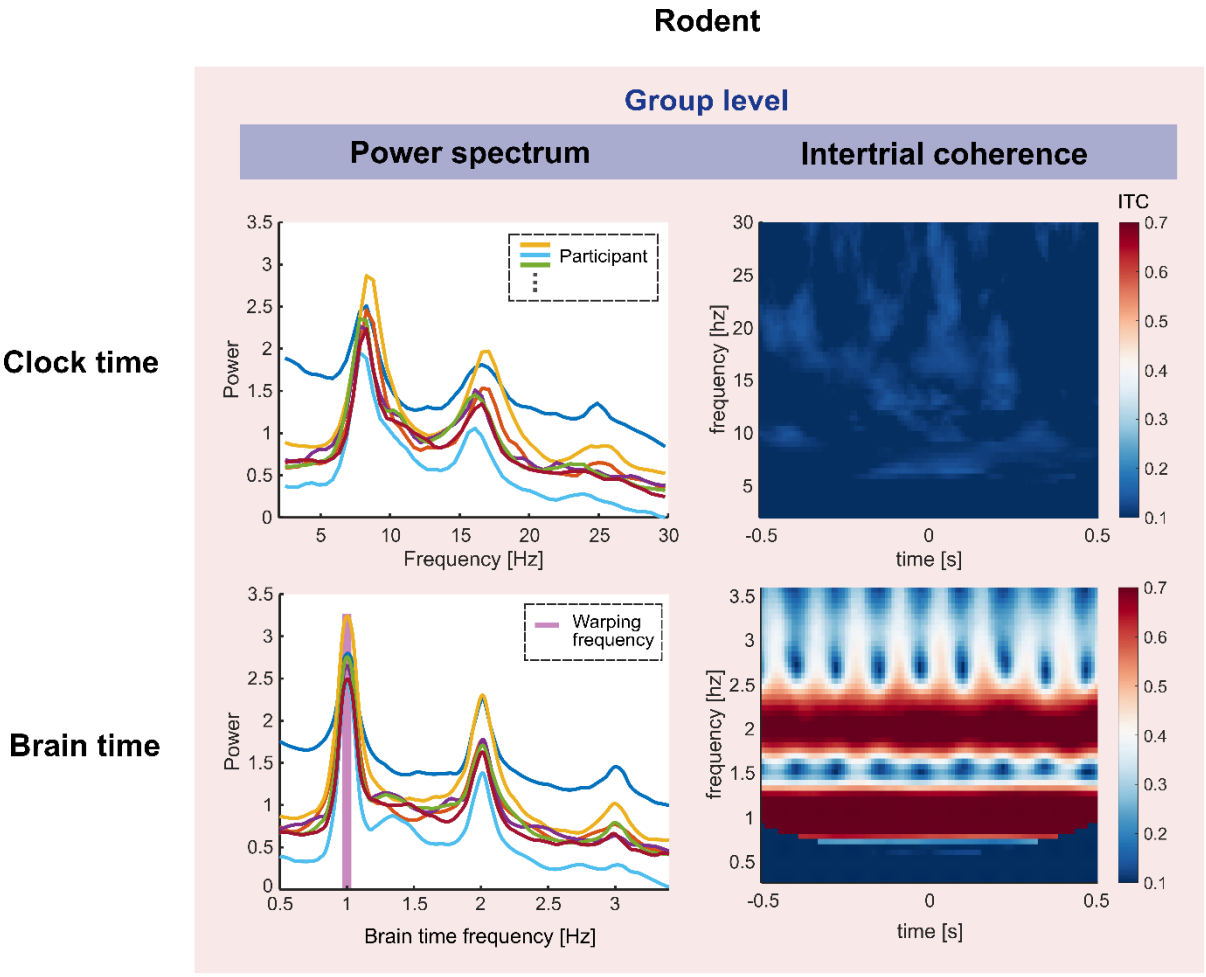

Power spectrum displays the power across frequencies in the local field potential of the entorhinal recordings.

3.2.2 Grid cells

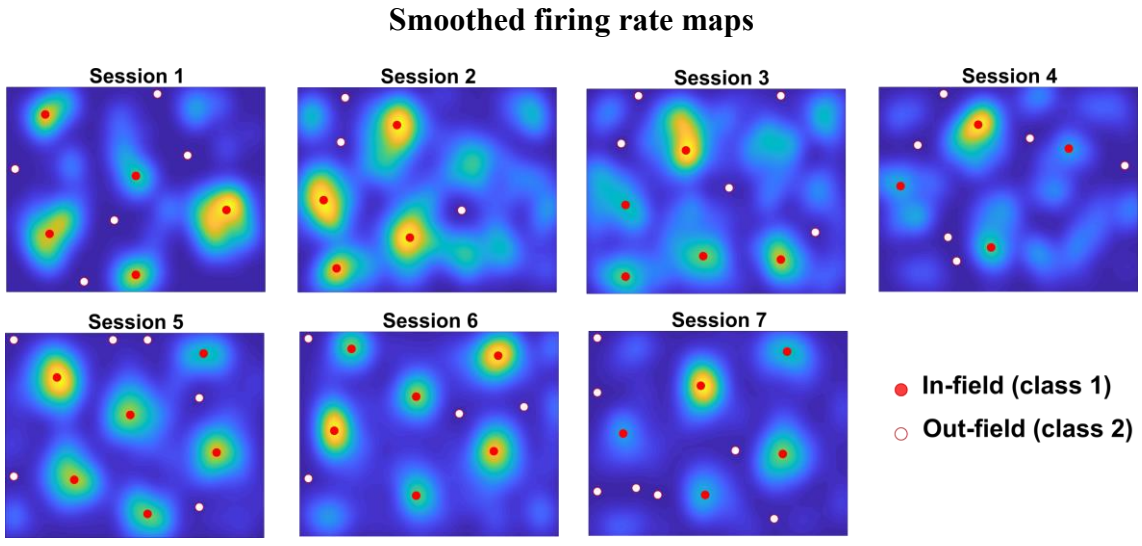

3.2.3 Spike-field coupling

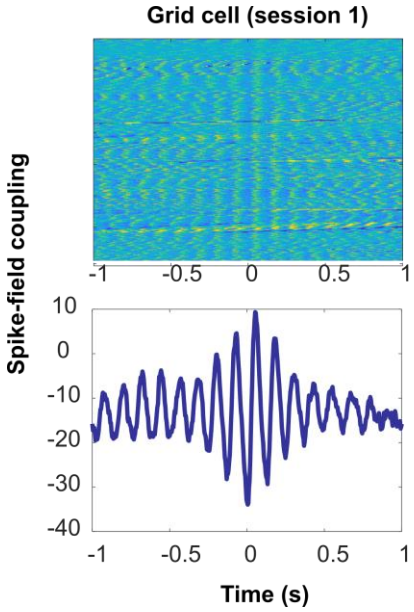

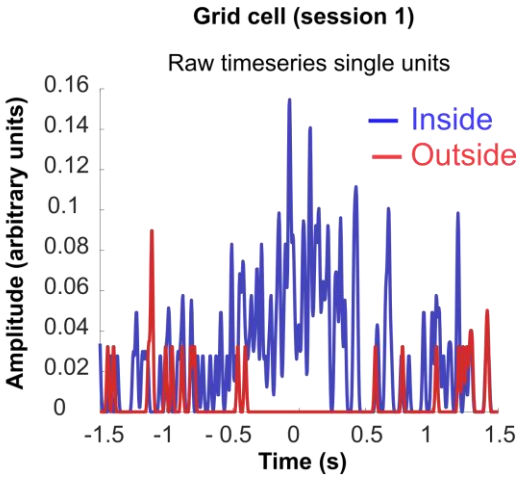

3.2.4 Advanced

Brain time TGM

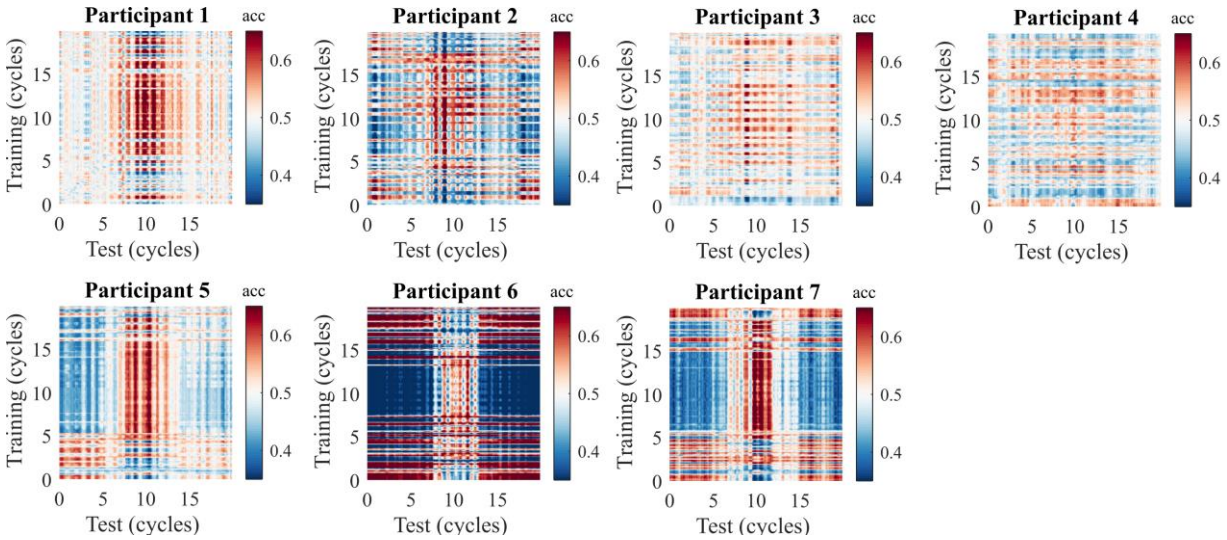

Brain time autocorrelation

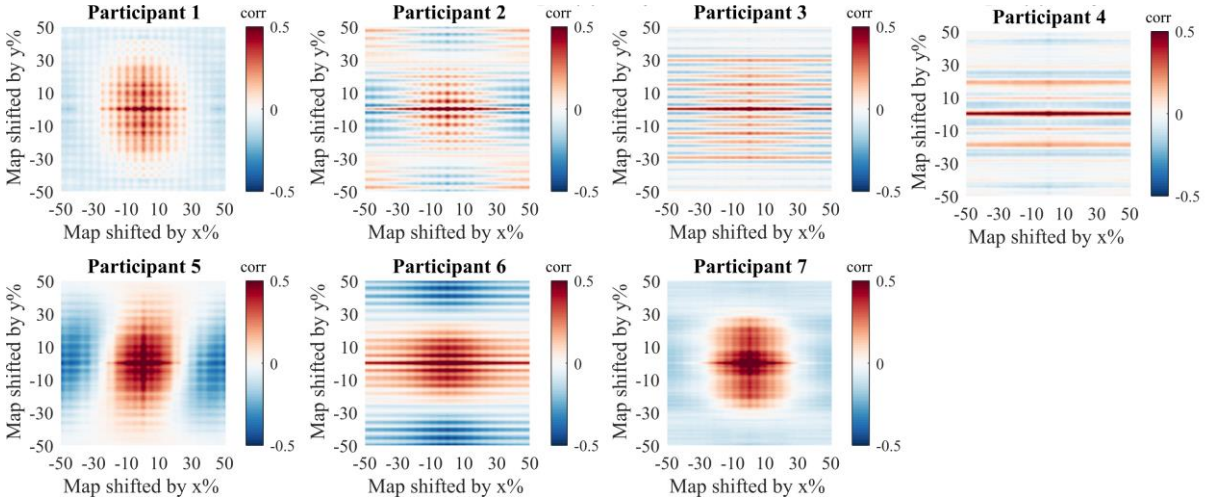

Brain time periodicity spectra (1st level)

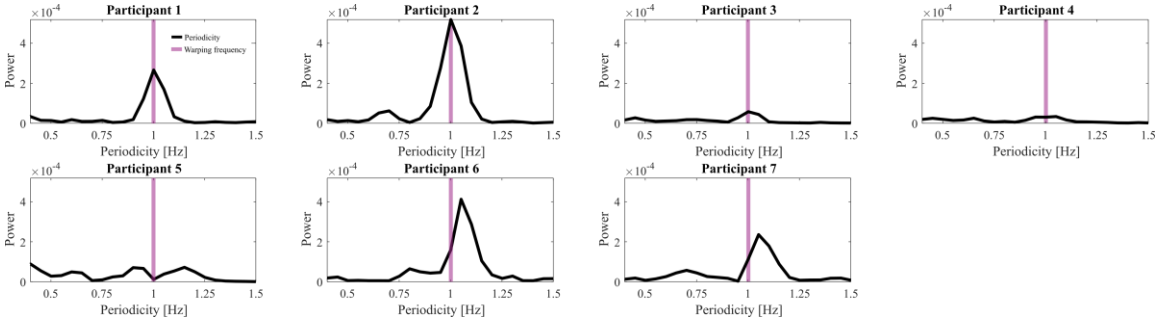

Brain time clusters

In line with our prediction, significant clusters occur in the period around t = 0, where the data was defined to contain a class difference.

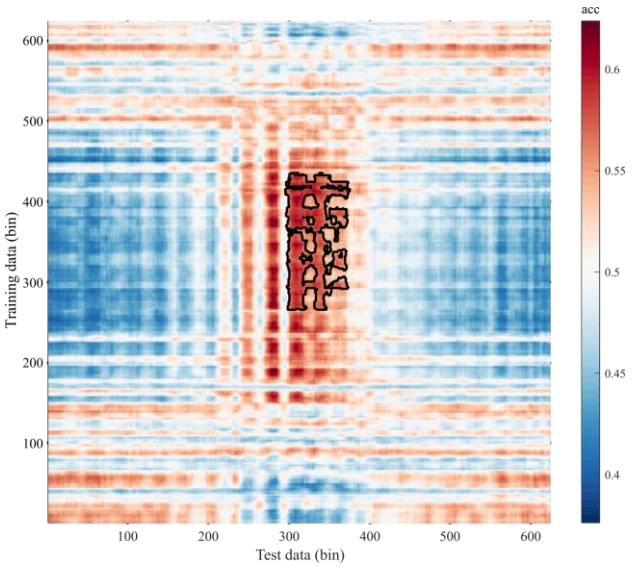

Clock time TGM

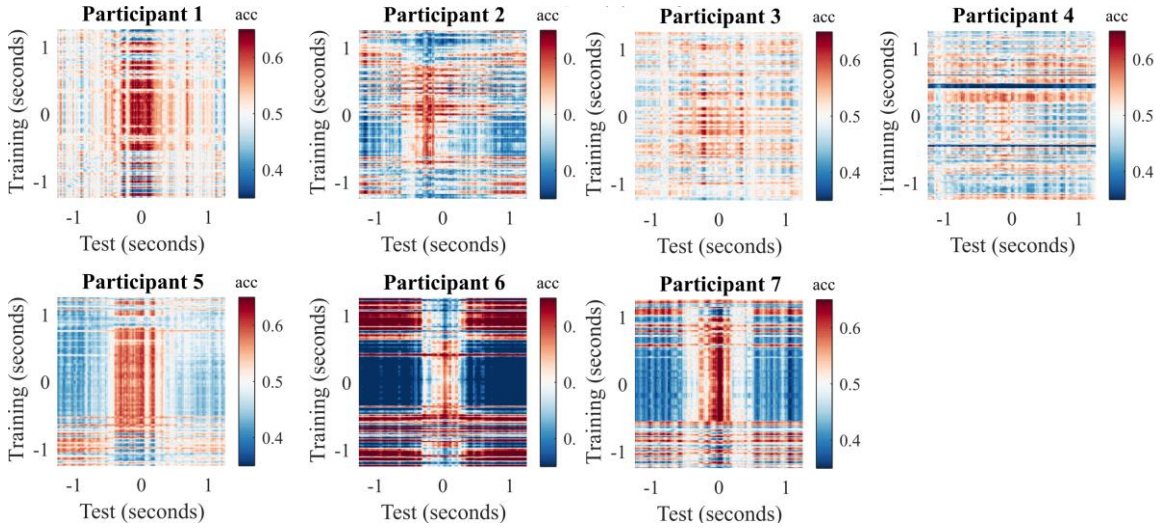

Clock time autocorrelation

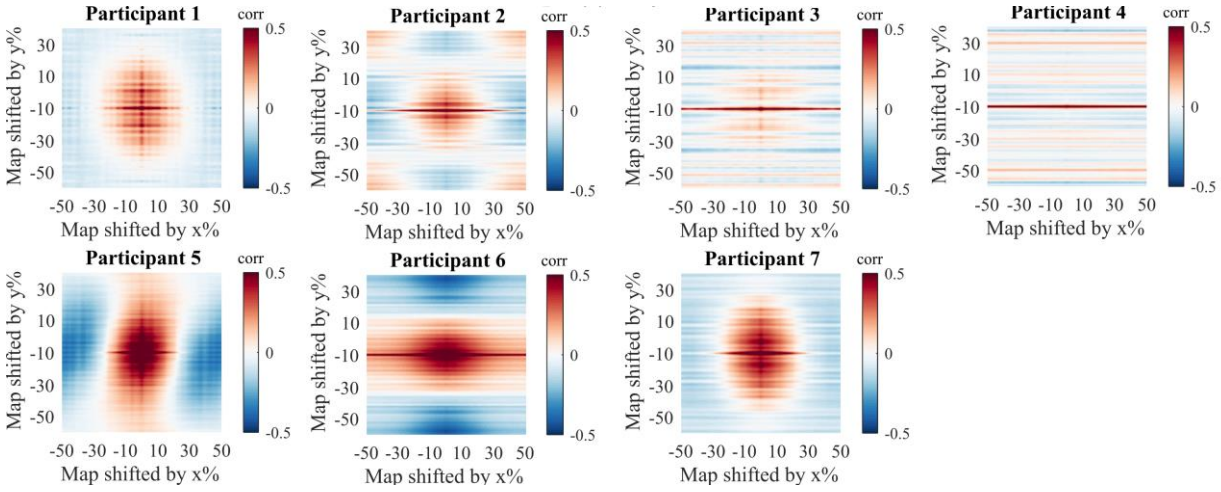

Clock time periodicity spectra (1st level)

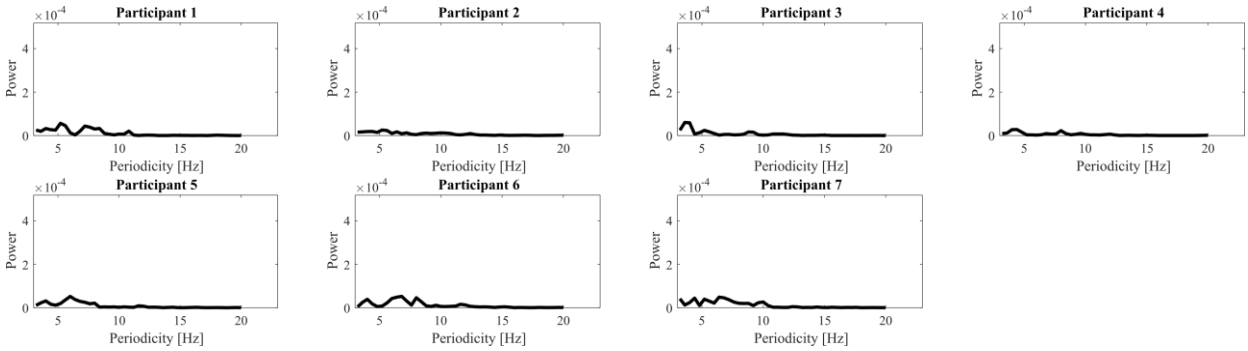

Clock time clusters

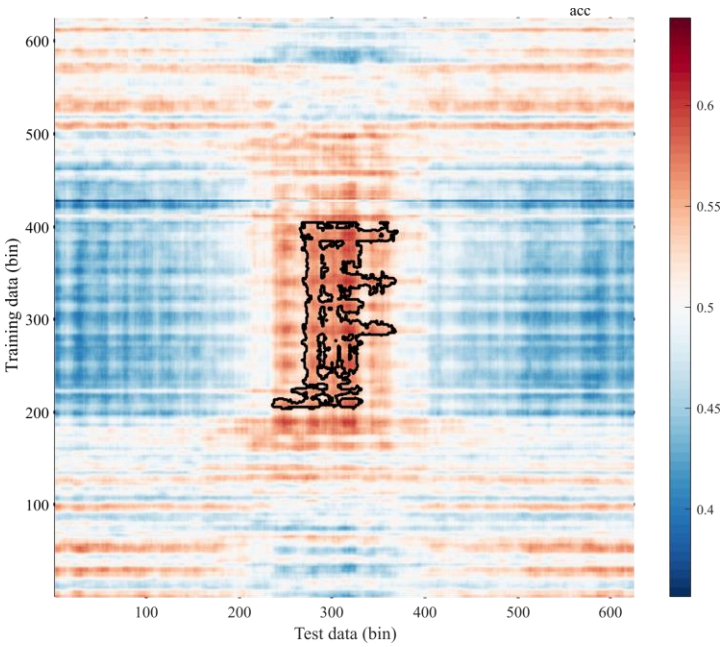

3.3 Human

3.3.1 Basic (main analysis)

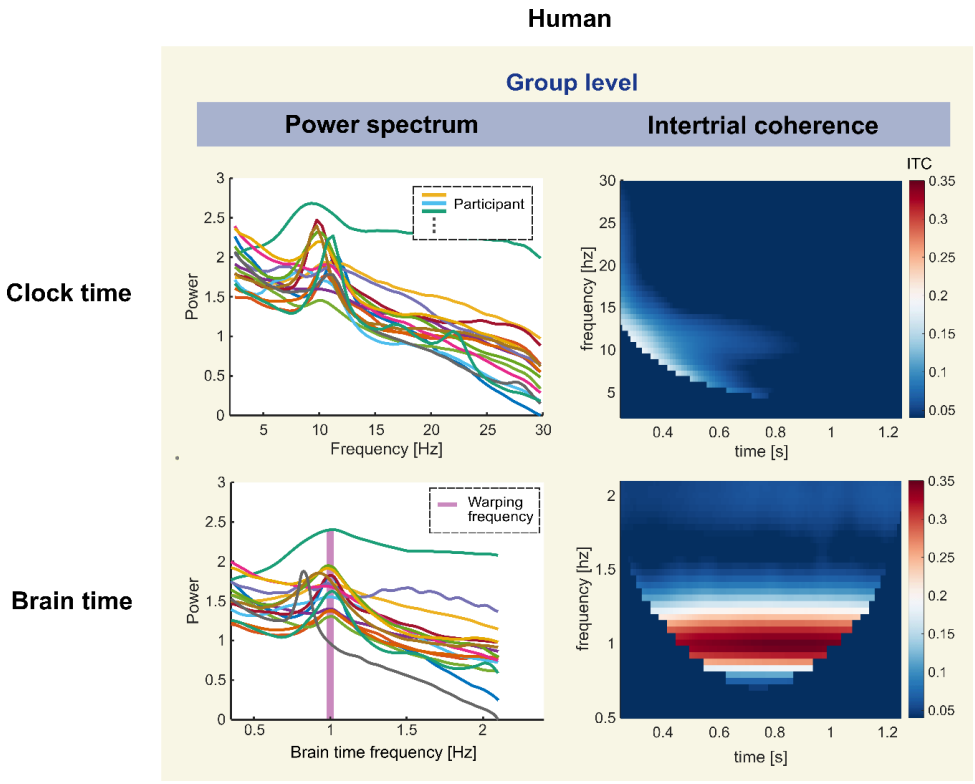

Power spectrum displays the power across frequencies in the EEG data across channels.

3.3.2 Advanced (main analysis)

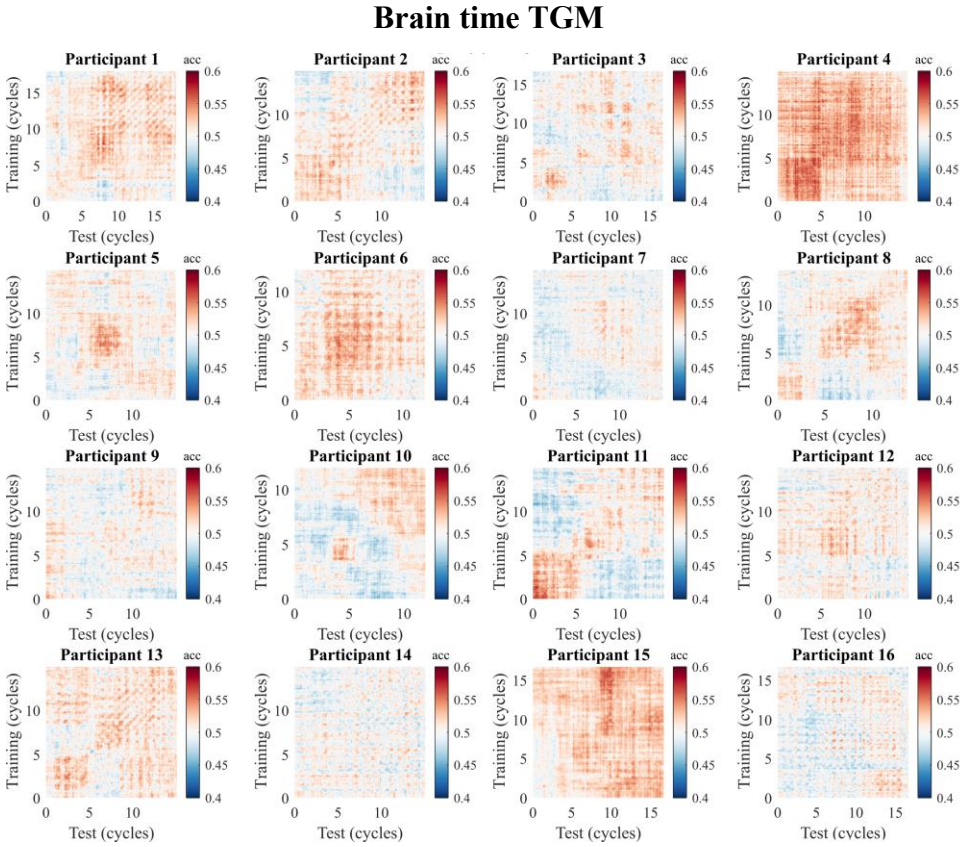

Brain time autocorrelation

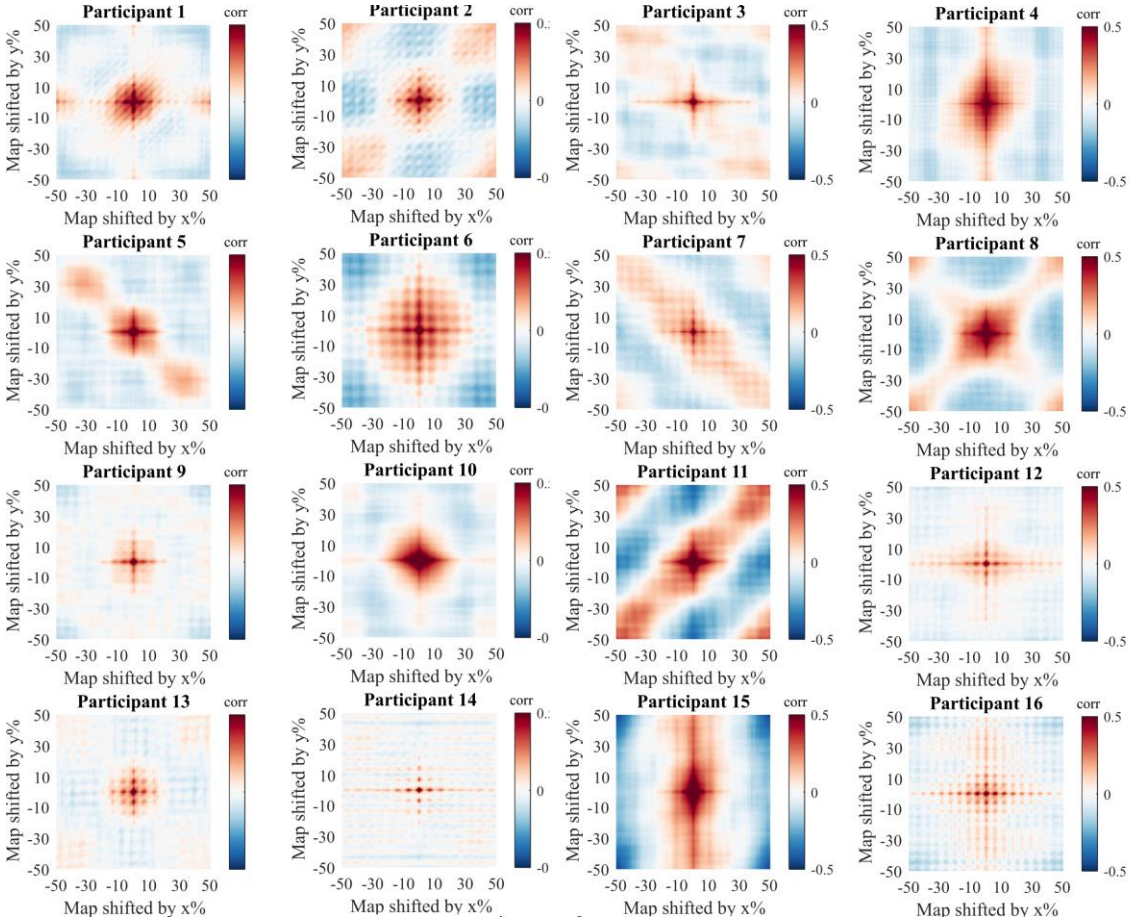

Brain time periodicity spectra (1st level)

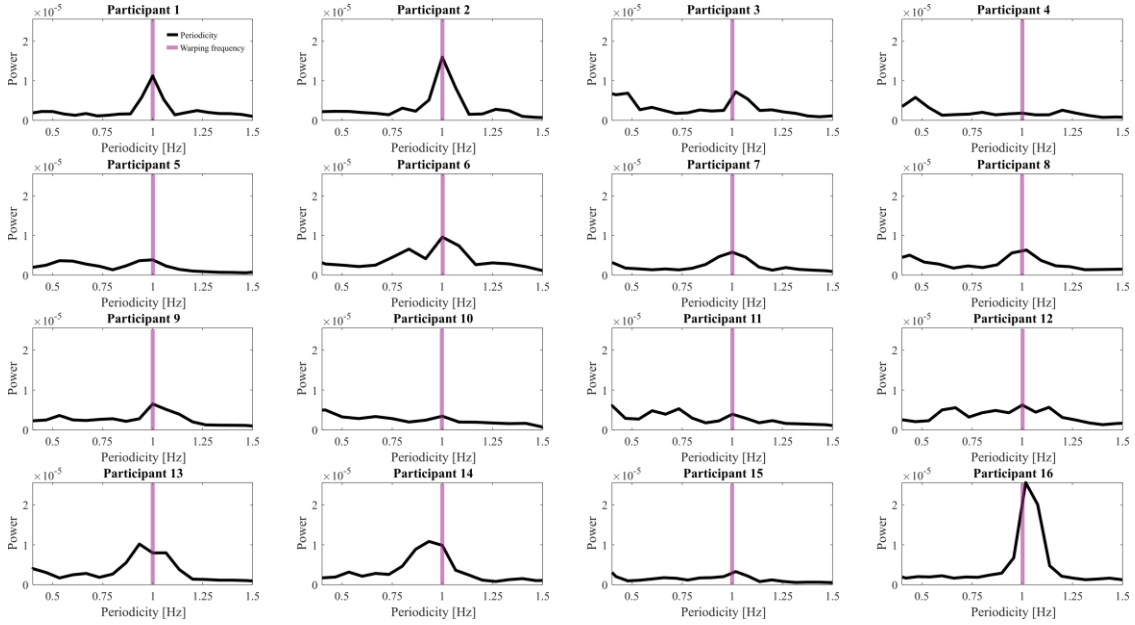

Brain time clusters

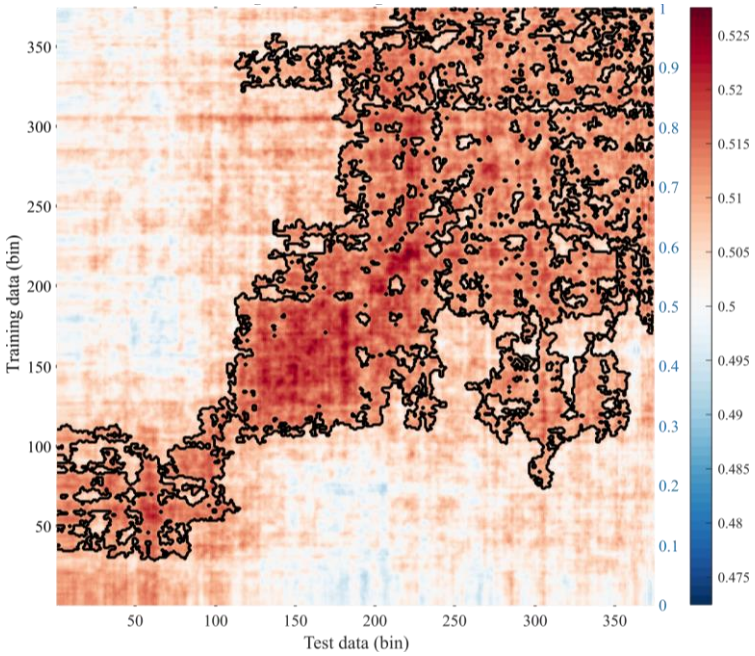

Clock time TGM

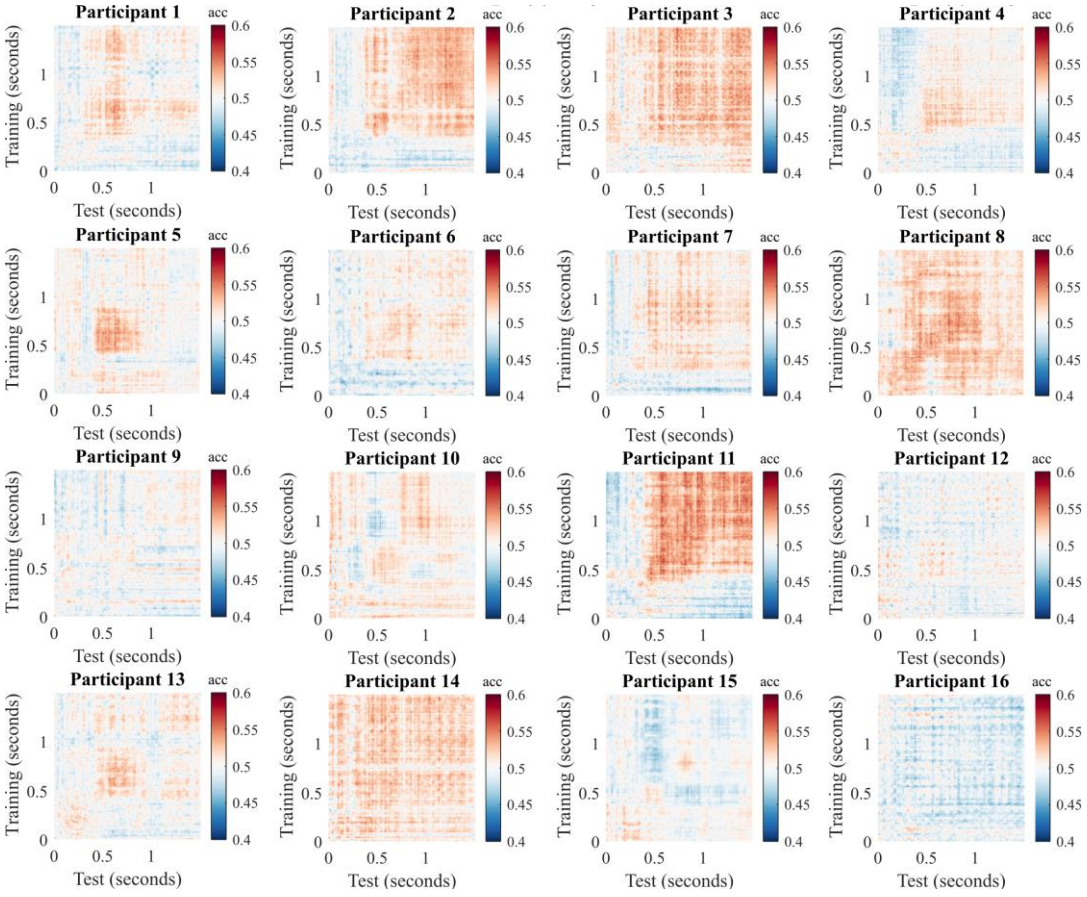

Clock time autocorrelation

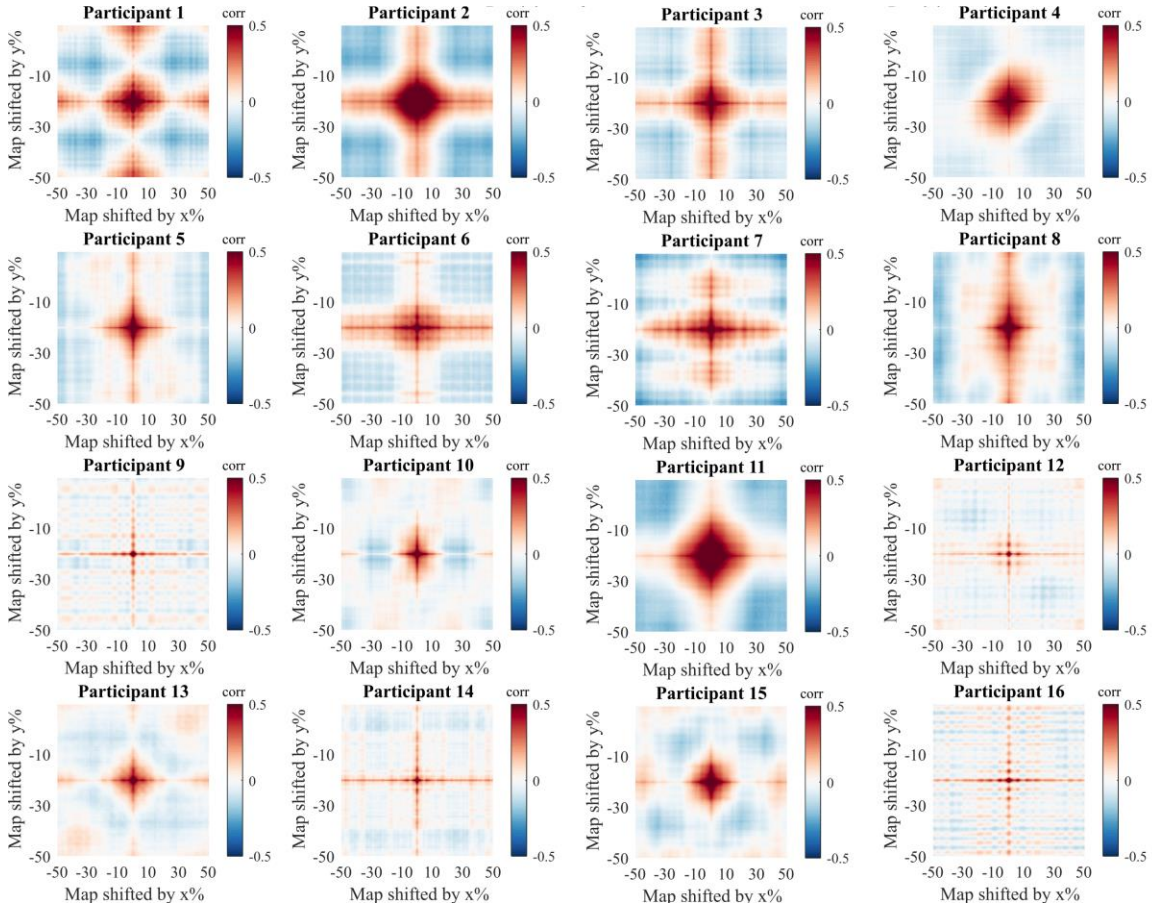

Clock time periodicity spectra (1st level)

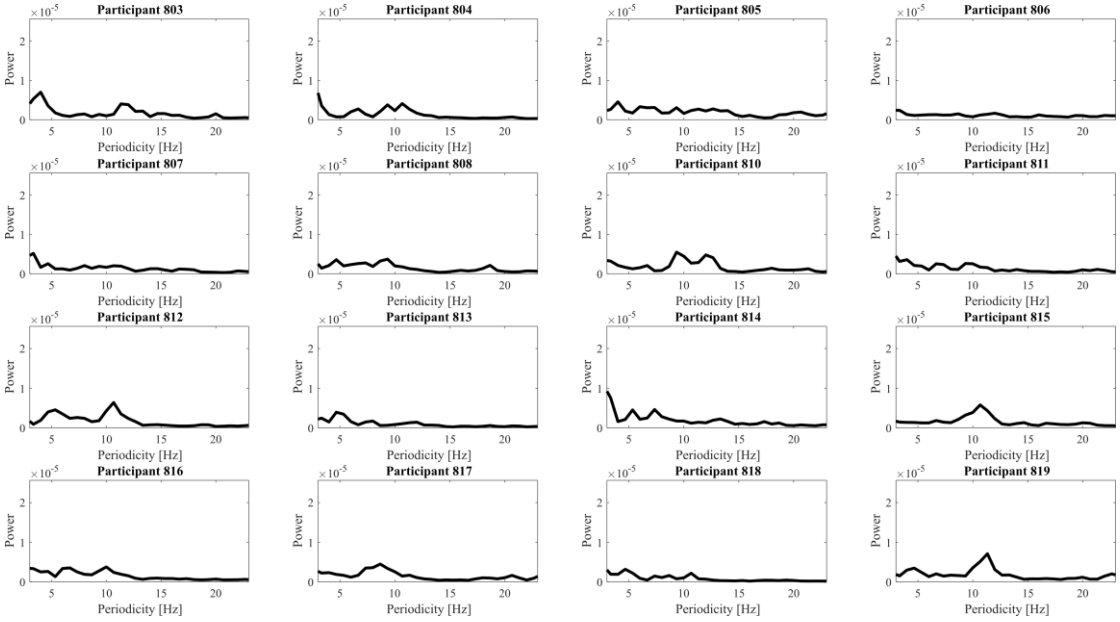

Clock time clusters

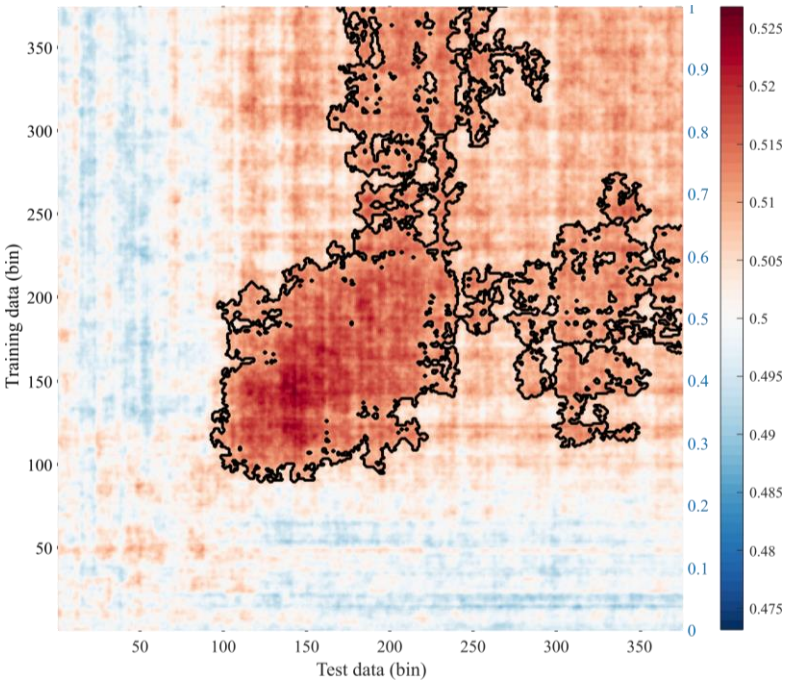
Training data (bin)
Test data (bin)
50
100
150
200
250
300
350
0
0.1
0.2
0.3
0.4
0.5
0.6
0.7
0.8
0.9
1
0.525
0.52
0.515
0.51
0.505
0.5
0.495
0.49
0.485
0.48
0.475

Supplementary material Chapter 4

1. Event-related potential

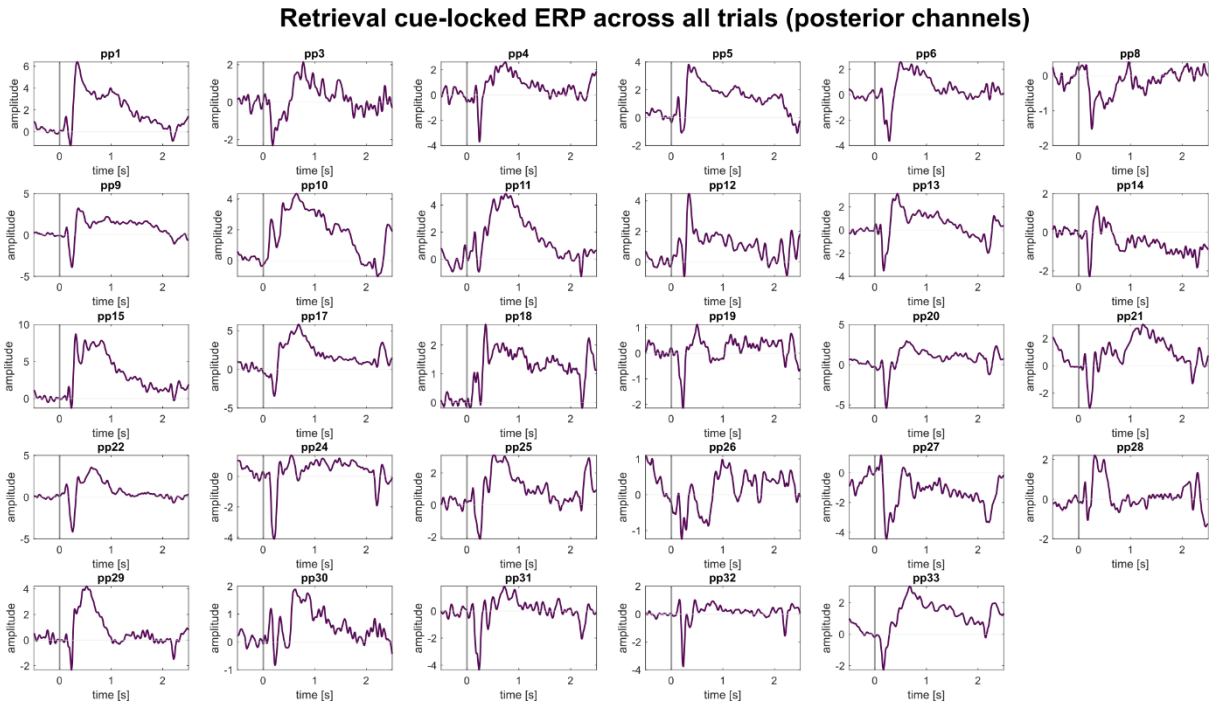

Supplementary Figure 1. Retrieval cue-locked ERP

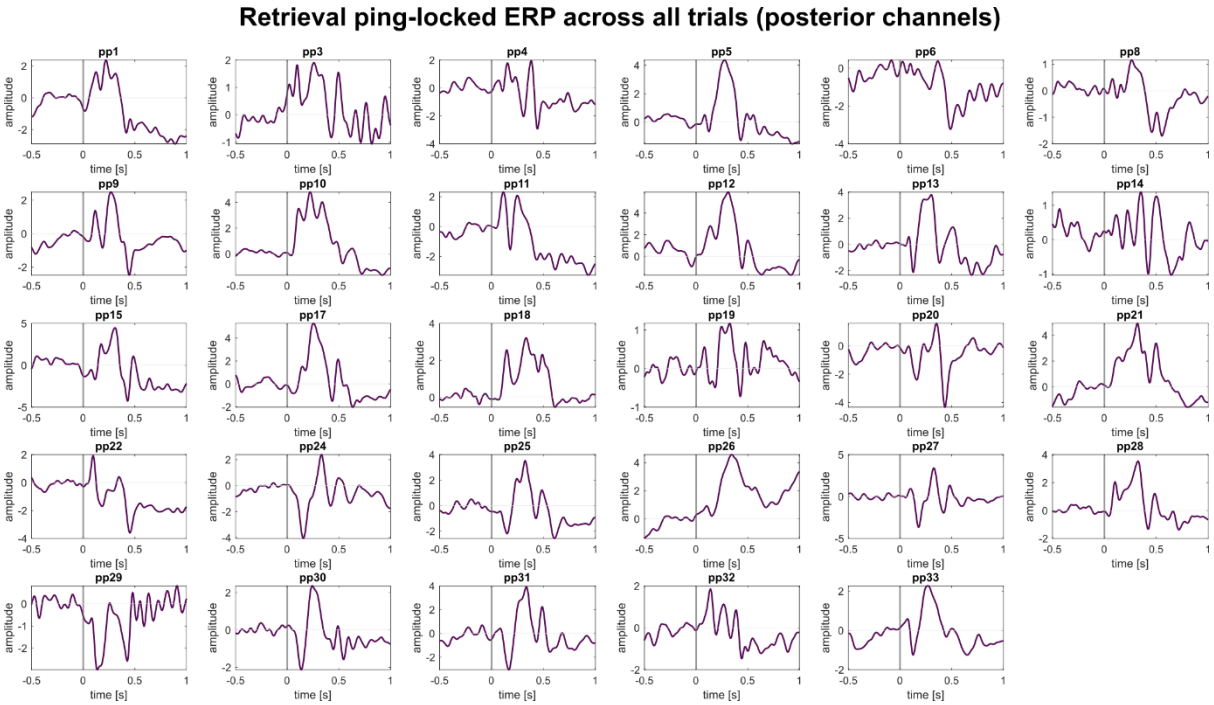

Supplementary Figure 2. Retrieval ping-locked ERP

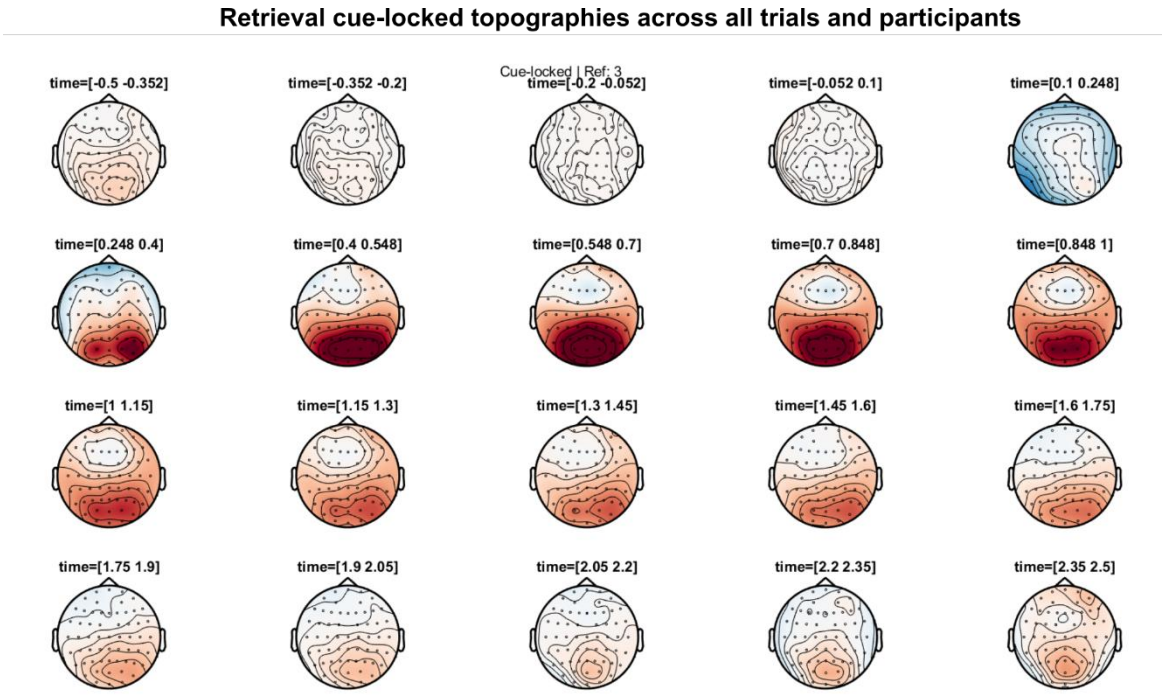

Supplementary Figure 3. Retrieval cue-locked topographies

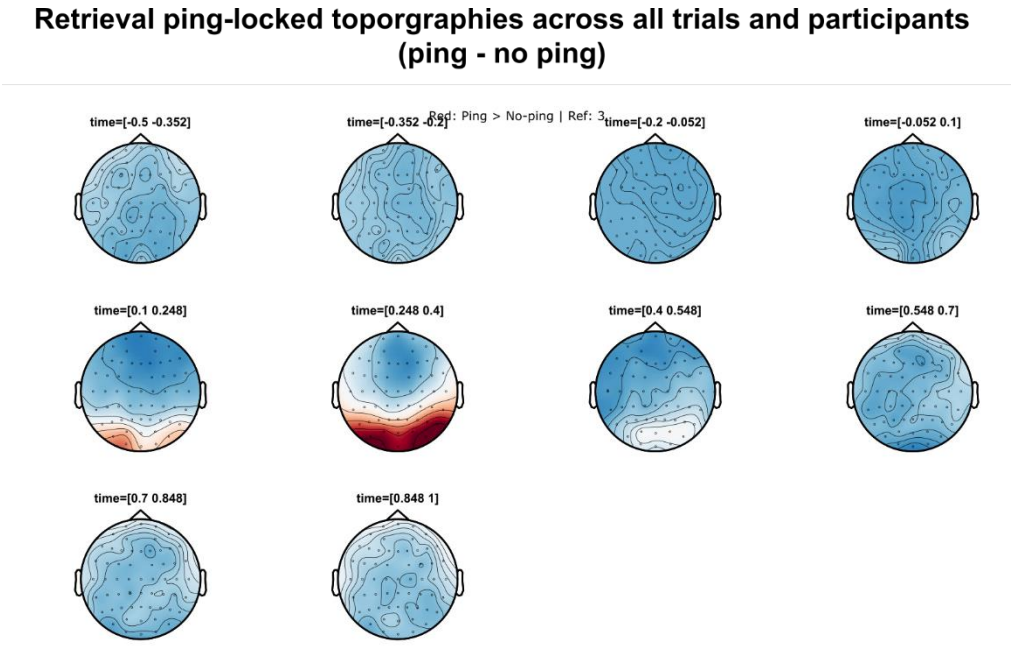

Supplementary Figure 4. Retrieval ping-locked topographies (ping vs. no ping trials)

Channel	Early ping (p-val)	Middle ping (p-val)	Late ping (p-val)
Fp1	0.032	0.616	0.246
Fpz	0.089	0.079	0.011
Fp2	0.042	0.537	0.115
AF8	0.119	0.422	0.318
AF7	0.014	0.272	0.954
AF3	0.439	0.23	0.123
AF4	0.712	0.541	0.014
F7	0.002	0.346	0.358
F5	0.068	0.439	0.33
F3	0.119	0.477	0.693
F1	0.597	0.662	0.119
Fz	0.053	0.551	0.003
F2	0.013	0.473	0
F4	0.341	0.939	0.049
F6	0.427	0.559	0.707
F8	0.131	0.826	0.825
FT8	0.001	0.097	0.049
FC6	0.177	0.142	0.78
FC4	0.962	0.176	0.881
FC2	0.245	0.276	0.09
FC1	0.969	0.503	0.881
FC3	0.176	0.279	0.28
FC5	0.011	0.083	0.112
FT7	0.002	0.298	0.127
T7	0.004	0.047	0.043
C5	0.013	0.027	0.051
C3	0.002	0.022	0.01
C1	0.148	0.049	0.04

Cz	0.144	0.155	0.114
C2	0.305	0.182	0.104
C4	0.02	0.004	0.014
C6	0.003	0	0.003
T8	0.002	0.002	0.003
TP10	0.002	0	0
TP8	0	0	0
CP6	0	0	0
CP4	0.001	0	0.001
CP2	0.006	0.001	0.001
CPz	0.019	0.006	0.01
CP1	0.272	0.002	0.003
CP3	0	0	0.001
CP5	0.002	0.001	0.001
TP7	0.002	0.008	0.001
TP9	0	0	0
P7	0	0	0
P5	0	0	0
P3	0	0	0
P1	0	0	0
Pz	0.001	0	0
P2	0.001	0	0
P4	0	0	0
P6	0	0	0
P8	0	0	0
PO8	0	0	0
PO4	0	0	0
POz	0	0	0
PO3	0	0	0
PO7	0	0	0
O1	0	0	0
Oz	0.001	0	0
O2	0	0	0

Supplementary Table 1. P-values associated with inset topographies in main text Fig. 2; rounded to three decimal points.

2. Peak order analysis simulation

2.1 Time series simulation

We used MATLAB (the MathWorks) to generate time series with two components: (1) a peak at a fixed time point (1000 ms), and (2) autocorrelated noise generated using a random walk procedure. We matched several characteristics of the simulated time series to our empirical decoding data, including the analysis period (500 to 2000 ms), sampling rate (50 Hz), and the number of (virtual) participants (N = 29). The signal-to-noise (SNR) ratio of the simulation was set to 1.15, qualitatively matching peaks observed in the empirical data. We found that varying the SNR does not significantly alter the results. We generated 1000 trials per participant, resulting in 29000 trials in total.

2.2 Analysis

We included a smoothing parameter that implemented one of four smoothing methods: no filter, a Gaussian filter, a Savitzky-Golay filter, and a median filter. We also included a window size for smoothing, set to 10 samples for our main analysis. We compared the performance of eight peak detection methods, evaluating each of them based on the absolute distance between estimated peaks and true peaks—amounting to a simplified version of the *peak order distance* score described under *condition-relative decoding peaks* in the main text. The winning method was locked in for our empirical analysis. We tested eight peak detection methods:

(1) Low-pass approach, where the maximum peak was computed after a low-pass filter was applied to the time series.
(2) Maximum value approach, which simply computed the maximum value per time series regardless of whether the surrounding data was peak-like.
(3) Cumulative sum approach, which computed the maximum peak in the derivative of the cumulative sum of the data.
(4) Cumulative integral approach, which computed the maximum peak in the cumulative integral of the data via the trapezoidal method.
(5) Integral cumulative sum approach, which worked as the previous method but which operates over the cumulative sum rather than raw time series.

(6) Wavelet transform-based method, which finds the maximum peak in a wavelet decomposed version of the data.

(7) Hilbert transform-based method, which find the maximum peak in the amplitude fluctuations in the envelope of the time series.

(8) Cross-correlation method, which finds the time lag with a maximal correlation between the signal and iteratively shifted versions of itself.

2.3 Results

We found that approach 5—the integral cumulative sum approach—reliably achieves low absolute distance errors across parameters (Supplementary Figure 5). These results were generally unchanged across adjustments of the parameters (to evaluate this, we refer to the code published with this manuscript). Thus, we used approach 5 in our main peak order detection analysis.

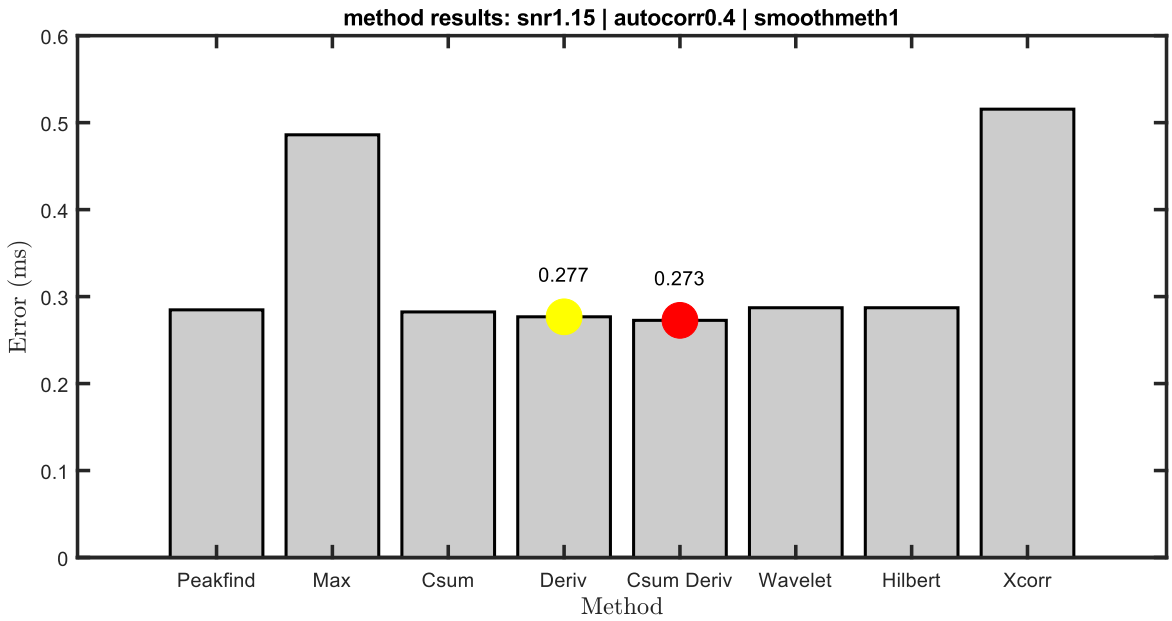

Supplementary Figure 5. In simulated time series, the integral cumulative sum approach works best for detecting a peak in noisy time series. The red circle indicates the best-performing method, and yellow the second best-performing method. Errors were computed based on the absolute distance in milliseconds (ms) between estimated and true peak location.

3. Class and trial number decoding simulation

We speculated based on a qualitative inspection of the empirical decoding results that the number of trials (N_{trials}) and classes ($N_{classes}$) reduces the statistical significance of decoding results. We evaluated this intuition by demonstrating using simulations that these two

parameters do indeed influence the variance of shuffled and empirical results, which in turn affects p-values but only if there is a true effect in the data.

3.1 Time series simulation

Using MATLAB, we generated one ground truth vector of class labels which represented the true class structure in the simulated data. This vector contained a random sequence of integers randomly grabbed between the interval 1 and $N_{classes}$. For example, with 16 classes, the ground truth pattern might have contained a sequence of [2,7,15,4,13,17] and with 2 classes a sequence of [2,2,1,2,1,2].

Then, to simulate shuffled decoding results, we generated a distribution of random sequences of integers identical the ground truth procedure, but with newly generated random integers. These random sequences represented shuffled decoding results and were scored based on their average element-wise correspondence to the ground truth pattern—which is how decoding accuracy is normally computed. For example, if the permuted vector is [2,1,2,2,1,1] and the true sequence is [2,2,1,2,1,2], the accuracy would be 50% because half of the class labels correspond to the true structure. Trivially, with increasing repetitions the shuffled distribution will approach chance level predictions of the ground truth pattern (i.e., the expected value is exactly at $1/ N_{classes}$).

Finally, to simulate empirical decoding results, we again generated a distribution of random integers identical to the procedure for shuffled and ground truth decoding results. However, for these data we manually injected between 0% and 60% of the ground truth pattern into the otherwise random vector, effectively modulating decoding accuracy. With 0% of the ground truth injected, there is no statistically detectable difference in accuracy between empirical and shuffled decoding results, because the vectors are equally random. With 60%, the encoding results are substantially more accurate than shuffled results, yielding above chance decoding accuracy.

We simplified our simulation by operationalizing the variable N_{trials} as the number of elements in the vector, allowing us to efficiently investigate how the number of observations influences statistical tests. We also compared $N_{classes} = 2$ and $N_{classes} = 16$, which respectively match the number of classes for top- and bottom-level category decoding in our main experiment. Both N_{trials} and $N_{classes}$ were independently manipulated in a 2x2 factorial design, allowing us to evaluate the contribution of each variable toward statistical outcomes (as a function of effect size).

3.2 Results

First, with respect to $N_{classes}$, we found that increasing the number of classes reduces the spread of both shuffled and empirical decoding results (Supplementary Figure 6; columns). This happens both if there is no true effect in the empirical data, and when a significant proportion of the ground truth is inserted into the empirical data. Second, we found that N_{trials} similarly reduces the variance of both shuffled and decoding results, both across low and high $N_{classes}$ (Supplementary Figure 6; top and bottom half). Thus, we conclude that both factors modulate the likelihood of finding a significant difference between empirical and shuffled results, but only if there is a true effect in the data. Indeed, as we can glean from the results based on non-existent effects, the distributions of empirical and shuffled will overlap regardless of N_{trials} or $N_{classes}$ (Supplementary Figure 6; left half). In contrast, if there is an effect (60% injected ground truth), both N_{trials} and $N_{classes}$ independently increase the distributional distance between empirical and shuffled accuracy values.

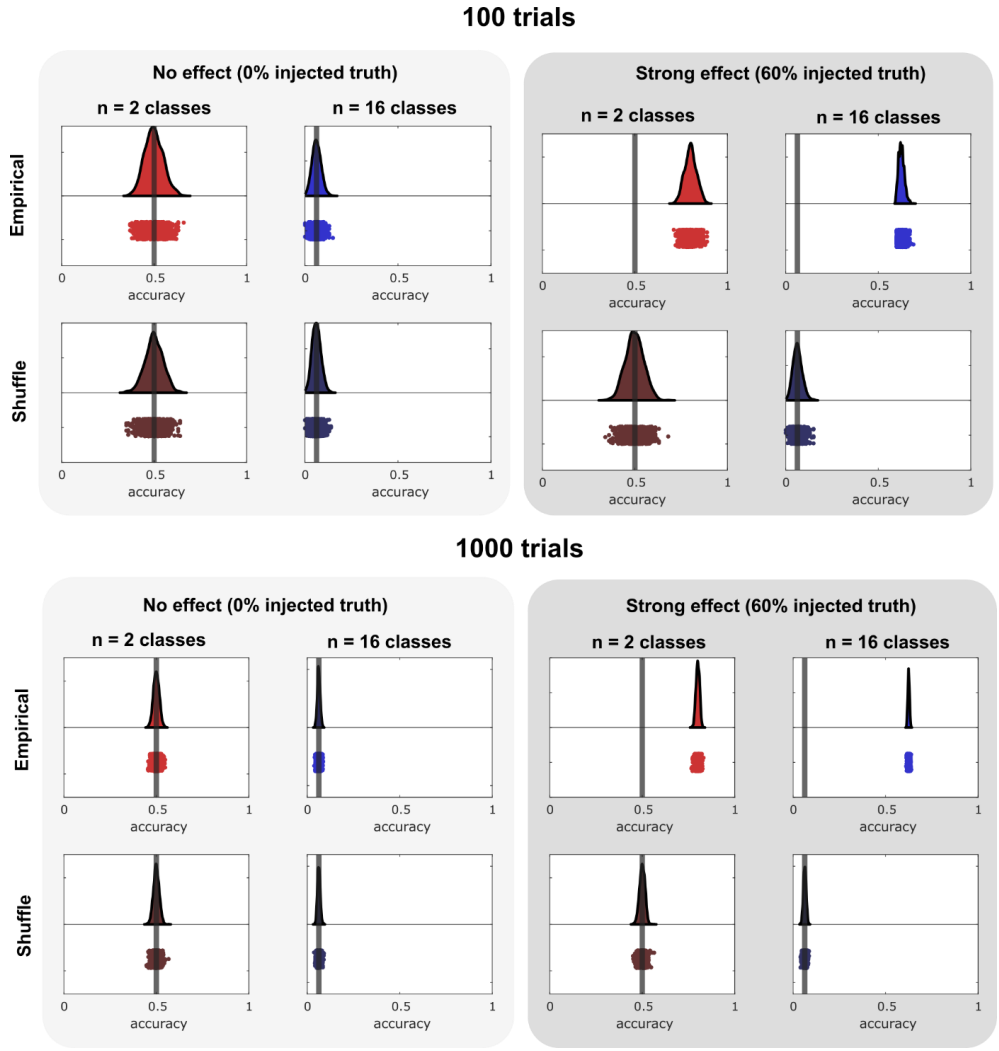

Supplementary Figure 6. The effects of class and trial number on decoding accuracy. Both the number of classes (columns) and trials (top vs. bottom half) influences the distance between shuffled and empirical distributions—but only if there is an effect in the data (left vs. right half).

3.3 Discussion

We found that N_{trials} and $N_{classes}$ independently reduce the variance of accuracy results, which will affect statistical tests between empirical and shuffled distributions but only if there is an effect in the data. As suggested in the main text, these findings suggest that statistical analyses that depend on variance comparisons between empirical and shuffled distributions should be interpreted with care if it is done across conditions with varying N_{trials} and $N_{classes}$. With regard to our main analysis for example, the fact that the decoder based on pinged trials yields more significant decodability compared to the decoder based on no-pinged trials should be interpreted with caution because there are differences in N_{trials} between the two conditions that could partially or fully explain this effect. More generally, we found that the condition with more trials or more classes is by default more likely to yield significant p-values—but only if a true effect exist.

These findings may be a manifestation of the classical notion of statistical power in statistical analysis but within the less intuitive context of decoding accuracy. Our interpretation then is not that N_{trials} and $N_{classes}$ must necessarily be equal between conditions for a statistical comparison to be meaningful. Rather, we wanted to err on the side of caution and ensure that analyses where power differences could possibly explain condition differences (e.g., Fig. 4.3 and Fig. 4.4A and 4B in the main text) do not inform subsequent analyses and scientific interpretations by themselves. Instead, we supplemented each of the implicated analyses with additional rationale (in the case of Fig. 4.3 main text) or analyses that do not involve empirical-to-shuffle decoding comparisons. Indeed, main text Fig. 4.4C and Fig. 4.4D involve direct comparisons between empirical and shuffled distributions, sidestepping the issue altogether.

References

Abbott, L. F., & Nelson, S. B. (2000). Synaptic plasticity: Taming the beast. *Nature Neuroscience*, *3*(11), Article 11. https://doi.org/10.1038/81453

Ai, L., & Ro, T. (2013). The phase of prestimulus alpha oscillations affects tactile perception. *Journal of Neurophysiology*, *111*(6), 1300–1307. https://doi.org/10.1152/jn.00125.2013

Akin, M. (2002). Comparison of Wavelet Transform and FFT Methods in the Analysis of EEG Signals. *Journal of Medical Systems*, *26*(3), 241–247. https://doi.org/10.1023/A:1015075101937

Antle, M. C., & Silver, R. (2005). Orchestrating time: Arrangements of the brain circadian clock. *Trends Neurosci.*, *28*. https://doi.org/10.1016/j.tins.2005.01.003

Backus, A. R., Schoffelen, J.-M., Szebényi, S., Hanslmayr, S., & Doeller, C. F. (2016). Hippocampal-Prefrontal Theta Oscillations Support Memory Integration. *Current Biology*, *26*(4), Article 4. https://doi.org/10.1016/j.cub.2015.12.048

Bae, G.-. Y., & Luck, S. J. (2019). Decoding motion direction using the topography of sustained ERPs and alpha oscillations. *NeuroImage*, *184*. https://doi.org/10.1016/j.neuroimage.2018.09.029

Bahramisharif, A., Jensen, O., Jacobs, J., & Lisman, J. (2018). Serial representation of items during working memory maintenance at letter-selective cortical sites. *PLoS Biology*, *16*(8), e2003805. https://doi.org/10.1371/journal.pbio.2003805

Barbosa, J., Lozano-Soldevilla, D., & Compte, A. (2021). Pinging the brain with visual impulses reveals electrically active, not activity-silent, working memories. *PLoS Biology*, *19*(10), e3001436. https://doi.org/10.1371/journal.pbio.3001436

Bastos, A. M., Vezoli, J., Bosman, C. A., Schoffelen, J.-M., Oostenveld, R., Dowdall, J. R., De Weerd, P., Kennedy, H., & Fries, P. (2015). Visual Areas Exert Feedforward and

Feedback Influences through Distinct Frequency Channels. *Neuron*, *85*(2), 390–401. https://doi.org/10.1016/j.neuron.2014.12.018

Battaglia, F. P., Benchenane, K., Sirota, A., Pennartz, C. M. A., & Wiener, S. I. (2011). The hippocampus: Hub of brain network communication for memory. *Trends in Cognitive Sciences*, *15*(7), 310–318. https://doi.org/10.1016/j.tics.2011.05.008

Belluscio, M. A., Mizuseki, K., Schmidt, R., Kempter, R., & Buzsáki, G. (2012). Cross-Frequency Phase–Phase Coupling between Theta and Gamma Oscillations in the Hippocampus. *The Journal of Neuroscience*, *32*(2), 423 LP – 435. https://doi.org/10.1523/JNEUROSCI.4122-11.2012

Benjamini, Y., & Yekutieli, D. (2001). The control of the false discovery rate in multiple testing under dependency. *The Annals of Statistics*, *29*(4), 1165–1188. https://doi.org/10.1214/aos/1013699998

Berger, H. (1929). Über das Elektrenkephalogramm des Menschen. *Archiv für Psychiatrie und Nervenkrankheiten*, *87*(1), 527–570. https://doi.org/10.1007/BF01797193

Berndt, D. J., & Clifford, J. (1994). Using Dynamic Time Warping to Find Patterns in Time Series. *Proceedings of the 3rd International Conference on Knowledge Discovery and Data Mining*, 359–370.

Beukers, A. O., Buschman, T. J., Cohen, J. D., & Norman, K. A. (2021). Is Activity Silent Working Memory Simply Episodic Memory? *Trends in Cognitive Sciences*, *25*(4), 284–293. https://doi.org/10.1016/j.tics.2021.01.003

Bi, G., & Poo, M. (1998). Synaptic Modifications in Cultured Hippocampal Neurons: Dependence on Spike Timing, Synaptic Strength, and Postsynaptic Cell Type. *Journal of Neuroscience*, *18*(24), 10464–10472. https://doi.org/10.1523/JNEUROSCI.18-24-10464.1998

Bi, G., & Poo, M. (2001). Synaptic modification by correlated activity: Hebb's postulate revisited. *Annual Review of Neuroscience*, *24*, 139–166. https://doi.org/10.1146/annurev.neuro.24.1.139

Bird, C. M., & Burgess, N. (2008). The hippocampus and memory: Insights from spatial processing. *Nature Reviews Neuroscience*, *9*(3), Article 3. https://doi.org/10.1038/nrn2335

Bonnefond, M., & Jensen, O. (2015). Gamma activity coupled to alpha phase as a mechanism for top-down controlled gating. *PLoS ONE*, *10*. https://doi.org/10.1371/journal.pone.0128667

Börgers, C., & Kopell, N. J. (2008). Gamma oscillations and stimulus selection. *Neural Computation*, *20*(2), 383–414. https://doi.org/10.1162/neco.2007.07-06-289

Bouwer, F. L., Honing, H., & Slagter, H. A. (2020). Beat-based and Memory-based Temporal Expectations in Rhythm: Similar Perceptual Effects, Different Underlying Mechanisms. *Journal of Cognitive Neuroscience*, *32*(7), 1221–1241. https://doi.org/10.1162/jocn_a_01529

Bragin, A., Jandó, G., Nádasdy, Z., Hetke, J., Wise, K., & Buzsáki, G. (1995). Gamma (40-100 Hz) oscillation in the hippocampus of the behaving rat. *The Journal of Neuroscience: The Official Journal of the Society for Neuroscience*, *15*(1 Pt 1), 47–60. https://doi.org/10.1523/JNEUROSCI.15-01-00047.1995

Bressler, S. L., & Kelso, J. a. S. (2001). Cortical coordination dynamics and cognition. *Trends in Cognitive Sciences*, *5*(1), 26–36. https://doi.org/10.1016/s1364-6613(00)01564-3

Broadbent, N. J., Squire, L. R., & Clark, R. E. (2004). Spatial memory, recognition memory, and the hippocampus. *Proceedings of the National Academy of Sciences*, *101*(40), 14515–14520. https://doi.org/10.1073/pnas.0406344101

Brodeur, M. B., Dionne-Dostie, E., Montreuil, T., & Lepage, M. (2010). The Bank of Standardized Stimuli (BOSS), a New Set of 480 Normative Photos of Objects to Be Used as Visual Stimuli in Cognitive Research. *PLOS ONE*, *5*(5), e10773. https://doi.org/10.1371/journal.pone.0010773

Burgess, N., Barry, C., & O'Keefe, J. (2007). An oscillatory interference model of grid cell firing. *Hippocampus*, *17*(9), 801–812. https://doi.org/10.1002/hipo.20327

Burgess, N., & O'Keefe, J. (2011). Models of place and grid cell firing and theta rhythmicity. *Curr. Opin. Neurobiol.*, *21*. https://doi.org/10.1016/j.conb.2011.07.002

Busch, N. A., Dubois, J., & VanRullen, R. (2009). The Phase of Ongoing EEG Oscillations Predicts Visual Perception. *The Journal of Neuroscience*, *29*(24), Article 24. https://doi.org/10.1523/JNEUROSCI.0113-09.2009

Bush, D., Bisby, J. A., Bird, C. M., Gollwitzer, S., Rodionov, R., Diehl, B., McEvoy, A. W., Walker, M. C., & Burgess, N. (2017). Human hippocampal theta power indicates movement onset and distance travelled. *Proceedings of the National Academy of Sciences*, *114*(46), 12297–12302. https://doi.org/10.1073/pnas.1708716114

Buzsáki, G. (1996). The hippocampo-neocortical dialogue. *Cerebral Cortex (New York, N.Y.: 1991)*, *6*(2), 81–92. https://doi.org/10.1093/cercor/6.2.81

Buzsáki, G. (2002). Theta oscillations in the hippocampus. *Neuron*, *33*(3), 325–340. https://doi.org/10.1016/s0896-6273(02)00586-x

Buzsáki, G. (2005). Theta rhythm of navigation: Link between path integration and landmark navigation, episodic and semantic memory. *Hippocampus*, *15*(7), 827–840. https://doi.org/10.1002/hipo.20113

Buzsáki, G. (2010). Neural syntax: Cell assemblies, synapsembles and readers. *Neuron*, *68*(3), 362–385. https://doi.org/10.1016/j.neuron.2010.09.023

Buzsáki, G. (2015). Hippocampal sharp wave-ripple: A cognitive biomarker for episodic memory and planning. *Hippocampus*, *25*(10), 1073–1188. https://doi.org/10.1002/hipo.22488

Buzsáki, G. (2019). *The Brain from Inside Out*. Oxford University Press. https://doi.org/10.1093/oso/9780190905385.001.0001

Buzsáki, G., Anastassiou, C. A., & Koch, C. (2012). The origin of extracellular fields and currents—EEG, ECoG, LFP and spikes. *Nature Reviews. Neuroscience*, *13*(6), 407–420. https://doi.org/10.1038/nrn3241

Buzsáki, G., & Draguhn, A. (2004). Neuronal oscillations in cortical networks. *Science (New York, N.Y.)*, *304*(5679), 1926–1929. https://doi.org/10.1126/science.1099745

Buzsáki, G., & Llinás, R. (2017). Space and time in the brain. *Science (New York, N.Y.)*, *358*(6362), 482–485. https://doi.org/10.1126/science.aan8869

Buzsáki, G., Logothetis, N., & Singer, W. (2013). Scaling Brain Size, Keeping Timing: Evolutionary Preservation of Brain Rhythms. *Neuron*, *80*(3), 751–764. https://doi.org/10.1016/j.neuron.2013.10.002

Buzsáki, G., & Vöröslakos, M. (2023). Brain rhythms have come of age. *Neuron*, *111*(7), 922–926. https://doi.org/10.1016/j.neuron.2023.03.018

Buzsáki, G., & Wang, X.-J. (2012). Mechanisms of Gamma Oscillations. *Annual Review of Neuroscience*, *35*(1), 203–225. https://doi.org/10.1146/annurev-neuro-062111-150444

Canavier, C. C. (2015). Phase-resetting as a tool of information transmission. *Current Opinion in Neurobiology*, *31*, 206–213. https://doi.org/10.1016/j.conb.2014.12.003

Capilla, A., Arana, L., García-Huéscar, M., Melcón, M., Gross, J., & Campo, P. (2022). The natural frequencies of the resting human brain: An MEG-based atlas. *NeuroImage*, *258*, 119373. https://doi.org/10.1016/j.neuroimage.2022.119373

Capotosto, P., Babiloni, C., Romani, G. L., & Corbetta, M. (2009). Frontoparietal cortex controls spatial attention through modulation of anticipatory alpha rhythms. *The Journal of Neuroscience : The Official Journal of the Society for Neuroscience*, *29*(18), 5863–5872. https://doi.org/10.1523/JNEUROSCI.0539-09.2009

Chase, S. M., & Young, E. D. (2007). First-spike latency information in single neurons increases when referenced to population onset. *Proceedings of the National Academy of Sciences*, *104*(12), 5175–5180. https://doi.org/10.1073/pnas.0610368104

Cisek, P. (2019). Resynthesizing behavior through phylogenetic refinement. *Attention, Perception, & Psychophysics*, *81*(7), 2265–2287. https://doi.org/10.3758/s13414-019-01760-1

Clouter, A., Shapiro, K. L., & Hanslmayr, S. (2017). Theta Phase Synchronization Is the Glue that Binds Human Associative Memory. *Current Biology: CB*, *27*(20), 3143-3148.e6. https://doi.org/10.1016/j.cub.2017.09.001

Cohen, M. X. (2017). Multivariate cross-frequency coupling via generalized eigendecomposition. *eLife*, *6*, e21792. https://doi.org/10.7554/eLife.21792

Cohen, M. X. (2021). A data-driven method to identify frequency boundaries in multichannel electrophysiology data. *Journal of Neuroscience Methods*, *347*, 108949. https://doi.org/10.1016/j.jneumeth.2020.108949

Cole, S., & Voytek, B. (2018). *Hippocampal theta bursting and waveform shape reflect CA1 spiking patterns* (p. 452987). bioRxiv. https://doi.org/10.1101/452987

Cole, S., & Voytek, B. (2019). Cycle-by-cycle analysis of neural oscillations. *Journal of Neurophysiology*, *122*(2), 849–861. https://doi.org/10.1152/jn.00273.2019

Cole, & Voytek. (2017). Brain oscillations and the importance of waveform shape. *Trends Cogn. Sci.*, *21*. https://doi.org/10.1016/j.tics.2016.12.008

Colgin, L. L., Denninger, T., Fyhn, M., Hafting, T., Bonnevie, T., Jensen, O., Moser, M.-B., & Moser, E. I. (2009). Frequency of gamma oscillations routes flow of information

in the hippocampus. *Nature*, *462*(7271), Article 7271. https://doi.org/10.1038/nature08573

Colgin, L. L., & Moser, E. I. (2010). Gamma oscillations in the hippocampus. *Physiology (Bethesda, Md.)*, *25*(5), 319–329. https://doi.org/10.1152/physiol.00021.2010

Cruzat, J., Torralba, M., Ruzzoli, M., Fernández, A., Deco, G., & Soto-Faraco, S. (2021). The phase of Theta oscillations modulates successful memory formation at encoding. *Neuropsychologia*, *154*, 107775. https://doi.org/10.1016/j.neuropsychologia.2021.107775

Csicsvari, J., Jamieson, B., Wise, K. D., & Buzsáki, G. (2003). Mechanisms of gamma oscillations in the hippocampus of the behaving rat. *Neuron*, *37*(2), 311–322. https://doi.org/10.1016/s0896-6273(02)01169-8

Cutsuridis, V., & Hasselmo, M. (2012). GABAergic contributions to gating, timing, and phase precession of hippocampal neuronal activity during theta oscillations. *Hippocampus*, *22*(7), 1597–1621. https://doi.org/10.1002/hipo.21002

Danker, J. F., & Anderson, J. R. (2010). The ghosts of brain states past: Remembering reactivates the brain regions engaged during encoding. *Psychological Bulletin*, *136*(1), 87–102. https://doi.org/10.1037/a0017937

de-Wit, L., Alexander, D., Ekroll, V., & Wagemans, J. (2016). Is neuroimaging measuring information in the brain? *Psychonomic Bulletin & Review*, *23*(5), 1415–1428. https://doi.org/10.3758/s13423-016-1002-0

Deuker, L., Olligs, J., Fell, J., Kranz, T. A., Mormann, F., Montag, C., Reuter, M., Elger, C. E., & Axmacher, N. (2013). Memory Consolidation by Replay of Stimulus-Specific Neural Activity. *Journal of Neuroscience*, *33*(49), 19373–19383. https://doi.org/10.1523/JNEUROSCI.0414-13.2013

Doelling, K. B., & Assaneo, M. F. (2021). Neural oscillations are a start toward understanding brain activity rather than the end. *PLOS Biology*, *19*(5), e3001234.

Donoghue, T., Haller, M., Peterson, E. J., Varma, P., Sebastian, P., Gao, R., Noto, T., Lara, A. H., Wallis, J. D., Knight, R. T., Shestyuk, A., & Voytek, B. (2020). Parameterizing neural power spectra into periodic and aperiodic components. *Nature Neuroscience*, *23*(12), 1655–1665. https://doi.org/10.1038/s41593-020-00744-x

Douchamps, V., Jeewajee, A., Blundell, P., Burgess, N., & Lever, C. (2013). Evidence for Encoding versus Retrieval Scheduling in the Hippocampus by Theta Phase and Acetylcholine. *Journal of Neuroscience*, *33*(20), 8689–8704. https://doi.org/10.1523/JNEUROSCI.4483-12.2013

Dragoi, G., & Buzsáki, G. (2006). Temporal encoding of place sequences by hippocampal cell assemblies. *Neuron*, *50*(1), 145–157. https://doi.org/10.1016/j.neuron.2006.02.023

Duncan, D. H., van Moorselaar, D., & Theeuwes, J. (2023). Pinging the brain to reveal the hidden attentional priority map using encephalography. *Nature Communications*, *14*(1), Article 1. https://doi.org/10.1038/s41467-023-40405-8

Duncan, K., Tompary, A., & Davachi, L. (2014). Associative Encoding and Retrieval Are Predicted by Functional Connectivity in Distinct Hippocampal Area CA1 Pathways. *Journal of Neuroscience*, *34*(34), 11188–11198. https://doi.org/10.1523/JNEUROSCI.0521-14.2014

Eichenbaum, H. (2000). A cortical–hippocampal system for declarative memory. *Nature Reviews Neuroscience*, *1*(1), Article 1. https://doi.org/10.1038/35036213

Einevoll, G. T., Kayser, C., Logothetis, N. K., & Panzeri, S. (2013). Modelling and analysis of local field potentials for studying the function of cortical circuits. *Nature Reviews Neuroscience*, *14*(11), Article 11. https://doi.org/10.1038/nrn3599

Ekstrom, A. D., Caplan, J. B., Ho, E., Shattuck, K., Fried, I., & Kahana, M. J. (2005). Human hippocampal theta activity during virtual navigation. *Hippocampus*, *15*(7), 881–889. https://doi.org/10.1002/hipo.20109

Eldridge, L. L., Engel, S. A., Zeineh, M. M., Bookheimer, S. Y., & Knowlton, B. J. (2005). A Dissociation of Encoding and Retrieval Processes in the Human Hippocampus. *Journal of Neuroscience*, *25*(13), 3280–3286. https://doi.org/10.1523/JNEUROSCI.3420-04.2005

Eliav, T., Geva-Sagiv, M., Yartsev, M. M., Finkelstein, A., Rubin, A., Las, L., & Ulanovsky, N. (2018). Nonoscillatory Phase Coding and Synchronization in the Bat Hippocampal Formation. *Cell*, *175*(4), 1119-1130.e15. https://doi.org/10.1016/j.cell.2018.09.017

Engel, A. K., Fries, P., & Singer, W. (2001). Dynamic predictions: Oscillations and synchrony in top-down processing. *Nat. Rev. Neurosci.*, *2*. https://doi.org/10.1038/35094565

Favila, S. E., Lee, H., & Kuhl, B. A. (2020). Transforming the Concept of Memory Reactivation. *Trends in Neurosciences*, *43*(12), 939–950. https://doi.org/10.1016/j.tins.2020.09.006

Fell, J., & Axmacher, N. (2011). The role of phase synchronization in memory processes. *Nature Reviews Neuroscience*, *12*(2), 105–118. https://doi.org/10.1038/nrn2979

Fernández-Ruiz, A., Oliva, A., Fermino de Oliveira, E., Rocha-Almeida, F., Tingley, D., & Buzsáki, G. (2019). Long-duration hippocampal sharp wave ripples improve memory. *Science*, *364*(6445), 1082–1086. https://doi.org/10.1126/science.aax0758

Foo, S., & Bohbot, V. D. (2020). Theta rhythm across the species: Bridging inconsistencies with a multiple memory systems approach. *Behavioral Neuroscience*, *134*(6), 475–490. https://doi.org/10.1037/bne0000440

Foster, D. J., & Wilson, M. A. (2007). Hippocampal theta sequences. *Hippocampus*, *17*(11), 1093–1099. https://doi.org/10.1002/hipo.20345

Fries, P. (2005). A mechanism for cognitive dynamics: Neuronal communication through neuronal coherence. *Trends in Cognitive Sciences*, *9*(10), 474–480. https://doi.org/10.1016/j.tics.2005.08.011

Fries, P. (2015). Rhythms For Cognition: Communication Through Coherence. *Neuron*, *88*(1), 220–235. https://doi.org/10.1016/j.neuron.2015.09.034

Fritch, H. A., MacEvoy, S. P., Thakral, P. P., Jeye, B. M., Ross, R. S., & Slotnick, S. D. (2020). The anterior hippocampus is associated with spatial memory encoding. *Brain Research*, *1732*, 146696. https://doi.org/10.1016/j.brainres.2020.146696

Fuster, J. M., & Alexander, G. E. (1971). Neuron Activity Related to Short-Term Memory. *Science*, *173*(3997), 652–654. https://doi.org/10.1126/science.173.3997.652

Gallistel, C. R. (2011). Chapter 1—Mental Magnitudes. In S. Dehaene & E. M. Brannon (Eds.), *Space, Time and Number in the Brain* (pp. 3–12). Academic Press. https://doi.org/10.1016/B978-0-12-385948-8.00001-3

Gallistel, C. R., & King, A. P. (2009). *Memory and the computational brain: Why cognitive science will transform neuroscience* (pp. xvi, 319). Wiley-Blackwell. https://doi.org/10.1002/9781444310498

Gallistel, C. R., & Matzel, L. D. (2013). The neuroscience of learning: Beyond the Hebbian synapse. *Annual Review of Psychology*, *64*, 169–200. https://doi.org/10.1146/annurev-psych-113011-143807

Gao, R., Peterson, E. J., & Voytek, B. (2017). Inferring synaptic excitation/inhibition balance from field potentials. *NeuroImage*, *158*, 70–78. https://doi.org/10.1016/j.neuroimage.2017.06.078

Gerster, M., Waterstraat, G., Litvak, V., Lehnertz, K., Schnitzler, A., Florin, E., Curio, G., & Nikulin, V. (2022). Separating Neural Oscillations from Aperiodic 1/f Activity: Challenges and Recommendations. *Neuroinformatics*, *20*(4), 991–1012. https://doi.org/10.1007/s12021-022-09581-8

Giovannini, F., Knauer, B., Yoshida, M., & Buhry, L. (2017). The CAN-In network: A biologically inspired model for self-sustained theta oscillations and memory maintenance in the hippocampus. *Hippocampus*, *27*(4), 450–463. https://doi.org/10.1002/hipo.22704

Girardeau, G., Benchenane, K., Wiener, S. I., Buzsáki, G., & Zugaro, M. B. (2009). Selective suppression of hippocampal ripples impairs spatial memory. *Nature Neuroscience*, *12*(10), Article 10. https://doi.org/10.1038/nn.2384

Givens, B., & Olton, D. S. (1994). Local modulation of basal forebrain: Effects on working and reference memory. *The Journal of Neuroscience*, *14*, 3578–3587.

Goldman-Rakic, P. S. (1995). Cellular basis of working memory. *Neuron*, *14*(3), 477–485. https://doi.org/10.1016/0896-6273(95)90304-6

Goyal, A., Miller, J., Qasim, S. E., Watrous, A. J., Zhang, H., Stein, J. M., Inman, C. S., Gross, R. E., Willie, J. T., Lega, B., Lin, J.-J., Sharan, A., Wu, C., Sperling, M. R., Sheth, S. A., McKhann, G. M., Smith, E. H., Schevon, C., & Jacobs, J. (2020). Functionally distinct high and low theta oscillations in the human hippocampus. *Nature Communications*, *11*(1), 2469. https://doi.org/10.1038/s41467-020-15670-6

Greicius, M. D., Krasnow, B., Boyett-Anderson, J. M., Eliez, S., Schatzberg, A. F., Reiss, A. L., & Menon, V. (2003). Regional analysis of hippocampal activation during memory encoding and retrieval: fMRI study. *Hippocampus*, *13*(1), 164–174. https://doi.org/10.1002/hipo.10064

Griffiths, B. J., & Jensen, O. (2023). Gamma oscillations and episodic memory. *Trends in Neurosciences*, *46*(10), 832–846. https://doi.org/10.1016/j.tins.2023.07.003

Grootswagers, T., Wardle, S. G., & Carlson, T. A. (2017). Decoding Dynamic Brain Patterns from Evoked Responses: A Tutorial on Multivariate Pattern Analysis Applied to Time Series Neuroimaging Data. *Journal of Cognitive Neuroscience*, *29*(4), 677–697. https://doi.org/10.1162/jocn_a_01068

Gruber, M. J., Hsieh, L.-T., Staresina, B. P., Elger, C. E., Fell, J., Axmacher, N., & Ranganath, C. (2018). Theta Phase Synchronization between the Human Hippocampus and Prefrontal Cortex Increases during Encoding of Unexpected Information: A Case Study. *Journal of Cognitive Neuroscience*, *30*(11), 1646–1656. https://doi.org/10.1162/jocn_a_01302

Haegens, S., Cousijn, H., Wallis, G., Harrison, P. J., & Nobre, A. C. (2014). Inter- and intra-individual variability in alpha peak frequency. *NeuroImage*, *92*(100), 46–55. https://doi.org/10.1016/j.neuroimage.2014.01.049

Hafting, T., Fyhn, M., Molden, S., Moser, M.-B., & Moser, E. I. (2005). Microstructure of a spatial map in the entorhinal cortex. *Nature*, *436*(7052), 801–806. https://doi.org/10.1038/nature03721

Halgren, M., Kang, R., Voytek, B., Ulbert, I., Fabo, D., Eross, L., Wittner, L., Madsen, J., Doyle, W. K., Devinsky, O., Halgren, E., Harnett, M. T., & Cash, S. S. (2021). *The timescale and magnitude of 1/f aperiodic activity decrease with cortical depth in humans, macaques, and mice* (p. 2021.07.28.454235). bioRxiv. https://doi.org/10.1101/2021.07.28.454235

Händel, B. F., Haarmeier, T., & Jensen, O. (2011). Alpha oscillations correlate with the successful inhibition of unattended stimuli. *Journal of Cognitive Neuroscience*, *23*(9), 2494–2502. https://doi.org/10.1162/jocn.2010.21557

Hanslmayr, S., Axmacher, N., & Inman, C. S. (2019). Modulating Human Memory via Entrainment of Brain Oscillations. *Trends in Neurosciences*, *42*(7), 485–499. https://doi.org/10.1016/j.tins.2019.04.004

Hanslmayr, S., & Staudigl, T. (2014). How brain oscillations form memories—A processing based perspective on oscillatory subsequent memory effects. *NeuroImage*, *85*, 648–655. https://doi.org/10.1016/j.neuroimage.2013.05.121

Haque, R. U., Wittig, J. H., Damera, S. R., Inati, S. K., & Zaghloul, K. A. (2015). Cortical Low-Frequency Power and Progressive Phase Synchrony Precede Successful Memory Encoding. *Journal of Neuroscience*, *35*(40), 13577–13586. https://doi.org/10.1523/JNEUROSCI.0687-15.2015

Hartman, P., & Wintner, A. (1949). Oscillatory and Non-Oscillatory Linear Differential Equations. *American Journal of Mathematics*, *71*(3), 627–649. https://doi.org/10.2307/2372355

Hasselmo, M. E. (2012). *How we remember: Brain mechanisms of episodic memory* (pp. xii, 366). MIT Press.

Hasselmo, M. E., Bodelón, C., & Wyble, B. P. (2002). A proposed function for hippocampal theta rhythm: Separate phases of encoding and retrieval enhance reversal of prior learning. *Neural Computation*, *14*(4), 793–817. https://doi.org/10.1162/089976602317318965

Hasselmo, M. E., & Stern, C. E. (2014). Theta rhythm and the encoding and retrieval of space and time. *NeuroImage*, *85*(0 2), 656–666. https://doi.org/10.1016/j.neuroimage.2013.06.022

Haxby, J. V., Connolly, A. C., & Guntupalli, J. S. (2014). Decoding Neural Representational Spaces Using Multivariate Pattern Analysis. *Annual Review of Neuroscience*, *37*(1), 435–456. https://doi.org/10.1146/annurev-neuro-062012-170325

Herweg, N. A., Solomon, E. A., & Kahana, M. J. (2020). Theta Oscillations in Human Memory. *Trends in Cognitive Sciences*, *24*(3), 208–227. https://doi.org/10.1016/j.tics.2019.12.006

Heusser, A. C., Poeppel, D., Ezzyat, Y., & Davachi, L. (2016). Episodic sequence memory is supported by a theta–gamma phase code. *Nature Neuroscience*, *19*(10), Article 10. https://doi.org/10.1038/nn.4374

Higgins, C., Liu, Y., Vidaurre, D., Kurth-Nelson, Z., Dolan, R., Behrens, T., & Woolrich, M. (2021). Replay bursts in humans coincide with activation of the default mode and parietal alpha networks. *Neuron*, *109*(5), 882-893.e7. https://doi.org/10.1016/j.neuron.2020.12.007

Hölscher, C., Anwyl, R., & Rowan, M. J. (1997). Stimulation on the Positive Phase of Hippocampal Theta Rhythm Induces Long-Term Potentiation That Can Be Depotentiated by Stimulation on the Negative Phase in Area CA1 In Vivo. *The Journal of Neuroscience*, *17*(16), 6470–6477. https://doi.org/10.1523/JNEUROSCI.17-16-06470.1997

Honey, C. J., Newman, E. L., & Schapiro, A. C. (2018). Switching between internal and external modes: A multiscale learning principle. *Network Neuroscience (Cambridge, Mass.)*, *1*(4), 339–356. https://doi.org/10.1162/NETN_a_00024

Huerta, P. T., & Lisman, J. (1995). Bidirectional synaptic plasticity induced by a single burst during cholinergic theta oscillation in CA1 in vitro. *Neuron*, *15*(5), 1053–1063. https://doi.org/10.1016/0896-6273(95)90094-2

Hughes, S. W. (2004). Synchronized oscillations at α and θ frequencies in the lateral geniculate nucleus. *Neuron*, *42*. https://doi.org/10.1016/S0896-6273(04)00191-6

Hülsemann, M. J., Naumann, E., & Rasch, B. (2019). Quantification of Phase-Amplitude Coupling in Neuronal Oscillations: Comparison of Phase-Locking Value, Mean Vector Length, Modulation Index, and Generalized-Linear-Modeling-Cross-Frequency-Coupling. *Frontiers in Neuroscience*, *13*, 573. https://doi.org/10.3389/fnins.2019.00573

Hutcheon, B., & Yarom, Y. (2000). Resonance, oscillation and the intrinsic frequency preferences of neurons. *Trends in Neurosciences*, *23*(5), 216–222. https://doi.org/10.1016/S0166-2236(00)01547-2

Hyman, J. M., Wyble, B. P., Goyal, V., Rossi, C. A., & Hasselmo, M. E. (2003). Stimulation in Hippocampal Region CA1 in Behaving Rats Yields Long-Term Potentiation when Delivered to the Peak of Theta and Long-Term Depression when Delivered to the Trough. *Journal of Neuroscience*, *23*(37), 11725–11731. https://doi.org/10.1523/JNEUROSCI.23-37-11725.2003

Jacobs, J. (2014). Hippocampal theta oscillations are slower in humans than in rodents: Implications for models of spatial navigation and memory. *Philosophical Transactions of the Royal Society of London. Series B, Biological Sciences*, *369*(1635), 20130304. https://doi.org/10.1098/rstb.2013.0304

Jacobs, J., Hwang, G., Curran, T., & Kahana, M. J. (2006). EEG oscillations and recognition memory: Theta correlates of memory retrieval and decision making. *NeuroImage*, *32*. https://doi.org/10.1016/j.neuroimage.2006.02.018

Jacobs, J., Weidemann, C. T., Miller, J. F., Solway, A., Burke, J. F., Wei, X.-X., Suthana, N., Sperling, M. R., Sharan, A. D., Fried, I., & Kahana, M. J. (2013). Direct recordings of grid-like neuronal activity in human spatial navigation. *Nature Neuroscience*, *16*(9), 1188–1190. https://doi.org/10.1038/nn.3466

Jadhav, S. P., Kemere, C., German, P. W., & Frank, L. M. (2012). Awake Hippocampal Sharp-Wave Ripples Support Spatial Memory. *Science*, *336*(6087), 1454–1458. https://doi.org/10.1126/science.1217230

Jahnke, S., Memmesheimer, R.-M., & Timme, M. (2014). Oscillation-Induced Signal Transmission and Gating in Neural Circuits. *PLOS Computational Biology*, *10*(12), e1003940. https://doi.org/10.1371/journal.pcbi.1003940

Jansen, B. H., Agarwal, G., Hegde, A., & Boutros, N. N. (2003). Phase synchronization of the ongoing EEG and auditory EP generation. *Clin. Neurophysiol.*, *114*. https://doi.org/10.1016/S1388-2457(02)00327-9

Jaramillo, J., & Kempter, R. (2017). Phase precession: A neural code underlying episodic memory? *Current Opinion in Neurobiology*, *43*, 130–138. https://doi.org/10.1016/j.conb.2017.02.006

Jensen, O. (2001). Information Transfer Between Rhythmically Coupled Networks: Reading the Hippocampal Phase Code. *Neural Computation*, *13*(12), 2743–2761. https://doi.org/10.1162/089976601317098510

Jensen, O. (2023). *Gating by alpha band inhibition revised: A case for a secondary control mechanism*.

Jensen, O., & Colgin, L. L. (2007). Cross-frequency coupling between neuronal oscillations. *Trends in Cognitive Sciences*, *11*(7), 267–269. https://doi.org/10.1016/j.tics.2007.05.003

Jensen, O., & Lisman, J. (1996). Hippocampal CA3 region predicts memory sequences: Accounting for the phase precession of place cells. *Learning & Memory (Cold Spring Harbor, N.Y.)*, *3*(2–3), 279–287. https://doi.org/10.1101/lm.3.2-3.279

Jensen, O., & Lisman, J. (2000). Position Reconstruction From an Ensemble of Hippocampal Place Cells: Contribution of Theta Phase Coding. *Journal of Neurophysiology*, *83*(5), 2602–2609. https://doi.org/10.1152/jn.2000.83.5.2602

Jensen, O., & Mazaheri, A. (2010). Shaping Functional Architecture by Oscillatory Alpha Activity: Gating by Inhibition. *Frontiers in Human Neuroscience*, *4*, 186. https://doi.org/10.3389/fnhum.2010.00186

Ji, D., & Wilson, M. A. (2007). Coordinated memory replay in the visual cortex and hippocampus during sleep. *Nature Neuroscience*, *10*(1), Article 1. https://doi.org/10.1038/nn1825

Joensen, B. H., Bush, D., Vivekananda, U., Horner, A. J., Bisby, J. A., Diehl, B., Miserocchi, A., McEvoy, A. W., Walker, M. C., & Burgess, N. (2023). Hippocampal theta

activity during encoding promotes subsequent associative memory in humans. *Cerebral Cortex*, *33*(13), 8792–8802. https://doi.org/10.1093/cercor/bhad162

Jones, S. R., Pritchett, D. L., Sikora, M. A., Stufflebeam, S. M., Hämäläinen, M., & Moore, C. I. (2009). Quantitative Analysis and Biophysically Realistic Neural Modeling of the MEG Mu Rhythm: Rhythmogenesis and Modulation of Sensory-Evoked Responses. *Journal of Neurophysiology*, *102*(6), 3554–3572. https://doi.org/10.1152/jn.00535.2009

Josselyn, S. A., & Tonegawa, S. (2020). Memory engrams: Recalling the past and imagining the future. *Science*, *367*(6473), eaaw4325. https://doi.org/10.1126/science.aaw4325

Joundi, R. A., Jenkinson, N., Brittain, J.-. S., Aziz, T. Z., & Brown, P. (2012). Driving oscillatory activity in the human cortex enhances motor performance. *Curr. Biol.*, *22*. https://doi.org/10.1016/j.cub.2012.01.024

Kahana, M. J., Seelig, D., & Madsen, J. R. (2001). Theta returns. *Current Opinion in Neurobiology*, *11*(6), 739–744. https://doi.org/10.1016/s0959-4388(01)00278-1

Kamiński, J., & Rutishauser, U. (2020). Between persistently active and activity-silent frameworks: Novel vistas on the cellular basis of working memory. *Annals of the New York Academy of Sciences*, *1464*(1), 64–75. https://doi.org/10.1111/nyas.14213

Kamondi, A., Acsády, L., Wang, X. J., & Buzsáki, G. (1998). Theta oscillations in somata and dendrites of hippocampal pyramidal cells in vivo: Activity-dependent phase-precession of action potentials. *Hippocampus*, *8*(3), 244–261. https://doi.org/10.1002/(SICI)1098-1063(1998)8:3<244::AID-HIPO7>3.0.CO;2-J

Kandemir, G., & Akyürek, E. G. (2023). Impulse perturbation reveals cross-modal access to sensory working memory through learned associations. *NeuroImage*, *274*, 120156. https://doi.org/10.1016/j.neuroimage.2023.120156

Kandemir, G., Wilhelm, S. A., Axmacher, N., & Akyürek, E. G. (2023). *Maintenance of colour memoranda in activity-quiescent working memory states: Evidence from*

impulse perturbation (p. 2023.07.03.547526). bioRxiv. https://doi.org/10.1101/2023.07.03.547526

Kaplan, R., Bush, D., Bonnefond, M., Bandettini, P. A., Barnes, G. R., Doeller, C. F., & Burgess, N. (2014). Medial prefrontal theta phase coupling during spatial memory retrieval. *Hippocampus*, *24*(6), 656–665. https://doi.org/10.1002/hipo.22255

Kayser, C., Ince, R. A. A., & Panzeri, S. (2012). Analysis of Slow (Theta) Oscillations as a Potential Temporal Reference Frame for Information Coding in Sensory Cortices. *PLoS Computational Biology*, *8*(10), e1002717. https://doi.org/10.1371/journal.pcbi.1002717

Kayser, J., & Tenke, C. E. (2015). On the benefits of using surface Laplacian (Current Source Density) methodology in electrophysiology. *International Journal of Psychophysiology : Official Journal of the International Organization of Psychophysiology*, *97*(3), 171–173. https://doi.org/10.1016/j.ijpsycho.2015.06.001

Kelso, J. A. S. (2001). Self-organizing Dynamical Systems. In N. J. Smelser & P. B. Baltes (Eds.), *International Encyclopedia of the Social & Behavioral Sciences* (pp. 13844–13850). Pergamon. https://doi.org/10.1016/B0-08-043076-7/00568-4

Kennedy, J. P., Zhou, Y., Qin, Y., Lovett, S. D., Sheremet, A., Burke, S. N., & Maurer, A. P. (2022). A Direct Comparison of Theta Power and Frequency to Speed and Acceleration. *Journal of Neuroscience*, *42*(21), 4326–4341. https://doi.org/10.1523/JNEUROSCI.0987-21.2022

Kerrén, C., Linde-Domingo, J., Hanslmayr, S., & Wimber, M. (2018). An Optimal Oscillatory Phase for Pattern Reactivation during Memory Retrieval. *Current Biology*, *28*(21), Article 21. https://doi.org/10.1016/j.cub.2018.08.065

Kerrén, C., van Bree, S., Griffiths, B. J., & Wimber, M. (2022). Phase separation of competing memories along the human hippocampal theta rhythm. *eLife*, *11*, e80633. https://doi.org/10.7554/eLife.80633

King, J.-R., & Dehaene, S. (2014). Characterizing the dynamics of mental representations: The temporal generalization method. *Trends in Cognitive Sciences*, *18*(4), 203–210. https://doi.org/10.1016/j.tics.2014.01.002

Klimesch, W. (1997). EEG-alpha rhythms and memory processes. *International Journal of Psychophysiology*, *26*(1), 319–340. https://doi.org/10.1016/S0167-8760(97)00773-3

Klimesch, W. (1999). EEG alpha and theta oscillations reflect cognitive and memory performance: A review and analysis. *Brain Res. Rev.*, *29*. https://doi.org/10.1016/S0165-0173(98)00056-3

Klimesch, W. (2012). α-band oscillations, attention, and controlled access to stored information. *Trends in Cognitive Sciences*, *16*(12), 606–617. https://doi.org/10.1016/j.tics.2012.10.007

Klimesch, W., Freunberger, R., Sauseng, P., & Gruber, W. (2008). A short review of slow phase synchronization and memory: Evidence for control processes in different memory systems? *Brain Research*, *1235*, 31–44. https://doi.org/10.1016/j.brainres.2008.06.049

Klimesch, W., Schimke, H., & Pfurtscheller, G. (1993). Alpha frequency, cognitive load and memory performance. *Brain Topography*, *5*(3), 241–251. https://doi.org/10.1007/BF01128991

Koepsell, K., Wang, X., Vaingankar, V., Wei, Y., Wang, Q., Rathbun, D. L., Usrey, W. M., Hirsch, J. A., & Sommer, F. T. (2009). Retinal Oscillations Carry Visual Information to Cortex. *Frontiers in Systems Neuroscience*, *3*, 4. https://doi.org/10.3389/neuro.06.004.2009

Kopell, N., Ermentrout, G. B., Whittington, M. A., & Traub, R. D. (2000). Gamma rhythms and beta rhythms have different synchronization properties. *Proceedings of the National Academy of Sciences*, *97*(4), 1867–1872. https://doi.org/10.1073/pnas.97.4.1867

Körner, T. W. (1988). *Fourier Analysis*. Cambridge University Press. https://books.google.co.uk/books?id=wwoETwEACAAJ

Kösem, A., Gramfort, A., & Wassenhove, V. (2014). Encoding of event timing in the phase of neural oscillations. *NeuroImage*, *92*. https://doi.org/10.1016/j.neuroimage.2014.02.010

Kostov, V. B., McCullough, P. R., Carter, J. A., Deleuil, M., Díaz, R. F., Fabrycky, D. C., Hébrard, G., Hinse, T. C., Mazeh, T., Orosz, J. A., Tsvetanov, Z. I., & Welsh, W. F. (2014). KEPLER-413B: A SLIGHTLY MISALIGNED, NEPTUNE-SIZE TRANSITING CIRCUMBINARY PLANET. *The Astrophysical Journal*, *784*(1), 14. https://doi.org/10.1088/0004-637X/784/1/14

Kota, S., Rugg, M. D., & Lega, B. C. (2020). Hippocampal Theta Oscillations Support Successful Associative Memory Formation. *Journal of Neuroscience*, *40*(49), Article 49. https://doi.org/10.1523/JNEUROSCI.0767-20.2020

Kragel, J. E., Ezzyat, Y., Sperling, M. R., Gorniak, R., Worrell, G. A., Berry, B. M., Inman, C., Lin, J.-J., Davis, K. A., Das, S. R., Stein, J. M., Jobst, B. C., Zaghloul, K. A., Sheth, S. A., Rizzuto, D. S., & Kahana, M. J. (2017). Similar patterns of neural activity predict memory function during encoding and retrieval. *NeuroImage*, *155*, 60–71. https://doi.org/10.1016/j.neuroimage.2017.03.042

Kramer, M. A., Roopun, A. K., Carracedo, L. M., Traub, R. D., Whittington, M. A., & Kopell, N. J. (2008). Rhythm Generation through Period Concatenation in Rat Somatosensory Cortex. *PLOS Computational Biology*, *4*(9), e1000169. https://doi.org/10.1371/journal.pcbi.1000169

Kriegeskorte, N., Simmons, W. K., Bellgowan, P. S. F., & Baker, C. I. (2009). Circular analysis in systems neuroscience: The dangers of double dipping. *Nature Neuroscience*, *12*(5), 535–540. https://doi.org/10.1038/nn.2303

Kuhl, B. A., Rissman, J., & Wagner, A. D. (2012). Multi-voxel patterns of visual category representation during episodic encoding are predictive of subsequent memory. *Neuropsychologia*, *50*(4), 458–469. https://doi.org/10.1016/j.neuropsychologia.2011.09.002

Kunec, S., Hasselmo, M. E., & Kopell, N. (2005). Encoding and retrieval in the CA3 region of the hippocampus: A model of theta-phase separation. *Journal of Neurophysiology*, *94*(1), 70–82. https://doi.org/10.1152/jn.00731.2004

Kunz, L., Wang, L., Lachner-Piza, D., Zhang, H., Brandt, A., Dümpelmann, M., Reinacher, P. C., Coenen, V. A., Chen, D., Wang, W.-X., Zhou, W., Liang, S., Grewe, P., Bien, C. G., Bierbrauer, A., Navarro Schröder, T., Schulze-Bonhage, A., & Axmacher, N. (2019). Hippocampal theta phases organize the reactivation of large-scale electrophysiological representations during goal-directed navigation. *Science Advances*, *5*(7), eaav8192. https://doi.org/10.1126/sciadv.aav8192

Lakatos, P., Chen, C.-M., O'Connell, M. N., Mills, A., & Schroeder, C. E. (2007). Neuronal Oscillations and Multisensory Interaction in Primary Auditory Cortex. *Neuron*, *53*(2), 279–292. https://doi.org/10.1016/j.neuron.2006.12.011

Lakatos, P., Shah, A. S., Knuth, K. H., Ulbert, I., Karmos, G., & Schroeder, C. E. (2005). An oscillatory hierarchy controlling neuronal excitability and stimulus processing in the auditory cortex. *Journal of Neurophysiology*, *94*(3), 1904–1911. https://doi.org/10.1152/jn.00263.2005

Lashley, K. S. (1958). Research publications of the Association for Research in Nervous & Mental Disease. Cerebral organization and behavior. *The Neuropsychology of Lashley*, 529–543.

Lea-Carnall, C. A., Montemurro, M. A., Trujillo-Barreto, N. J., Parkes, L. M., & El-Deredy, W. (2016). Cortical Resonance Frequencies Emerge from Network Size and

Connectivity. *PLoS Computational Biology*, *12*(2), e1004740. https://doi.org/10.1371/journal.pcbi.1004740

Lega, B. C., Jacobs, J., & Kahana, M. (2012). Human hippocampal theta oscillations and the formation of episodic memories. *Hippocampus*, *22*(4), 748–761. https://doi.org/10.1002/hipo.20937

Liebe, S., Niediek, J., Pals, M., Reber, T. P., Faber, J., Bostroem, J., Elger, C. E., Macke, J. H., & Mormann, F. (2022). *Phase of firing does not reflect temporal order in sequence memory of humans and recurrent neural networks* [Preprint]. Neuroscience. https://doi.org/10.1101/2022.09.25.509370

Linde-Domingo, J., Treder, M. S., Kerrén, C., & Wimber, M. (2019). Evidence that neural information flow is reversed between object perception and object reconstruction from memory. *Nature Communications*, *10*(1), 179. https://doi.org/10.1038/s41467-018-08080-2

Lisman, J. (2005). The theta/gamma discrete phase code occuring during the hippocampal phase precession may be a more general brain coding scheme. *Hippocampus*, *15*(7), 913–922. https://doi.org/10.1002/hipo.20121

Lisman, J., & Buzsáki, G. (2008). A Neural Coding Scheme Formed by the Combined Function of Gamma and Theta Oscillations. *Schizophrenia Bulletin*, *34*(5), 974–980. https://doi.org/10.1093/schbul/sbn060

Lisman, J., & Jensen, O. (2013). The theta-gamma neural code. *Neuron*, *77*(6), 1002–1016.

Liu, C., Todorova, R., Tang, W., Oliva, A., & Fernandez-Ruiz, A. (2023). Associative and predictive hippocampal codes support memory-guided behaviors. *Science*, *382*(6668), eadi8237. https://doi.org/10.1126/science.adi8237

Liu, Y., Dolan, R. J., Kurth-Nelson, Z., & Behrens, T. E. J. (2019). Human Replay Spontaneously Reorganizes Experience. *Cell*, *178*(3), 640-652.e14. https://doi.org/10.1016/j.cell.2019.06.012

Llinás, R. R. (1988). The intrinsic electrophysiological properties of mammalian neurons: Insights into central nervous system function. *Science (New York, N.Y.)*, *242*(4886), 1654–1664. https://doi.org/10.1126/science.3059497

Llinás, R., & Yarom, Y. (1981). Properties and distribution of ionic conductances generating electroresponsiveness of mammalian inferior olivary neurones in vitro. *The Journal of Physiology*, *315*, 569–584. https://doi.org/10.1113/jphysiol.1981.sp013764

Lombardi, F., Herrmann, H. J., & de Arcangelis, L. (2017). Balance of excitation and inhibition determines 1/f power spectrum in neuronal networks. *Chaos (Woodbury, N.Y.)*, *27*(4), 047402. https://doi.org/10.1063/1.4979043

Luo, H., & Poeppel, D. (2012). Cortical oscillations in auditory perception and speech: Evidence for two temporal windows in human auditory cortex. *Frontiers in Psychology*, *3*, 170. https://doi.org/10.3389/fpsyg.2012.00170

M. Aghajan, Z., Schuette, P., Fields, T. A., Tran, M. E., Siddiqui, S. M., Hasulak, N. R., Tcheng, T. K., Eliashiv, D., Mankin, E. A., Stern, J., Fried, I., & Suthana, N. (2017). Theta Oscillations in the Human Medial Temporal Lobe during Real-World Ambulatory Movement. *Current Biology*, *27*(24), 3743-3751.e3. https://doi.org/10.1016/j.cub.2017.10.062

MacDonald, C. J., Lepage, K. Q., Eden, U. T., & Eichenbaum, H. (2011). Hippocampal "time cells" bridge the gap in memory for discontiguous events. *Neuron*, *71*. https://doi.org/10.1016/j.neuron.2011.07.012

Madore, K. P., & Wagner, A. D. (2022). Readiness to remember: Predicting variability in episodic memory. *Trends in Cognitive Sciences*, *26*(8), 707–723. https://doi.org/10.1016/j.tics.2022.05.006

Maguire, E. A. (2014). Memory consolidation in humans: New evidence and opportunities. *Experimental Physiology*, *99*(3), 471–486. https://doi.org/10.1113/expphysiol.2013.072157

Makeig, S., Bell, A. J., Jung, T.-P., & Sejnowski, T. J. (1995). Independent Component Analysis of Electroencephalographic Data. *Proceedings of the 8th International Conference on Neural Information Processing Systems*, 145–151.

Malhotra, S., Cross, R. W. A., & van der Meer, M. A. A. (2012). Theta phase precession beyond the hippocampus. *Reviews in the Neurosciences*, *23*(1), 39–65. https://doi.org/10.1515/revneuro-2011-0064

Manning, J. R., Jacobs, J., Fried, I., & Kahana, M. J. (2009). Broadband Shifts in Local Field Potential Power Spectra Are Correlated with Single-Neuron Spiking in Humans. *Journal of Neuroscience*, *29*(43), 13613–13620. https://doi.org/10.1523/JNEUROSCI.2041-09.2009

Manns, J. R., Zilli, E. A., Ong, K. C., Hasselmo, M. E., & Eichenbaum, H. (2007). Hippocampal CA1 spiking during encoding and retrieval: Relation to theta phase. *Neurobiology of Learning and Memory*, *87*(1), 9–20. https://doi.org/10.1016/j.nlm.2006.05.007

Mansvelder, H. D., Verhoog, M. B., & Goriounova, N. A. (2019). Synaptic plasticity in human cortical circuits: Cellular mechanisms of learning and memory in the human brain? *Current Opinion in Neurobiology*, *54*, 186–193. https://doi.org/10.1016/j.conb.2018.06.013

Maris, E., & Oostenveld, R. (2007). Nonparametric statistical testing of EEG- and MEG-data. *Journal of Neuroscience Methods*, *164*(1), 177–190. https://doi.org/10.1016/j.jneumeth.2007.03.024

Markram, H., Lübke, J., Frotscher, M., & Sakmann, B. (1997). Regulation of Synaptic Efficacy by Coincidence of Postsynaptic APs and EPSPs. *Science*, *275*(5297), 213–215. https://doi.org/10.1126/science.275.5297.213

Marshall, L., Kirov, R., Brade, J., Mölle, M., & Born, J. (2011). Transcranial Electrical Currents to Probe EEG Brain Rhythms and Memory Consolidation during Sleep in Humans. *PLOS ONE*, *6*(2), e16905. https://doi.org/10.1371/journal.pone.0016905

Martín-Buro, M. C., Wimber, M., Henson, R. N., & Staresina, B. P. (2020). Alpha Rhythms Reveal When and Where Item and Associative Memories Are Retrieved. *The Journal of Neuroscience: The Official Journal of the Society for Neuroscience*, *40*(12), 2510–2518. https://doi.org/10.1523/JNEUROSCI.1982-19.2020

Martínez, M., & Artiga, M. (2023). Neural Oscillations as Representations. *British Journal for the Philosophy of Science*, *74*(3), 619–648.

Masse, N. Y., Rosen, M. C., & Freedman, D. J. (2020). Reevaluating the Role of Persistent Neural Activity in Short-Term Memory. *Trends in Cognitive Sciences*, *24*(3), 242–258. https://doi.org/10.1016/j.tics.2019.12.014

Matsuoka, K. (1985). Sustained oscillations generated by mutually inhibiting neurons with adaptation. *Biological Cybernetics*, *52*(6), 367–376. https://doi.org/10.1007/BF00449593

Maurer, A. P., & McNaughton, B. L. (2007). Network and intrinsic cellular mechanisms underlying theta phase precession of hippocampal neurons. *Trends in Neurosciences*, *30*(7), 325–333. https://doi.org/10.1016/j.tins.2007.05.002

Mazaheri, A., & Jensen, O. (2006). Posterior α activity is not phase-reset by visual stimuli. *Proc. Natl Acad. Sci. USA*, *103*. https://doi.org/10.1073/pnas.0505785103

Mazzoni, A., Lindén, H., Cuntz, H., Lansner, A., Panzeri, S., & Einevoll, G. T. (2015). Computing the Local Field Potential (LFP) from Integrate-and-Fire Network Models. *PLoS Computational Biology*, *11*(12), e1004584. https://doi.org/10.1371/journal.pcbi.1004584

McClelland, J. L., McNaughton, B. L., & O'Reilly, R. C. (1995). Why there are complementary learning systems in the hippocampus and neocortex: Insights from

the successes and failures of connectionist models of learning and memory. *Psychological Review*, *102*(3), 419–457. https://doi.org/10.1037/0033-295X.102.3.419

McFarland, W. L., Teitelbaum, H., & Hedges, E. K. (1975). Relationship between hippocampal theta activity and running speed in the rat. *Journal of Comparative and Physiological Psychology*, *88*(1), 324–328. https://doi.org/10.1037/h0076177

McNaughton, N., Ruan, M., & Woodnorth, M.-A. (2006). Restoring theta-like rhythmicity in rats restores initial learning in the Morris water maze. *Hippocampus*, *16*(12), 1102–1110. https://doi.org/10.1002/hipo.20235

Mehta, M. R., Lee, A. K., & Wilson, M. A. (2002). Role of experience and oscillations in transforming a rate code into a temporal code. *Nature*, *417*(6890), 741–746. https://doi.org/10.1038/nature00807

Merkow, M. B., Burke, J. F., & Kahana, M. J. (2015). The human hippocampus contributes to both the recollection and familiarity components of recognition memory. *Proceedings of the National Academy of Sciences*, *112*(46), 14378–14383. https://doi.org/10.1073/pnas.1513145112

Michelmann, S., Staresina, B. P., Bowman, H., & Hanslmayr, S. (2019). Speed of time-compressed forward replay flexibly changes in human episodic memory. *Nature Human Behaviour*, *3*(2), Article 2. https://doi.org/10.1038/s41562-018-0491-4

Mirjalili, S., Powell, P., Strunk, J., James, T., & Duarte, A. (2021). Context Memory Encoding and Retrieval Temporal Dynamics are Modulated by Attention across the Adult Lifespan. *eNeuro*, *8*(1), ENEURO.0387-20.2020. https://doi.org/10.1523/ENEURO.0387-20.2020

Moliadze, V., Zhao, Y., Eysel, U., & Funke, K. (2003). Effect of transcranial magnetic stimulation on single-unit activity in the cat primary visual cortex. *The Journal of Physiology*, *553*(Pt 2), 665–679. https://doi.org/10.1113/jphysiol.2003.050153

Molina, J. L., Voytek, B., Thomas, M. L., Joshi, Y. B., Bhakta, S. G., Talledo, J. A., Swerdlow, N. R., & Light, G. A. (2020). Memantine Effects on Electroencephalographic Measures of Putative Excitatory/Inhibitory Balance in Schizophrenia. *Biological Psychiatry: Cognitive Neuroscience and Neuroimaging*, *5*(6), 562–568. https://doi.org/10.1016/j.bpsc.2020.02.004

Mongillo, G., Barak, O., & Tsodyks, M. (2008). Synaptic Theory of Working Memory. *Science*, *319*(5869), 1543–1546. https://doi.org/10.1126/science.1150769

Mormann, F., Fell, J., Axmacher, N., Weber, B., Lehnertz, K., Elger, C. E., & Fernández, G. (2005). Phase/amplitude reset and theta–gamma interaction in the human medial temporal lobe during a continuous word recognition memory task. *Hippocampus*, *15*(7), 890–900. https://doi.org/10.1002/hipo.20117

Mueller, J., Legon, W., Opitz, A., Sato, T. F., & Tyler, W. J. (2014). Transcranial Focused Ultrasound Modulates Intrinsic and Evoked EEG Dynamics. *Brain Stimulation*, *7*(6), 900–908. https://doi.org/10.1016/j.brs.2014.08.008

Murphy, E. (2024). ROSE: A neurocomputational architecture for syntax. *Journal of Neurolinguistics*, *70*, 101180. https://doi.org/10.1016/j.jneuroling.2023.101180

Nádasdy, Z., Hirase, H., Czurkó, A., Csicsvari, J., & Buzsáki, G. (1999). Replay and Time Compression of Recurring Spike Sequences in the Hippocampus. *Journal of Neuroscience*, *19*(21), 9497–9507. https://doi.org/10.1523/JNEUROSCI.19-21-09497.1999

Newman, E. L., & Hasselmo, M. E. (2014). Grid cell firing properties vary as a function of theta phase locking preferences in the rat medial entorhinal cortex. *Frontiers in Systems Neuroscience*, *8*, 193. https://doi.org/10.3389/fnsys.2014.00193

Norman, K., Newman, E., Detre, G., & Polyn, S. (2006). How inhibitory oscillations can train neural networks and punish competitors. *Neural Computation*, *18*(7), 1577–1610. https://doi.org/10.1162/neco.2006.18.7.1577

Norman, Y., Yeagle, E. M., Khuvis, S., Harel, M., Mehta, A. D., & Malach, R. (2019). Hippocampal sharp-wave ripples linked to visual episodic recollection in humans. *Science*, *365*(6454), eaax1030. https://doi.org/10.1126/science.aax1030

Nowak, M., Zich, C., & Stagg, C. J. (2018). Motor cortical gamma oscillations: What have we learnt and where are we headed? *Curr. Behav. Neurosci. Rep.*, *5*. https://doi.org/10.1007/s40473-018-0151-z

Nyhus, E., & Curran, T. (2010). Functional role of gamma and theta oscillations in episodic memory. *Neuroscience and Biobehavioral Reviews*, *34*(7), 1023–1035. https://doi.org/10.1016/j.neubiorev.2009.12.014

O'Keefe, J., & Recce, M. L. (1993). Phase relationship between hippocampal place units and the EEG theta rhythm. *Hippocampus*, *3*(3), 317–330. https://doi.org/10.1002/hipo.450030307

Ólafsdóttir, H. F., Bush, D., & Barry, C. (2018). The Role of Hippocampal Replay in Memory and Planning. *Current Biology: CB*, *28*(1), R37–R50. https://doi.org/10.1016/j.cub.2017.10.073

Oostenveld, R., Fries, P., Maris, E., & Schoffelen, J.-M. (2011). FieldTrip: Open source software for advanced analysis of MEG, EEG, and invasive electrophysiological data. *Computational Intelligence and Neuroscience*, *2011*, 156869. https://doi.org/10.1155/2011/156869

Ouyang, G., Hildebrandt, A., Schmitz, F., & Herrmann, C. S. (2020). Decomposing alpha and 1/f brain activities reveals their differential associations with cognitive processing speed. *NeuroImage*, *205*, 116304. https://doi.org/10.1016/j.neuroimage.2019.116304

Pacheco Estefan, D., Zucca, R., Arsiwalla, X., Principe, A., Zhang, H., Rocamora, R., Axmacher, N., & Verschure, P. F. M. J. (2021). Volitional learning promotes theta

phase coding in the human hippocampus. *Proceedings of the National Academy of Sciences*, *118*(10), e2021238118. https://doi.org/10.1073/pnas.2021238118

Panzeri, S., Ince, R. A. A., Diamond, M. E., & Kayser, C. (2014). Reading spike timing without a clock: Intrinsic decoding of spike trains. *Philosophical Transactions of the Royal Society B: Biological Sciences*, *369*(1637), 20120467. https://doi.org/10.1098/rstb.2012.0467

Parra, L. C., Spence, C. D., Gerson, A. D., & Sajda, P. (2005). Recipes for the linear analysis of EEG. *NeuroImage*, *28*(2), 326–341. https://doi.org/10.1016/j.neuroimage.2005.05.032

Pavlides, C., Greenstein, Y. J., Grudman, M., & Winson, J. (1988). Long-term potentiation in the dentate gyrus is induced preferentially on the positive phase of θ-rhythm. *Brain Research*, *439*(1), 383–387. https://doi.org/10.1016/0006-8993(88)91499-0

Pearson, J., Naselaris, T., Holmes, E. A., & Kosslyn, S. M. (2015). Mental Imagery: Functional Mechanisms and Clinical Applications. *Trends in Cognitive Sciences*, *19*(10), 590–602. https://doi.org/10.1016/j.tics.2015.08.003

Peirce, J., Gray, J. R., Simpson, S., MacAskill, M., Höchenberger, R., Sogo, H., Kastman, E., & Lindeløv, J. K. (2019). PsychoPy2: Experiments in behavior made easy. *Behavior Research Methods*, *51*(1), 195–203. https://doi.org/10.3758/s13428-018-01193-y

Petersen, P. C., & Buzsáki, G. (2020). Cooling of Medial Septum Reveals Theta Phase Lag Coordination of Hippocampal Cell Assemblies. *Neuron*, *107*(4), 731-744.e3. https://doi.org/10.1016/j.neuron.2020.05.023

Petsche, H., Stumpf, Ch., & Gogolak, G. (1962). The significance of the rabbit's septum as a relay station between the midbrain and the hippocampus I. The control of hippocampus arousal activity by the septum cells. *Electroencephalography and*

Clinical Neurophysiology, *14*(2), 202–211. https://doi.org/10.1016/0013-4694(62)90030-5

Pezzulo, G., van der Meer, M. A. A., Lansink, C. S., & Pennartz, C. M. A. (2014). Internally generated sequences in learning and executing goal-directed behavior. *Trends in Cognitive Sciences*, *18*(12), 647–657. https://doi.org/10.1016/j.tics.2014.06.011

Piccinini, G., & Bahar, S. (2013). Neural Computation and the Computational Theory of Cognition. *Cognitive Science*, *37*(3), 453–488. https://doi.org/10.1111/cogs.12012

Pletzer, B., Kerschbaum, H., & Klimesch, W. (2010). When frequencies never synchronize: The golden mean and the resting EEG. *Brain Research*, *1335*, 91–102. https://doi.org/10.1016/j.brainres.2010.03.074

Polanía, R., Moisa, M., Opitz, A., Grueschow, M., & Ruff, C. C. (2015). The precision of value-based choices depends causally on fronto-parietal phase coupling. *Nat. Commun.*, *6*. https://doi.org/10.1038/ncomms9090

Poldrack, R. A. (2006). Can cognitive processes be inferred from neuroimaging data? *Trends in Cognitive Sciences*, *10*(2), 59–63. https://doi.org/10.1016/j.tics.2005.12.004

Poldrack, R. A., & Yarkoni, T. (2016). From brain maps to cognitive ontologies: Informatics and the search for mental structure. *Annual Review of Psychology*, *67*, 587–612. https://doi.org/10.1146/annurev-psych-122414-033729

Preston, A. R., & Eichenbaum, H. (2013). Interplay of hippocampus and prefrontal cortex in memory. *Current Biology : CB*, *23*(17), R764–R773. https://doi.org/10.1016/j.cub.2013.05.041

Qasim, S. E., Fried, I., & Jacobs, J. (2021). Phase precession in the human hippocampus and entorhinal cortex. *Cell*, *184*(12), 3242-3255.e10. https://doi.org/10.1016/j.cell.2021.04.017

Rabinovich, M., Huerta, R., & Laurent, G. (2008). Neuroscience. Transient dynamics for neural processing. *Science (New York, N.Y.)*, *321*(5885), 48–50. https://doi.org/10.1126/science.1155564

Rahi, P. K., & Mehra, R. (2014). Analysis of power spectrum estimation using welch method for various window techniques. *International Journal of Emerging Technologies and Engineering*, *2*(6), 106–109.

Reddy, L., Self, M. W., Zoefel, B., Poncet, M., Possel, J. K., Peters, J. C., Baayen, J. C., Idema, S., VanRullen, R., & Roelfsema, P. R. (2021). Theta-phase dependent neuronal coding during sequence learning in human single neurons. *Nature Communications*, *12*(1), Article 1. https://doi.org/10.1038/s41467-021-25150-0

Reifenstein, E. T., Bin Khalid, I., & Kempter, R. (2021). Synaptic learning rules for sequence learning. *eLife*, *10*, e67171. https://doi.org/10.7554/eLife.67171

Reifenstein, E. T., Kempter, R., Schreiber, S., Stemmler, M. B., & Herz, A. V. M. (2012). Grid cells in rat entorhinal cortex encode physical space with independent firing fields and phase precession at the single-trial level. *Proceedings of the National Academy of Sciences*, *109*(16), 6301–6306. https://doi.org/10.1073/pnas.1109599109

Reimann, M. W., Anastassiou, C. A., Perin, R., Hill, S., Markram, H., & Koch, C. (2013). A biophysically detailed model of neocortical Local Field Potentials predicts the critical role of active membrane currents. *Neuron*, *79*(2), 375–390. https://doi.org/10.1016/j.neuron.2013.05.023

Rissman, J., & Wagner, A. D. (2012). Distributed representations in memory: Insights from functional brain imaging. *Annual Review of Psychology*, *63*, 101–128. https://doi.org/10.1146/annurev-psych-120710-100344

Ritchie, J. B., Kaplan, D. M., & Klein, C. (2019). Decoding the Brain: Neural Representation and the Limits of Multivariate Pattern Analysis in Cognitive Neuroscience. *The*

British Journal for the Philosophy of Science, *70*(2), 581–607. https://doi.org/10.1093/bjps/axx023

Rizzuto, D. S., Madsen, J. R., Bromfield, E. B., Schulze-Bonhage, A., & Kahana, M. J. (2006). Human neocortical oscillations exhibit theta phase differences between encoding and retrieval. *NeuroImage*, *31*(3), 1352–1358. https://doi.org/10.1016/j.neuroimage.2006.01.009

Rizzuto, D. S., Madsen, J. R., Bromfield, E. B., Schulze-Bonhage, A., Seelig, D., Aschenbrenner-Scheibe, R., & Kahana, M. J. (2003). Reset of human neocortical oscillations during a working memory task. *Proceedings of the National Academy of Sciences*, *100*(13), 7931–7936. https://doi.org/10.1073/pnas.0732061100

Rolls, E. (2013). The mechanisms for pattern completion and pattern separation in the hippocampus. *Frontiers in Systems Neuroscience*, *7*. https://www.frontiersin.org/articles/10.3389/fnsys.2013.00074

Romei, V., Gross, J., & Thut, G. (2010). On the role of prestimulus alpha rhythms over occipito-parietal areas in visual input regulation: Correlation or causation? *J. Neurosci.*, *30*. https://doi.org/10.1523/JNEUROSCI.0160-10.2010

Ruzzoli, M., & Soto-Faraco, S. (2014). Alpha Stimulation of the Human Parietal Cortex Attunes Tactile Perception to External Space. *Current Biology*, *24*(3), 329–332. https://doi.org/10.1016/j.cub.2013.12.029

Sakoe, H., & Chiba, S. (1978). Dynamic programming algorithm optimization for spoken word recognition. *IEEE Transactions on Acoustics, Speech, and Signal Processing*, *26*(1), 43–49. https://doi.org/10.1109/TASSP.1978.1163055

Salinas, E., & Sejnowski, T. J. (2001). Correlated neuronal activity and the flow of neural information. *Nature Reviews Neuroscience*, *2*(8), Article 8. https://doi.org/10.1038/35086012

Sauseng, P., Conci, M., Wild, B., & Geyer, T. (2015). Predictive coding in visual search as revealed by cross-frequency EEG phase synchronization. *Frontiers in Psychology*, *6*. https://www.frontiersin.org/articles/10.3389/fpsyg.2015.01655

Sauseng, P., Klimesch, W., Stadler, W., Schabus, M., Doppelmayr, M., Hanslmayr, S., Gruber, W. R., & Birbaumer, N. (2005). A shift of visual spatial attention is selectively associated with human EEG alpha activity. *The European Journal of Neuroscience*, *22*(11), 2917–2926. https://doi.org/10.1111/j.1460-9568.2005.04482.x

Scharnowski, F., Rees, G., & Walsh, V. (2013). Time and the brain: Neurorelativity: The chronoarchitecture of the brain from the neuronal rather than the observer's perspective. *Trends in Cognitive Sciences*, *17*(2), Article 2. https://doi.org/10.1016/j.tics.2012.12.005

Schneider, M., Broggini, A. C., Dann, B., Tzanou, A., Uran, C., Sheshadri, S., Scherberger, H., & Vinck, M. (2021). A mechanism for inter-areal coherence through communication based on connectivity and oscillatory power. *Neuron*, *109*(24), 4050-4067.e12. https://doi.org/10.1016/j.neuron.2021.09.037

Schreiner, T., Petzka, M., Staudigl, T., & Staresina, B. P. (2021). Endogenous memory reactivation during sleep in humans is clocked by slow oscillation-spindle complexes. *Nature Communications*, *12*(1), Article 1. https://doi.org/10.1038/s41467-021-23520-2

Sekeres, M. J., Winocur, G., & Moscovitch, M. (2018). The hippocampus and related neocortical structures in memory transformation. *Neuroscience Letters*, *680*, 39–53. https://doi.org/10.1016/j.neulet.2018.05.006

Siebenhühner, F., Wang, S. H., Palva, J. M., & Palva, S. (2016). Cross-frequency synchronization connects networks of fast and slow oscillations during visual working memory maintenance. *eLife*, *5*, e13451. https://doi.org/10.7554/eLife.13451

Siegle, J. H., & Wilson, M. A. (2014). Enhancement of encoding and retrieval functions through theta phase-specific manipulation of hippocampus. *eLife*, *3*, e03061. https://doi.org/10.7554/eLife.03061

Singer, W. (1999). Neuronal Synchrony: A Versatile Code for the Definition of Relations? *Neuron*, *24*(1), 49–65. https://doi.org/10.1016/S0896-6273(00)80821-1

Singer, W. (2007). Binding by synchrony. *Scholarpedia*, *2*(12), 1657. https://doi.org/10.4249/scholarpedia.1657

Singer, W. (2018). Neuronal oscillations: Unavoidable and useful? *The European Journal of Neuroscience*, *48*(7), 2389–2398. https://doi.org/10.1111/ejn.13796

Skaggs, W. E., McNaughton, B. L., Wilson, M. A., & Barnes, C. A. (1996). Theta phase precession in hippocampal neuronal populations and the compression of temporal sequences. *Hippocampus*, *6*(2), 149–172. https://doi.org/10.1002/(SICI)1098-1063(1996)6:2<149::AID-HIPO6>3.0.CO;2-K

Small, S. A., Nava, A. S., Perera, G. M., DeLaPaz, R., Mayeux, R., & Stern, Y. (2001). Circuit mechanisms underlying memory encoding and retrieval in the long axis of the hippocampal formation. *Nature Neuroscience*, *4*(4), Article 4. https://doi.org/10.1038/86115

Solomon, E. A., Stein, J. M., Das, S., Gorniak, R., Sperling, M. R., Worrell, G., Inman, C. S., Tan, R. J., Jobst, B. C., Rizzuto, D. S., & Kahana, M. J. (2019). Dynamic Theta Networks in the Human Medial Temporal Lobe Support Episodic Memory. *Current Biology*, *29*(7), 1100-1111.e4. https://doi.org/10.1016/j.cub.2019.02.020

Sotomayor-Gómez, B., Battaglia, F. P., & Vinck, M. (2023). SpikeShip: A method for fast, unsupervised discovery of high-dimensional neural spiking patterns. *PLOS Computational Biology*, *19*(7), e1011335. https://doi.org/10.1371/journal.pcbi.1011335

Squire, L. R., Genzel, L., Wixted, J. T., & Morris, R. G. (2015). Memory Consolidation. *Cold Spring Harbor Perspectives in Biology*, *7*(8), a021766. https://doi.org/10.1101/cshperspect.a021766

Stangl, M., Maoz, S. L., & Suthana, N. (2023). Mobile cognition: Imaging the human brain in the 'real world.' *Nature Reviews Neuroscience*, *24*(6), Article 6. https://doi.org/10.1038/s41583-023-00692-y

Stangl, M., Topalovic, U., Inman, C. S., Hiller, S., Villaroman, D., Aghajan, Z. M., Christov-Moore, L., Hasulak, N. R., Rao, V. R., Halpern, C. H., Eliashiv, D., Fried, I., & Suthana, N. (2021). Boundary-anchored neural mechanisms of location-encoding for self and others. *Nature*, *589*(7842), 420–425. https://doi.org/10.1038/s41586-020-03073-y

Staresina, B. P., & Wimber, M. (2019). A Neural Chronometry of Memory Recall. *Trends in Cognitive Sciences*, *23*(12), 1071–1085. https://doi.org/10.1016/j.tics.2019.09.011

Steriade, M. (2001). Impact of network activities on neuronal properties in corticothalamic systems. *Journal of Neurophysiology*, *86*(1), 1–39. https://doi.org/10.1152/jn.2001.86.1.1

Stokes, M. G. (2015). "Activity-silent" working memory in prefrontal cortex: A dynamic coding framework. *Trends in Cognitive Sciences*, *19*(7), 394–405. https://doi.org/10.1016/j.tics.2015.05.004

Strüber, M., Sauer, J.-F., & Bartos, M. (2022). Parvalbumin expressing interneurons control spike-phase coupling of hippocampal cells to theta oscillations. *Scientific Reports*, *12*(1), Article 1. https://doi.org/10.1038/s41598-022-05004-5

Szendro, P., Vincze, G., & Szasz, A. (2001). Pink-noise behaviour of biosystems. *European Biophysics Journal*, *30*(3), 227–231. https://doi.org/10.1007/s002490100143

Ten Oever, S., De Weerd, P., & Sack, A. T. (2020). Phase-dependent amplification of working memory content and performance. *Nature Communications*, *11*(1), 1832. https://doi.org/10.1038/s41467-020-15629-7

Ter Wal, M., Linde-Domingo, J., Lifanov, J., Roux, F., Kolibius, L. D., Gollwitzer, S., Lang, J., Hamer, H., Rollings, D., Sawlani, V., Chelvarajah, R., Staresina, B., Hanslmayr, S., & Wimber, M. (2021). Theta rhythmicity governs human behavior and hippocampal signals during memory-dependent tasks. *Nature Communications*, *12*(1), 7048. https://doi.org/10.1038/s41467-021-27323-3

Terada, S., Sakurai, Y., Nakahara, H., & Fujisawa, S. (2017). Temporal and Rate Coding for Discrete Event Sequences in the Hippocampus. *Neuron*, *94*(6), 1248-1262.e4. https://doi.org/10.1016/j.neuron.2017.05.024

Terrazas, A., Krause, M., Lipa, P., Gothard, K. M., Barnes, C. A., & McNaughton, B. L. (2005). Self-Motion and the Hippocampal Spatial Metric. *Journal of Neuroscience*, *25*(35), 8085–8096. https://doi.org/10.1523/JNEUROSCI.0693-05.2005

Teyler, T. J., & DiScenna, P. (1985). The role of hippocampus in memory: A hypothesis. *Neuroscience & Biobehavioral Reviews*, *9*(3), 377–389. https://doi.org/10.1016/0149-7634(85)90016-8

Thut, G., Nietzel, A., Brandt, S. A., & Pascual-Leone, A. (2006). Alpha-band electroencephalographic activity over occipital cortex indexes visuospatial attention bias and predicts visual target detection. *The Journal of Neuroscience: The Official Journal of the Society for Neuroscience*, *26*(37), 9494–9502. https://doi.org/10.1523/JNEUROSCI.0875-06.2006

Trautmann, E. M., Hesse, J. K., Stine, G. M., Xia, R., Zhu, S., O'Shea, D. J., Karsh, B., Colonell, J., Lanfranchi, F. F., Vyas, S., Zimnik, A., Steinmann, N. A., Wagenaar, D. A., Andrei, A., Lopez, C. M., O'Callaghan, J., Putzeys, J., Raducanu, B. C., Welkenhuysen, M., … Harris, T. (2023). Large-scale high-density brain-wide neural

recording in nonhuman primates. *bioRxiv: The Preprint Server for Biology*, 2023.02.01.526664. https://doi.org/10.1101/2023.02.01.526664

Treder, M. S. (2020). MVPA-Light: A Classification and Regression Toolbox for Multi-Dimensional Data. In *Frontiers in Neuroscience* (Vol. 14). https://www.frontiersin.org/article/10.3389/fnins.2020.00289

Uhlhaas, P. J., & Singer, W. (2013). High-frequency oscillations and the neurobiology of schizophrenia. *Dialogues in Clinical Neuroscience*, *15*(3), 301–313. https://doi.org/10.31887/DCNS.2013.15.3/puhlhaas

van Bree, S. (2023). A Critical Perspective on Neural Mechanisms in Cognitive Neuroscience: Towards Unification. *Perspectives on Psychological Science: A Journal of the Association for Psychological Science*, 17456916231191744. https://doi.org/10.1177/17456916231191744

van Bree, S., Alamia, A., & Zoefel, B. (2022). Oscillation or not—Why we can and need to know (commentary on Doelling and Assaneo, 2021). *European Journal of Neuroscience*, *55*(1), 201–204. https://doi.org/10.1111/ejn.15542

van Bree, S., Melcón, M., Kolibius, L. D., Kerrén, C., Wimber, M., & Hanslmayr, S. (2022). The brain time toolbox, a software library to retune electrophysiology data to brain dynamics. *Nature Human Behaviour*, *6*(10), 1430–1439. https://doi.org/10.1038/s41562-022-01386-8

van Bree, S., Sohoglu, E., Davis, M. H., & Zoefel, B. (2021). Sustained neural rhythms reveal endogenous oscillations supporting speech perception. *PLOS Biology*, *19*(2), e3001142.

van Driel, J., Olivers, C. N. L., & Fahrenfort, J. J. (2021). High-pass filtering artifacts in multivariate classification of neural time series data. *Journal of Neuroscience Methods*, *352*, 109080. https://doi.org/10.1016/j.jneumeth.2021.109080

van Gelder, T. (1995). What Might Cognition Be, If Not Computation? *Journal of Philosophy*, *92*(7), 345–381. https://doi.org/jphil199592719

Vanderwolf, C. H. (1969). Hippocampal electrical activity and voluntary movement in the rat. *Electroencephalography and Clinical Neurophysiology*, *26*(4), 407–418. https://doi.org/10.1016/0013-4694(69)90092-3

VanRullen, R. (2016). Perceptual Cycles. *Trends in Cognitive Sciences*, *20*(10), 723–735. https://doi.org/10.1016/j.tics.2016.07.006

Vertes, R. P., & Kocsis, B. (1997). Brainstem-diencephalo-septohippocampal systems controlling the theta rhythm of the hippocampus. *Neuroscience*, *81*(4), 893–926. https://doi.org/10.1016/s0306-4522(97)00239-x

Vijayan, S., & Kopell, N. J. (2012). Thalamic model of awake alpha oscillations and implications for stimulus processing. *Proc. Natl Acad. Sci. USA*, *109*. https://doi.org/10.1073/pnas.1215385109

Vivekananda, U., Bush, D., Bisby, J. A., Baxendale, S., Rodionov, R., Diehl, B., Chowdhury, F. A., McEvoy, A. W., Miserocchi, A., Walker, M. C., & Burgess, N. (2021). Theta power and theta-gamma coupling support long-term spatial memory retrieval. *Hippocampus*, *31*(2), 213–220. https://doi.org/10.1002/hipo.23284

Wang, D., Clouter, A., Chen, Q., Shapiro, K. L., & Hanslmayr, S. (2018). Single-Trial Phase Entrainment of Theta Oscillations in Sensory Regions Predicts Human Associative Memory Performance. *Journal of Neuroscience*, *38*(28), 6299–6309. https://doi.org/10.1523/JNEUROSCI.0349-18.2018

Wang, D., Parish, G., Shapiro, K. L., & Hanslmayr, S. (2023). Interaction between Theta Phase and Spike Timing-Dependent Plasticity Simulates Theta-Induced Memory Effects. *eNeuro*, *10*(3), ENEURO.0333-22.2023. https://doi.org/10.1523/ENEURO.0333-22.2023

Ward, L. M., & Greenwood, P. E. (2007). 1/f noise. *Scholarpedia*, *2*(12), 1537. https://doi.org/10.4249/scholarpedia.1537

Wassenhove, V. (2016). Temporal cognition and neural oscillations. *Curr. Opin. Behav. Sci.*, *8*. https://doi.org/10.1016/j.cobeha.2016.02.012

Watrous, A. J., Fried, I., & Ekstrom, A. D. (2011). Behavioral correlates of human hippocampal delta and theta oscillations during navigation. *Journal of Neurophysiology*, *105*(4), 1747–1755. https://doi.org/10.1152/jn.00921.2010

Watrous, A. J., Lee, D. J., Izadi, A., Gurkoff, G. G., Shahlaie, K., & Ekstrom, A. D. (2013). A comparative study of human and rat hippocampal low-frequency oscillations during spatial navigation. *Hippocampus*, *23*(8), 656–661. https://doi.org/10.1002/hipo.22124

Watrous, A. J., Miller, J., Qasim, S. E., Fried, I., & Jacobs, J. (2018). Phase-tuned neuronal firing encodes human contextual representations for navigational goals. *eLife*, *7*, e32554. https://doi.org/10.7554/eLife.32554

Watrous, A. J., Tandon, N., Conner, C. R., Pieters, T., & Ekstrom, A. D. (2013). Frequency-specific network connectivity increases underlie accurate spatiotemporal memory retrieval. *Nature Neuroscience*, *16*(3), Article 3. https://doi.org/10.1038/nn.3315

Weiss, S., Müller, H. M., & Rappelsberger, P. (2000). Theta synchronization predicts efficient memory encoding of concrete and abstract nouns. *Neuroreport*, *11*(11), 2357–2361. https://doi.org/10.1097/00001756-200008030-00005

Weiss, S., & Rappelsberger, P. (2000). Long-range EEG synchronization during word encoding correlates with successful memory performance. *Brain Research. Cognitive Brain Research*, *9*(3), 299–312. https://doi.org/10.1016/s0926-6410(00)00011-2

Welch, P. (1967). The use of fast Fourier transform for the estimation of power spectra: A method based on time averaging over short, modified periodograms. *IEEE*

Transactions on Audio and Electroacoustics, *15*(2), 70–73. https://doi.org/10.1109/TAU.1967.1161901

Wen, H., & Liu, Z. (2016). Separating Fractal and Oscillatory Components in the Power Spectrum of Neurophysiological Signal. *Brain Topography*, *29*(1), 13–26. https://doi.org/10.1007/s10548-015-0448-0

Whittington, M. A., Traub, R. D., Kopell, N., Ermentrout, B., & Buhl, E. H. (2000). Inhibition-based rhythms: Experimental and mathematical observations on network dynamics. *International Journal of Psychophysiology*, *38*(3), 315–336. https://doi.org/10.1016/S0167-8760(00)00173-2

Widmann, A., Schröger, E., & Maess, B. (2015). Digital filter design for electrophysiological data – a practical approach. *Journal of Neuroscience Methods*, *250*, 34–46. https://doi.org/10.1016/j.jneumeth.2014.08.002

Wikenheiser, A. M., & Redish, A. D. (2015). Hippocampal theta sequences reflect current goals. *Nature Neuroscience*, *18*(2), 289–294. https://doi.org/10.1038/nn.3909

Wilcoxon, F. (1945). Individual Comparisons by Ranking Methods. *Biometrics Bulletin*, *1*(6), 80–83. https://doi.org/10.2307/3001968

Williams, A. H. (2020). Discovering precise temporal patterns in large-scale neural recordings through robust and interpretable time warping. *Neuron*, *105*. https://doi.org/10.1016/j.neuron.2019.10.020

Williams, A. H., Poole, B., Maheswaranathan, N., Dhawale, A. K., Fisher, T., Wilson, C. D., Brann, D. H., Trautmann, E. M., Ryu, S., Shusterman, R., Rinberg, D., Ölveczky, B. P., Shenoy, K. V., & Ganguli, S. (2020). Discovering Precise Temporal Patterns in Large-Scale Neural Recordings through Robust and Interpretable Time Warping. *Neuron*, *105*(2), 246-259.e8. https://doi.org/10.1016/j.neuron.2019.10.020

Winawer, J., Kay, K. N., Foster, B. L., Rauschecker, A. M., Parvizi, J., & Wandell, B. A. (2013). Asynchronous broadband signals are the principal source of the BOLD

response in human visual cortex. *Current Biology: CB*, *23*(13), 1145–1153. https://doi.org/10.1016/j.cub.2013.05.001

Winson, J. (1978). Loss of hippocampal theta rhythm results in spatial memory deficit in the rat. *Science (New York, N.Y.)*, *201*(4351), Article 4351. https://doi.org/10.1126/science.663646

Wolff, Ding, Myers, & Stokes. (2015). Revealing hidden states in visual working memory using electroencephalography. *Frontiers in Systems Neuroscience*, *9*. https://www.frontiersin.org/articles/10.3389/fnsys.2015.00123

Wolff, Jochim, Akyürek, Buschman, & Stokes. (2020). Drifting codes within a stable coding scheme for working memory. *PLOS Biology*, *18*(3), e3000625. https://doi.org/10.1371/journal.pbio.3000625

Wolff, Jochim, Akyürek, & Stokes. (2017). Dynamic hidden states underlying working-memory-guided behavior. *Nature Neuroscience*, *20*(6), 864–871. https://doi.org/10.1038/nn.4546

Womelsdorf, T., Valiante, T. A., Sahin, N. T., Miller, K. J., & Tiesinga, P. (2014). Dynamic circuit motifs underlying rhythmic gain control, gating and integration. *Nature Neuroscience*, *17*(8), Article 8. https://doi.org/10.1038/nn.3764

Worden, M. S., Foxe, J. J., Wang, N., & Simpson, G. V. (2000). Anticipatory biasing of visuospatial attention indexed by retinotopically specific alpha-band electroencephalography increases over occipital cortex. *The Journal of Neuroscience: The Official Journal of the Society for Neuroscience*, *20*(6), RC63.

Xiao, J., Hays, J., Ehinger, K. A., Oliva, A., & Torralba, A. (2010). SUN database: Large-scale scene recognition from abbey to zoo. *2010 IEEE Computer Society Conference on Computer Vision and Pattern Recognition*, 3485–3492. https://doi.org/10.1109/CVPR.2010.5539970

Xie, J., & Qiu, Z. (2007). The effect of imbalanced data sets on LDA: A theoretical and empirical analysis. *Pattern Recognition*, *40*(2), 557–562. https://doi.org/10.1016/j.patcog.2006.01.009

Xue, G. (2018). The Neural Representations Underlying Human Episodic Memory. *Trends in Cognitive Sciences*, *22*(6), 544–561. https://doi.org/10.1016/j.tics.2018.03.004

Yamaguchi, Y., Sato, N., Wagatsuma, H., Wu, Z., Molter, C., & Aota, Y. (2007). A unified view of theta-phase coding in the entorhinal–hippocampal system. *Current Opinion in Neurobiology*, *17*(2), 197–204. https://doi.org/10.1016/j.conb.2007.03.007

Yang, C., He, X., & Cai, Y. (2023). *Reactivating and reorganizing activity-silent working memory: Two distinct mechanisms underlying pinging the brain* (p. 2023.07.16.549254). bioRxiv. https://doi.org/10.1101/2023.07.16.549254

Ye, Z., Shelton, A. M., Shaker, J. R., Boussard, J., Colonell, J., Manavi, S., Chen, S., Windolf, C., Hurwitz, C., Namima, T., Pedraja, F., Weiss, S., Raducanu, B., Ness, T. V., Einevoll, G. T., Laurent, G., Sawtell, N. B., Bair, W., Pasupathy, A., … Steinmetz, N. A. (2023). Ultra-high density electrodes improve detection, yield, and cell type specificity of brain recordings. *bioRxiv: The Preprint Server for Biology*, 2023.08.23.554527. https://doi.org/10.1101/2023.08.23.554527

Zeineh, M. M., Engel, S. A., Thompson, P. M., & Bookheimer, S. Y. (2003). Dynamics of the Hippocampus During Encoding and Retrieval of Face-Name Pairs. *Science*, *299*(5606), 577–580. https://doi.org/10.1126/science.1077775

Zheng, C., Hwaun, E., Loza, C. A., & Colgin, L. L. (2021). Hippocampal place cell sequences differ during correct and error trials in a spatial memory task. *Nature Communications*, *12*, 3373. https://doi.org/10.1038/s41467-021-23765-x

Zoefel, B., Ten Oever, S., & Sack, A. T. (2018). The Involvement of Endogenous Neural Oscillations in the Processing of Rhythmic Input: More Than a Regular Repetition

of Evoked Neural Responses. *Frontiers in Neuroscience*, *12*, 95. https://doi.org/10.3389/fnins.2018.00095